ABSTRACT

INA, MARIA. The Synthesis of Poly *N*-acetyl iodo Glucosamine and its Gelation of Blood. (Under the direction of Dr. Samuel Hudson and Dr. Wendy Krause).

A variety of advanced hemostats have been brought to market, where most products work by simply absorbing the blood at the site of the wound rather than by actively coagulating the blood. In this study, a new hemostatic system that causes an induced blood clot formation via simultaneous gelation of blood proteins and agglutination of the various suspended cells, transforming a liquid blood into an elastic gel, selectively at the site of injury.

The key chemistry of this study postulates the formation of covalent crosslinks between a hemostat matrix with sulfhydryl-reactive sites and sulfhydryl compounds in the blood. Chitosan-iodoacetic acid derivative was successfully prepared by substituting amino groups of chitosan at its C-2 position with iodoacetic acid which is an irreversible inhibitor of all cysteine peptidases, to interact with the free thiol group of cysteine. Mass spectrometry demonstrated the clear reaction between iodoacetic acid and L-cysteine, suggesting the possibility of a reaction between chitosan-iodoacetic acid derivative and cysteine residues in the blood proteins. A series of rheological experiments were carried out on the mixture of 2 wt% chitosan-iodoacetic acid/acetic acid solution and sodium citrated blood in order to investigate the rheological properties of the mixture. The steady shear measurement indicated that the viscosity of the blood increased by nearly a million-fold after being mixed with the derivative solution. The dynamic oscillatory measurement revealed that the mixture sample reached its gel state in approximately 10 minutes after the mixing. Moreover, changing the ratio of the derivative content to the blood content demonstrated that chitosan-iodoacetic acid

enables the blood to be a gel within seconds upon mixing.

Next, the detailed mechanism of the observed enhanced clots formation was investigated. The blood was separated into the cells and the plasma, then, each was tested on its rheological behavior with chitosan-iodoacetic acid solution. The plasma never became a gel, confirming the presence of the blood cells is necessary for the gelation of the blood. In addition, separated cells re-suspended in the phosphate buffered saline (PBS) exhibited gelation, which indicates that the chitosan-iodoacetic acid derivative works independently of the natural coagulation pathways. This supports our assumption that this system would interact with cysteine-rich domains of the blood cells via covalent crosslinkings.

Lastly, additional rheological studies were conducted on a thiolated chitosan, chitosan-L-cysteine. Chitosan-L-cysteine derivative caused somewhat increased viscosity of the blood, which is in agreement with the assumption that the enhanced blood coagulation is caused by the covalent crosslinking between the sulfhydryl reactive-chitosan derivative and sulfhydryl compounds in the blood. In contrast, significant gelation between chitosan-iodoacetic acid and chitosan-L-cysteine derivative was not observed. Also, the expected *in situ* gelation of chitosan-L-cysteine derivative through disulfide crosslinking was not confirmed. The substitution ratio of the sulfhydryl reactive moieties into chitosan is low so as not to insolubilize the derivative. These results suggest the sulfhydryl groups found in the blood plasma proteins are not reactive. *In vitro* experiments using albumin, a model blood, also suggest that sulfhydryl groups in the albumin are not reactive enough to cause the sample-spanned gelling. Nevertheless, the chitosan-iodoacetic acid derivatives demonstrated gelation of blood, much faster than the chitosan controls.

© Copyright 2013 Maria Ina

All Rights Reserved

The Synthesis of Poly *N*-acetyl iodo Glucosamine and its Gelation of Blood

by
Maria Ina

A dissertation submitted to the Graduate Faculty of
North Carolina State University
in partial fulfillment of the
requirements for the degree of
Doctor of Philosophy

Fiber and Polymer Science

Raleigh, North Carolina

2013

APPROVED BY:

_____	_____
Dr. Samuel Hudson Co-Chair of Advisory Committee	Dr. Wendy Krause Co-Chair of Advisory Committee
_____	_____
Dr. Martin King	Dr. Saad Khan

DEDICATION

Dedicated to all people who always supported and encouraged me to complete this work.

BIOGRAPHY

Maria Ina grew up in Ueda, Japan. She received her Bachelor of Science in Materials Chemistry in 2007 from Shinshu University, Japan. A long-term study abroad fellowship from Japanese Ministry of Education, Culture, Sports, Science and Technology gave her a chance to pursue further studies in a graduate school. In 2007 she came to the United States and started her Master Program in College of Textiles at North Carolina State University under the direction of Dr. Samuel Hudson. After graduation in 2009 with Master of Science in Textile Engineering, she continuously started her Doctoral Program in Fiber and Polymer Science in College of Textiles, minoring in Chemical Engineering, under Drs. Samuel Hudson and Wendy Krause. She expects to complete her Ph.D. degree in summer 2013.

ACKNOWLEDGMENTS

I would like to gratefully acknowledge all who have helped me complete this work. First of all, I am sincerely grateful to my advisor, Dr. Samuel Hudson, for his continuous support and guidance throughout my graduate study for six years. Additionally, I would like to thank Dr. Wendy Krause, the co-chair of committee, for her helpful suggestions and encouragement, as well as my committee members, Dr. Martin King and Dr. Saad Khan.

I would also like to thank Ms. Birgit Andersen form Department of Textile Engineering, Chemistry, and Science and Dr. Xiaoyan Sun from the Department of Chemistry for the training in the use of FTIR and NMR. My special thanks go to Dr. Taufika Williams and Ms. Danielle Lehman from the Department of Chemistry for the LC-TOF operating. A great appreciation is extended to Mr. Chris Pernell from the Department of Food, Bioprocessing and Nutrition Sciences for his assistance with ATS Rheometer. I would also like to thank Dr. Jennifer Davis from the Veterinary School and Medicine for the blood supply. I would sincerely appreciate the Japanese study-abroad fellowship which gave me a chance to pursue my study in the United States.

Last but not least, I have had many precious friendships. I would like to thank all my friends inside and outside of the campus who have supported and encouraged me to achieve this work and spent valuable time together. Finally, I would like to express my sincere appreciation to my family for their unending patience and support.

TABLE OF CONTENTS

LIST OF TABLES

LIST OF FIGURES

CHAPTER 1

1 Introduction

Hemostasis is the physiological process to arrest bleeding and minimize blood loss from the damaged blood vessels. The hemostatic process is accelerated when blood contacts a majority of foreign materials, either rapidly or over the course of long-term exposure. Uncontrolled hemorrhage from severe injuries remains one of the leading causes of pre-hospital trauma deaths in both the battlefield and civilian settings.[1-5] Champion et al.[3] reported that extensive hemodynamic and biochemical measurements, which were made in several hundred seriously wounded combat casualties at an average time of about 6.5 hours after an injury, demonstrate that casualties with the greatest blood loss were most likely to die, also a blood volume reduced to 50% of normal was likely to be fatal. The majority of trauma deaths occur in the first few hours following injury, often before the injured patient reaches a hospital.[6,7,8] Hemorrhage, in fact, contributes to the pre-hospital deaths in 33 to 56% of cases.[7] Moreover, hemorrhage accounts for the largest proportion of mortality occurring within the first hour of trauma center care, over 80% of operating room deaths after major trauma, and almost 50% of deaths in the first 24 hours of trauma care,[6,7,9] also the presence of early hemorrhagic shock as defined by a systolic blood pressure less than or equal to 90 mmHg in the pre-hospital setting or emergency department is associated with high rates of organ failure (24%) and infection (39%).[10] On the other hand, very few hemorrhagic deaths occur after the first day of the injury.[6,7] The Wound Data and Munitions Effectiveness Team (WDMET) database suggests that more than half of the potentially

preventable deaths in combat related to the lack of first aid after the exsanguinations from extremity wounds.[11,12] Therefore, hemostatic agents that can arrest bleeding and stabilize the casualty before evacuation is done, are desired for both the battlefield and civilian medicine.

The control of bleeding and limitation of blood loss is the only means of avoiding the problems associated with the large trauma hemorrhage. The development of prospective powerful hemostatic wound dressings for traumatic hemorrhages has been investigated. Progress has been made in the development and testing of novel dressings and dressing-adjuncts for use in compressed arrest of bleeding on external or visceral hemorrhage. Several of these commercial hemostatic products have been used routinely in the battlefield. Some case reports show that agents are effective in reducing or stopping bleeding in more than 90% of applications.[13,14]

The most promising of these in pre-clinical studies has been the fibrin dressing developed by the American Red Cross which has shown superior hemostatic effect in models of severe arterial and hepatic hemorrhage.[15-18] The fibrin dressing is distinguished from other available agents in that it contains purified human fibrinogen and thrombin, both are plasma coagulation factors, and this is inherently hemostatic while other products support hemostasis primarily through adherence to and desiccation of the bleeding wound, not directly through thrombogenesis.[17-21]

1.1 Blood Coagulation Cascade

Blood loss at the site of a wound in mammals is curtailed by the rapid formation of a hemostatic plug, i.e., a self-assembled network of the plasma protein. Several studies reported that the physiological hemostatic process consists of a series of cascade reactions in which 11 plasma coagulation factors are involved: six in the intrinsic pathway (factor VIII, IX, XI, XII, prekallikrein (PK), and high-molecular weight kininpgen (HMWK)), one in the extrinsic pathway (factor VII), and four in the common pathway (prothrombin (factor II), V, X, and fibrinogen (factor I)). The blood coagulation consists of a cascade of precursor protein activation reactions, where each precursor protein is converted to an active protease by cleavage of one or more peptide bonds in the precursor molecule. The final protease generated is thrombin (factor IIa, the subscript "a" stands for the activated form of each factor). The schematic image of coagulation pathways is shown in Figure 1-1.[22]

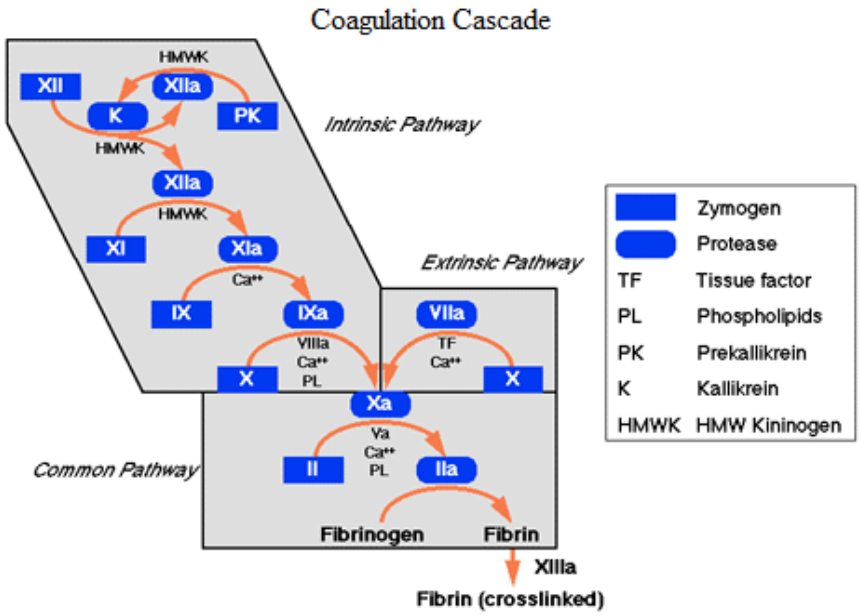

Figure 1-1 Sequence of coagulation reactions. The classical model of blood coagulation involves a cascade of precursor protein (zymogen) activation reactions. At each stage a precursor protein is converted to an active protease by cleavage of one or more peptide bonds in the precursor molecule.[22]

There are two different pathways that lead to thrombin formation; extrinsic pathway and intrinsic pathway.[22,23] The extrinsic pathway, also referred to as the tissue factor pathway, is initiated when blood plasma is exposed to tissue factor. Tissue factor (factor III) is a non-enzymatic lipoprotein constitutively expressed on the surface of cells that are not normally in contact with plasma. Exposure of plasma to these cells initiates coagulation outside a broken blood vessel. Tissue factor binds factor VIIa and accelerates factor X activation about 30000-fold in the presence of calcium ions. Then, factor Xa converts prothrombin (factor II) into thrombin (factor IIa). A trace amount of factor VIIa appears to be available in plasma at all times to interact with tissue factor, also, factor VII is activated by its product, factor Xa. For

example, NovoSeven® (Novo Nordisk Inc., Princeton, NJ), recombinant physiological blood coagulation factor VIIa, is intended to promote hemostasis by activating the extrinsic pathway of the coagulation and has demonstrated promise in clinical series as an adjunct to traditional measures in controlling hemorrhage in acute, life-threatening traumatic coagulopathy. The extrinsic pathway is a very rapid process, i.e., within 12 to 15 seconds, however, the produced thrombin is low and the resulting clot is small.

The intrinsic pathway, also referred to as the contact activation pathway, is initiated when blood, mainly factor XII, contact with negatively charged surfaces like exposed collagen in the blood vessel wall, glass, kaolin, or another artificial surface. Once bound, reciprocal activation of factor XII occurs. Factor XII triggers clotting via the sequential activation of factors XI, IX, X, and II (prothrombin). This process is considerably slower, i.e., five to ten minutes, but results in the formation of larger amounts of thrombin. Kaolin is an inert mineral and is utilized routinely to assay blood clotting times by clinical laboratories because it promotes clotting by the intrinsic pathway. Lately, kaolin-based QuikClot® gauze, which is the third generation of QuikClot® (Z-Medica Corp., Wallingford, CT), has been subjected to safety and efficacy studies performed by the US Army Institute of Surgical Research (USAISR) and the Naval Medical Research Center and was found to be the most effective product among the tested in the USAISR study, allowing the least amount of hemorrhage and resulted in the highest survival rate in the animals tested.[24] This product is designed as rayon/polyester gauze impregnated with kaolin, not containing botanicals or materials from animal or human sources.

Factor VIIa also activates factor IX in the presence of tissue factor, providing a connection between the extrinsic and intrinsic pathways. Tissue factor pathway inhibitor (TFPI) is a protein that binds to factor Xa. The Xa-TFPI complex then interacts with VIIa/tissue factor and inhibits activation of factors X and IX unless the VIIa/tissue factor initially present, generates a sufficient amount of factor IXa to sustain factor X activation via the intrinsic pathway. Thus, VIIa/tissue factor may provide the initial stimulus to clot and then be rapidly turned off, while IXa in the intrinsic pathway may be responsible for generating the larger amounts of Xa and thrombin required for clot formation.

The final common pathway is the conversion of the soluble protein fibrinogen into an insoluble fibrin gel by the action of thrombin, which the fibrin is strengthened further through covalent crosslinking catalyzed by factor XIIIa. In this pathway, factor Xa converts prothrombin (factor II) to thrombin (factor IIa) by cleaving two peptide bonds. Activation of prothrombin by Xa is accelerated by factor Va, platelets *in vivo* (or phospholipids *in vitro*), and calcium ions. Rapid activation occurs only when prothrombin and Xa have the ability to bind calcium. Binding of calcium alters the conformation of these factors to interact with a membrane surface provided by platelets *in vivo* (or phospholipids *in vitro*). That is, aggregated platelets are thought to provide the surface upon which prothrombin activation occurs at a site of hemostasis. This leads to local generation of large amounts of Xa and thrombin (factor IIa), followed by conversion of fibrinogen to fibrin by thrombin (factor IIa). Finally, numerous blood cells and other molecules are trapped in the crosslinked fibrin mesh and a blood clot is formed. Fibrin is the primary scaffold that induces angiogenesis and fibroblast migration. Once fibroblasts have migrated into fibrin, synthesis of collagen and

other extracellular matrix molecules is induced. The concentrations of coagulation factors required for normal hemostasis are summarized in Table 1-1.[22]

Table 1-1 Concentrations of coagulation factors required for normal hemostasis. With the exception of fibrinogen, factor levels are usually reported as percentages of the concentrations present in plasma pooled from normal individuals. Tissue factor is not present in plasma and cannot be quantified in patients[22]

Factor	Molecular Weight	Plasma Concentration (μg/ml)	Required for Hemostasis (% of normal concentration)
Fibrinogen	330,000	3000	30
Prothrombin	72,000	100	40
Factor V	300,000	10	10-15
Factor VII	50,000	0.5	5-10
Factor VIII	300,000	0.1	10-40
Factor IX	56,000	5	10-40
Factor X	56,000	10	10-15
Factor XI	160,000	5	20-30
Factor XIII	320,000	30	1-5
Factor XII	76,000	30	0
Prekallikrein	82,000	40	0
HMWK	108,000	100	0

1.1.1 Fibrin Crosslinking

Fibrin, also called factor Ia, is a fibrillar protein played an important role in blood coagulation cascade, which is converted from a soluble globular plasma glycoprotein fibrinogen by the action of thrombin. Human fibrinogen is a soluble precursor of polymeric fibrin. The human fibrinogen molecule is a large dimeric protein that consists of 2964 amino acid residues and four carbohydrate residues. Every subunit contains three pairs of

polypeptide chains covalently linked by disulfide bonds, which are α-chain, β-chain, and γ-chain,[25] as shown in Figure 1-2.[22]

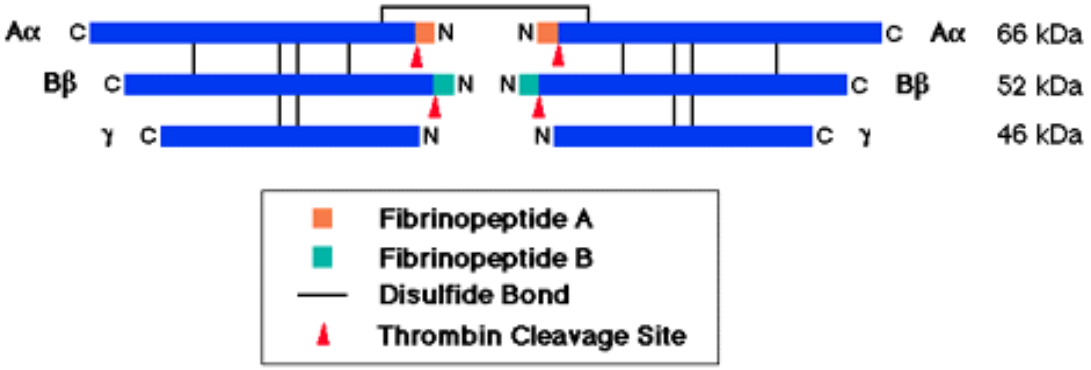

Figure 1-2 Structure of fibrinogen.[22] N and C represent the nitrogen and carbon terminus, respectively. Fibrinogen consists of three pairs of polypeptide chains covalently linked by disulfide bonds and has a molecular weight of approximately 330, 000. Thrombin converts fibrinogen to fibrin monomers by cleaving fibrinopeptides A (16 amino acid residues) and B (14 amino acid residues) from the N-terminal ends of the Aα and Bβ chains, allowing the fibrin monomers to form a gel.

When thrombin catalyzes the cleavage of fibrinogen to fibrin segments, it cleaves specific fibrinopeptide bonds in the α- and β-chains. Removal of the fibrinopeptides allows the fibrin monomers to form a gel consisting of long polymers. At this stage, the fibrin monomers are bound to each other non-covalently, making a physically crosslinked fibrin gel (Figure 1-3[22]).

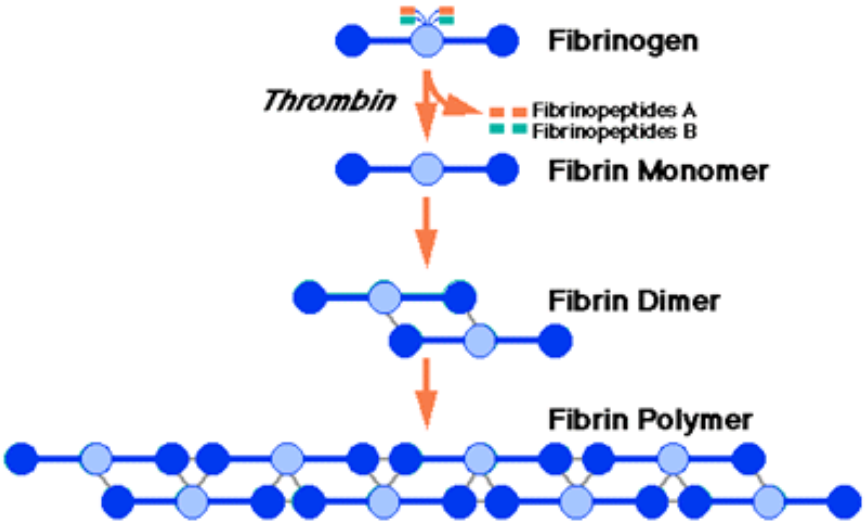

Figure 1-3 Fibrin polymerization.[22]

Simultaneously, thrombin activates factor XIII and converts it into active factor XIIIa that stabilizes the polymeric fibrin gel through the covalent disulfide crosslinkages of its γ- and, then α- polypeptide chains.[26] Such stabilization of fibrin give the clot adequate mechanical rigidity and stability towards the plasmin cleavage,[27,28] where plasmin provides the subsequent cleavage of the fibrin network and acts to dissolve the fibrin clot in the final step of healing, referred to as fibrinolysis.[29] Finally, soluble fibrin is converted to three-dimensional, covalent structure of cross-linked, insoluble fibrin. Hemostasis proceeds when serum proteins, such as platelets and red blood cells, are caught by this polymerized fibrin mesh and aggregate at the site of injury, forming the hemostatic plug. This locally transforms liquid blood into a gelled clot.

Factor XIIIa is a thiol enzyme (protein-glutamine-γ-transferase) that belongs to the transglutaminase family. This family catalyzes the formation of γ-glutamyl-lysine isopeptide bonds.[30] An isopeptide bond is a bond between the carboxyl terminus of one protein and the amino group of a lysine residue on another protein. McKee et al.[25] reported that crosslinking of fibrin by the action of XIIIa consists of the rapid formation of crosslinks between γ-chains that produces γ-γ dimers, and a much slower formation of crosslinks between α-chains that produce higher molecular weight polymers of at least six α-chains. In addition, β-chains are not involved directly in the crosslinking of fibrin. The faster crosslinking between γ-chain completes within five minutes of the onset of clot formation, while the slower crosslinking between α-chains completes only after 90 minutes. Moreover, they found that the more extensive the crosslinks in α-chain, the greater the insolubility of the fibrin. Authors concluded that although it is still uncertain whether the γ-γ dimmers are formed by intra- or intermolecular reaction, higher molecular weight α-chains could only be formed by crosslinkage between α-chains in different molecules. Thus, the extensive crosslink among fibrin molecules on formation of insoluble fibrin mesh must largely depend on formation of insoluble crosslinks between α-chains. It is noteworthy that the extent of crosslinking in fibrin is reflected by the solubility of the fibrin in 10 M urea, turning out that the more extensive the crosslinks in α-chain, the greater the insolubility of the fibrin (Figure 1-4).[25] Besides, it is also notable that formation of the γ-γ and the -α-α- crosslinks was accelerated by calcium in the presence of excess ethylenediaminetetraacetic acid (EDTA), which is a versatile chelating agent that binds to the metal ions like Ca^{2+} and forms 1:1 metal-to-EDTA complexes.

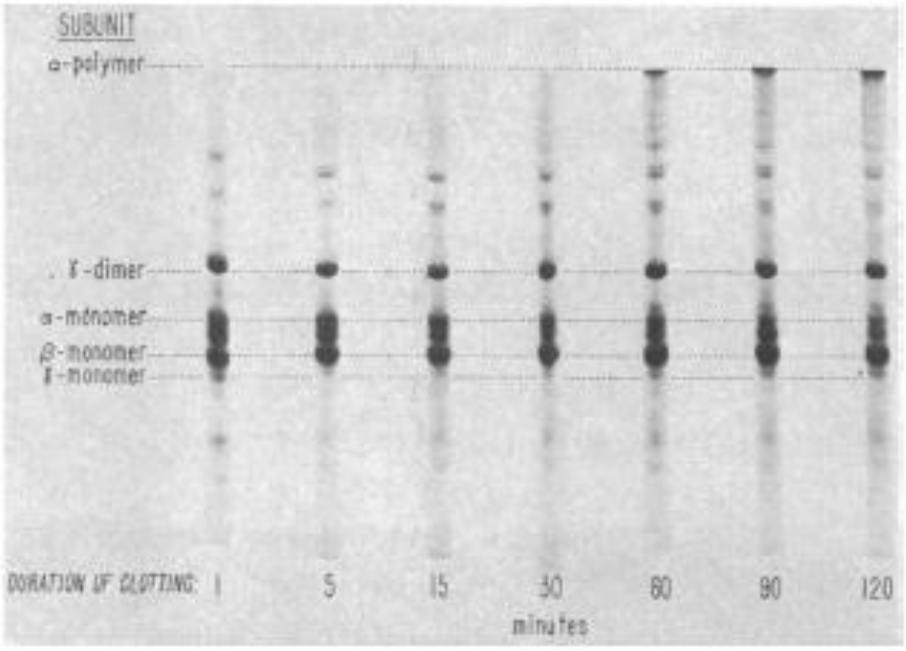

Figure 1-4 Gel electrophoresis of fibrin as a function of time of crosslinking by fibrin stabilizing factor (factor Xllla). Fibrinogen was reacted with thrombin and the above factor for the intervals indicated as described in the text, and the resulting fibrin was reduced and analyzed on the gels.[25]

1.1.2 Fibrin-based Hemostatic Wound Dressing

Current investigated hemostatic agents include surgical gauze, gelatin foam, oxidized cellulose, microfibrillar collagen powder, collagen fleece modified collagen and fibrin. Generally, these agents are applied to the injury with gentle to moderate digital pressure to establish hemostasis within three to four minutes.[31-33] However, these hemostatic agents are ineffective in many conditions because the hemostatic properties of these agents depend on adequate platelet and the clotting factors. On the other hand, fibrin is a natural hemostat and scaffold, guiding the direction of wound contraction and closure. *In vivo*, fibrin protects wounded tissues by providing a moist environment and forms a provisional matrix through

which cells migrate during the healing process. Thus, many researchers attempted to take advantage of natural fibrinogen, the precursor of the fibrin, and its derivatives as effective hemostatic agents.

Fibrin-based sealants were first-developed in the 1940s and have proven to be quite effective.[16,34] For example, one form involves a dry powdered mixture of human fibrinogen and thrombin packed onto a solid bandage backing. When such a bandage is firmly pressed onto a bleeding injury, a strong fibrin seal quickly forms and bleeding is stopped.[16] Fibrin-based hemostatic agent has been found to be effective in achieving hemostasis of superficial and deep liver and splenic injuries in experimental and clinical studies.[35,36] In general, almost all formulations of fibrin sealants are presented in two-component systems in which a solution of concentrated fibrinogen and factor XIII are combined with a solution of thrombin and calcium in order to form a coagulum, simulating the final stage of the clotting cascade. Once the thrombin/calcium is combined with the fibrinogen/factor XIII, a fibrin clot forms in seconds, or somewhat slower if a more dilute form of thrombin is used. The application devices are designed to mix the fibrinogen and thrombin components either just prior to contact with tissue or on the tissue itself. Problems associated with application include immediate clotting between the two components before binding with the tissues and/or poor mixing of the components, which result in low bonding strength.[37-39]

For the purpose of maximizing the ease of application, fibrin has been associated with sponges made of cellulose[40] or collagen[41] to improve wound healing ability. Fibrin sealant in combination with collagen also has been shown to be a safe and effective method for control of hemorrhage from splenic and liver injuries, with no evidence of increased infections or

hemorrhagic complications.[42,43] Moreover, Krishnan et al.[44] prepared a composite sheet of human fibrin and gelatin with improved mechanical strength. The sheets being porous, blood oozing from the injured site would penetrate and react with the excess thrombin in the sheet to clot and arrest bleeding. Also, Noorjahan et al.[45] reported that gelatin is a good candidate to give fibrin film better mechanical properties with compatible wound healing properties. However, fibrin bandages have limited practical applicability in trauma medicine because human fibrinogen and thrombin are highly expensive molecules that are scarce in supply.[34] If a biomimetic crosslinked fibrous mat of approximately the same dimensions as a naturally occurring fibrin network based on an inexpensive and widely available biomaterial would be developed, it should be possible to construct an artificial blood clot that accelerate the clotting process than those possible in the unaided physiological processes.

1.1.3 Evaluation of Blood Clotting Time

When blood is removed from the body and placed in a glass test tube, it clots in around four to eight minutes. Calcium ions are required for this process. Added EDTA or citrate prevents clotting by binding calcium. Therefore, clotting can be initiated *in vitro* at a later time by adding an excess of calcium ions. The clotting time can also be shortened by adding an emulsion of negatively-charged phospholipids (PL). The clotting time is further shortened to 21 to 32 seconds by pre-incubation of the plasma with particulate activator substances, such as kaolin, silica. The blood clotting initiated by kaolin, PL, and calcium is

termed the activated partial thromboplastin time (aPPT, APTT) or the partial thromboplastin time (PTT), where the thromboplastin is a synonym of tissue factor.

Alternatively, the clotting time of blood plasma can be shortened to 11 to 12 seconds by adding thromboplastin (tissue factor) and calcium ions. The reaction initiated by thromboplastin and calcium is termed the prothrombin time (PT). Since patients with inherited bleeding disorders have prolongation of the aPTT, the PT, or both, these are useful clinical screening tests to detect abnormalities of the extrinsic, intrinsic, and the common pathways. For example, a patient with a prolonged aPTT and a normal PT is considered to have a defect in the intrinsic coagulation pathway since all of the components of the aPTT test, i.e., negative-charged surfaces, initiate the intrinsic pathway. On the other hand, a patient with a prolonged PT and a normal aPTT has a defect in the extrinsic pathway since the component of the PT test, i.e., tissue factor, initiates extrinsic pathway. Prolongation of both the aPTT and the PT suggests that the defect lies in a common pathway (Figure 1-5).

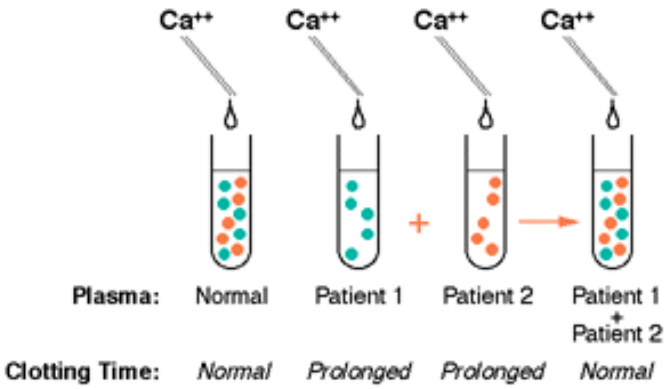

Figure 1-5 Identification of distinct coagulation factors.[22] If mixing plasma from two patients with defect in either of the coagulation pathways would correct the clotting time to normal, this suggests that the two patients have different coagulation factor deficiencies.

1.2 Chitosan as Hemostat

Chitosan is a linear polysaccharide composed of randomly distributed β-(1-4)-linked D-glucosamine and *N*-acetyl-D-glucosamine. Chitosan is the fully or partially *N*-deacetylated derivative of chitin, which is the structural element in the exoskeleton of crustaceans and cell walls of fungi. Both chitin and chitosan have been commercially interesting due to their high percentage of nitrogen content (6.89%) compared to synthetically substituted cellulose (1.25%).[46] This provides chitin and chitosan different properties from that of cellulose although they are structurally similar (Figure 1-6[46]). The application of chitin and chitosan and their derivatives are widespread from agriculture, medicine, environment, to food. Especially, much attention has been paid to chitosan as a polysaccharide with many potential biomedical applications.

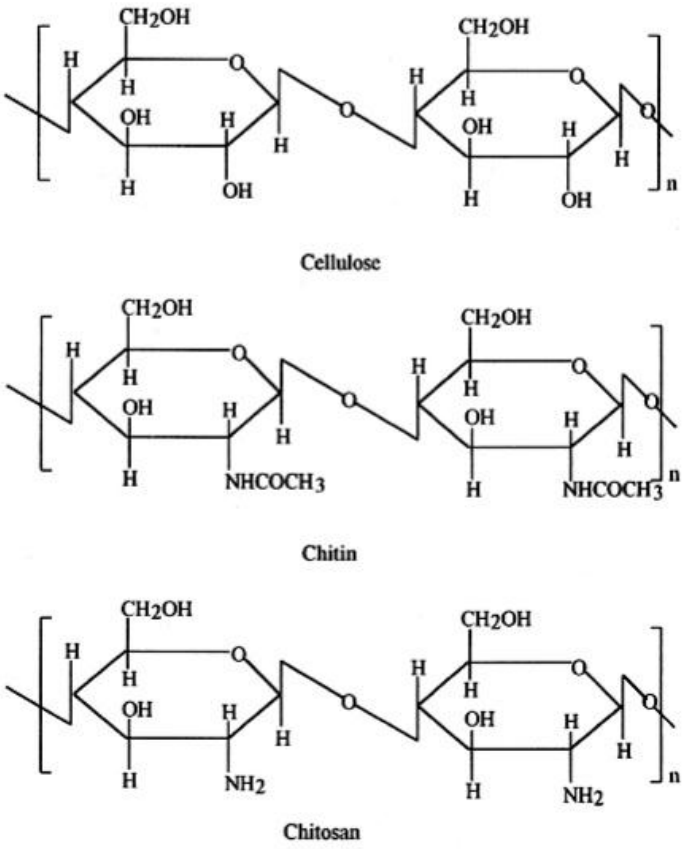

Figure 1-6 Structures of cellulose, chitin, and chitosan.[46]

Chitosan is interesting in the way that it maintains its hydrated gel-like structure in a neutral and basic pH environment but is solubilized in an acidic environment due to the positive charge that comes from protonation of its free amino groups. In particular, chitosan becomes soluble in aqueous solutions due to the protonation of its amine groups in acidic environments. Once dissolved, chitosan remains in solution up to around pH 6.2, since the amino groups of chitosan have a pKa value in the vicinity of 6.4.[47,48] Increasing the pH of chitosan aqueous solution to above 6.2 leads to the formation of a hydrated gel-like

precipitate.[49] This provides a substantial bioadhesive quality, which readily binds chitosan to negatively charged surfaces such as the mucosal membrane and chelates metal ions. Thus, chitosan has been of interest as a promising biodegradable/ biocompatible cationic biomaterial for a wide range of medical applications over the last three decades. Chenite et al.[49] demonstrated that the combination of chitosan and polyol-phosphate salt, which is a well-known thermoset-gel forming material, results in a temperature-controlled pH-dependent chitosan reverse gel, allowing the chitosan solutions to remain liquid at physiological pH and at room temperature and then turn into gel if heated to body temperature (37˚C) without any crosslinkers. This could be a potential non-surgically applied drug delivery vehicle. Furthermore, recent studies suggested that chitosan and its derivatives are great candidates as supporting material for tissue engineering that inhibit fibroplasias in wound healing and promote tissue growth and differentiation in tissue culture due to their porous structure, gel forming properties, high mucoadhesion (high affinity to protein), and ease of chemical modification.[50-53] In addition, this indicates that chitosan can be potentially used as controlled drug carriers that transport a drug to an acidic environment like the human stomach, where the chitosan drug carrier degrades and releases the drug rapidly.[54-63]

One of the important parameters of chitosan is the degree of *N*-deacetylation (DD%), i.e., the ratio of 2-acetamido-2-deoxy-D-glucopyranose to 2-amino-2-deoxy-D-glucopyranose structural units. A common method for the synthesis of chitosan is the alkaline deacetylation of chitin in concentrated sodium hydroxide aqueous solution at an elevated temperature. Although typical DD% of commercial chitosans is 65% or more,[46] this method makes it possible to produce chitosan with DD% of up to 98%.[64] This ratio has a

striking effect on its solubility and solution properties. As mentioned earlier, the derived amino group in chitosan has a pKa of 6.3-6.5,[47,48] which makes chitosan protonated in acidic to neutral solution with a charge density dependent on the environmental pH and the degree of deacetylation. Due to this, chitosan is soluble in dilute aqueous acids, such as acetic acid and formic acid, moreover, the low molecular weight chitosan can be soluble in water. Furthermore, chitosan with a low degree of deacetylation ~40% has been found to be soluble up to pH 9.0.[65] Solubility is greatly influenced by the addition of salt to the solution. The higher the ionic strength, the lower the solubility.[65] This is due to the fact that chitosan in solution exists in an extended conformation with a more flexible chain due to the repelling effect of each positively charged deacetylated unit on the neighboring glucosamine unit. Addition of an electrolyte reduces this effect, resulting in a more random coil-like conformation in the molecule. A higher electrolyte concentration, thus, results in a salting-out effect leading to the precipitation of chitosan from solution.[66] Increasing degree of deacetylation increases the viscosity of chitosan solution due to the extended conformation in highly deacetylated chitosan. In addition, high molecular weight and a linear unbranched structure of chitosan bring about an excellent viscosity enhancing effect in an acidic environment with the shear-thinning behavior. The viscosity also increases with an increase in chitosan concentration, but decreases with an increase in temperature.

In order to determine DD %, several methods have been used, including IR spectroscopy,[67-69] X-ray diffraction (XRD),[70] gel permeation chromatography,[71] UV spectrophotometry,[71-73] ^{1}H-NMR spectroscopy,[74] ^{13}C-NMR spectroscopy,[66,75] conductometric titration,[75,76] potentiometric titration,[77,78] or mass spectrometry.[78]

1.2.1 Chitosan-based Hemostatic Wound Dressing

Chitosan is an attractive biomaterial for wound care due to its biocompatibility and antimicrobial properties.[79-81] Chitosan's mechanism of action functions independently of either the intrinsic or extrinsic clotting cascades, and forms an immediate seal on wounds. The hemostatic effect of chitosan was proposed to be due to an interaction between the negatively charged cell membrane of erythrocytes and positively charged chitosan, and to be independent of the classical coagulation cascade.[82] Recently, chitosan has gained approval in the United State and Europe for use in bandage and other hemostatic agents.[83,84] CELOX™ (Medtrade Products Ltd., UK), one of the chitosan-based hemostatic dressing products, has been shown to arrest bleeding quickly and result in high survival of lethal arterial wounds in swine, reducing blood loss.[85] There are several chitosan-based hemostatic dressings for the control of bleeding in small wounds and have applications in maxillofacial, general, trauma, and neuro surgeries. Some commercially available chitosan based hemostatic dressings are HemCon® (HemCon Inc., Portland, OR), Chitoflex® (HemCon Inc., Portland, OR), SyvekPatch® (Marine Polymer Technologies Inc., Danvers, MA), Clo-Sur P.A.D.™ (Scion Cardio-Vascular, Miami, FL), and ChitoSeal™ (Abbott Vascular Devices, Redwood City, CA) in Figure 1-7. The mechanism of action for chitosan is believed to be tissue adhesion, attraction of circulating blood cells, and vasospasm. A representative chitosan-based hemostatic pad, HemCon® bandage, incorporates chitosan into a flexible bandage which becomes sticky when it contacts blood or other moisture, and adheres to the wound site and seals it with an antimicrobial barrier.[86] HemCon® works through ionic interaction by drawing negatively charged red blood cells and platelets to the positively charged bandage,

forming a clot and creating an anti-bacterial barrier that protects the wound from infection.[81,86 ,87]

Figure 1-7 Commercial chitosan-based hemostatic wound dressing products; Clo-Sur PLUS P.A.D. ™ (Scion Cardio-Vascular, Inc. Miami, FL) (left) and ChitoFlex® Dressing (HemCon Medical Technologies, Inc. Portland, Oregon) (right).

One challenge facing the design of hemostatic dressings is the growing incidence of infection by antibiotic-resistant bacteria strains in battlefield trauma wounds.[88,89] Although the use of broad range of antibiotics has been implicated in the selection of these resistant pathogens, surgical debridement to reduce wound bacteria bioburden may not be possible under combat conditions.[89,90] Chitosan itself and several chitosan derivatives are known for their antimicrobial activity. In view of both arrest of bleeding and reducing of contamination in the bleeding wounds, chitosan has attracted attentions as an improved hemostatic and antimicrobial wound dressing material.

The antimicrobial activity of chitosan depend on several factors, such as the nature of chitosan (degree of deacetylation, molecular weight), the pH of the medium, the temperature,

etc. The mechanism of the antimicrobial activity has not been fully elucidated yet, but several hypotheses have been postulated. The most feasible hypothesis proposed is a crosslinking between polycations of chitosan and the anions on the bacterial surface like *E. coli*, which alter the cell membrane permeability, resulting in the leakage of glucose and lactate dehydrogenase from *E. coli* cells. Tsai et al.[91] demonstrated that the antibacterial effect was potentiated in an acidic pH and a higher temperature, while presence of divalent cations in the external medium reduced this antibacterial activity. This result can be considered as chelate formation between chitosan and divalent cations that suppresses the crosslinking between chitosan and bacterial surface. Similar results were earlier reported by Valenta et al.[92] for chitosan-EDTA conjugate neutralized with sodium hydroxide. The antibacterial effect of chitosan-EDTA was explained by its high binding affinity for Mg^{2+}, which was responsible for the stabilization of the outer membranes of Gram-negative bacteria.

Although a number of chitosan-based hemostatic wound dressing products are available, the mechanism of wound healing acceleration by chitosan is still under investigation. Some researchers have concluded that chitosan accelerates blood coagulation *in vivo* by activating platelets.[93-95] Okamoto et al.[96] evaluated the effects of chitin and chitosan on blood coagulation, particularly focusing on the function of platelets. They found that both chitosan and chitin shorten the blood coagulation time (BCT), indicating that chitin also has a potency of hemostasis as well as chitosan. It has been reported that fine powders of chitosan causes the reduction of the blood coagulation time by 4.7 min in a dose dependent manner, as shown in Figure 1-8.[96] They demonstrated that chitosan enhanced the release of the platelet-derived growth factor-AB (plays a significant role in blood vessel formation, the

growth of blood vessels from already-existing blood vessel tissue) and the transforming growth factor-β-1(performs many cellular functions, including the control of cell growth, cell proliferation, cell differentiation, and apoptosis). Interestingly, chitin was less effective for blood coagulation, however, it enhanced aggregation of platelets more than chitosan, pointing out that platelets aggregation is not the only factor to affect blood coagulation.

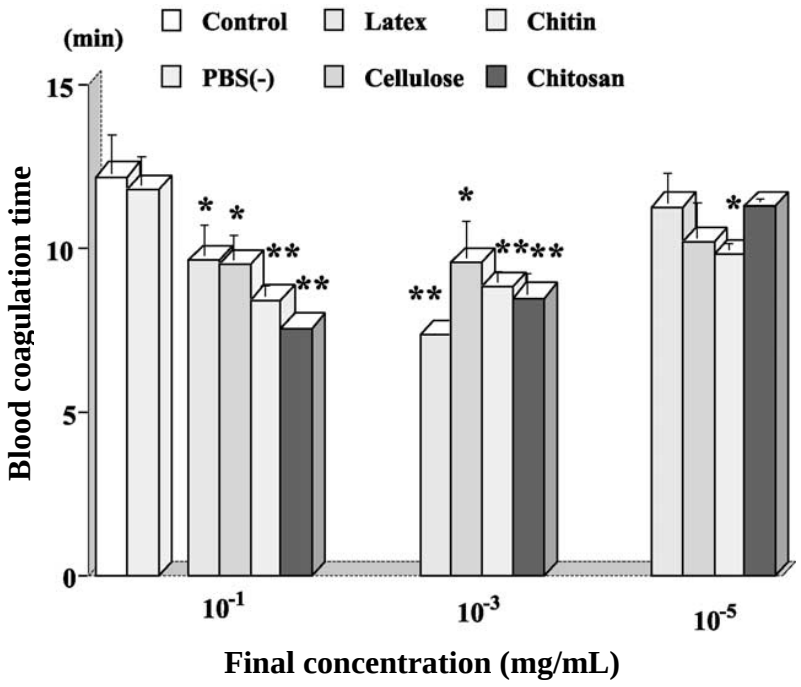

Figure 1-8 Effect of chitin and chitosan on blood coagulation time. Chitin and chitosan with particle size of 2.8 mm were mixed with whole blood: *(p < 0.05 vs. Control), **(p < 0.01vs. Control).[96]

Moreover, it has been reported that chitosan shows high-compatibility against erythrocytes morphologically and induces erythrocytes aggregation, which influences the

shortening of BCT. In addition, Dowling et al.[97] reported that the hydrophobically modified chitosan is capable of transforming rapidly the liquid blood into an elastic gel when it contacts heparinized human blood. When added to liquid blood, the hydrophobes on the hydrophobically modified chitosan derivatives are inserted into blood cell membranes and connect the cells into a three-dimensional network (gel structure).

1.2.2 Improved Hemostatic Ability of Chitosan

Both poorly deacetylated chitin and chitosan are interesting polysaccharides with ease of chemical modification because of the presence of the amino groups at the C-2 position, which can be suitably modified to impart desired properties and distinctive biological functions, including water solubility.[98-100] Apart from the amino groups, they have two hydroxyl groups for effecting appropriate chemical modifications to enhance solubility.[101] Due to these functional groups, chitin and chitosan can undergo many chemical modifications, like esterification, etherification, urethane formation, cross-linking with poly-functional reagents and graft copolymerization,[99,100] also such as quaternization, formation of Schiff bases and other NH_2-specific reactions,[98] which opens the way to their use in a wide variety of biomedical and biomaterial applications.[99]

In recent years, hydrophobically modified chitosan has attracted attention. The first investigation upon chitosan solubility properties and increases in its hydrophobic character was reported by Yalpani and Hall[102] in 1984. The progressive decrease in water solubility of the initially highly polar modified chitosan was attained by appending alkyl chains of

growing length. Furthermore, Desbrieres et al.[103] substituted amino groups of chitosan with C3 (three carbon atoms) to C12-alkyl chains by reductive amination, and demonstrated that a minimum of six carbon atoms was required to impart hydrophobic characteristics to chitosan within the experimental conditions studied.

As mentioned above, native chitosan has been used as a hemostatic material due to its cationic and antimicrobial nature, however, its hemostatic efficacy in dealing with severe wounds has been questioned.[104] Dowling et al.[97] hypothesized the mechanism of hemostatic action of hydrophobically modified chitosan involves the anchoring of hydrophobes from the polymer into the hydrophobic interiors of blood cell membranes. That is, blood cells would become connected by biopolymer chains into a sample-spanning gel network, which could potentially transform liquid blood into a gelled clot, i.e., a hemostatic plug. In particular, they attached a small number of hydrophobic alkyl tails to the backbone of chitosan, as shown in Figure 1-9.[97]

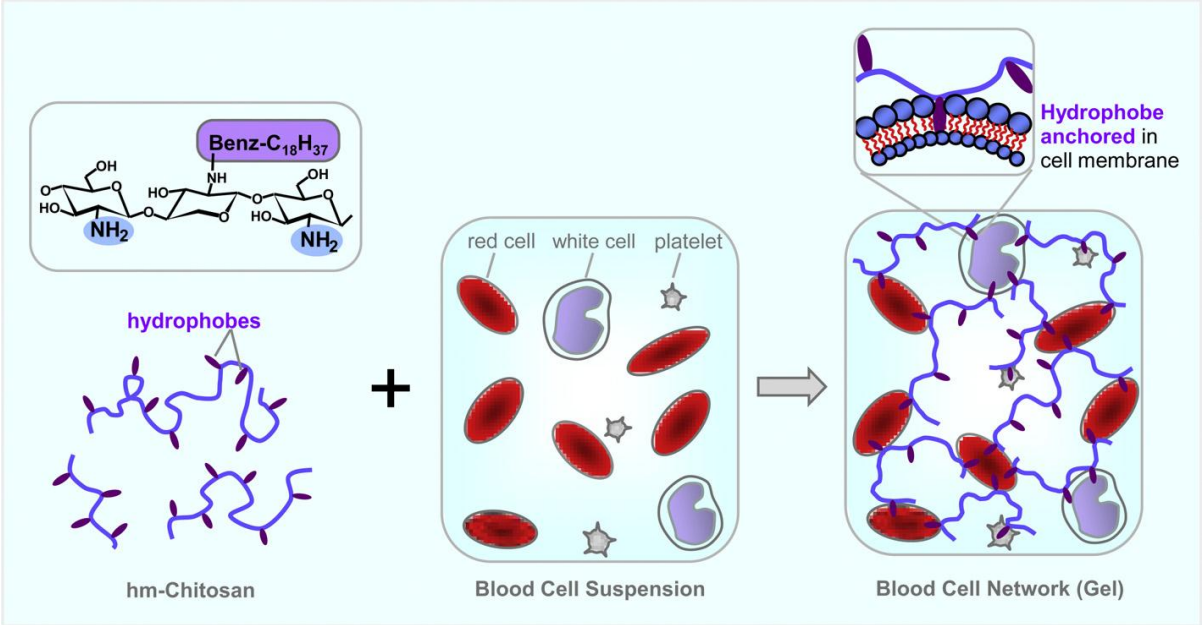

Figure 1-9 Mechanism for gelation of blood by hydrophobically modified (hm)-chitosan. On the left the polymer is shown schematically with its hydrophilic backbone in blue and the grafted benzyloctadecyl hydrophobes in purple. When added to liquid blood, the components assemble into a three-dimensional network (gel), as shown on the right. This is driven by insertion of hydrophobes into blood cell membranes (as depicted in the top inset); thereby the polymer chains connect (bridge) the cells into a self-supporting network.[97]

They successfully demonstrated that when hydrophobically modified chitosan contacted heparinized human blood, it rapidly transformed the liquid in to an elastic gel. In contrast, the native chitosan does not gel blood. Gelation occurs within a few seconds of mixing the polymer into blood and the gel remains stable indefinitely. Rheological tests revealed that the chitosan/blood sample has a constant viscosity of about 0.01 Pa s, which is about four times that of blood alone. In contrast, the mixture of 0.25 wt% solution of hydrophobically modified chitosan (viscosity of about 0.07 Pa s) and blood has a low-shear viscosity around 10,000 Pa s, which is a million-fold higher than that of blood. Also, in this case, the steep drop in viscosity around a stress of 2 Pa is indicative of a yield stress,[105] meaning that the

sample hardly flows at stresses below this value. According to this result, they assumed the structure of the blood gels as illustrated in Figure 1-9, where some of the hydrophobes from hydrophobically modified chitosan chains are shown embedded within the hydrophobic cores of cell membranes. Individual polymer chains thereby connect adjacent cells, and the net result is a sample-spanning three-dimensional network in which the cells act as the crosslink points or nodes.

1.2.3 Improved Mocoadhesion of Chitosan

Recently, thiolated polymers, or thiomers, bearing free thiol side groups on their backbone chains, have been widely studied as a prospective new generation of mucoadhesive polymers.[106-136] Many mucoadhesive approaches are based on the formation of non-covalent bonds including hydrogen bonds, van der Waals interactions, or ionic interaction, but providing only weak mucoadhesion.[123] By contrast, thiomers are capable of establishing strong mucoadhesion, by forming covalent bonds. The most common mucoadhesive structure in biological systems is the formation of disulfide covalent bonds between cysteine-rich subdomains of mucus glycoproteins of the mucus gel layer and the free thiol groups of thiomers through either thiol/disulfide exchange reactions or a simple oxidation process of free thiol groups[113,114] as shown in Figure 1-10[114].

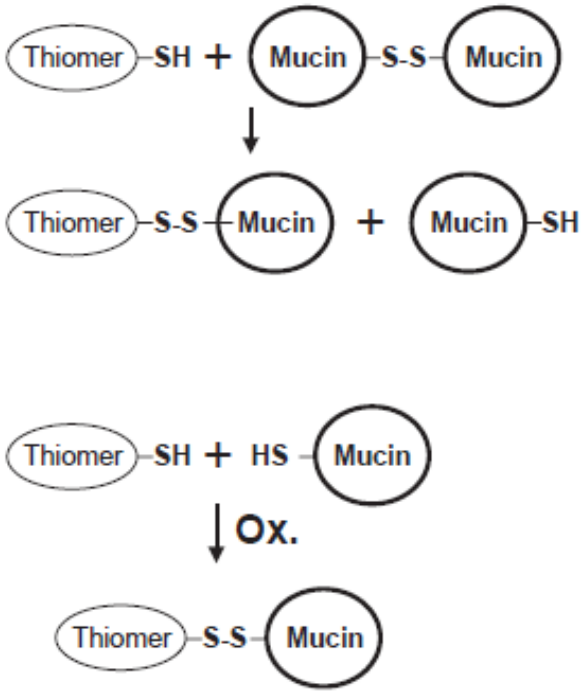

Figure 1-10 Mechanism of disulfide bond formation between thiomers and mucus glycoproteins (mucins) according to Leitner et al.[114]

As mentioned above, chitosan is a cationic polymer with positively charged primary amino groups in the acidic condition. This cationic character of chitosan provides mucoadhesive properties that can be mainly attributed to ionic interaction between the cationic amino groups of chitosan and the negative substructures of the mucus, such as sialic acid moieties.[114] Moreover, the primary amino group at the C-2 position of chitosan can react with sulfhydryl compounds to produce thiolated chitosan derivatives, which can form the covalent disulfide bond with the mucus glycoproteins, which are also covalently anchored in the mucus layer by disulfide bonds. Therefore, thiolated chitosan derivatives have been known to mimic the natural behavior of secreted mucus glycoproteins.[106-111]

In general, sulfhydryl bearing compounds are covalently attached to the primary amino group via the formation of amide or amidine bonds. Numerous thiolated chitosan derivatives have been synthesized, including chitosan–cysteine (chitosan-Cys) conjugate,[124] chitosan–4-thio-butyl-amidine (chitosan-TBA) conjugate,[109] chitosan–thioglycolic acid (chitosan-TGA) conjugate,[107,108,110,125] chitosan–*N*-acetylcysteine (chitosan-NAC) conjugate,[126] chitosan–2-thio-ethyl-amidine (chitosan-TEA) conjugate,[127] chitosan–glutathione (chitosan-GSH) conjugate,[128] the aryl thiolated chitosans chitosan–6-mercaptonicotinic acid (chitosan-MNA),[120] and chitosan–4-mercaptobenzoic acid (chitosan-MBA).[130] All of these structures are summarized in Figure 1-11[131].

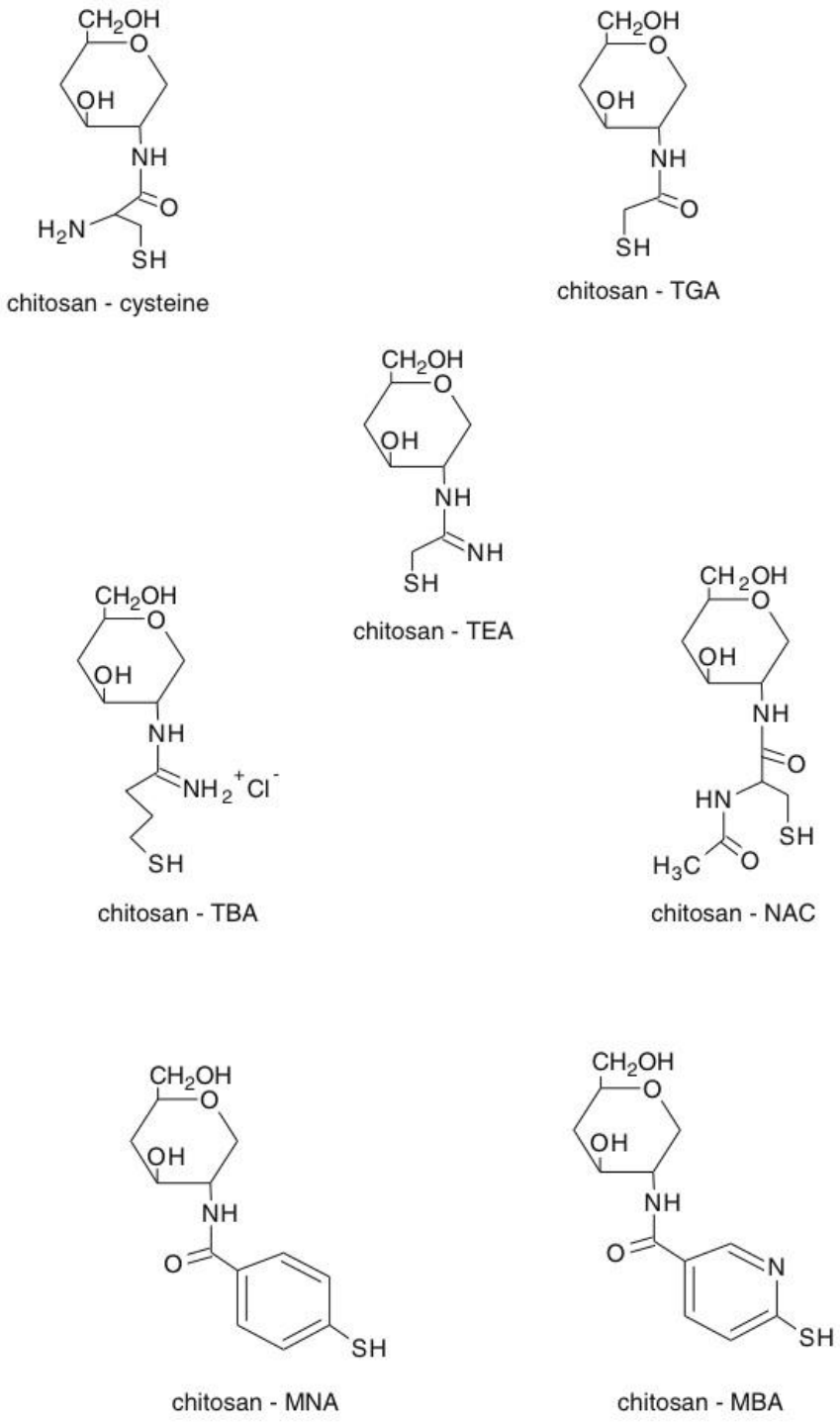

Figure 1-11 Structures of established thiolated chitosans.[131]

These chitosan derivatives have demonstrated greater formation of disulfide crosslinking and resultant *in situ* gelling of the thiolated chitosan, as well as a significantly improved mucoadhesiveness. Bernkop-Schnurch et al.[109] obtained the result that the viscosity of chitosan-4-thio-butyl-amidine (chitosan-TBA) conjugate increased more than 100-fold in comparison to unmodified chitosan, as well as a significant improvement of the mucoadhesive properties in comparison to unmodified chitosan and chitosan-thioglycolic acid (chitosan-TGA) conjugates, which were tested under the same conditions as shown in Table 1-2.[109]

Table 1-2 Comparison of the mucoadhesive properties of chitosan–TBA conjugates, chitosan–TGA conjugates, and unmodified chitosan[109]

Polymer	Time (h)	Improvement ratio
Unmodified chitosan	1.2 ± 0.8	1
Chitosan-TGA conjugate 10a	1.05 ± 0.05	0.88
Chitosan-TGA conjugate 30a	4.0 ± 0.1	5
Chitosan-TBA conjugate 60	148 ± 25	123
Chitosan-TBA conjugate 100	>168	>140

Test discs of each polymer were attached to excised porcine mucosa, which has been spanned on a cylinder and agitated with 125 rpm in a 100 mM phosphate buffer pH 6.0 at 37± 0.5˚C. The indicated time of adhesion represents the mean (±S.D.) of at least three experiments. The improvement ratio is calculated by adhesion time of conjugates versus adhesion time of control. *a According to Kast and Bernkop-Schnurch (2001); chitosan-TGA 10 and 30 display 9.9 and 27.4 μM thiol groups per g polymer, respectively.

Furthermore, for the future applications of the thiomers including non-chitosan based thiomers, the use in oral-,[120,132-135] nasal-,[121] and ocular[136] delivery systems have been investigated. Guggi et al.[133,135] proposed a potential oral mucoadhesive drug delivery system that comprise chitosan-TBA conjugate and salmon calcitonin as a model drug which act to reduce blood calcium. The tablets comprised of chitosan-TBA conjugate and unmodified chitosan were, respectively, orally given to rats and the plasma calcium level was monitored with time. The data showed that only chitosan-TBA based tablets caused a decrease of plasma calcium level of more than 5% for several hours. Further studies would lead to the expansion of proposed biomedical applications of thiolated chitosan derivatives. At present, the thiolation has been successfully accomplished for several polymers, not only chitosan,[106-111] but also alginate,[112] poly(acrylic acid),[115-118] polycarbophil,[119-121] and pectin.[122]

1.3 Concept of Artificial Blood Clot Model

Crosslinking or modification reactions using disulfide exchange processes form disulfide linkages with sulfhydryl-containing molecules. These bonds are reversible using disulfide reducing agents. Compounds containing a disulfide group are able to participate in disulfide exchange reactions with another sulfhydryl compounds. The disulfide exchange process involves attack of the thiol at the disulfide, breaking S-S bond, with subsequent formation of a new mixed disulfide constituting a portion of the original disulfide compound. The reduction of disulfide groups to sulfhydryls in proteins using thiol-containing reductants proceeds through the intermediate formation of a mixed disulfide. If the thiol is present in

excess, the mixed disulfide can go on to form a symmetrical disulfide consisting entirely of the thiol reducing agent, thus completely reducing the original disulfide to free sulfhydryls. Disulfide exchange reactions occur over a broad range of conditions from acid to basic pH and in a wide variety of buffer constituents. Most crosslinking reactions involving disulfide exchange are done under physiological conditions or those most appropriate to maintain stability of the protein or other molecule being modified.

Cysteine is a sulfur-containing (sulfhydryl or thiol) amino acid (Figure 1-12), which is present in many proteins throughout the body including blood plasma. For example, in serum albumin which is the most abundant plasma protein in mammals, there are 17 cystine residues and 6 glutamylcystine (Glu-Cys) dipeptides. Previously, Triantaphyllopoulos et al. quantified the amino acid composition of human fibrinogen.[137] As shown in Table 1-3, there is remarkable amount of cysteine content in human fibrinogen.

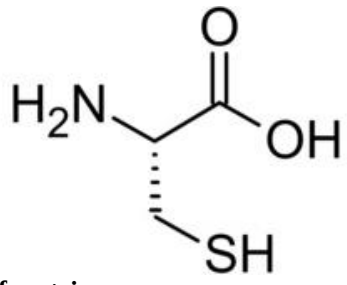

Figure 1-12 The chemical structure of cysteine.

Table 1-3 Amino acid composition of human fibrinogen and three intermediate anticoagulant derivatives isolated from fibrinogen solutions by ammonium sulfate fractionation and column electrophoresis[137]

Residues/ 10^5 g of protein moiety exactly

Amino acid	Fibrinogen	LP_{100}	LP_{200}	SP_{200}
Lys	60.9	61.1	63.6	55.7
His	18.3	17.5	16.6	16.4
NH_3*	97.3	99.2	103.9	129.3
Arg	45.2	43.3	46.8	36.0
Trp	24.1	25.1	27.7	17.4
Asp	107.2	109.3	109.0	137.7
Thr	59.4	59.5	48.2	41.2
Ser	77.6	78.4	64.6	61.5
Glu	105.0	103.7	111.0	118.4
Pro	46.4	41.9	35.7	33.3
Gly	87.1	90.5	82.2	47.8
Ala	43.9	41.9	37.6	40.3
Cys	6.0	4.9	4.4	22.6
Val	41.6	41.3	44.6	48.2
Met	19.9	20.5	21.9	9.3
Ile	32.4	35.5	44.1	29.3
Leu	54.7	53.9	56.2	77.3
Tyr	31.3	32.6	37.1	30.3
Phe	28.9	28.1	22.9	30.0
Total	889.9	889.0	874.2	852.7

*** Ammonia values were not included in the totals.**

LP_{100}: a derivative isolated as the large electrophoretic peak at the end of the clottable period (100% CP) of the parent fibrinogen solution; LP_{200} and SP_{200}: derivatives obtained as the large peak and small peak, respectively, at twice this period (200% CP)

Cysteine is a potent nucleophile, which is often linked to another cysteine to form a dimer cystine through the covalent disulfide bond. This leads to the idea that incorporation of thiol reactive groups into chitosan, which react with cysteine or cysteine found in blood plasma proteins, would induce crosslinking between the chitosan derivative hemostat and blood cells and elicit chemical gelation of the blood plasma. In order to accelerate gel formation, there is

a need to identify and induce crosslinking reactions to interact with as many blood proteins as possible. There are several candidates for the derivatization of chitosan to yield a material capable of gelling blood plasma proteins; thiolated chitosan, chitosan/iodoacetate, and Sanger's reagent.

First, as mentioned before, thiol bearing chitosan has been reported to have enhanced mucoadhesion through the formation of covalent disulfide bonds with cysteine-rich subdomains of mucus glycoproteins building up the mucus gel layer. This would apply for formation of crosslinking with cysteine (or cystine) in blood plasma proteins. Thiomers have pH-dependent reactivity. Thus, the thiol-modified chitosan system would require a desired pH range to induce *in situ* gelling. The reactive form of thiomers is the thiolate anion. The pKa of alkyl thiols is in the range of 8 to 10.[138] This means that thiomers will be most reactive in a pH range slightly above the physiological intestinal pH, for example, the stomach pH is very low, the small intestine pH is around 5, or vaginal pH is in the range of 3.5-5. Ideally, a system should be a non-pH-dependent. Millotti et al.[139] reported on the pH-independent *in situ* gelling properties of thiolated chitosan by 6-Mercaptonicotinic acid.

Secondary, iodoacetic acid has been known as an irreversible inhibitor of all cysteine peptidases by interacting with the free thiol group of cysteine. This research mainly focuses on the gelation of blood protein via this approach, thereby, the detail reaction mechanism between cysteine and iodoacetate will be discussed in following section.

Finally, another approach is the incorporation of moiety as an analog to thiol groups, such as Sanger's reagent, also referred as to 1-fluoro-2,4-dinitrobenzene (FDNB). In 1950, Shaltiel et al.[140] demonstrated that proteins react with Sanger's reagent selectively at cysteine

residue sites within the protein structure. They reported that treatment of a dehydrogenase enzyme with Sanger's reagent at pH 8 at 22˚C for 30 minutes resulted in the complete loss of enzymatic activity. This gives the possibility that Sanger's reagent introduced to the backbone of chitosan would also be a good bridge between cysteine. Nevertheless, Sanger's reagent would possibly be toxic due to the bearing fluorine. The structures of all of these are shown in Figure 1-13.

.

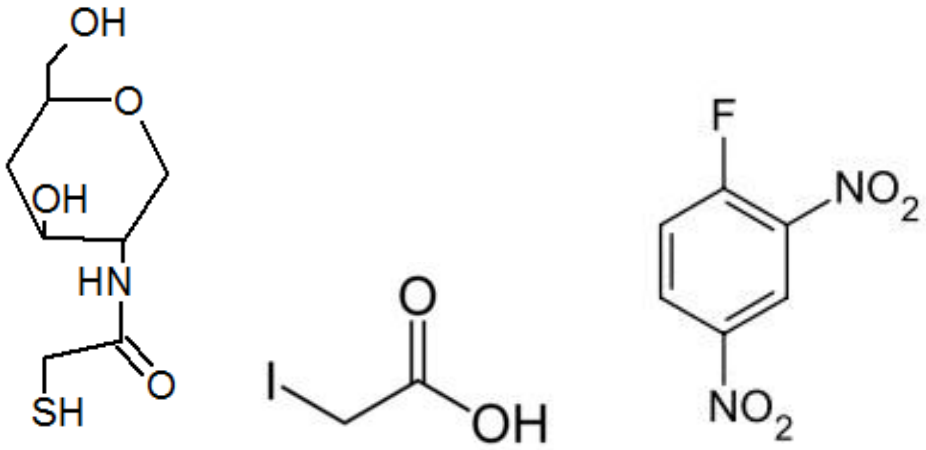

Figure 1-13 Chemical structures of chitosan-TGA, iodoacetic acid, and Sanger's reagent (1-Fluoro-2,4-dinitrobenzene) from left to right.

1.4 Purpose of Research

Although a variety of advanced hemostats have been brought to market, several products work simply by absorbing the blood at the site of the wound rather than by actively

coagulating the blood.[141,142] The fibrin sealants (ref. Sect. 1.1.2) are useful hemostatic materials that simulate the final stage of the clotting cascade, nevertheless, the efficacy of fibrin sealants have been still under investigation.[141,143] Recently, a new approach has been put forward by Ellis-Behnke et al.,[144] where the self-assembly of a synthetic peptide into a nano-fibrous network[145] is used to achieve hemostasis independent of the natural coagulation cascade. While this method is promising, the synthetic peptides employed are expensive and difficult to synthesize, therefore their practical viability is unclear. Furthermore, most of current hemostatic agents employ the patches that are firmly compressed on open wound sites until arrest of bleedings are completed. These patches, however, cannot be applied on non-compressible wound sites, such as the brain, peritoneal cavity, etc. Therefore, a new hemostatic system that is intended for the use in the form of injected liquids would be useful for these non-compressible sites.

The objective of this research is to propose a new hemostatic system based on chitosan derivative that relies on *in situ* formation of artificial blood clots via simultaneous gelation of blood plasma proteins and agglutination of the various suspended cells found in blood without the risk of undesired gelation or clotting in parts of the body that are not involved in the site of injury. In particular, we prepared a chitosan derivative hemostat matrix that could crosslink covalently with the cysteine-rich domains existing in the serum proteins, such as albumin, to cause the transformation of liquid blood into gel and act synergistically to enhance clot formation. The formation of the artificial blood clot relies upon the derivatization of chitosan to yield a material capable of gelling blood plasma proteins. In this research, first, thiolated chitosan composed of chitosan and thioglycolic acid (TGA) was

considered on its blood coagulation ability through the formation of disulfide crosslinking with cysteine since its high mucoadhesiveness between cysteine-rich domains of glycoproteins was expected to be an useful approach for this new type of hemostatic agent. This brought us to investigate the potential of chitosan modified by iodoacetic acid. This is a novel chemical structure which has not been synthesized before. It is expected that chitosan easily undergoes the amidation by iodoacetic acid to produce chitosan iodoacetamide (CIA) derivative. This study emphasizes the first synthesis of CIA and the investigation of its ability to interact with cysteine in the blood protein.

Gelling by chitosan derivatives is caused by the formation of chemical three-dimensional crosslinking networks. In order to accelerate gel formation, there is a need to understand the gelling behavior and identify and induce crosslinking reactions to turn as many blood proteins to a gel as possible. Rheological study is necessary to understand the crosslinking behavior of blood cells, plasma protein and the hemostat matrix, and resultant hemostatic ability. The effect of the concentration, molecular weight (chain entanglement), or DD% (charge density) of chitosan and its derivatives on the rheological properties have been investigated through steady shear experiments or dynamic oscillatory experiments. These results are discussed in the following chapters.

CHAPTER 2

2 Preparation of Chitosan Derivatives as Improved Hemostat

Chitosan has been of interest as a promising biodegradable,[146-149] biocompatible,[147,149,150] and low toxic[151] biomaterial with antimicrobial activity for a wide range of medical applications in the form of films,[147,148,152-155] fibers,[156-159] sponges,[149,160] porous scaffolds,[161,162] gels,[163-165] tubes,[166] microspheres,[167] microcapsules,[168] and nanoparticles.[169-172] Chitosan is much easier to undergo chemical modifications than chitin.[173] The availability of numerous amino and hydroxyl groups allows chitosan to be conjugated with antiviral,[174] antimicrobial,[175] antitumor,[176,177] and anticoagulant agents,[178] as well as peptides.[179] Various reactions have been proposed to introduce different functional groups on chitosan. Generally, chitosan derivatives can be obtained through specific reactions involving the amino group at the C-2 position or nonspecific reactions involving hydroxyl groups at the C-3 and C-6 positions, especially esterification and etherification.[180-183]

The most important fields for chitosan and its derivatives have been cosmetic, pharmaceutical, and biomedical applications, including surgical sutures, dental implants, artificial skin, rebuilding of bone, corneal contact lenses, wound dressings, bone tissue engineering, and drugs delivery systems. Chitosan materials are also known to activate biological defense mechanisms. Nishimura et al.[184] reported that chitosan with degree of deacetylation (DD%) of 70% showed macrophage activation, cytokine production, and anti-infectious activity. The cytotoxicity of chitosan is reported to be dose dependent and decreases with a decrease in molecular weight and degree of deacetylation,[185] while chitosan

of 700 kDa or larger has been used safely in actual clinical applications.[149,186] Additionally, chitosan and its derivatives have been investigated as tissue engineering scaffold for bone,[148] liver,[154] nerve,[166] cartilage,[148,153,155,157,162] and skin[161,165,187] since chitosan has partially similar structure to glycosaminoglycans, which are essential structural elements of the extracellular matrix of most tissues. Therefore, chitosan has been reported to accelerate early phase healing of open skin wounds by increasing the rate of infiltration of polymorphonuclear cells and the production of collagen by fibroblasts.[188]

These properties make chitosan a useful candidate as the basement material for hemostatic wound dressings. As mentioned earlier, thiolated chitosans have been proved to enhance the mucoadhesion due to their disulfide bonds formation with cysteine-rich mucus layer. In this chapter, a chitosan derivative that bears a moiety that reacts with cysteine was prepared and characterized in terms of its ability to induce the interaction with cysteine existing in the blood protein.

2.1 Deacetylated Chitosan

Finely ground chitosan with a degree of deacetylation of around 96%, which was previously obtained in this lab through the alkalin deacetylation of commercial chitin [Sigma chitin Lot 21 HO189], was used as a starting material for this work. First, the chitin was soaked for two days in 14% NaOH at 5˚C to decolorize. The decolorized chitin was washed with distilled water and filtered through polypropylene screen until the filtrate was neutral to pH paper. Then, the chitin was placed in additional distilled water and heated at 80˚C for 30

minutes, filtered and washed with distilled water. The moist chitin was dried at 115˚C for 20 hours, and cooled in a vacuum desiccator. The dry decolorized chitin was mixed with 50% NaOH for 30 minutes and heated to 120-130˚C for 2 hours under N_2 purge. After the reaction was completed, the mixture was washed with distilled water repeatedly until the filtrate is neutral. Finally, the chitosan was dried overnight in an oven at 115˚C, then cooled under vacuum.

2.2 Obtaining of Chitosan Derivatives

For the purpose of this work, any moieties that react with thiol groups found in cysteine need to be introduced on the chitosan. The modification of chitosan proceeds through the amino groups at its C-2 position. First of all, chitosan-thioglycolic acid (TGA) derivative with % sulfur content of 4.54 wt% was obtained from Luna Innovations, Inc. (Charlottesville, VA). Several tests were done on this chitosan-TGA/blood mixture, but data were not shown in this research. Introducing iodoacetic acid into chitosan is performed by a previously described method,[107,108] which is described in detail in the following section. This is the first reported synthesis of this derivative.

2.2.1 Synthesis of CIA Derivative

Chitosan (2 g) is dissolved in 1.0 wt % acetic acid (200 mL) to prepare chitosan/acetic acid solution of 1 % (w/v). In order to facilitate the reaction, 1-ethyl-3-(3-dimethylaminopropyl) carbodiimide hydrochloride (EDAC HCl) (Sigma-Aldrich, 400 mg) as

a coupling agent is added to the chitosan solution. After EDAC is dissolved, iodoacetic acid (Sigma-Aldrich ≥99.0%, 2.4 g) is added and the pH is adjusted to 5.0 with 3N NaOH. The reaction mixture is stirred for 3 h at room temperature. After the reaction is completed, an excess amount of isopropanol is added to the mixture to precipitate the derivative. Then, the precipitate is filtered and dried in the vacuum desiccator at room temperature. The reaction scheme is shown in Figure 2-1. All chemicals were purchased from Sigma Aldrich.

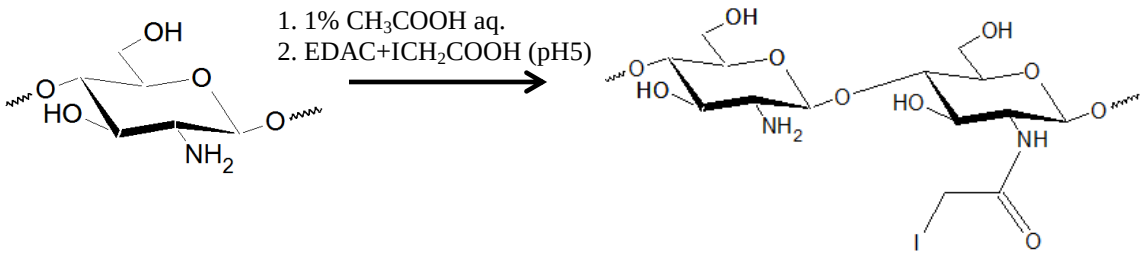

Figure 2-1 Synthetic scheme of chitosan-iodoacetamide (CIA) by a reaction coupled with 1-ethyl-3-(3-dimethylaminopropyl) carbodiimide hydrochloride (EDAC HCl).

2.3 Characterization

To measure the degree of deacetylation of the chitosan, conductometric titration, ^{1}H-NMR, and FTIR were used. The molecular weight (MW) of chitosan was obtained by means of viscometric method using intrinsic viscosity and Mark-Houwink equation. The degree of substitution of amino groups of each chitosan derivatives at the C-2 position was elucidated by a series of characterization techniques of elemental analysis, FTIR, ^{1}H-NMR, and conductometric titration, comparing to the control unmodified chitosan sample.

2.3.1 Conductometric Titration

A known mass of dried chitosan sample (0.0935 g) and the prepared CIA derivative (0.0870 g) were respectively dissolved into 10 mL of 0.1 N hydrochloric acid (HCl) then 90 mL of distilled water, and several drops of phenolphthalein as an indicator was added. Each solution was then titrated with a standard 0.1 N sodium hydroxide (NaOH) solution using a 10-mL buret while the solution conductivity was monitored as a function of the volume of NaOH added with an Orion Benchtop Conductivity Meter (Model 162) equipped with an Orion Conductivity Cell (Model 013030). During the titration, the temperature of the solution was kept constant (25 ˚C) by using a water bath since the conductivity is a function of temperature.

In a typical conductometric titration curve, there are two deflection points. The first deflection point corresponds to the neutralization of excess H^+ ions of the strong acid, HCl. After all excess H^+ ions are neutralized, then the neutralization of the weak acid, the ammonium salt in chitosan starts. After all of the ammonium is neutralized, the conductivity again goes up with a higher value of slope due to the excess OH^- ions of NaOH added, which is the second deflection point and the phenolphthalein turns pink. Thus, the range between the first and the second deflection points corresponds to the neutralization of the protonated amine groups of chitosan. Therefore, the number of moles of NaOH used between the first and the second deflection points equals the number of moles of amine groups of the chitosan sample. The percent degree of deacetylation was calculated by the following equation:

$$\%DD = \frac{(v2-v1)(L)\, M_{NaOH}\left(\frac{mol}{L}\right) Unit\ mass\ of\ chitosan\left(=\frac{161.16g}{mol}\right)}{Mass\ of\ chitosan\ sample\ (g)} \times 100$$

where (v_2-v_1) is the difference in volume in mL between the two deflection points, M_{NaOH} is the molarity (mol/L) of standard NaOH solution.

2.3.2 FTIR Spectroscopy

FT-IR is one of the useful techniques in polymer characterization. All IR spectra in this work were obtained by using a Nicolet 510P FT-IR spectrophotometer. The data collection parameters employed were as follows unless specified otherwise: Gain 1, Resolution: 4.0 cm^{-1}, and Scans: 32. Sample solutions, including unmodified chitosan and its derivative, were cast to make films for analysis in the following way. A total amount of 20.0 g of 2% (w/w) solution of CIA derivative and unmodified chitosan in 0.3 M acetic acid were prepared, respectively. These solutions were cast into 85 mm diameter petri dishes. They were allowed to evaporate at room temperature over two days. All of the films were easy to peel and remove from the dishes.

Chitin and chitosan can be differentiated by IR peak analysis. There are two characteristic bands for amides: amide I corresponds to C=O stretching vibration at 1695-1630 cm^{-1} and amide II corresponds to in-plane N-H bending vibration at 1650-1590 cm^{-1} for primary NH and at 1560-1500 cm^{-1} for secondary NH, respectively. Besides, the N-H stretches of amines appear in the region of 3300-3000 cm^{-1}. In primary amines (RNH_2), there are two bands in this region corresponding to the exiting two N-H stretches, the asymmetrical

N-H stretch and the symmetrical N-H stretch. Secondary amines (R_2NH) show only a single weak band in the 3300-3000 cm^{-1} region, since they have only one N-H bond. Another band attributed to amines is observed in the region of 910-665 cm^{-1}. This strong, broad band is due to N-H wag and is observed only for primary and secondary amines. In addition, the C–N stretching vibration of aliphatic amines is observed in the region 1250-1020 cm^{-1}.

Chitin shows amide I band (C=O stretch) and amide II band (secondary NH bending) at 1695-1630 cm^{-1} and 1560-1500 cm^{-1}, respectively. Whereas, in highly deacetylated chitosan, amide I band disappears and primary NH bending band appears at 1650-1590 cm^{-1} by the conversion of acetyl groups into amino groups. Therefore, this is often used to evaluate the degree of deacetylation of chitosan sample.

2.3.3 Nuclear Magnetic Resonance (NMR) Spectroscopy

^1H NMR is one of the simplest and most precise methods to determine the DD % of chitosan. Chitosan with a high MW does not give a good NMR spectrum due to its high viscosity. The MW of chitosan used in this study lies in the medium range of the molecular weight and ^1H NMR was used to determine %DD. ^1H NMR measurement was performed on a Varian Mercury 300 NMR spectrometer operating at 300 MHz for the ^1H nucleus at room temperature for all samples. Chemical shifts for ^1H NMR spectra were reported in δ (ppm), where increasing values indicates downfield shifts from an internal reference, tetramethylsilane (TMS) or 3-(trimethylsilyl)propionic 2,2,3,3,-d4 acid sodium salt (TSP)

was used. The solvent signals were as follows: D_2O (Aldrich, 99.9 atom % D) 4.65 ppm and CD_3COOD (Aldrich, 99.5 atom % D) 2.03 ppm, 11.53 ppm.

A known amount of chitosan (5 mg) and CIA derivative (7 mg) were, respectively, dissolved in 0.765mL of 2% (v/v) CD_3COOD/D_2O solution and introduced into a 5 mm NMR tube. The degree of deacetylation was calculated based on the integral ratio of peaks by the following equation:[189]

$$\%DD = 100\% - \frac{I_{CH3}/3}{I_{H2-H6}/6} \times 100\%$$

where I_{CH3} is the integral intensity of *N*-acetyl protons and $I_{H2\text{-}H6}$ is the sum of integral intensities of H2,3,4,5,6, and 6' protons (see Figure 2-3).

2.3.4 Molecular Weight (MW)

Although viscometry is not an absolute method for determining the MW of chitosan, it is one of the simplest and most rapid methods. The viscosity average molecular weight (M_v) of chitosan can be determined by the following Mark-Houwink equation, where [η] is intrinsic viscosity determined from a Huggins plot, and k and α are empirical coefficients that are dependent on the solvent systems, temperature employed, and the DD of chitosan.

$[\eta] = k M_v^{\alpha}$ (Mark-Houwink equation)

$\frac{\eta_{sp}}{c} = [\eta] + k_H[\eta]^2 c$ (Huggins equation)

$$[\eta] = \lim_{c \to 0} \eta_{sp}/c$$

where [η] is an intrinsic viscosity (mL/g), M_v is the viscosity-average molecular weight, k (mL/g) and α are empirical Mark-Houwink parameters, c is the concentration of solution (g/mL), η_{sp} is a specific viscosity, k_H is the Huggins coefficient, respectively.

Specific viscosity (η_{sp}) is calculated by using the following equation;

$$\eta_{sp} = \frac{t - t_s}{t_s}$$

where t is a sample flow time and t_s is a solvent flow time.

A number of different values of k and α depending on different solvent systems can be found in a recent literature review.[190] Wang et al.[191] presented the dependence of k and α on the DD of chitosan when chitosan is dissolved in 0.2 M CH_3COOH/0.1M CH_3COONa aqueous solution at 30˚C:

$$k = 1.64 \times 10^{-30} \times (\%DD)^{14}$$

$$\alpha = -1.02 \times 10^{-2} \times (\%DD) + 1.82$$

A known amount of dried chitosan was dissolved in 0.2M CH_3COOH/0.1M CH_3COONa aqueous solution and a series of dilute solutions were prepared. A Cannon®-

Ubbelohde Viscometer (size 1, No. J437, Viscometer Constant = 0.01 mm^2/s^2) is loaded with 10 mL of each solution. The η_{sp} was calculated by taking the average of five measurements for each concentration solution and η_{sp}/c is plotted against the concentration.

2.4 Results and Discussion

2.4.1 Determination of DD% of Chitosan (conductometric titration, FTIR, NMR)

The IR absorption peaks of the Amide I band (C=O stretching of secondary amide) and the Amide II (NH bending of primary and secondary amides coupled with C-N stretching vibration) can be used for the qualitative evaluation of the deacetylation of chitosan. Figure 2-2 shows the spectrum of the highly deacetylated chitosan.

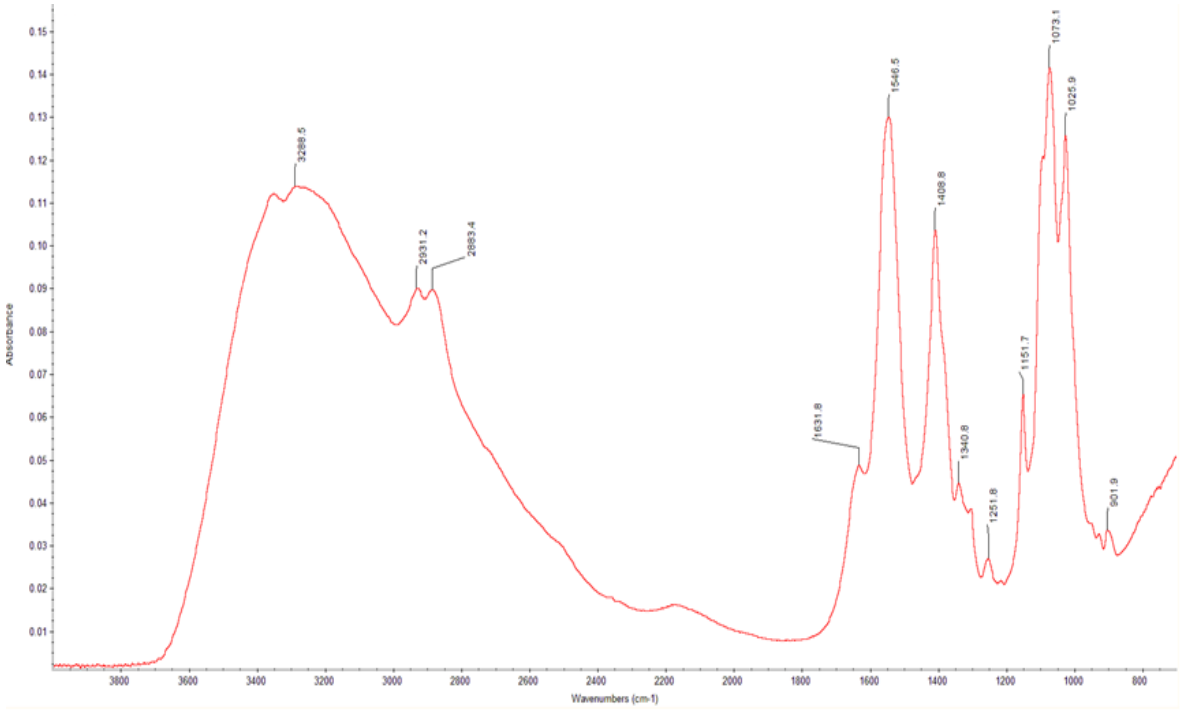

Figure 2-2 FTIR spectrum of the chitosan sample used in this study.

In the IR spectrum of the deacetylated chitosan, there were evidences of high degree of deacetylation of pure chitosan due to the presence of characteristic absorption peaks for the primary amine. First, two N-H stretch bands were observed at 3350 cm^{-1} and 3288 cm^{-1}. The peaks at 2931 cm^{-1} and 2883 cm^{-1} are assigned as C-H stretching vibration of CH, CH_2, CH_3. Also, a strong peak of the NH_2 scissoring vibration was observed at 1546 cm^{-1}. Moreover, a very weak absorption peak of C=O stretching vibration for the secondary amide (Amide I) was observed at 1631 cm^{-1}, which is attributed to the *N*-acetyl groups and indicates that most acetyl groups at the C-2 position were almost completely changed to primary

amino groups by alkali deacetylation. The strong peak at 1408 cm^{-1} comes from CH_2 bending vibration and the weak peak at 1340 cm^{-1} indicates the CH_3 bending of remaining acetyl groups. Moreover, several peaks were observed at 1251, 1151, 1073, and 1025 cm^{-1}. The absorptions at 1251 cm^{-1} should be assigned as a C-N stretching coupled with N-H in-plane bending (Amide III). The absorption at 1073 cm^{-1} corresponds to the symmetric stretch of C-O-C. This peak had a shoulder at 1151 cm^{-1} which also indicated the presence of C-O-C asymmetric stretch of ether bonds. The absorption at 1025 cm^{-1} was assigned to the C-OH stretch of C-6 of chitosan (primary OH) in the sugar ring.

Subsequently, the evidence of the high deacetylation of chitosan can also be obtained by means of ^1H NMR. Figure 2-3 shows the ^1H-NMR spectrum of chitosan. The degree of deacetylation was calculated as follows:

$$\%DD = 100\% - \frac{I_{CH3}/3}{I_{H2-H6}/6} \times 100\%$$

$$= 100\% - \frac{1.85/3}{(42.91+26.54+27.47)/6} \times 100\%$$

$$= 96.18\%$$

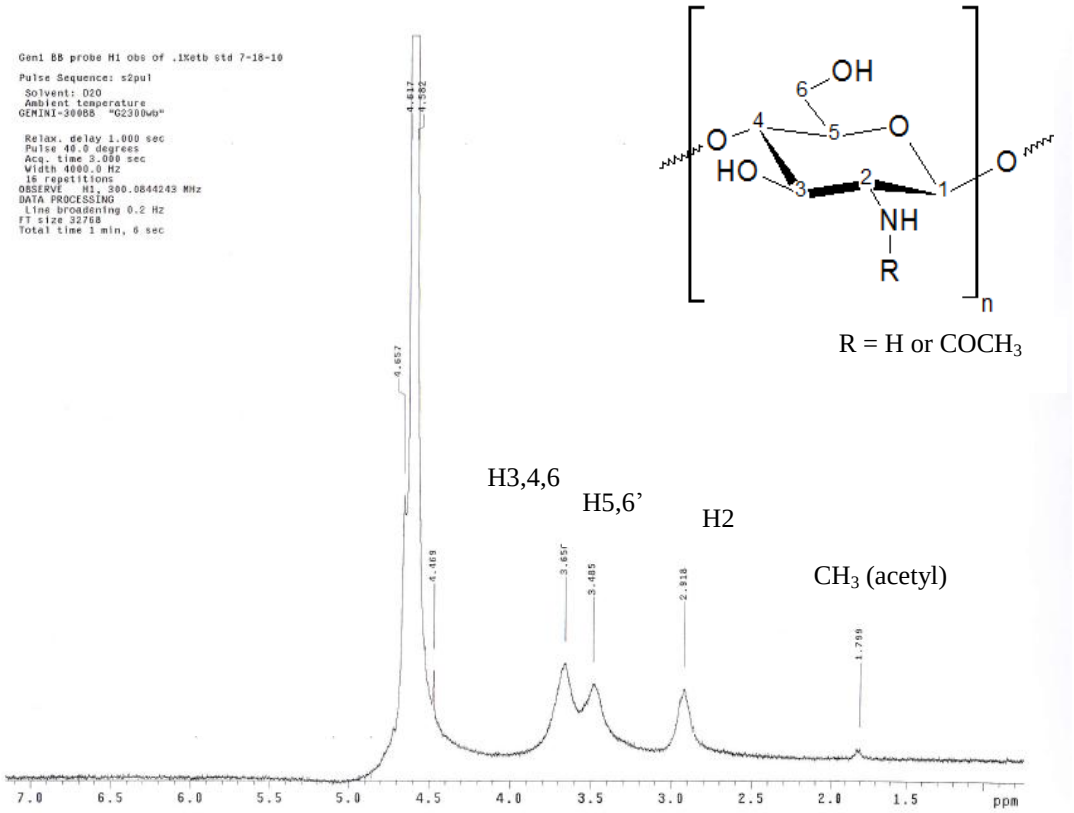

Figure 2-3 NMR spectrum of the chitosan sample used in this study.

In the spectrum it is notable that the *N*-acetyl peak at 1.799 ppm is very small, which indicates that the chitosan is highly deacetylated (100% deacetylated chitosan will not show this peak). The H1 and H2 appeared at 4.469 and 2.918 ppm, respectively. The remaining protons, H3, 4, 5, and 6 appeared as a clustered signal between 4.0 and 3.5 ppm.[192] Finally, we calculated the values of %DD of 96% for the chitosan sample used in this study. This high value of %DD is reasonable since this chitosan sample underwent the alkaline deacetylation twice.

The determination of %DD of chitosan was also attempted by the titration of chitosan/HCl solution conductometrically with NaOH solution. The titration curve is provided in Figure 2-4. Before the inflection point, the curve has a negative slope, which corresponds to the decrease in conductivity due to the neutralization of excess H^+ of HCl by OH^- of NaOH. The slightly positive slope after the inflection point results from the neutralization of protonated amino groups on chitosan. The amount of NaOH used (9.35 mL – 3.90 mL = 5.45 mL) at the inflection point equals to the amount of NH_3^+ ions present on chitosan. Since the mole of 0.1N NaOH between the first and second inflection points is equivalent to the mole of NH_3^+ ions existed, the DD of chitosan can be calculated as 93.44 % in the following way:

$$\%DD = \frac{(v2-v1)(L)\, M_{NaOH}\left(\frac{mol}{L}\right) Unit\ mass\ of\ chitosan\left(=\frac{161.16\ g}{mol}\right)}{Mass\ of\ chitosan\ sample\ (g)} \times 100$$

$$= \frac{\frac{(9.35-3.90)}{1000}(L) \times 0.1\left(\frac{mol}{L}\right) \times 161.16\left(\frac{g}{mol}\right)}{0.0935(g)} \times 100$$

$$= 93.94\ \%$$

In terms of the difference in %DD from NMR and conductometric titration, NMR data would be taken precedence due to their greater accuracy. The conductometric titration is susceptible since the conductivity is a function of temperature, also the data is dependent on the plot although it is technically useful to know the amount of amino groups charged.

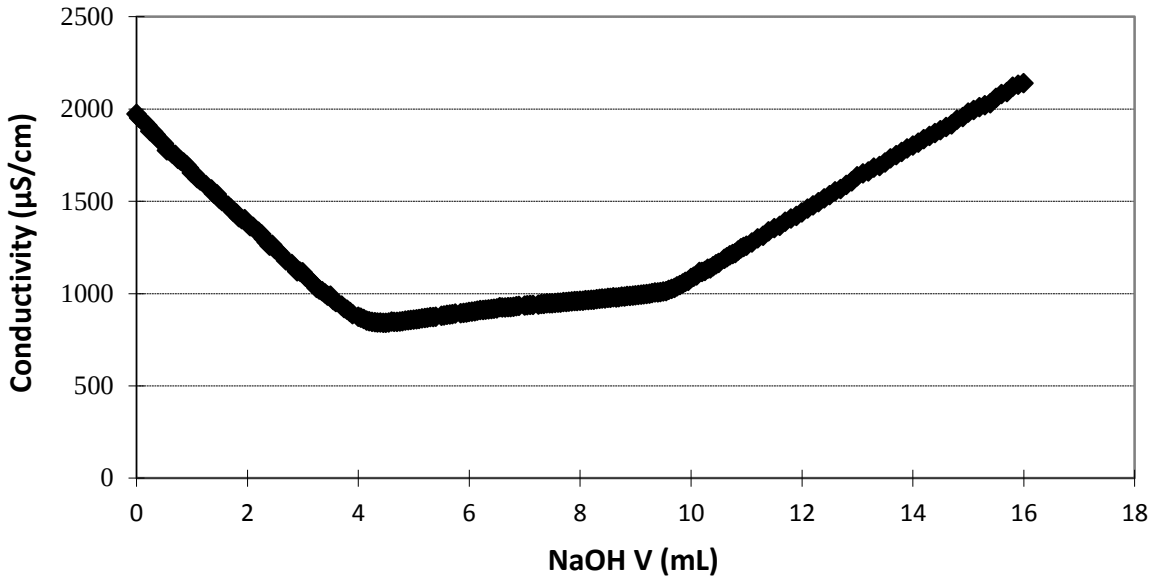

Figure 2-4 Conductometric titration curve of the chitosan sample.

2.4.2 Degree of Substitution (elemental analysis, FTIR, conductometric titration, NMR)

The prepared samples of CIA derivative were preliminary subjected to an elemental analysis to determine the iodine content at Atlantic Microlab, Inc. (Norcross, GA). The results from the elementary analysis confirmed that iodine present in CIA derivatives varied from 4.41 wt% up to 10.38 wt%, indicating that the iodine content in the sample of 100 g is 4.41 g-10.38 g. In this study, most of the experiments were done on the sample which contains 4.41 wt% of iodine.

The degree of iodine substitution of amino groups of chitosan at the C-2 position is calculated in the following way:

4.41/126.91 (MW of iodine) = 0.03475 mole of I

(100 – 4.41)/162.84 (MW of chitosan) = 0.5870 mole of average chitosan structural unit

Here the molecular weight of chitosan sample is calculated, assuming %DD of 96%. Then,

The mole ratio of iodine to chitosan = 0.03475/0.5870 = 0.05920 ≈ 0.06 ≈1/17

Therefore, approximately, one amino group at C-2 position should be substituted by a iodoacetic acid moiety every 17 sugar rings of chitosan.

The degree of substitution of amino groups into iodoacetic acid moiety at the C-2 position of chitosan was also measured by conductometric titration. The titration curve for CIA in HCl is provided in Figure 2-5. Before the first inflection point, the curve has a negative slope, which corresponds to the decrease in conductivity due to the consumption of excess acid. The positive slope after the second inflection point results from the excess NaOH added. As before, the amount of NaOH used between the two inflection points (13.41 mL - 8.70 mL = 4.71 mL) equals to the amount of NH_3^+ ions present on the CIA. Comparing with the titration curve for unmodified chitosan in Section 2.4.1, the amounts of NaOH used for the neutralization of protonated NH_3^+ ions for CIA and unmodified chitosan were 4.71 mL and 5.45 mL, respectively. Then the mole amount of amino groups present for each sample per gram is:

Mole of amino groups present in 1 g of CIA

$$= \frac{(v2-v1)(L)\, M_{NaOH}\left(\frac{mol}{L}\right)}{Mass\ of\ chitosan\ sample\ (g)}$$

$$= \frac{\frac{(4.71)}{1000}(L) \times 0.1\left(\frac{mol}{L}\right)}{0.0871(g)}$$

$= 5.41 \times 10^{-3}$ (mol)

Mole of amino groups present in unmodified chitosan of 1 g

$$= \frac{(v2-v1)(L)\, M_{NaOH}\left(\frac{mol}{L}\right)}{Mass\ of\ chitosan\ sample\ (g)}$$

$$= \frac{\frac{(5.45)}{1000}(L) \times 0.1\left(\frac{mol}{L}\right)}{0.0940(g)}$$

$= 5.80 \times 10^{-3}$ (mol)

Then, the mole amount of $–NH_2$ on chitosan that converted into $–NHCOCH_2I$ after the reaction with iodoacetic acid is calculated as 3.90×10^{-4} (mol) (= $5.80 \times 10^{-3} – 5.41 \times 10^{-3}$). Finally, the amount of iodine present in CIA is 4.95×10^{-2} (g) (= 3.90×10^{-4} (mol) x 126.91 (g/mol)), and the weight percent of iodine content in1g of CIA, i.e., the value of degree of substitution, is 4.95 % (= 4.95×10^{-2} (g)/ 1 (g) x 100 (%)). This is consistent with the result from the elementary analysis, which is 4.41 %.

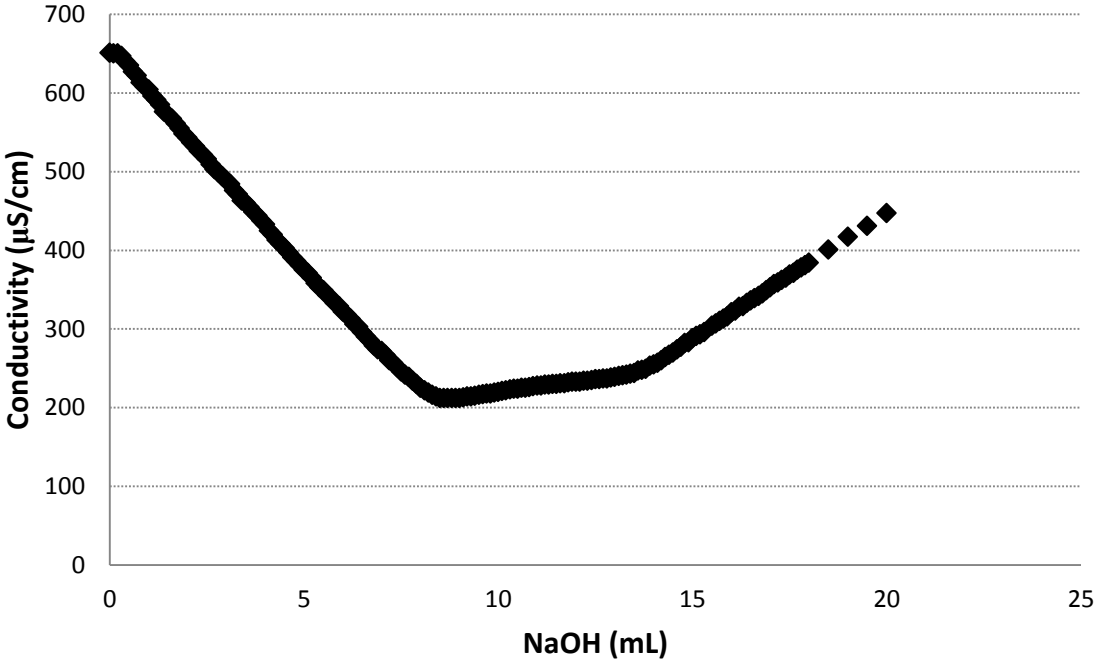

Figure 2-5 Conductometric titration curve of CIA derivative.

Furthermore, the IR spectra of native chitosan and its derivative of iodoacetic acid derivative are shown in Figure 2-6. The significant differences in spectra between the unmodified chitosan and CIA derivative are that CIA exhibits a single band at 3350 cm^{-1} that attributes to N-H stretching, a strong peak at 1630 cm^{-1} that attributes to C=O stretching of amides, and a strong N-H bending vibration band coupled with C-N stretching for secondary amides at 1570 cm^{-1}. Also they show two peaks at 1395 cm^{-1} and 1380 cm^{-1}. The single N-H stretching band at 3350 cm^{-1} indicates that the derivative has only one –NH, indicating the amino groups at C-2 position were substituted with iodoacetic acid moiety and changed into secondary amide. Also, the strong bands at 1630 cm^{-1} and 1570 cm^{-1} observed for the derivative would be assigned for the Amide I band and the Amide II band, respectively. On

the other hand, the native chitosan shows two N-H stretching bands at 3350 and 3288 cm^{-1}, suggesting the presence of primary amine (-NH_2). In addition, the chitosan sample shows only weak peak at 1631 cm^{-1} which is likely to come from C=O stretching of acetyl groups remained in this chitosan sample. Besides, the strong peak of primary NH_2 scissoring vibration was observed at 1546 cm^{-1}, which disappears in the spectrum of the derivative.

In summary, the strong Amide I and Amide II bands demonstrate that the amide group was introduced into the chitosan sample after the reaction with iodoacetic acid through the substitution of amino group at C-2 position. In addition, two peaks at 1395 cm^{-1} and 1380 cm^{-1} would be assigned for CH_2 and CH_3 deformations. Since native chitosan shows only one weak peak at 1340 cm^{-1} that attributes to CH_3 deformation of –$NHCOCH_3$, these two peaks also support the reaction of chitosan and iodoacetic acid at its C-2 position of chitosan, substituting –NH_2 with –$NHCOCH_2I$.

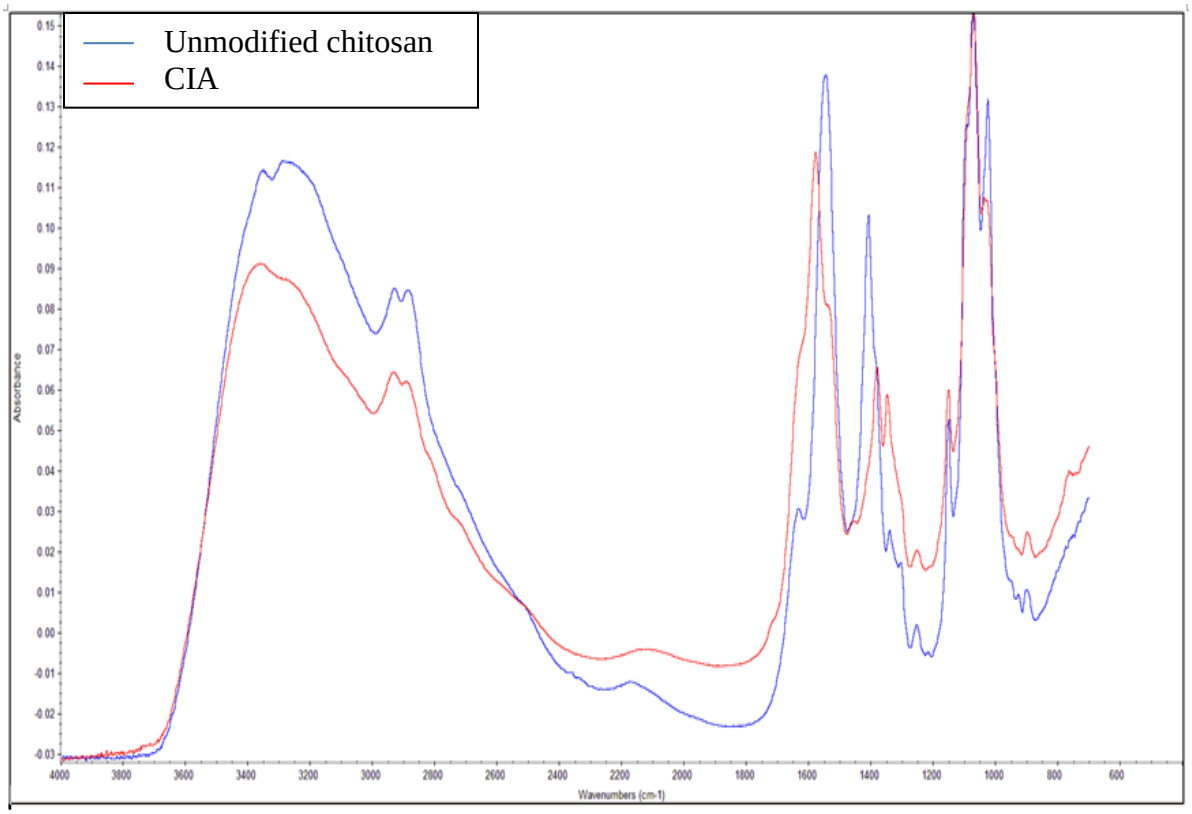

Figure 2-6 Comparison of the FTIR spectra between the unmodified chitosan and CIA derivative.

Finally, the introduction of iodoacetic acid moiety into chitosan was also confirmed with ^{1}H-NMR. The NMR spectrum of the CIA derivative and that of the unmodified chitosan are shown in Figure 2-7. As an evidence of the reaction, the methylene group in the iodoacetic acid moiety was observed as a very strong peak at 2.909 ppm. The H2 signal in the derivative appears at around 2.7 ppm and shifted to upfield compared to that in the unmodified chitosan, which appeared at 2.918 ppm. This would indicate that the electron density around the proton at C-2 increased because of the adjacent iodoacetyl group. Also,

the peak appeared at 3.770 ppm should be assigned to protons on unreacted iodoacetic acid (ref. the spectrum of iodoacetic acid in Figure 3-5).

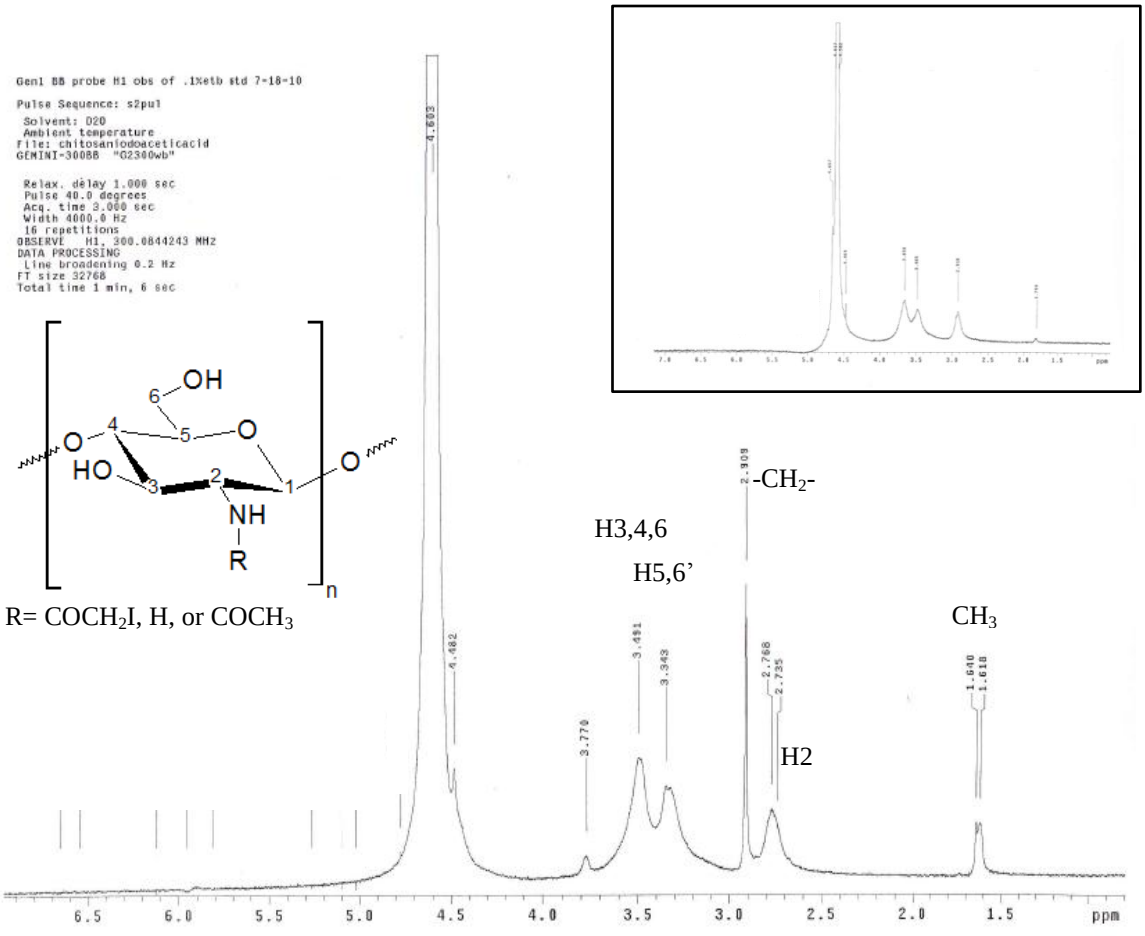

Figure 2-7 NMR spectrum of the CIA sample. The inset shows NMR spectrum of the unmodified chitosan sample.

2.4.3 Derivatives with Different Substitution Ratio

In this study, the CIA derivative with iodine content of 4.4 wt% was used since this sample showed good blood gelation. Several batches with different degree of introduction of iodoacetic acid residue into chitosan were obtained as before. The iodine content in each batch was determined by elemental analysis at Atlantic Microlab, Inc. The analysis is performed by flask combustion followed by ion chromatography with duplicate tests. The degree of iodoacetyl substitution varies from 4wt% to 10 wt%, as summarized in Table 2-1. Comparing the IR spectrum of the unmodified chitosan with those of CIA derivatives in Figure 2-8 and 2-9, C=O stretching vibration coupled with N-H bending vibration of the secondary amide, which is known as the Amide I band, at 1630 cm^{-1} can be observed for the CIA derivatives, which is hardly seen for the chitosan spectra. Also, a very strong absorption at 1546 cm^{-1} due to the NH_2 scissoring vibration for primary amines is observed for the chitosan while it disappears for the derivatives. Moreover, the N-H stretching band exhibits a doublet peaks at around 3300 cm^{-1} for the chitosan, while it exhibits a single peak for the three CIA derivatives. These results clearly indicate that carbonyl groups were introduced into the derivative after the reaction with iodoacetic acid by forming the amide bond between the amino groups of the chitosan as assumed. As a result, the primary amine groups turned to be the secondary amide.

Furthermore, the Amide I band becomes stronger with the increase in the iodine contents, while the NH_2 scissoring band becomes weaker in the same way (Figure 2-10). There are few differences in the spectra for the derivatives with the iodine contents of above

9 wt%, suggesting the limitation of introduction of iodoacetic acid compound under this synthesis procedure.

Table 2-1 Summary of iodine contents for several different CIA batches obtained by elemental analysis

# of batch	**1**	**2**	**3**	**4**	**5**
Iodine content (wt%)	4.33 4.48	6.20 6.09	9.43 9.33	10.44 10.32	9.30 9.14
Average (wt%)	4.41	6.15	9.38	10.38	9.22

The error limit is ± 0.3% for both accuracy and precision.

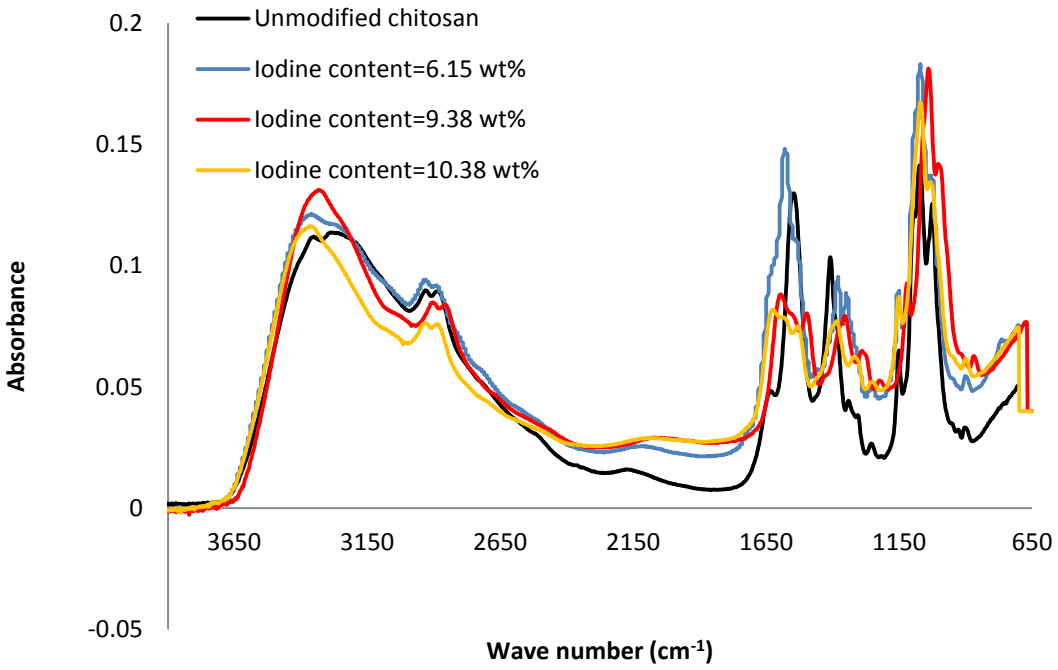

Figure 2-8 FTIR spectra for the unmodified chitosan and several different CIA derivatives.

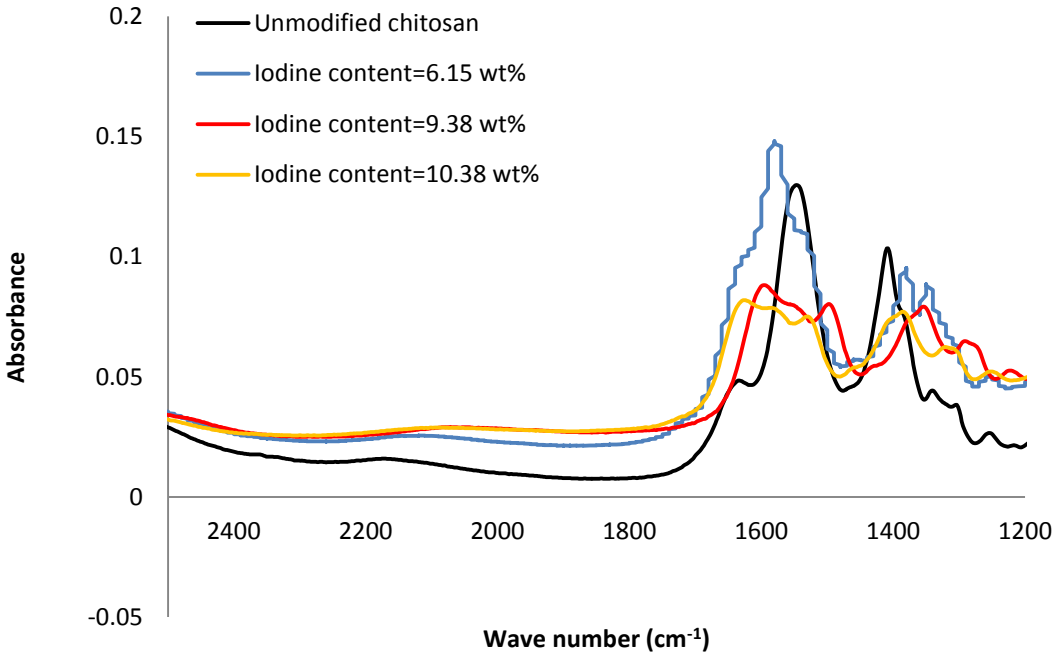

Figure 2-9 FTIR spectra for the unmodified chitosan and several different CIA derivatives, which is expanded between 2500cm^{-1} and 1200 cm^{-1}.

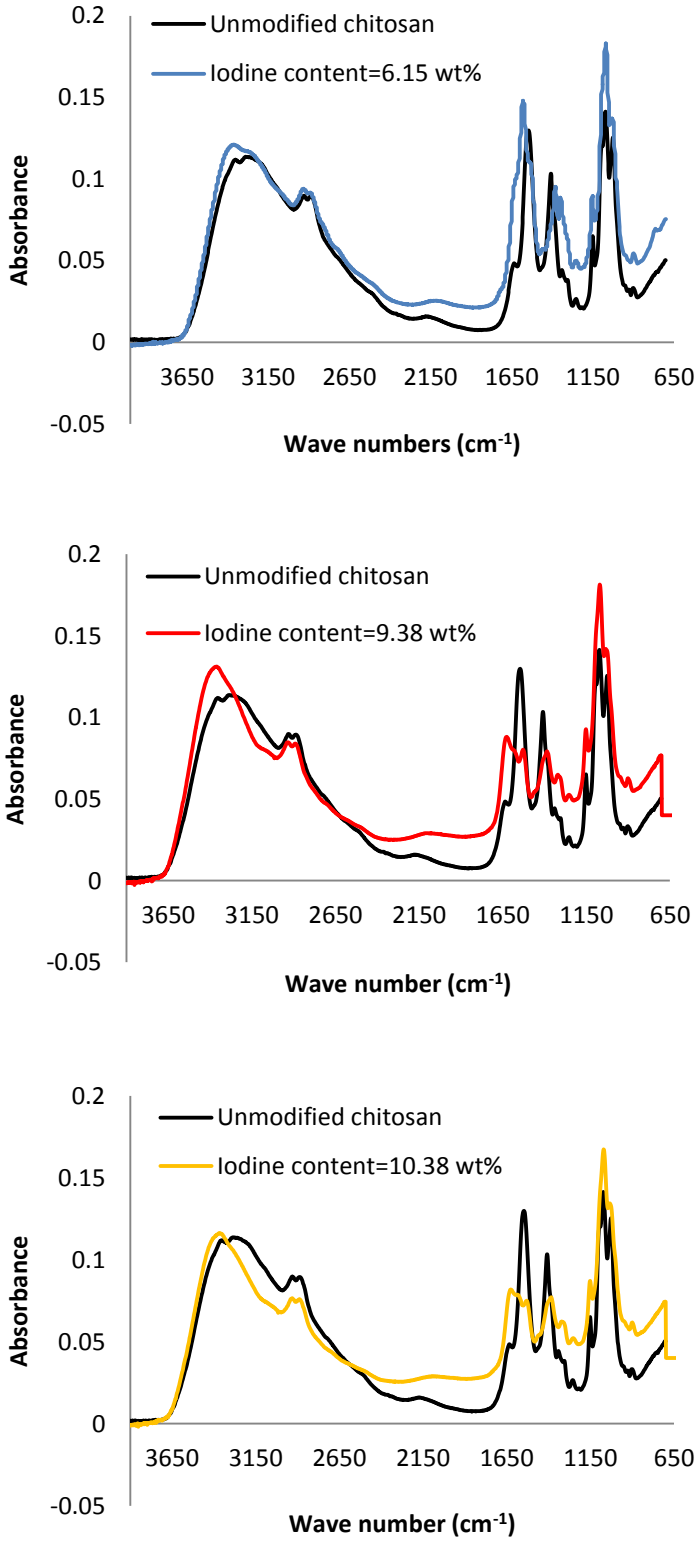

Figure 2-10 IR spectra of the CIA derivatives with three different iodine contents.

2.4.4 Molecular Weight

As a result of the polyelectrolyte nature of chitosan in a dilute aqueous acid, the linear charge density along the chitosan chain increases with the increase in %DD, which results in a gradual increase in intrinsic viscosity due to the coil expansion between electrostatically repelled segments. The intrinsic viscosity [η] was determined by extrapolating the linear regression of plots of η_{sp}/c versus c, to zero concentration, where c is concentration of chitosan solution (g/mL) (Figure 2-11 and Table 2-2).

The DD obtained by ^{1}H NMR was used to calculate k and α, which were used together with [η] to calculate M_v of chitosan using the Mark-Houwink equation. The average molecular weight was confirmed to be $M = ([\eta]/k)^{1/\alpha} \approx 312000$, using the Mark-Houwink equation, $[\eta] = k M_v^{\alpha}$, where $k = 1.64 \times 10^{-30} \times (\%DD)^{14} = 9.51 \times 10^{-3}$ mL/g and $\alpha = -1.02 \times 10^{-2} \times (\%DD) + 1.82 = 0.84$, and the [η] = 392 mL/g. The properties of chitosan are provided in Table 2-3. As a result of the alkaline treatment, a highly deacetylated chitosan with low MW was obtained. The deacetylated chitosan will be used for the synthesis.

Table 2-2 Scheme of intrinsic viscosity measurement for the chitosan sample

C (g/mL)	0 (solvent)	0.002300	0.001150	0.0007667
Time (sec)	114	251	174	152
η_{sp}		1.2018	0.5263	0.3333
η_{sp}/c (mL/g)		522.50	457.67	434.78

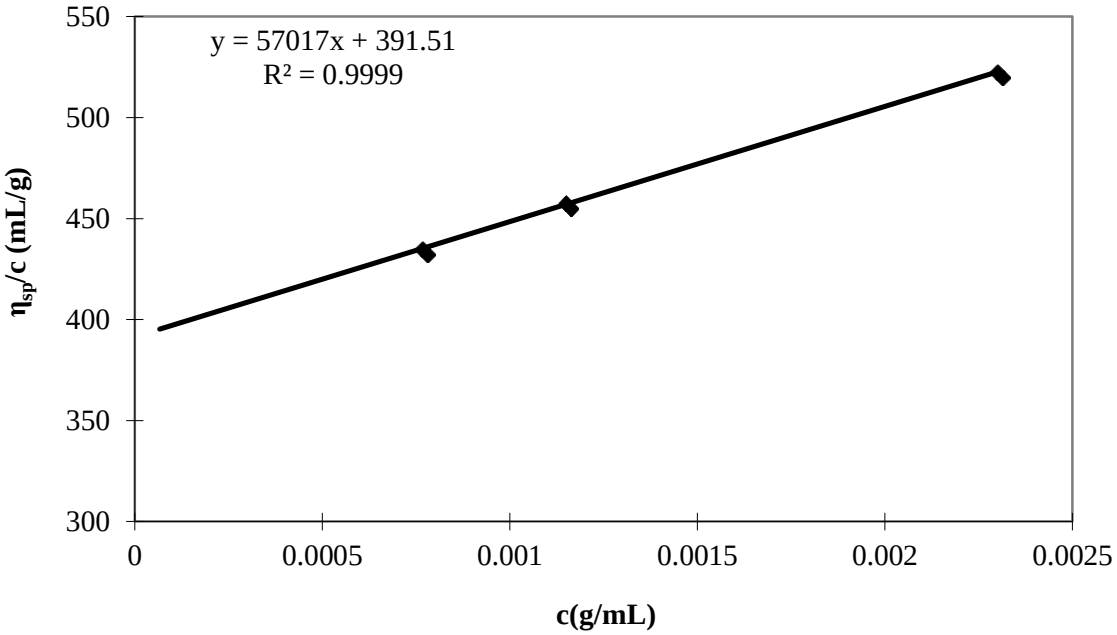

Figure 2-11 Huggins plot of η_{sp}/c vs. c for the chitosan in 0.2M CH_3COOH/0.1M CH_3COONa aq. solution.

Table 2-3 Properties of the chitosan sample

Results	%DD	k	α	[η]	M_v
Chitosan	96.18	9.51×10^{-3}	0.84	392	312000

2.5 Conclusion

In this chapter, the original chitosan sample, first, was characterized in terms of its degree of deacetylation and molecular weight. The degree of deacetylation is an important parameter that strikingly influences the chemical and physical properties of chitosan due to the protonation/deprotonation of the introduced amino group in response to the external pH environment. The chitosan sample used in this study was determined to have %DD of 96% based on ^{1}H-NMR, FTIR, and conductometric titration. Also, the molecular weight of this chitosan was determined as approximately 312 kDa by the viscometric method.

Next, the CIA derivative was synthesized in order to introduce a moiety that potentially reacts with the free thiol of cysteine that exists in blood proteins. Several tests were done to characterize the prepared derivative, including ^{1}H-NMR, FTIR, elemental analysis, and conductometric titration. NMR and FTIR data successfully demonstrated that the iodoacetic acid moiety was introduced into the chitosan through the reaction between amino group at C-2 position of chitosan and carboxyl group of iodoacetic acid. The elemental analysis showed that the degree of substitution was in the range of 4 wt% to 10 wt%, which the conductometric titration result supported. Several different CIA derivatives with different substitution ratio were studied on their effect on the gelation of blood proteins. At present, the sample with the substitution ratio of 4% shows the maximized effect on blood gelation (the detail was discussed in Chapter 4).

The degree of substitution was varied even if chitosan and iodoacetic acid were reacted with the constant concentrations. The future work would address the control of the substitution ratio. The key for this synthesis would be to increase the reactivity of carboxyl

group of iodoacetic acid against amino group of chitosan. EDAC was used to activate carboxyl group in this study. Some investigated the action of EDAC in different pH environment. In terms of this, the optimum solution pH would need to be determined to maximize the reaction between chitosan and iodoacetic acid. In contrast, the higher degree of substitution would not necessarily bring in the more effective gelation behavior with blood, as it will eventually insolubilize CIA in water.

CHAPTER 3

3 Reactivity of Iodoacetic acid and Cysteine

Reacting groups that are able to couple with sulfhydryl-containing molecules are one of the common functional groups present on crosslinking or modification reagents. The thiolated polymers or the so-called thiomers exhibit improved mucoadhesive properties by forming covalent disulfide bonds with the mucus layer. Based on a simple oxidation process between free thiol groups and/or thiol/disulfide exchange reactions, disulfide bonds are formed between cysteine-rich subdomains of mucus glycoproteins and such thiomers, building up the mucus gel layer.[194] For example, chitosan-thioglycolic acid (TGA) and polycarbophil-cysteine conjugates have been reported to display more than four-fold higher and more than two-fold higher adhesive properties on freshly excised intestinal mucosa than the corresponding unmodified polymers, respectively.[195,196] Thus, the formation of the covalent crosslinking between thiolated chitosan derivatives and cysteine in the blood protein with (di)sulfide interactions may result in a novel hemostatic approach, establishing the gelation of the blood at the site of injury. Moreover, the introduction of the other moieties but thiols that interact with cysteine into chitosan would be another candidate.

Iodoacetic acid is an irreversible inhibitor of all cysteine peptidases with the mechanism of inhibition occurring from alkylation of the catalytic cysteine residue according to the equation:

$$R\text{-}SH + ICH_2\,COOH \rightarrow R\text{-}SCH_2\,COOH + HI$$

Iodoacetyl derivatives can react with a number of functional groups within proteins: the

sulfhydryl group of cysteine, both imidazolyl side chain nitrogens of histidine, the thioether of methionine, and the primary ε-amine group of lysine residues and *N*-terminal α-amines.[197] The relative rate of reaction with each of these residues is generally dependent on the degree of ionization and thus the pH at which the modification is done. Generally, the relative reactivity of α-haloacetates toward protein functionalities is sulfhydryl > imidazolyl > thioether > amine. Among halo derivatives, the relative reactivity is I > Br > Cl > F, with fluorine being almost unreactive. Thus, iodoacetate has the highest reactivity toward sulfhydryl cysteine residues and the alkylation of cysteine sulfhydryls has previously been reported to give the carboxymethylcysteinyl derivative.[198]

3.1 Background of Reaction between Iodoacetic acid and Cysteine Sulfhydryls

The reaction between iodoacetic acid and sulfhydryl compounds was first reported in the 1930s'. Dickens[199] has shown that this reaction proceeds through the substitution of a carboxymethyl group (-CH_2-COOH) of iodoacetic acid for the hydrogen of the thiol group with the formation of HI. Smythe et al.[200] has measured the rate of reaction of iodoacetic acid with various sulfhydryl compounds by estimation of the carbon dioxide change in a CO_2-bicarbonate buffer as a result of the HI produced (Figure 3-1, Table 3-1[200]).

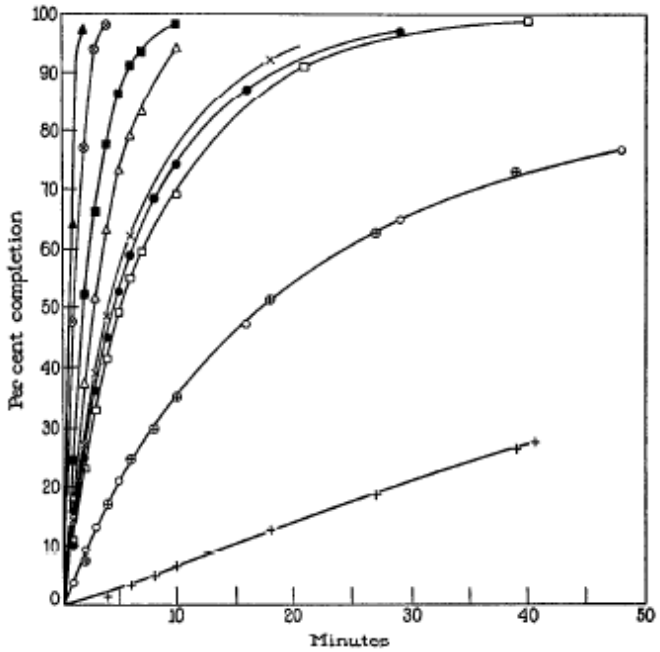

Figure 3-1 The rate of reaction of iodoacetate and of iodoacetamide with various sulfhydryl groups at pH 6.1 and 28°C. The amount of -SH present was 0.2 cc. of a 0.1 M solution in each case and the amount of iodo compound 0.2 cc. of a 0.5 M solution. The total volume was 1.4 cc. ⊗ represents thiosalicylic acid and iodoacetamide; × represents thiosalicylic acid and iodoacetate; ▲ thioglucose and iodoacetamide; △ thioglucose and iodoacetate; ■ cysteine and iodoacetamide; □ cysteine and iodoacetate; ● glutathione and iodoacetamide; ○ glutathione and iodoacetate; ⊕ thioglycol and iodoacetamide; + thioglycol and iodoacetate.[200]

Table 3-1 Reactions of –SH Compounds with Iodo Compounds[200]

-SH compound	Iodo compound	pH = 7.1		pH = 6.1	
		Time for 50% reaction (min)	Time for iodoacetate + time for iodoacetamide	Time for 50% reaction (min)	Time for iodoacetate + time for iodoacetamide
Thioglucose	Acetamide	0.57	1.42	0.7	4.15
"	Acetate	0.81		2.9	
Thiosalicylic acid	Acetamide	0.58	1.45	1.0	4.00
"	Acetate	0.84		4.0	
Cysteine	Acetamide	0.81	1.38	1.9	2.68
"	Acetate	1.12		5.1	
Glutathione	Acetamide	1.10	1.82	4.5	3.84
"	Acetate	2.0		17.3	
Thioglycol	Acetamide	2.0	3.50	17.3	5.40
"	Acetate	7.0		93.5	

Rapkine[201] showed that iodoacetic acid may react not only with the sulfhydryl groups of relatively simple molecules, such as cysteine and glutathione, but also with those of proteins. Subsequently, Rapkine[201] and Mirsky and Anson[202] found that iodoacetic acid might react with only a portion or with none of the sulfhydryl groups of native proteins, as evidenced by the continued presence of part or all of the original protein cysteine in the protein hydrolysate after the reaction. They reported that denaturation of the protein causes all of the sulfhydryl groups to be capable of interaction with iodoacetic acid, resulting in no free cysteine left in the protein hydrolysate after the reaction.[202] In these experiments, iodoacetic acid was reacted with coagulated denatured egg albumin, revealing that 3 hours were required for the completion of the reaction. Later, Rosner[203] carried out the reaction of iodoacetic acid with heat- (urea-) denatured egg albumin at pH 7.3 (0.01 N KOH), and confirmed an initial sharp

rise in the formation of iodide is mainly a result of the reaction between the iodoacetic acid and the thiol groups of the denatured egg albumin. This initial rapid iodide production lasted no longer than 10 minutes, followed by the continued slower rate of iodide production that possibly results from the reaction of iodoacetate with amino groups of the denatured egg albumin,[204] as shown in Figure 3-2.[203] Furthermore, it is of interest that when a solution of native egg albumin was tested in the same manner, no iodide was found at the end of a 5 h period. This indicates that not only the sulfhydryl but all of the groups in the native egg albumin are non-reactive toward iodoacetate.

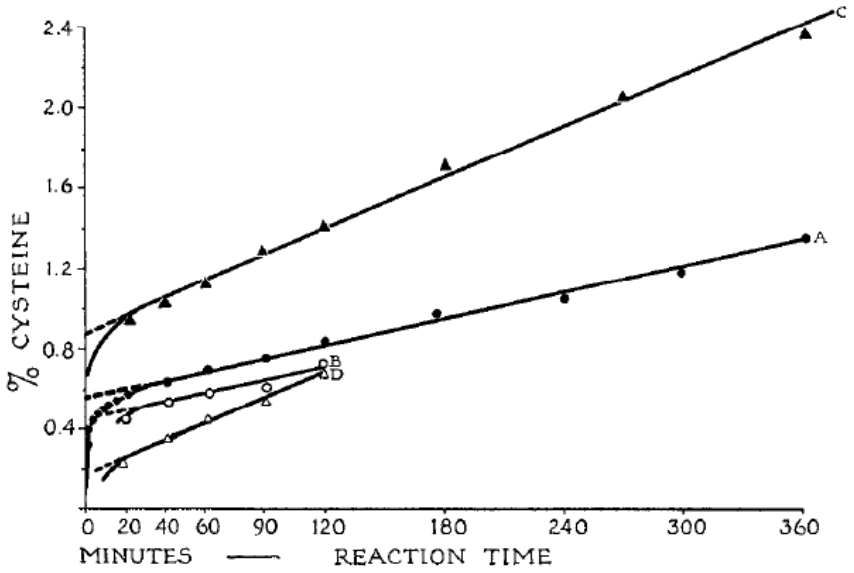

Figure 3-2 The production of iodide upon reaction of iodoacetic acid with denatured egg albumin at pH 7.3. The iodide is expresses in terms of its equivalent percent cysteine of the total weight of egg albumin. Curve A: heat-denatured egg albumin which was treated with iodoacetate immediately following denaturation; Curve B: heat-denatured egg albumin which was treated with iodoacetate after standing 4 hours following denaturation; Curve C: urea-denatured egg albumin which was treated with iodoacetate after 1 hour in urea solution; Curve D: urea-denatured egg albumin which was treated with iodoacetate after 20 hours in urea solution.[203]

Furthermore, the interesting observation of Greenstein[205] is that denaturation of egg albumin by urea, guanidine, and various derivatives causes markedly greater initial iodide production than that given by heat-denatured egg albumin. In addition, they demonstrated that the characteristics of urea-denaturation as compared with that of heat-denaturation is that it makes a greater number of thiol groups, as well as other groups, available for the reaction with the iodoacetic acid. Therefore, if iodoacetic acid is present in limiting quantities, relative to the number of sulfhydryl groups present, and at slightly alkaline pH, cysteine modification will be the exclusive reaction. This gives us a possibility that chitosan modified by iodoacetic acid derivatives would crosslink with the blood plasma protein that contains cysteine at the biological pH range of ~7.4 and form the three dimensional gel network, resulting in the gelation of blood.

3.2 Sulfhydryl and Disulfide Groups of Proteins

In general, native proteins have few, if any, free sulfhydryl and disulfide groups, while denatured proteins have a number of such groups corresponding to the total number of cysteine and cysteine groups existed in the protein. Serum albumin treated with acid acetone (an effective denaturing agent) or trichloracetic acid has the number of free sulfhydryl and disulfide groups that is a characteristic of a denatured protein.[206] Mirsky and Anson[202] described the methods for estimating quantitatively the sulfhydryl (SH) and disulfide (S-S) groups available in proteins, using the reaction between iodoacetic acid and cysteine. They developed two independent methods. In the direct method, the SH groups are oxidized by

cystine, which is a dimer formed from the oxidation of two cysteine residues by a disulfide bridge. After oxidization, the formed cystine is, then again, reduced to cysteine. Thereby the number of free SH groups in the protein is estimated by measuring the amount of newly formed cysteine. (Cystine oxidizes all SH groups and no other groups in the protein.) In the indirect method, SH groups are first eliminated by a treatment with iodoacetic acid. The protein is then hydrolyzed, the existed SH groups is estimated by comparing its total cysteine content with that of untreated protein. Also, the number of S-S groups in unhydrolyzed protein is estimated by the increase in number of SH groups caused by reducing the S-S groups to SH with thioglycolic acid ($HSCH_2COOH$).

Seen from Figure 3-2, groups other than sulfhydryl produce iodide with iodoacetic acid as a linear function of time. If the non-sulfhydryl iodide is extrapolated to zero time, a value for the iodide formed from the reaction of the sulfhydryl groups and iodoacetic acid is obtained. Assuming all of these sulfhydryl groups to be part of the cysteine moiety of the protein molecule, Rosner[203] estimated the cysteine content in the protein. This method gives a value of available cysteine of 0.55% in heat-denatured egg albumin (average of ten determinations with a range of 0.53 to 0.57% cysteine). This result is in good agreement with those reported by Mirsky and Anson, 0.56 to 0.61 %.[202] In the same way, they reported the much higher content of SH groups in the denatured serum albumin of 4.57 to 4.85%.[202] Also, they found a value of available cysteine in urea-denatured egg albumin of 0.87%,[203] confirming the previous finding[205] that the greater increase in availability, not only of sulfhydryl groups but of other iodoacetate reacting groups, in urea-denatured egg albumin than in heat-denatured egg albumin. Finally, one more interesting finding is that the thiol

groups in the denatured egg albumin, both heat- and urea-denatured, are quite labile. If the denatured egg albumin was permitted to stand for a few hours at pH 7.3 before being treated with iodoacetate, the cysteine content calculated was markedly decreased compared to that was immediately treated with iodoacetate.[203] This disappearance of sulfhydryl groups does not represent a reversal of the denaturation of egg albumin, it probably indicates their oxidation.

3.3 Materials and Methods

3.3.1 ^{1}H NMR spectroscopy

The reaction between L-cysteine and iodoacetic acid was first tested through ^{1}H NMR. A known amount of L-cysteine (Sigma bioreagent ≥ 98%, 5 mg) and iodoacetic acid (Sigma-Aldrich ≥ 99.0%, 7.67 mg) were dissolved in 0.75mL of D_2O (Aldrich 99.9 atom %D) and introduced into a 5 mm NMR tube, respectively. Also, L-cysteine (5 mg) in 0.75 mL D_2O and iodoacetic acid (7.67 mg) in 0.75 mL D_2O were mixed for 30 minutes at room temperature and then 0.6 mL from the mixed solution were introduced into 5 mm NMR tube.

^{1}H NMR measurement was performed on a Varian Mercury 300 NMR spectrometer operating at 300 MHz for the ^{1}H nucleus in 16 scans at room temperature for all samples. Chemical shifts for ^{1}H NMR spectra were expressed in δ (ppm) downfield from the signal for 3-(trimethylsilyl)-2,2',3,3',-tetradeuteropropionic acid (TSP-d4), the internal reference. The solvent signal was as follows: D_2O, 4.65 ppm.

3.3.2 Liquid Chromatography-Time of Flight Mass Spectrometry (LC-TOF)/MS

A 0.1 M iodoacetic acid aqueous solution of 0.75 mL was prepared. The solution pH was raised to 8.5 by 0.1N NaOH (The pH was kept as it is for a control). The solution was stored in cool darkness. Next, 0.05 M L-cysteine aqueous solution of 0.75 mL was prepared in a vial. The vial was wrapped in aluminium foil and then the iodoacetic acid solution was added dropwise with stirring. The reactant was incubated in the dark for 30 minutes at 37˚C water bath.

The high resolution (≥ 10,000 R FWHM) exact mass measurement of the sample was made using Electrospray Ionization (ESI) on an Agilent Technologies (Santa Clara, California) 6210 LC-TOF mass spectrometer. Samples were diluted in water and analyzed via a 1μL flow injection at 300 μL/min in a water: methanol mixture (25:75) (v:v) with 0.1% formic acid. The mass spectrometer was operated in positive-ion mode with a capillary voltage of 4 kV, nebulizer pressure of 35 psig, and a drying gas flow rate of 12 L/min at 350˚C. The fragmentor and skimmer voltages were 130 and 60 V, respectively. Reference ions of purine at *m/z* 121.0509 and HP-0921 at *m/z* 922.0098 were simultaneously introduced via a second orthogonal sprayer, and used as internal calibrants.

Mass spectra were obtained at the NCSU Department of Chemistry Mass Spectrometry Facility. Funding was obtained from the North Carolina Biotechnology Center, and the NCSU Department of Chemistry.

3.4 Results and Discussion

3.4.1 Reactivity between Iodoacetic acid and Cysteine from ^{1}H-NMR

The reaction between iodoacetic acid and free thiol groups of cysteine is crucial for this work (Figure 3-3).

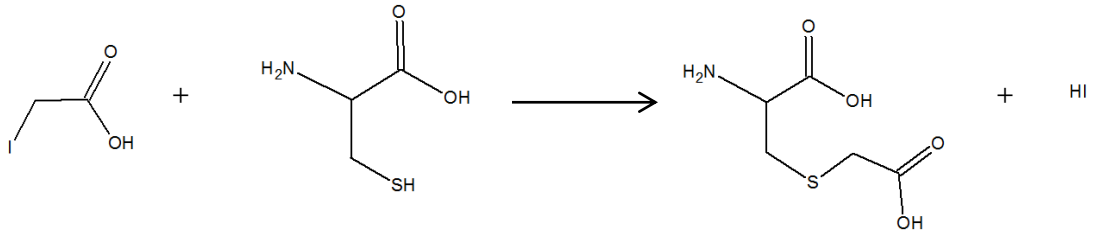

Figure 3-3 Scheme of reaction between L-cysteine and iodoacetic acid.

^{1}H-NMR can be useful to demonstrate the reaction between these two functional groups. The two carbon-protons of iodoacetic acid have a specific peak. The signal of these protons should be shifted after the reaction with L-cysteine since an iodine atom from iodoacetic acid should be replaced with a sulfur atom from L-cysteine after the reaction. The iodoacetic acid and L-cysteine themselves can be used as controls.

Figure 3-4 and 3-5 are the ^{1}H-NMR spectra of L-cysteine and iodoacetic acid, respectively. In Figure 3-4, the peak at 3.779 ppm is assigned to H1 in L-cysteine. Since the adjacent carbon has two hydrogen atoms, H1 peak appears as a triplet. The peaks of -CH_2- (H2 and H2') appear as clustered signals at around 2.8 ppm. Generally, a proton on –CH_2- is shifted upfield (low chemical shift) than that of a proton on –CH- due to higher electron

density. Next, Figure 3-5 shows the spectrum of iodoacetic acid. The peak of -CH_2- (H3, H3') in iodoacetic acid appears at 3.576 ppm. The frequency was shifted downfield (high chemical shift) due to the two adjacent electron withdrawing groups, carboxyl group and iodine. Figure 3-6 shows the NMR spectrum of the product between L-cysteine and iodoacetic acid. In the spectrum, the peak of –CH_2- from the iodoacetic acid moiety was shifted slightly upfield from 3.576 ppm to 3.544 ppm, compared to that which appeared in the iodoacetic acid spectrum (Figure 3-5). The two compounds would bond via a sulfur linkage, removing HI. It could be considered that the –CH_2- group in iodoacetic acid lies next to iodine which is a strong electronegative atom and, thus, its NMR frequency appears at a higher chemical shift. The reaction with L-cysteine removed the iodine from the structure, as a result, made it shift slightly upfield. Furthermore, the integration gives us additional information. The integration reveals the relative numbers for the different hydrogens in the molecule. There are supposed to be three different kinds of hydrogens in the product if L-cysteine and iodoacetic acid successfully react with one another, which are H1 and H2, 2' from L-cysteine residue and H3, 3' from iodoacetic acid residue. As seen in Figure 3-6, the ratio of H1 to (H2 and H2') to (H3 and H3') turned out to be 1: 2: 2 (18.02: 38.58: 43.40), which supports the predicted product structure.

Nevertheless, there still is a possibility that this spectrum reflects the presence of unreacted L-cysteine or unreacted iodoacetic acid in a mixed solution since ^{1}H NMR was done on the reaction mixture solution, not on the separated product. The reactivity between these two, therefore, was investigated by Mass Spectrometry in the following section.

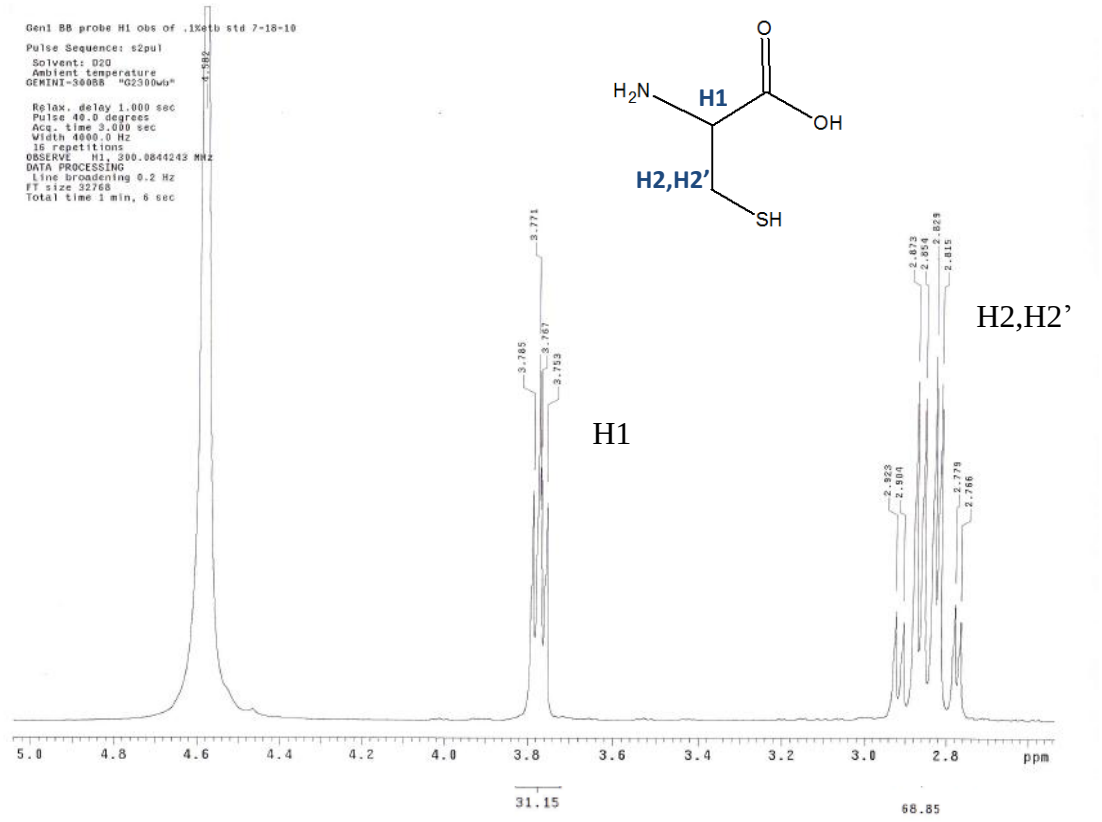

Figure 3-4 ^{1}H NMR spectrum of L-cysteine.

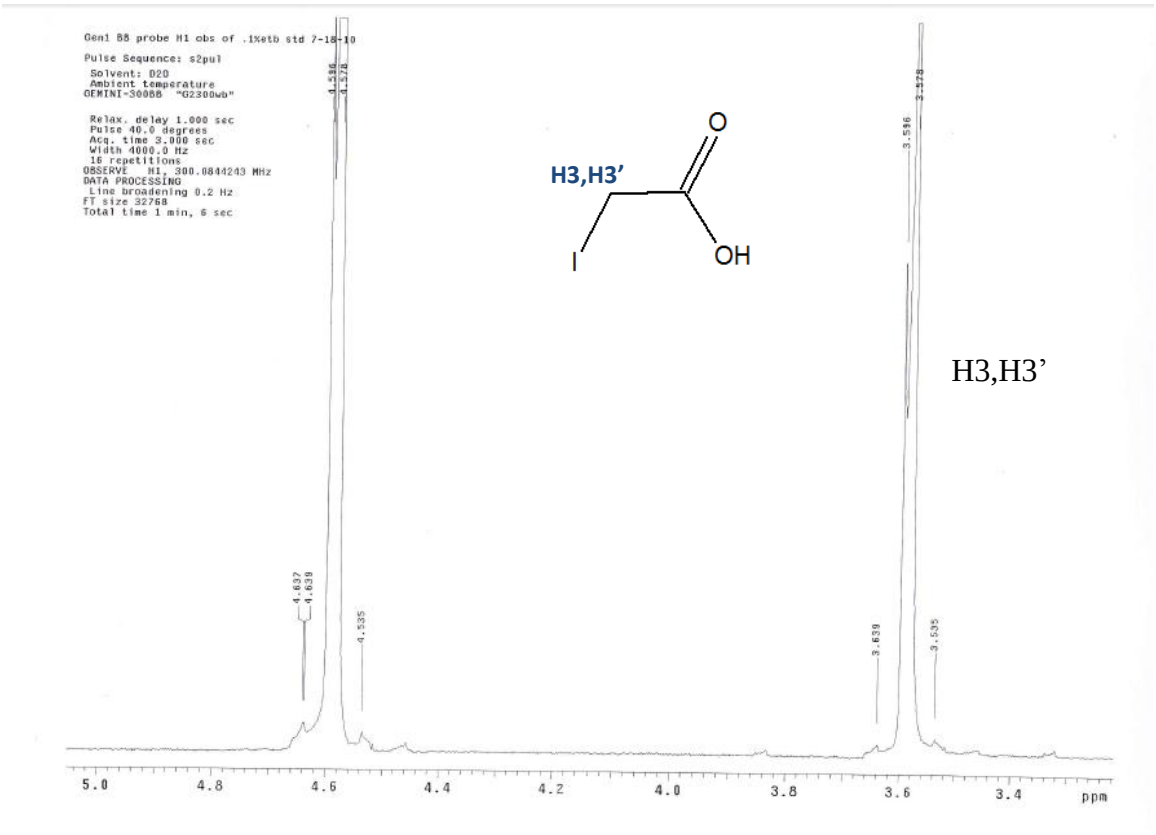

Figure 3-5 ^{1}H NMR spectrum of iodoacetic acid.

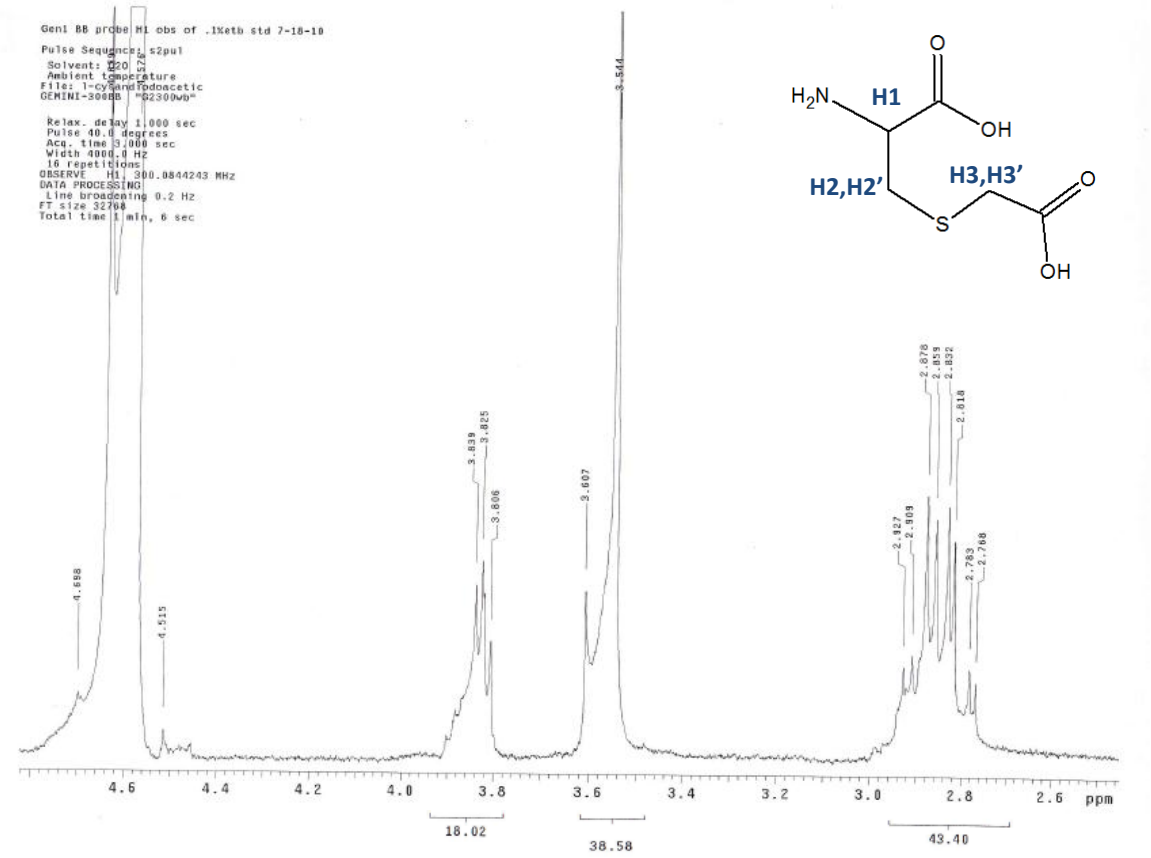

Figure 3-6 ^{1}H NMR spectrum of the reaction mixture between L-cysteine and iodoacetic acid.

3.4.2 Reactivity between Iodoacetic acid and Cysteine from Mass Spectrometry (MS)

Since ^{1}H NMR was not enough to prove the reaction between L-cysteine and iodoacetic acid, Liquid Chromatography-Time of Flight (LC-TOF)/MS was used to obtain a strong evidence of the reaction between these two compounds. The two compounds were reacted at slightly basic aqueous solution in dark at 37˚C because the thiol group has pKa value of ~8 and the iodoacetyl group is light sensitive. The theoretically calculated molecular weights of each compound are: L-cysteine ($C_3H_7NO_2S$, MW 121.16), iodoacetic acid ($C_2H_3O_2I$, MW 185.95), and their derivative ($C_5H_9NO_4S$, MW 179.19). After 30 minutes reaction, a clear and colorless solution was obtained. This solution was submitted to LC-TOF/MS. The results are summarized in Table 3-2. Also, Figure 3-7 shows the LC-TOF spectra of the resulting product between L-cysteine and iodoacetic acid. A clear peak for the targeted reaction product is observed at *m/z* 180.0322. This suggests the presence of the targeted product of $C_5H_9NO_4S$ ($[M+H]^+$ $C_5H_{10}NO_4S$). The peak at *m/z* 241.0307 is assigned to cystine ($C_6H_{13}N_2O_4S_2$, MW 241.32) that is a dimer of cysteine, indicating some cysteine molecules linked each other through disulfide linkage. Since the pKa of alkyl thiols is in the range of 8 to 10,[138] the reactivity of free thiol groups in L-cysteine was high and caused intermolecular disulfide linkage at this pH 8.5 although the reaction with iodoacetic acid was still dominant. The rest of the weak peaks are assigned to the fragments due to the breakdown of the product, also unreacted iodoacetic acid and L-cysteine, and resulting HI (MW 127.91). It is reasonable to consider that excess iodoacetic acid should remain in the sample solution because L-cysteine and iodoacetic acid was mixed in molar ratio of 1:2. The obtained data clearly proved that the free thiol group in L-cysteine reacts with iodoacetic acid.

The predicted reaction scheme that occurs between iodoacetic acid and L-cysteine was shown in Figure 3-8.

Table 3-2 Summary of the results obtained from mass spectrometry at pH 8.5

Sample	$M_{theoretical}$	M_{sample}	ΔM		Corresponding elemental composition
			millimass units	ppm	
11/1	180.0325	180.0322	0.33	1.87	$C_5H_9NO_4S$

MS Formula Results: + Scan (0.177-0.236 min) Sub - 121944.d (121944.d)

m/z	Ion	Formula	Abundance
180.0322	(M+H)+	C5 H10 N O4 S	148888.7

Best	Formula (M)	Ion Formula	Calc Mass	m/z	Calc m/z	Diff (ppm)	Diff (mDa)	DBE
☑	C5 H9 N O4 S	C5 H10 N O4 S	179.0252	180.0322	180.0325	1.87	0.33	2
☐	C6 H5 N5 S	C6 H6 N5 S	179.0266	180.0322	180.0338	9.34	1.67	7

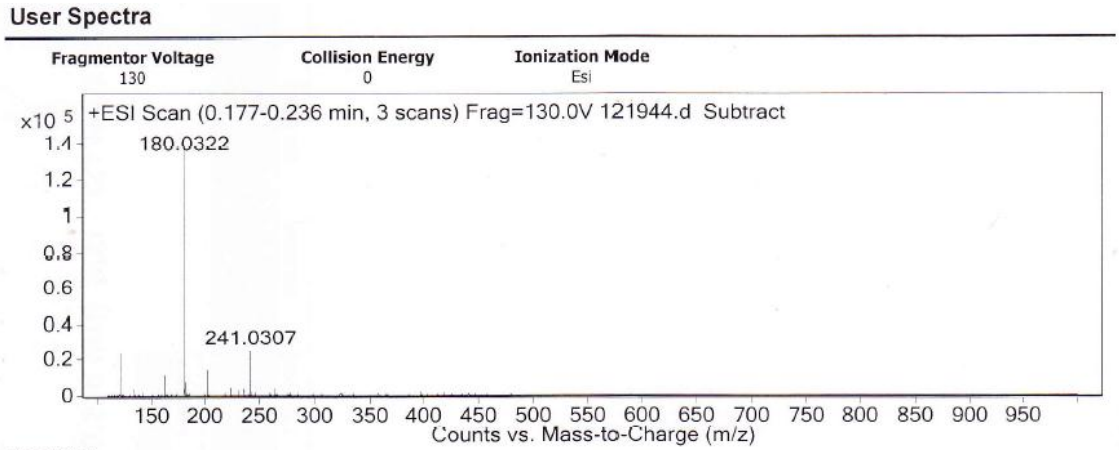

Peak List

m/z	z	Abund	Formula	Ion
122.0273		23543		
163.0062		11709		
180.0322	1	148889	C5 H10 N O4 S	(M+H)+
181.0352	1	7747	C5 H10 N O4 S	(M+H)+
202.0144		14740		
241.0307		26842		

Figure 3-7 Mass spectrum of the reaction product between L-cysteine and iodoacetic acid at pH 8.5.

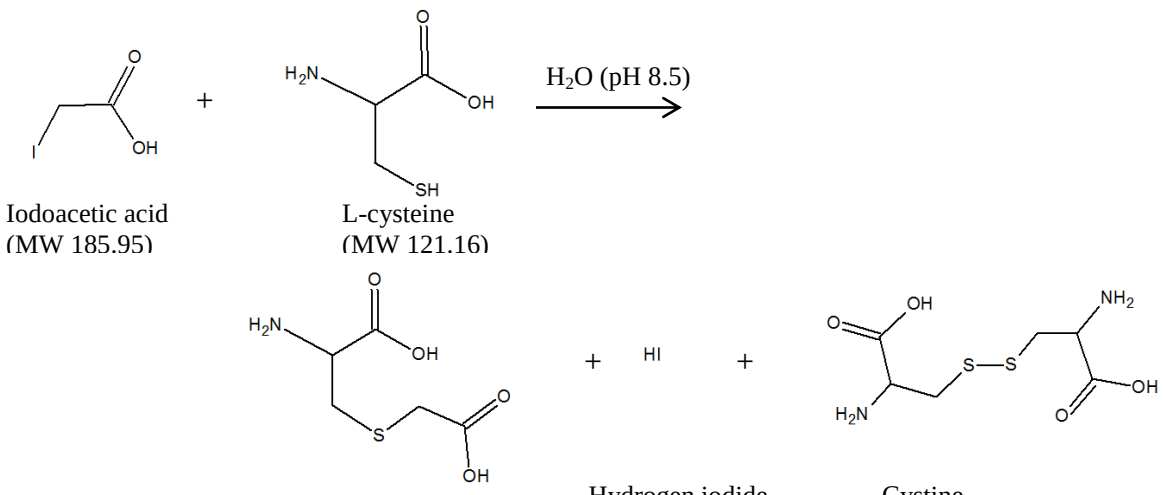

Figure 3-8 The predicted reaction scheme between iodoacetic acid and L-cysteine based on the results of MS.

As mentioned above, the reaction between iodoacetic acid and L-cysteine requires alkaline condition since the sulfhydryl group has the pKa value in the range of 8-10. Here we further studied how much the reaction proceeds at physiological condition (~pH7.4). The same experiment was carried out except the pH was not raised, and the reacted solution was analyzed by LC-TOF. The results are shown in Table 3-3 and Figure 3-9. As seen, the results confirm the formation of the targeted product of $C_5H_9NO_4S$ ($[M+H]^+$ $C_5H_{10}NO_4S$) at *m/z* 180.0320. At the same time, this peak did not predominate compared to that obtained at pH 8.5, indicating the reactivity between iodoacetic acid and L-cysteine was slightly reduced. Also, some cystine ($C_6H_{13}N_2O_4S_2$) formation is seen at *m/z* 241.0310 as well. The second largest peak at m/z 230.8882 is assigned to be a fragment ion of cystine dimer. All other peaks are considered as the breakdown weight loss of the targeted product, excess iodoacetic acid, cystine, or impurities. These give us further information that the free thiol group of cysteine selectively reacts with iodoacetic acid in the alkaline environment, however, it has some reactivity in physiological solution of pH 7.4 as well. Furthermore, the obtained data explains previous studies that the reactions between iodoacetic acid (or iodoacetamide) and sulfhydryl compounds go faster at pH 7.1 than at pH 6.1 (ref. Table 3-1).[200]

The pH of blood is 7.35-7.45. The obtained results support the iodoacetic acid derivative system can interact with cysteine in the blood protein at physiological condition.

Table 3-3 Summary of the results obtained from mass spectrometry at pH 7.4

Sample	$M_{theoretical}$	M_{sample}	ΔM millimass units	ΔM ppm	Corresponding elemental composition
11/19	180.0325	80.0320	0.53	2.96	$C_5H_9NO_4S$

MS Formula Results: + Scan (0.255-0.314 min) Sub - 122137.d (122137.d)

m/z	Ion	Formula	Abundance
180.032	(M+H)+	C5 H10 N O4 S	12057.4

Best	Formula (M)	Ion Formula	Calc Mass	m/z	Calc m/z	Diff (ppm)	Diff (mDa)	DBE
☑	C5 H9 N O4 S	C5 H10 N O4 S	179.0252	180.032	180.0325	2.96	0.53	2
☐	C5 H5 D2 N O4 S	C5 H6 D2 N O4 S	179.0221	180.032	180.0294	-14.34	-2.57	3
☐	C8 H5 N O4	C8 H6 N O4	179.0219	180.032	180.0291	-15.86	-2.84	7

User Spectra

Fragmentor Voltage	Collision Energy	Ionization Mode
150	0	Esi

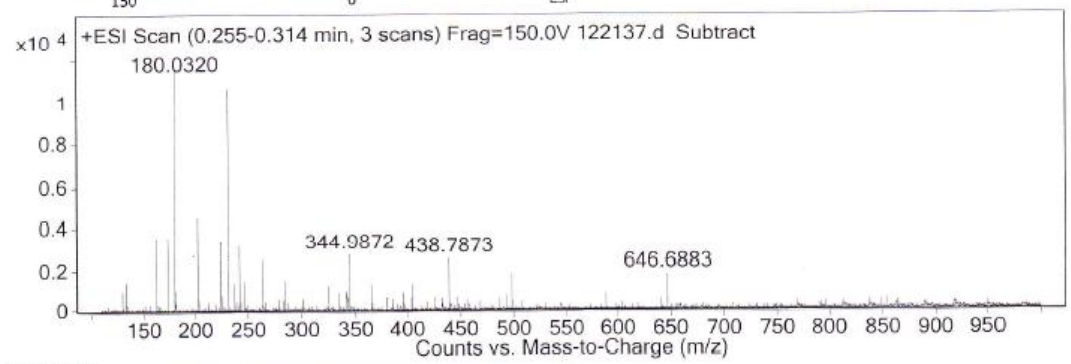

Peak List

m/z	z	Abund	Formula	Ion
163.0066		3486		
172.8825		3740		
180.0320	1	12057	C5 H10 N O4 S	(M+H)+
202.0143		4455		
223.9955		3400		
230.8882		11629		
241.0310		3226		
263.0112		2604		
344.9872		2681		
438.7873		2684		

Figure 3-9 Mass spectrum of the reaction product between L-cysteine and iodoacetic acid at pH 7.4.

3.5 Conclusion

Iodoacetic acid is known as an irreversible inhibitor of all cysteine peptidase by causing alkylation of the cysteine residue. This reaction mechanism was adopted for this study in order to explore the possibility to create sulfide links between a chitosan derivative and the cysteine residue sulfhydryl groups that exist in blood serum proteins. This chapter focuses on the reaction between iodoacetic acid and L-cysteine and addressed the evidence of the reactivity of the two compounds. ^{1}H NMR and Mass Spectrometry were applied for this purpose. ^{1}H NMR was not sufficient to determine that the reaction occurred since the two compounds bond one another through a sulfur and the protons from each compound did not interact. ^{13}C NMR would be worth trying, it could give us additional useful information to prove the reaction. Also, ^{1}H NMR test on a product between iodoacetic acid and other amino acid that does not contain sulfhydryl group can be used as a control.

The reaction was, furthermore, studied by MS. It successfully demonstrated that L-cysteine and iodoacetic acid react, releasing HI and cysteine alkylation occurred. In addition, two different pH conditions were attempted to find the appropriate condition that maximizes the reaction between iodoacetic acid and L-cysteine, and what is more, the reaction between CIA derivative and sulfhydryl groups in the blood proteins. The alkaline condition caused a higher reactivity between iodoacetic acid and cysteine, nevertheless, we can still expect a sufficiently high reactivity even at physiological condition.

CHAPTER 4

4 Rheology and Gelation of Chitosan-iodoacetamide (CIA) and blood

As polymers undergo crosslinking in solution, they undergo a phase transition from liquid to solid at a critical extent of reaction. This phenomenon is called gelation.[207] Gels consist of a solid three-dimensional crosslinked network that spans the volume of a liquid medium inside the network. Thus, gels are mostly liquid, but they behave like solids due to their three-dimensional crosslinked network within the liquid medium, depending on time scale, temperature, or applied stress. For example, the gel shows elastic response like a solid for quick deformation or at low temperature, on the other hand, the gel behaves more like a liquid for slow deformation or at high temperature. Such behavior may be described as viscoelasticity for the solution or the elastoviscous solid. Gels are divided into chemical gels which are linked by covalent bonds and cannot undergo the reversible sol-gel transition by changing the temperature or applied stress, and physical gels which are linked through weak forces, such as hydrogen bonds, van der Waals interaction, hydrophobic interactions, or electrostatic interactions and undergo reversible sol-gel transition by changing temperature and pressure.

Its cationic character, ease of chemical modification and gel forming ability make chitosan a promising candidate for tissue engineering scaffolds, drug delivery vehicles, or wound dressings. Gelling of chitosan is caused by the formation of physical or chemical three-dimensional crosslinking networks. The formation of covalent crosslinking of chitosan with glutaraldehyde has been widely studied.[208-210] Researchers have proposed the detailed

mechanism for the crosslinking reaction between glutaraldehyde and chitosan.[211-214] In recent years, thiolated chitosan derivatives have been getting attentions as a new generation of mucoadhesive polymers since they are capable of establishing much stronger mucoadhesion than existing non-covalent mucoadhesion approaches, based on the formation of the covalent disulfide crosslinkings.[106-136] As described earlier, thiolated chitosan derivatives have attractive potential as mucoadhesive biomaterials that can be the bridging structure with cysteine-rich subdomains of mucus glycoproteins, building up the mucus layers through the disulfide crosslinkings. Also, they are capable of self-gelling through the formation of inter- and intramolecular disulfide crosslinkings. The purpose of this chapter is to study the gelation of blood plasma protein, especially focusing on cysteine in the plasma, when mixed with the chitosan derivative solutions. This gelation would be caused by the interaction between cysteine-specific moieties in the chitosan derivatives and cysteine residue in the blood plasma proteins, followed by the formation of three dimensional crosslinking network that mimics the natural fibrin crosslinked mesh.

4.1 Introduction to Rheology

Rheology attempts to quantify the way a material deforms when forces are applied, or is a measure of the resistance of a fluid to flow. Generally, the rheological properties can be studied by measuring either the deformation resulting from a stress induced by an applied force on the sample or the force required to obtain a certain amount of deformation. Ideal solids deform elastically, where the deformation is fully recovered when the stress is

removed. On the other hand, ideal liquids deform irreversibly, where the deformation cannot be recovered, even upon the removal of the applied stress. Viscoelastic materials, such as polymers, show both solid- and liquid-like response when a stress is applied. (Figure 4-1)

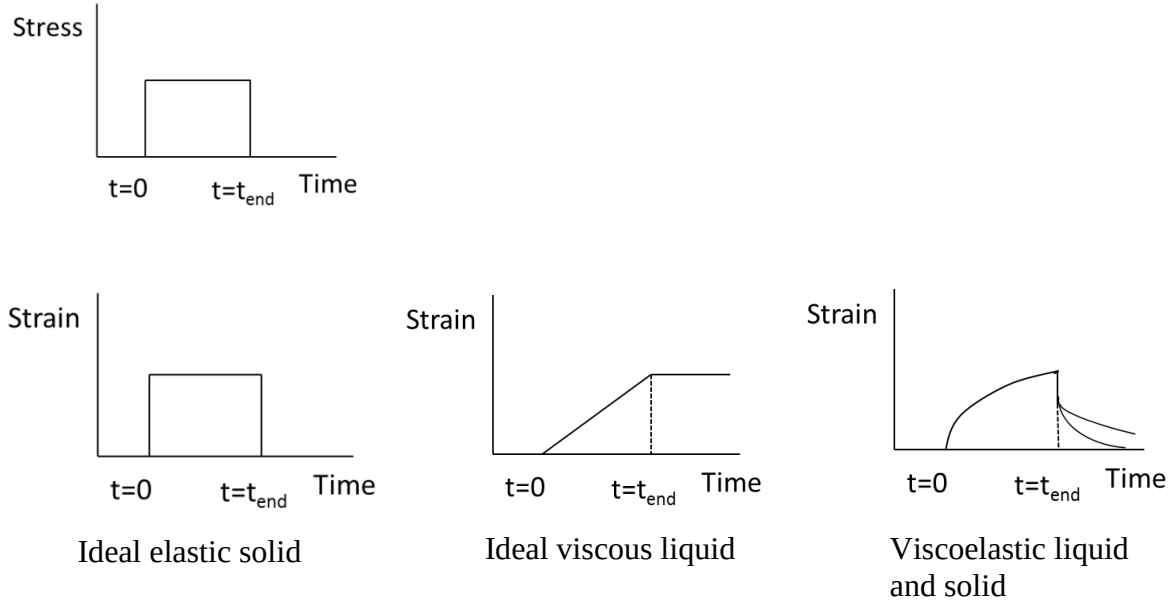

Figure 4-1 Creep responses for an ideal elastic solid, an ideal viscous liquid, and two different viscoelastic materials. A stress is applied to each sample at t=0 and is removed at $t=t_{end}$. Ideal solid recovers from the deformation perfectly after stress is removed. Ideal liquid cannot go back to the original state even after stress is removed. Viscoelastic materials show delayed recovery of deformation.

The fluid whose stress is linearly proportional to shear rate, i.e., the viscosity is constant over the entire shear rate range, is called a Newtonian fluid. The viscosity of an ideal liquid is defined as the ratio of the shear stress to the shear rate;

$$\frac{\sigma}{\dot{\gamma}} = \mu = \text{constant}$$

where σ is the shear stress, μ is the viscosity of the material, and $\dot{\gamma}$ is the shear rate.

Materials which cannot be defined by a single viscosity at a specified temperature are called non-Newtonian. The viscosity of these materials changes, corresponding to temperature and shear rate. Solution viscosity also depends heavily on both the size and concentration of the polymer molecules in solution. For these non-Newtonian fluids, the relationship between the shear stress and the shear rate is described as:

$$\frac{\sigma}{\dot{\gamma}} = \eta$$

where σ is the shear stress, η is the apparent viscosity, and $\dot{\gamma}$ is the shear rate.

In general, polymer solutions exhibit a Newtonian plateau at low shear rates, where the viscosity is independent of shear rate. At higher shear rates, a non-Newtonian region appears. For example, pseudoplastic polymer solutions show the shear thinning behavior, that the viscosity decreases as a function of shear rate, while dilatant polymer solutions show the shear thickening behavior that the viscosity increases as a function of shear rate, as seen in Figure 4-2. The power law is the empirical model that describes the change in viscosity with the shear rate:

$$\tau = k\,\dot{\gamma}^{n}$$

or

$$\eta = k\,\dot{\gamma}^{n-1}$$

if

n < 1 Shear thinning

n = 1 Newtonian

n >1 Shear thickening

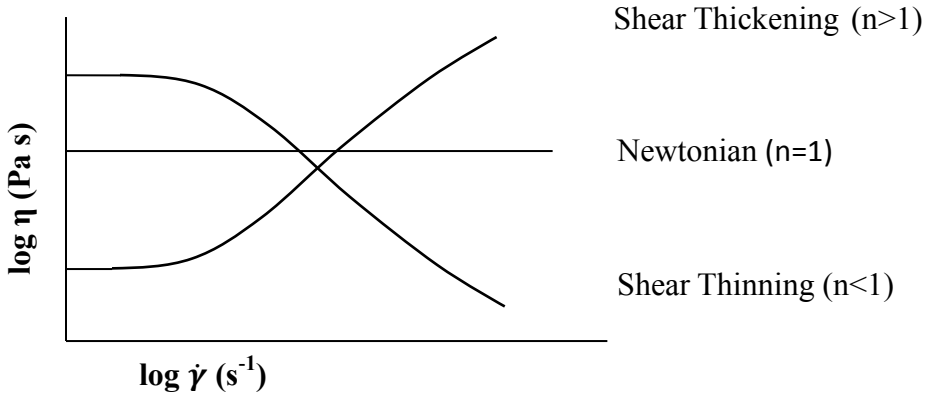

Figure 4-2 A typical viscosity versus shear rate plot for Newtonian fluids and non-Newtonian fluids, including pseudoplastic fluids (shear thinning) and dilatant fluids (shear thickening).

The viscoelastic materials have a stress relaxation time, that is, it takes time for a material to adjust to applied stresses or deformations, and is the inverse of the shear rate. The Deborah number (De) is defined as the ratio of the relaxation time to a characteristic time scale of deformation:

$$De = t_c/t_p$$

where t_c refers to the stress relaxation time and t_p refers to the process time. De incorporates

both the elasticity and viscosity of the material. When De >> 1, the material behaves like an ideal elastic solid, while if De << 1, then the material behaves like a purely viscous liquid. Moreover, there are some time-dependent viscoelastic behaviors including thixotropy and rheopexy. Thixotropy is defined as the decrease in the viscosity of certain gels and fluids that are viscous at rest over time when shaken, agitated, or otherwise stressed. On the other hand, rheopexy is the increase in the viscosity or even solidification under constant shear stress over time, which is much less common.

Rheometers are instruments that measure the rheological response of solids, semi-solids, and liquids. There are both shear and extensional rheometers, corresponding to a stress or strain that is applied to the material, which can be a shear stress/strain or an extensional stress/strain, respectively. Shear rheometers can be further classified into a strain-controlled rheometer that measures stress resulting from applied strain and a stress-controlled rheometer that measures strain resulting from applied stress. Rotational rheometers are most often used as shear rheometers, and involve two surfaces that contact the material, which are a stationary surface and rotational surface. The two surfaces can come in a variety of geometries. The three most popular geometries are cup/bob (couette), cone/plate, and parallel plates, as seen in Figure 4-3. In many cases, the bottom surface is fixed while the top surface (bob, cone, or plate) rotates. Furthermore, two different shear measurements can be obtained by rotational rheometers. First, the steady shear experiment measures a stress or a strain induced on a sample that contacts the surface rotating in a direction. Additionally, oscillatory shear measurements can be conducted, where the bottom plate is again stationary, while the top plate moves at a user prescribed oscillatory frequency or stress and strain amplitude.

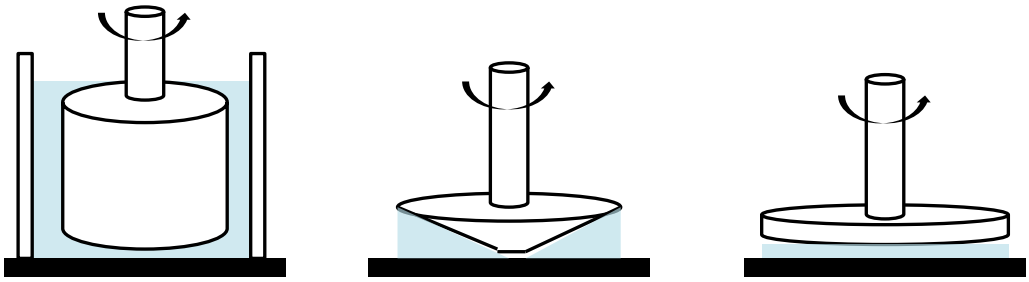

Figure 4-3 Measuring geometries for the rotational rheometer; couette, cone/plate, and parallel plates (from left to right).

There are two different frequency (ω) dependent functions that describe the viscoelastic properties of the gel, the storage modulus (G') and the loss modulus (G"). G' is the measure of elasticity of a material and it is the ability of the material to store potential energy and G" is the measure of the viscous behavior of the material and it is the ability of the material to dissipate energy, representing the elastic portion and the viscous portion, respectively. In general, the oscillatory test is performed in the linear viscoelastic regime, where the storage and loss moduli are independent of the strain amplitude. The phase lag (δ) between stress and strain, which changes between 0 and π/2, can also be used to describe the material behavior. When a material is ideally elastic, δ equals to zero, while a material is ideally viscous, δ equals to π/2. Viscoelastic materials exhibit behavior between purely elastic materials and purely viscous materials, resulting in δ values between 0 and π/2.

When a material is subjected to a shear deformation, the shear modulus is defined as a complex number;

$G^* = \tau_0/\gamma_0 = G' + iG'' = \sqrt{(G')^2 + (G'')^2}$

$G' = G^* \cos(\delta)$

$G'' = G^* \sin(\delta)$

where G* is the complex modulus, which is the ratio of the stress amplitude (τ_0) to the strain amplitude (γ_0). Another commonly used function, loss tangent (tan δ), denotes the ratio of viscous component to elastic component in a viscoelastic behavior of the material. The material exhibits a gel character if tan $\delta < 1$ ($G' > G''$), a viscous character if tan $\delta > 1$ ($G' < G''$), and a viscoelastic character if tan $\delta \leq 1$ ($G' \geq G''$). The point at tan $\delta = 1$ is the cross over where G' equals to G". Also, complex viscosity（η*）is a frequency-dependent viscosity function, which is defined as the difference between the dynamic viscosity (η') and the out-of-phase viscosity (η"). The dynamic viscosity and the out-of-phase viscosity are the real part and the imaginary part of the complex viscosity, respectively;

Loss tangent, $\tan \delta = G''/G'$

Complex viscosity, $\eta^*(i\omega) = \eta'(\omega) - i\eta''(\omega)$

Dynamic viscosity, $\eta' = G''/\omega$

Out-of phase viscosity, $\eta'' = G'/\omega$

The time it takes for G' and G" to intersect (G'= G") is called the crossover gel point, and has been known to be a function of frequency. This makes it difficult to determine

the exact gel point. A complementary criterion has been reported by Winter and Chambon[215] in 1985. They concluded that the critical gel point is defined as the point at which the following two conditions hold:

$$G'(\omega) \sim G''(\omega) \sim \omega^n, \quad 0 < n < 1$$

and

$$\tan \delta = G''/G' = \tan (n\pi/2)$$

where n is given by $n = 2\delta/\pi$, and called a relaxation exponent. It is independent of frequency. At the critical gel state, G' and G" are perfectly parallel with the same slope of n with independence of frequencies. That is, changes in tan δ over time (or over temperature) measured under different frequencies intersect at the gel point.

4.2 Materials and Methods

4.2.1 Preparation of Chitosan Derivative Solutions

Chitosan and the prepared chitosan derivatives were dissolved in 0.3 M of acetic acid (from Sigma-Aldrich) aqueous solution so as to mimic physiological ionic strength. The concentration of 0.02 g/mL was used as a basic sample solution, through the entire experiments.

4.2.2 Fabrication of Chitosan Derivative Film

The total amount of 20.0 g of 2% (w/w) solution of CIA derivative and unmodified chitosan in 0.3 M acetic acid were prepared, respectively. These solutions were cast into 85 mm diameter petri dishes. They were allowed to evaporate at room temperature over two days. All of the films were easy to peel and remove from the dishes.

4.2.3 Obtaining Blood

Venous blood from a donor horse was obtained by a venipuncture in the laboratory of Dr. Jennifer Davis, at Clinical Science, College of Veterinary Medicine, NC State University. The blood was collected into 2.7 mL plastic tube (light blue-top) containing 3.2 wt% of sodium citrate (0.109 M) as an anticoagulant. Also, bovine whole blood (gender unspecified) with 3.8 % sodium citrate (anticoagulant ratio of 1:9), sodium EDTA (anticoagulant ratio of 7.5:92.5), and sodium heparin (anticoagulant ratio of 1:99) were purchased from Lampire Biological Laboratories, Inc. (Ottsville, PA). Due to its less influence on the blood coagulation test, the sodium citrated blood was used for this study.

4.2.4 Rheological Tests on Chitosan Derivative/Horse Blood Mixture

Steady and dynamic rheological experiments were performed on a StressTech HR stress-controlled rheometer (ATS Rheosystems, Bordentown, NJ) with parallel plates geometry of 50 mm diameter and a plate gap of 0.4 mm. The chitosan derivative in 0.3 M acetic acid aqueous solution is mixed with certain amount of whole horse blood. The mixture

is put on the rheometer and changes in viscosity over stress, time, and frequency were measured at the physiological temperature of 37˚C. Dynamic frequency spectra were obtained in the linear viscoelastic regime of the samples, which storage modulus G' is constant with applied stress, as determined from dynamic strain sweep experiments.

4.2.5 Blood Coagulation Tests for Fabricated Films

A total of 1 mL of blood was transferred to each glass tube (10 x 75 mm) and it was pre-incubated for 5 minutes in a water bath at 37 ˚C. CIA film and unmodified chitosan film as control were cut into 1 x 1 cm in size. Half of the films were soaked in phosphate buffered saline (PBS, pH 7.4) for 30 minutes to be wet, while other half of the films were dried before the test. Each film specimen was put into the blood, and the tubes were placed and incubated at 37˚C until the blood was separated into two phases, supernatant and red blood cell aggregation. The tube was checked every 30 sec until the blood sedimentation was completed at almost 1:1 ratio of two phases.[216] The time of blood sedimentation was recorded for each sample. Four replicates or more were conducted. After 1.5 h, all tests were stopped and films were taken out from the blood. The blood clot formed on each film was captured by a digital camera.

4.3 Results and Discussion

4.3.1 Viscosity of Chitosan Derivatives

In order to determine the effect of the interaction between blood plasma protein and CIA derivative on the rheology of the blood, a series of rheological studies were carried out. First, the molecular weight has a profound effect on the viscosity of a solution. The molecular weight of chitosan used in this study is 312 kDa. Chitosan is a cationic polyelectrolyte in acidic solutions due to the protonation of its amino groups. The protonated polymer chains associate with each other in solutions, resulting in the much higher solution viscosity than a neutral polymer of similar size. Also, the coil expansion by the electrostatic repulsion due to charges on the polyelectrolyte contributes to this effect.

In addition, the solution can be divided into different viscometric regimes, depending on the polymer concentration; the dilute regime, semi-dilute regime, and concentrated regime. In dilute solutions, the polymer chains are isolated from each other in the solvent and the hydrodynamic volume and the conformation of the molecules are the most important parameters that determine the physical properties. As the concentration increases and the chain density in the solution becomes higher, the chains overlap with each other. The overlap concentration (c*) is defined as the boundary between the dilute regime and the semi-dilute regime, at which chains start overlapping. Further increase in the concentration causes chain entanglements. The entanglement concentration (c_e) is the boundary between the semi-dilute unentangled regime, where polymer chains overlap one another but are not entangled, and

the semi-dilute entangled regime, where the polymer chains significantly overlap one another and topologically constrain each other's motion.[217]

To determine entanglement concentration (c_e) for the chitosan sample, specific viscosity ($\eta_{sp} = (\eta_0 - \eta_s)/\eta_s$, where η_0 is the zero shear rate viscosity and η_s is the solvent viscosity) data are plotted against the solution concentration in Figure 4-4. Solutions span nearly two orders of magnitude concentration and a crossover from the semi-dilute unentangled to the semi-dilute entangled regime is observed as a change in slope at the solution concentration of 2.5 wt%. The c_e was, therefore, determined to be 2.5 wt%. The dependency of the specific viscosity on the polymer concentration has been investigated in the concentrated regime.[218-221] Dobrynin et al.[222] presented the scaling prediction for the specific viscosity for polyelectrolytes in excess salt;

$\eta_{sp} \sim c^{5/4(=1.25)}$ semi-dilute unentangled

$\eta_{sp} \sim c^{15/4(=3.75)}$ semi-dilute entangled

In semi-dilute unentangled solution, $\eta_{sp} \sim c^{1.56}$ was found in this investigation. This concentration dependence is in more or less agreement with the predicted relationship ($\eta_{sp} \sim c^{1.25}$).[222] In semi-dilute entangled solution, this study found $\eta_{sp} \sim c^{4.30}$. This concentration dependence is much stronger than predicted ($\eta_{sp} \sim c^{3.75}$).[222] This strong scaling dependence indicates the polymer chains are associating in solution.

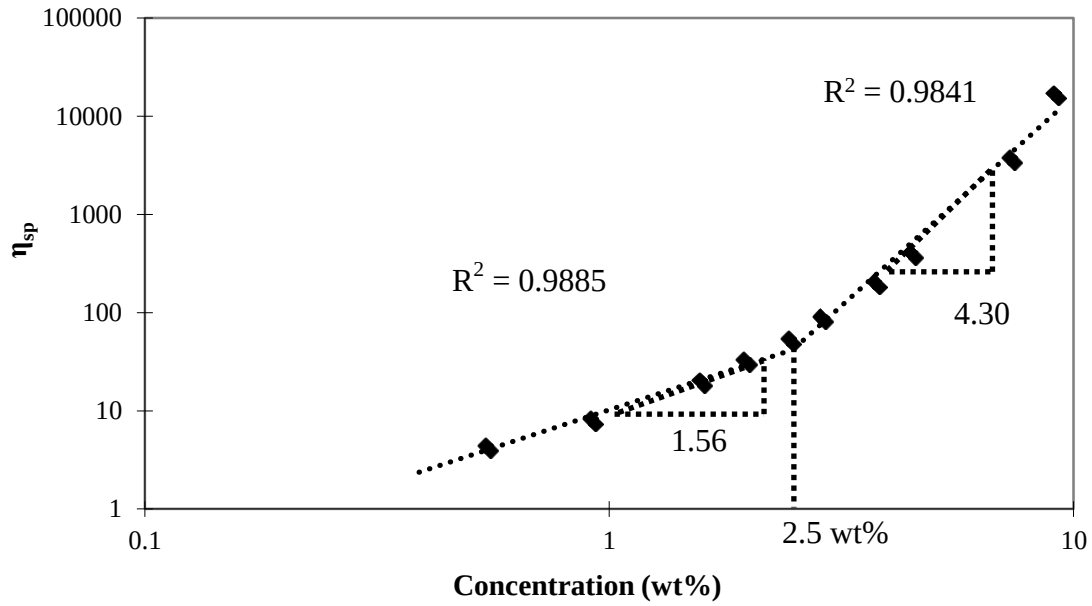

Figure 4-4 Plot of specific viscosity (η_{sp}) versus concentration for chitosan in 0.3M AcOH/0.2M AcONa aqueous solution. The entanglement concentration (c_e) of 2.5 wt% is determined by the change in slope (scaling exponent) on the above log-log plot.

4.3.2 Kinetics of Gelation of Blood Plasma Protein

The effects of CIA derivative and native chitosan on Na-citrated horse whole blood were investigated. Upon addition of CIA solution, liquid blood is instantly transformed into a self-supporting stable gel within a few seconds of mixing the polymer into blood, where the sample holds its weight upon tube inversion, while the mixture of chitosan and blood remains a freely flowing liquid as seen in Figure 4-5 (picture). These differences in flow properties were quantified by rheological measurements. First, the viscosity of the mixture is measured by changing applied stress to obtain the linear viscoelastic regime, where elastic modulus G'

is constant with stress. Then, time sweep tests at a constant frequency and frequency sweep tests at a constant stress were done on the mixture to understand gelling behavior of chitosan derivative and blood proteins. In each case, the polymer concentration in the overall mixture was adjusted to 1 wt% (1 mL of CIA/0.3 M AcOH (0.02 g/mL) + 0.8 mL of whole blood). Figures 4-6 shows data from oscillatory shear measurements on chitosan derivative/whole blood mixture and native chitosan/blood mixture, respectively. The data plotted are for the elastic and viscous moduli as functions of the angular frequency ω.

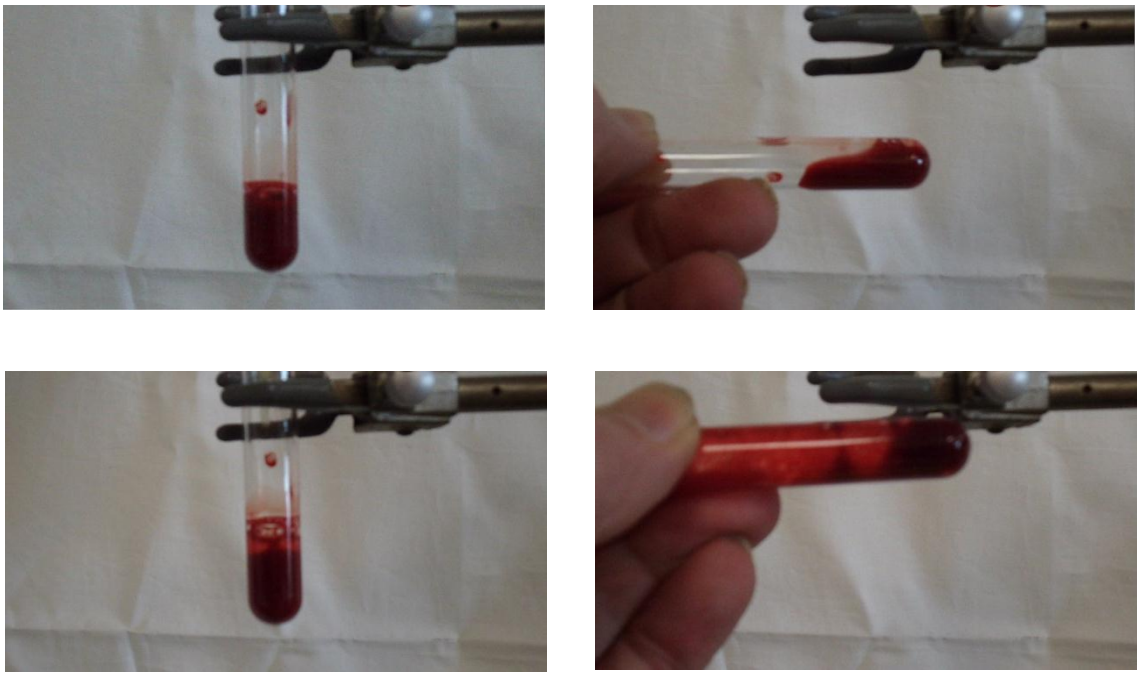

Figure 4-5 Effect of 2 wt% CIA in 0.3M aqueous AcOH on 3.2 % Na-citrated horse whole blood (anticoagulant ratio of Na-citrate to whole blood is 1 to 9). The photographs show that the freely flowing blood before the CIA solution was added turned to be a self-supporting gel that holds its weight in the inverted test tube.

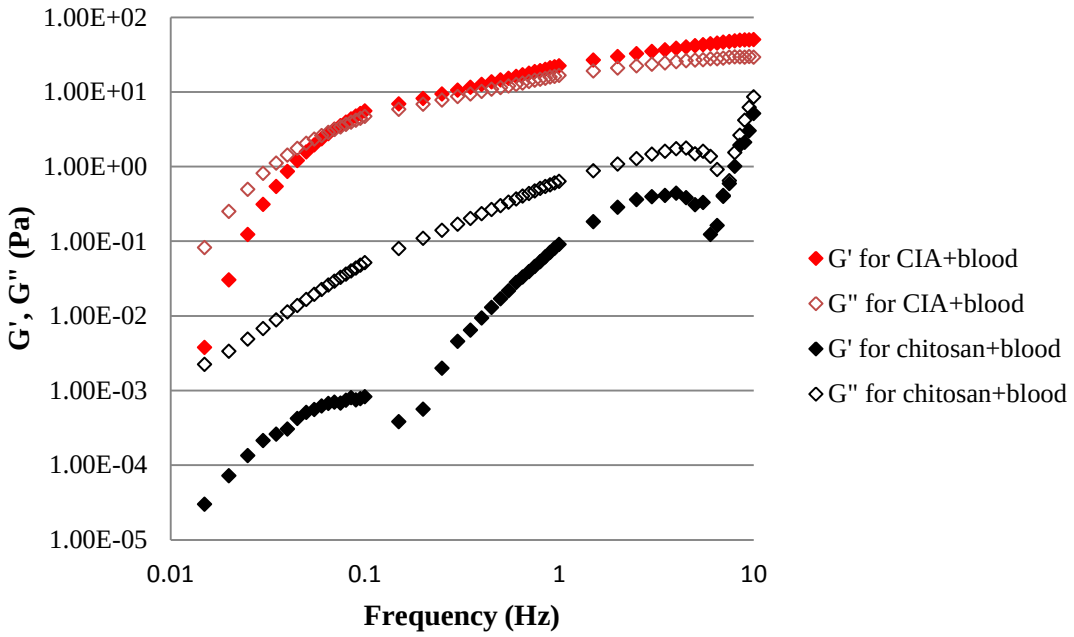

Figure 4-6 The dynamic rheological data for the elastic modulus (G') and the viscous modulus (G") versus frequency for the two samples. The CIA/blood mixture (red symbols) shows the rheology of an elastic gel (G' > G") whereas the chitosan/blood mixture (black symbols) responds like a viscous solution over the measurement frequency range.

As seen in Figure 4-6, the CIA/blood mixture shows an elastic response, which both moduli increase with the increase in the frequency but G' increases more sharply and it finally crosses over G" at a certain frequency. This frequency dependence of the moduli for CIA/blood mixture evidences the gel structure that is able to store the shear deformation, i.e., stress relaxation of this network occurs very slowly over long time scales. In contrast, native chitosan/blood mixture shows a viscous liquid response that G" exceeds G' over almost the entire frequency range.

Next, the changes in G’ and G” as functions of time is plotted in Figure 4-7. The polymer concentration in the overall mixture is also fixed to 1 wt%. As well as the result of the frequency sweep, this measurement also clearly confirmed that CIA solution induces the phase transition of the horse whole blood from a viscous liquid to an elastic gel in approximately 15 minutes after mixing. This profile is apparently different from those of the CIA solution itself without blood, or horse whole blood itself, that behave as typical viscoelastic liquids, indicating CIA solution has a possibility of interacting with certain blood factors and inducing its gelation. The unmodified chitosan solution also caused the phase transition, however, the crossover point of G’ and G” was reached in around 40 minutes.

Moreover, the sol-gel transitions of these samples were described with different rheological parameter. Figure 4-8 shows a change in tan δ (=G”/G’) as a function of time for the samples above. For the gel formation, the storage modulus rises much more sharply than the viscous modulus ($G' \sim \omega^2$; $G'' \sim \omega$) until it intersects with the loss modulus ($G' = G''$), then finally exceeds the loss modulus, corresponding to the increase in physical crosslink density. Therefore, the rate of change in tan δ for each sample over time can be a parameter to evaluate its gelation rate. This result confirmed that CIA/blood mixture exhibits highly elastic response with time, compared to unmodified chitosan/blood mixture. The mixtures show the decrease in tan δ with time, indicating the elastic component predominates over the viscous component in these samples. The two controls retain their viscous solution properties, although the viscosity values gradually increase over time because of the slightly-higher measurement temperature of 37˚C. Table 4-1 shows the time which it takes for G’ and G” to

be twice, equal, and half to each other, comparing the chitosan derivative sample to the unmodified chitosan sample.

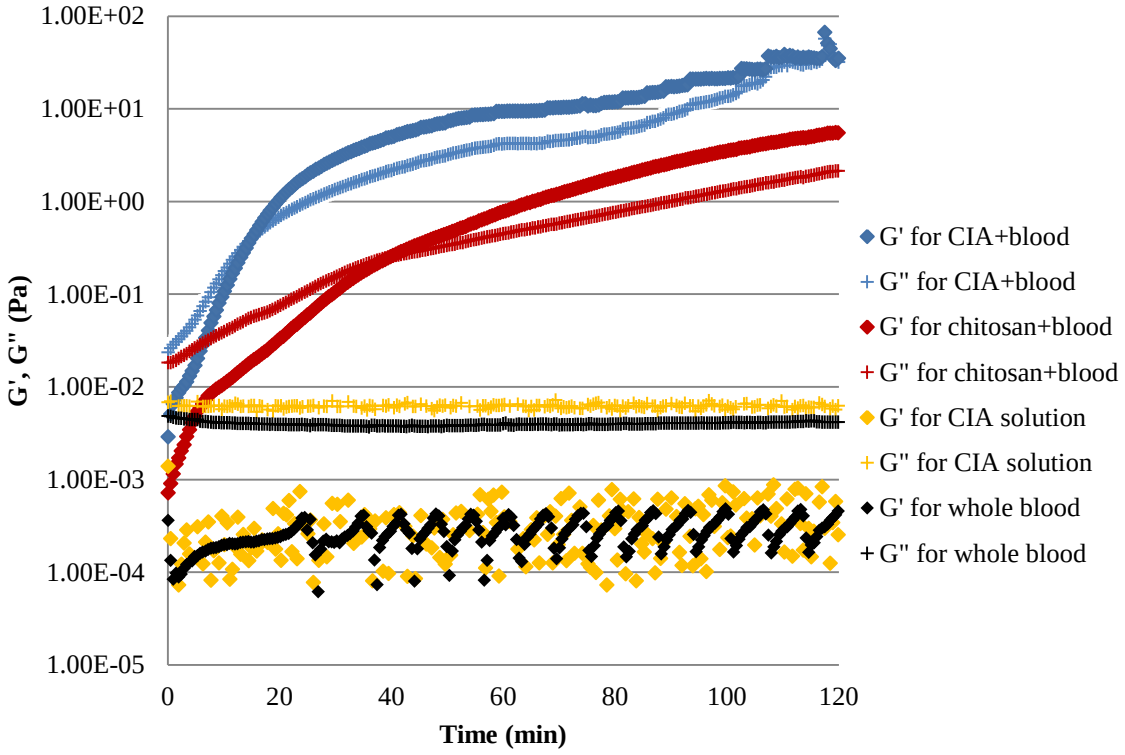

Figure 4-7 The dynamic rheological data for the elastic modulus G' and the viscous modulus G" versus time are shown for the two samples and two controls. The CIA sample (blue symbols) displays a gel response (G' > G") much faster than the chitosan sample (red symbols). The CIA solution (yellow symbols) and the Na-citrated horse whole blood (black symbols) respond like viscoelastic solution (G' < G") throughout the measurement.

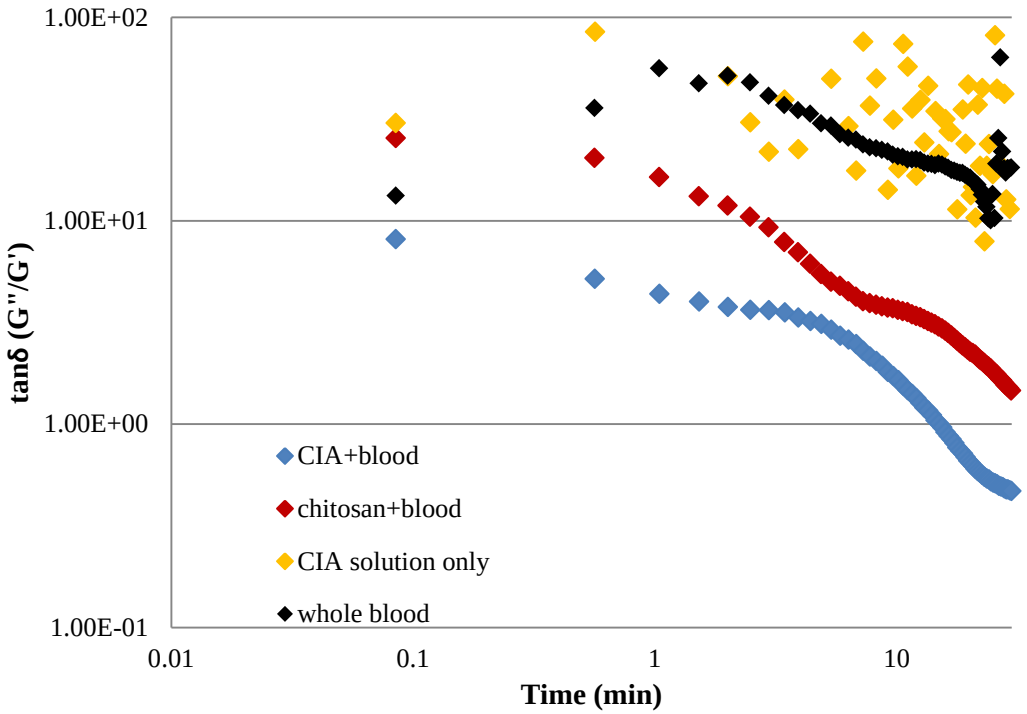

Figure 4-8 The changes in tan δ as a function of time (log-log scale) for the various samples. The CIA/blood sample (blue symbols) and chitosan/blood sample(red symbols) exhibit the significant decrease in tan δ with time whereas the CIA solution (yellow symbols) and Na-citrated horse whole blood (black symbols) exhibit little change in tan δ with time.

Table 4-1 Gel time of the CIA/horse whole blood and the chitosan/horse whole blood systems at 37 ˚C

Sample	Time (min) at G"/G' = 2	Time (min) at G"/G' = 1 (crossover time)	Time (min) at G"/G' = 1/2
CIA/blood	8.30	15.01	26.30
Chitosan/blood	23.10	39.87	67.21

G"/G' = 1 indicates the onset of gelation.

Moreover, the changes in complex viscosity (η*) of various samples are plotted in Figure 4-9. The complex viscosity increases considerably on the addition of CIA solution into the whole blood. The Na-citrated horse blood did not show any observable increase in the complex viscosity, proving that the CIA solution interacts with the blood and somehow triggers the rapid gel formation.

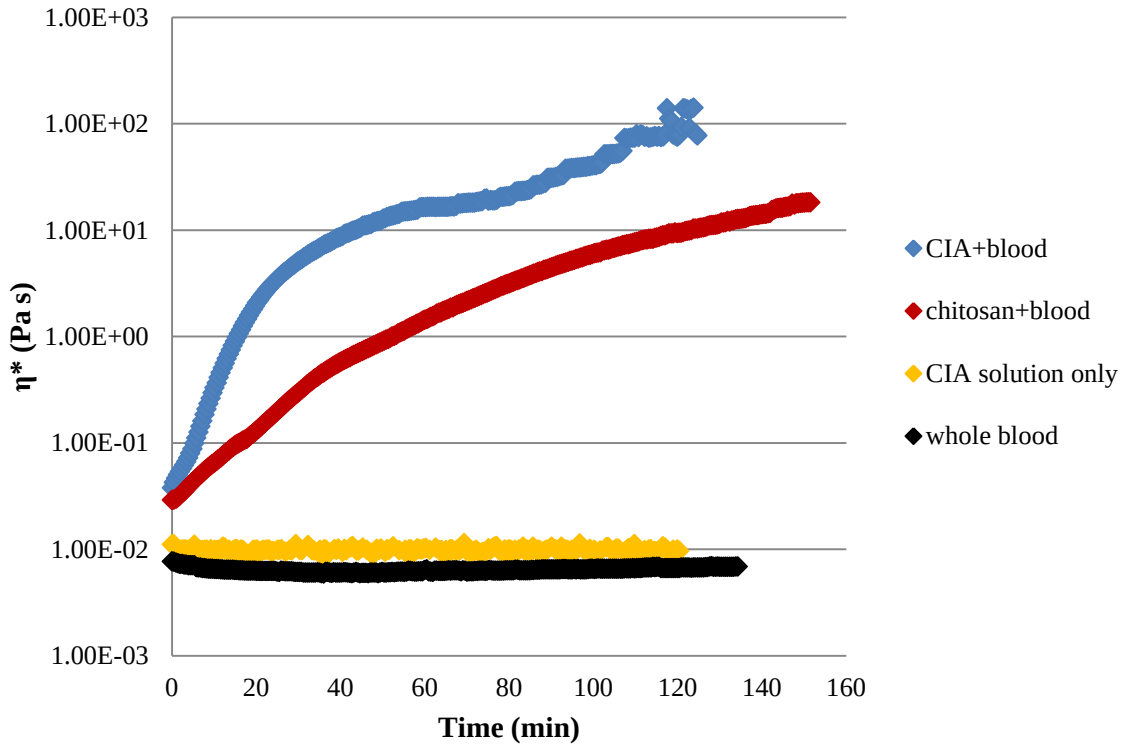

Figure 4-9 Complex dynamic viscosity (η*) versus time for CIA/horse whole blood mixture and the several controls.

Next, the changes in G' and G" on CIA /blood sample (0.02 g in 1mL 0.3 M AcOH/ 0.8 mL blood) over time were measured at three different frequencies (Figure 4-10). The mixture underwent the change from a viscous solution to an elastic gel at certain crossover points for all three frequencies. The increase in frequency causes the shift of the crossover points to shorter times, which is indicative that the sample is exposed to faster deformations at higher frequencies, as a result, it exhibits the gel response earlier.

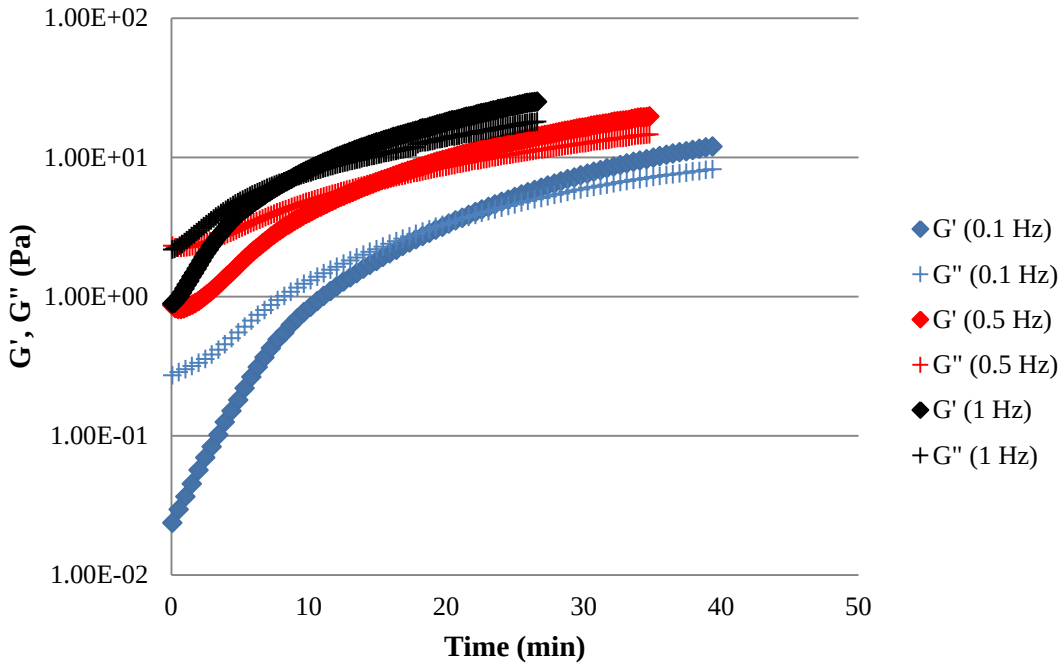

Figure 4-10 The changes in G' and G" over time for the 2 wt% CIA solution/Na-citrated horse whole blood under three different frequencies; 0.1 Hz, 0.5 Hz, and 1.0 Hz.

The variation in loss factor (tan δ) at various frequencies can be used to determine the gel point based on the criteria defined by Winter and Chambon.[215] At the gel point, G' equals to G" with independence of frequencies, resulting in the constant tan δ at different frequencies at the gel point. The change in tan δ over time at several frequencies is shown in Figure 4-11 for the mixture above. The crossover was reached at around 22 minutes, 15 minutes, and 10 minutes at 0.1 Hz, 0.5 Hz, and 1 Hz, respectively. From the Figure, tan δ becomes independent of frequency at approximately 26 minutes, indicating the formation of a gel. Table 4-2 lists the gel time measured for the mixture of 1 mL of 2 wt% CIA in 0.3 M aq. AcOH/ 0.8 mL of horse whole blood. The gelation relaxation exponent (n) is the power law index of G' and G" as a function of frequency and is calculated by following the Winter and Chambon[215] criteria. The relaxation exponent is a specific parameter that is related to the growing clusters in a material near the gelation threshold. The relaxation exponent at the gel point was determined as 0.41 for this sample from the tan δ plots.

At a gel point,

$$G'(\omega) \sim G''(\omega) \sim \omega^n, \quad 0 < n < 1$$

and

$$\tan \delta = G''/G' = \tan (n\pi/2)$$

where n is the relaxation exponent.

Table 4-2 Gel point, tan δ, and relaxation exponent (n) of CIA/horse whole blood mixture

Gel point (min)	tan δ	n
26	0.75	0.41*

$* \ \mathrm{n} = \ \tan^{-1}(\tan\delta, radian) * (\frac{2}{\pi})$ [215]

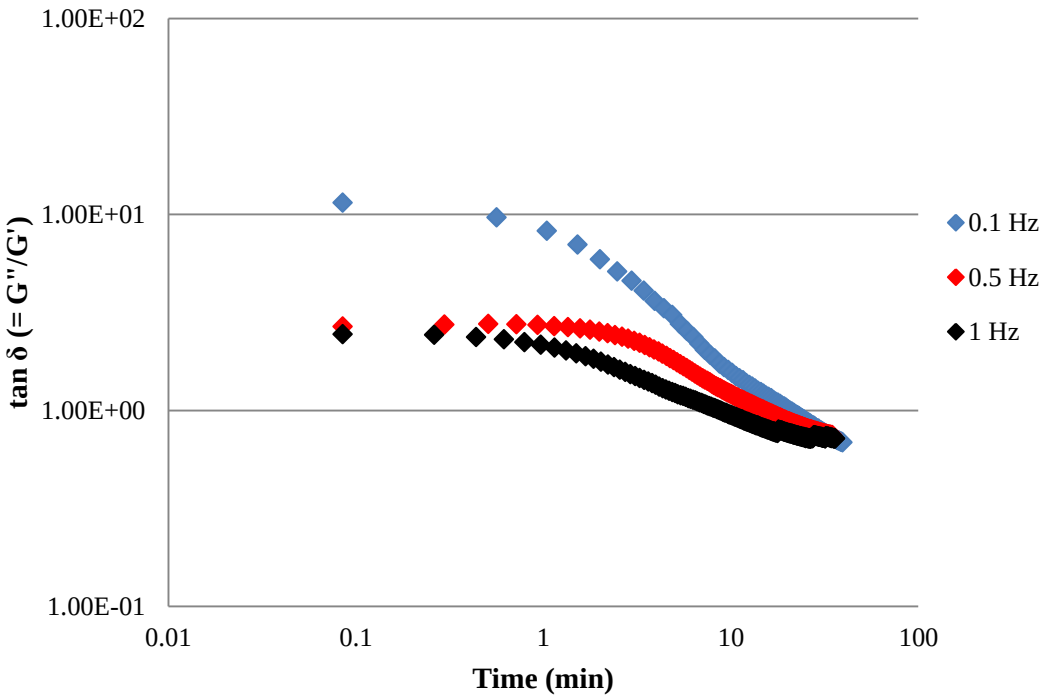

Figure 4-11 The plot of tan δ versus time for the CIA/horse whole blood mixture at three different frequencies; 0.1 Hz, 0.5 Hz, and 1.0 Hz.

4.3.3 Effect of Concentration of Chitosan Derivative on Blood Coagulation

In the previous section, the mixture of 1 mL of 2wt% CIA in 0.3 M AcOH mixed with 0.8 mL of whole blood was shown to induce the transformation of liquid blood into an

elastic gel in approximately 15 minutes. In this section, three different ratios of CIA/blood mixture were studied on their blood gelation in order to determine the best ratio for inducing the rapid gelation. In particular, CIA solutions were mixed with the blood by volume ratio of 3:1, 1:1, and 1:3 (CIA: blood), keeping the total mixture volume constant (1.8 mL). The rheological tests were carried out on each mixture. Figure 4-12 shows the both elastic and viscous moduli of each sample as functions of frequency. The CIA solutions all have a very different response, especially at low frequencies. As seen in this Figure, the mixture whose ratio of polymer content to blood content equals to 1:3 (vol:vol) immediately turned into an elastic gel, right after mixing, which can be seen in Figure 4-5. This gelation is incomparably faster than that seen in the mixture by ratio of 3:1 (CIA: blood).

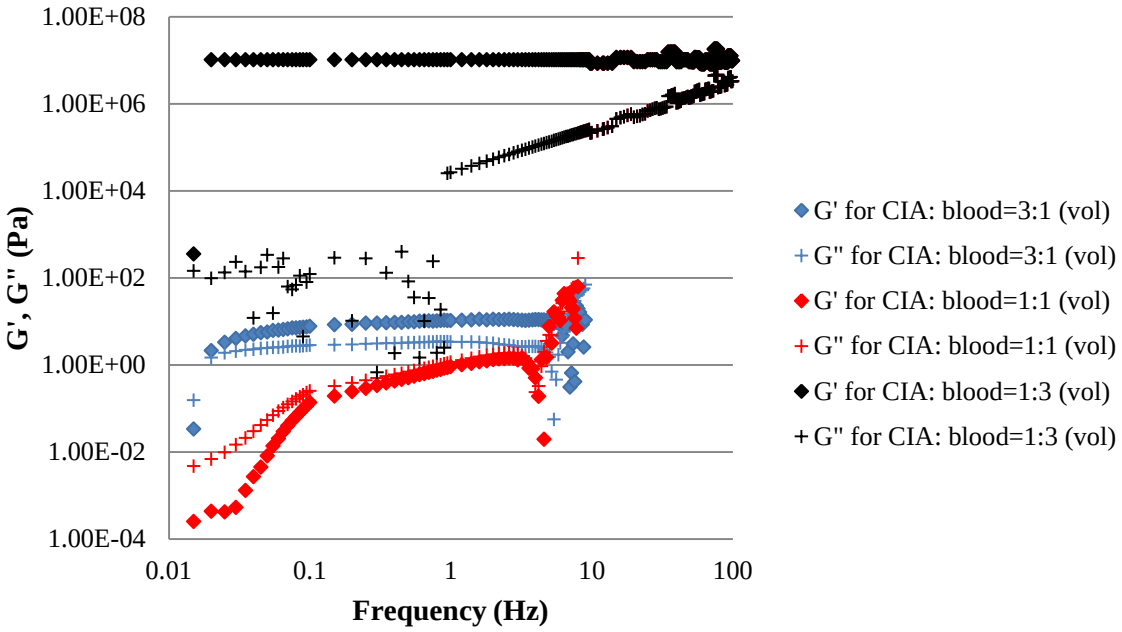

Figure 4-12 The elastic modulus (G') and the viscous modulus (G") versus frequency for the three CIA/blood mixture samples with different volume ratios of the CIA component to Na-citrated horse whole blood content; 3:1 (blue symbols), 1:1 (red symbols), and 1:3 (black symbols).

In addition, the change in both elastic and viscous moduli over time under constant stress and frequency was tested on three mixtures by the different ratio of polymer content to blood content, as shown in Figure 4-13. The mixture of 3:1 exhibited the solution property at first that G" is larger than G' and subsequently G' became over G" after 15 minutes. The mixture of 1:1 showed similar moduli changes over time, but the crossover of both moduli, in contrast, happened at 9 minutes after the mixing. The initial viscosity of this mixture was lower than that of the mixture of 3:1. This would be explained in that the viscosity of blood is much lower than that of CIA solution, thus, the raise of blood content from 1/4 to half in the mixture leads to the reduction of overall viscosity of the mixture. However, the viscosity of the mixture of 1:1 increased much faster and reached the crossover point earlier. In sharp contrast to these two mixtures, the mixture of 1:3 became an elastic gel before measurements could begin, confirming the rapid blood gelation at this concentration ratio. This gel structure, however, cannot be retained approximately after 70 minutes, when G" becomes larger than G' again. Figure 4-14 demonstrates the change in tan δ with time. This result supports that the mixture of 1:3 reaches the gel state right after the mixing and consequently tan δ (= G"/G') stays constant, keeping G' larger than G" over time. In addition, the mixture of 3:1 and 1:1 also gradually become gels with time, however, these gel structures are not stable as seen for the mixture of 1:3, and the solution behavior appears again approximately after 1 hour of mixing.

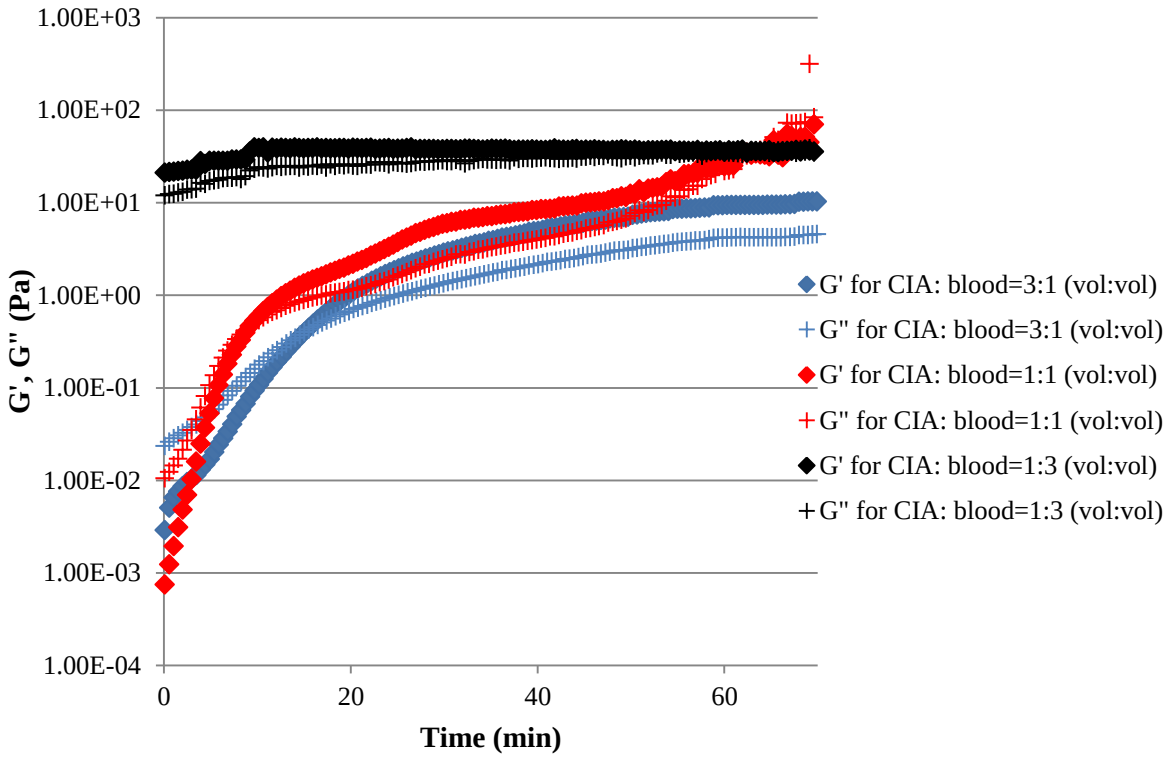

Figure 4-13 The elastic modulus (G') and the viscous modulus (G") versus time for the CIA/horse whole blood mixture samples with three different volume ratios of the CIA component to whole blood content; 3:1 (blue symbols), 1:1 (red symbols), and 1:3 (black symbols). The measurements were done under a constant frequency of 0.1 Hz.

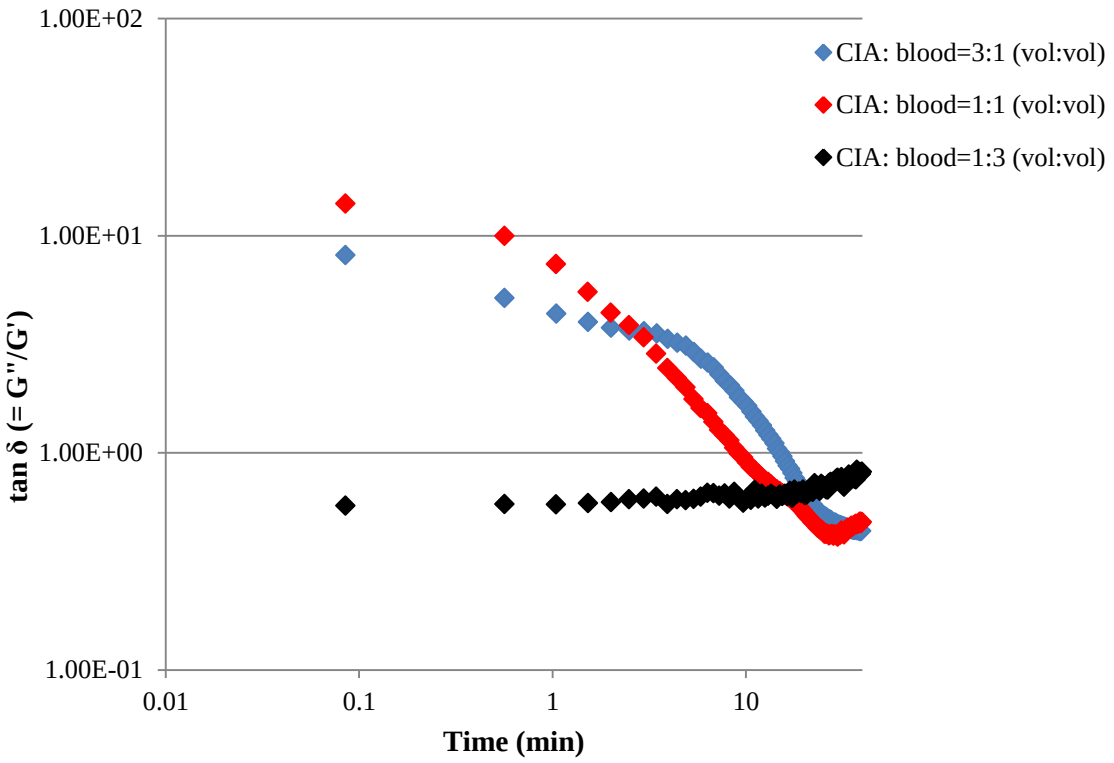

Figure 4-14 The plot of tan δ versus time (log-log scale) for the CIA/horse whole blood mixture with the three different volume ratios of the CIA content to horse whole blood content; 3:1 (blue symbols), 1:1 (red symbols), and 1:3 (black symbols).

Table 4-3 Gelation kinetics of the three different CIA/horse whole blood mixtures

Composition of CIA:blood (vol:vol)	Time (min) at G"/G' = 2	Time (min) at G"/G' = 1	Time (min) at G"/G' = 1/2
3:1	8.30	15.01	26.30
1:1	4.88	8.95	21.18
1:3	NA	NA	Upon mixing

4.3.4 Yield Stress of Chitosan Derivative/Blood Mixtures

Next, steady shear stress was applied on the sample whose ratio of CIA content to blood content was equal to 1:1 (vol:vol) and the change in its viscosity was measured as shown in Figure 4-15, where the apparent viscosity is plotted as a function of shear stress. Under the same condition, the measurements were applied on unmodified chitosan/blood mixture and whole blood itself as controls.

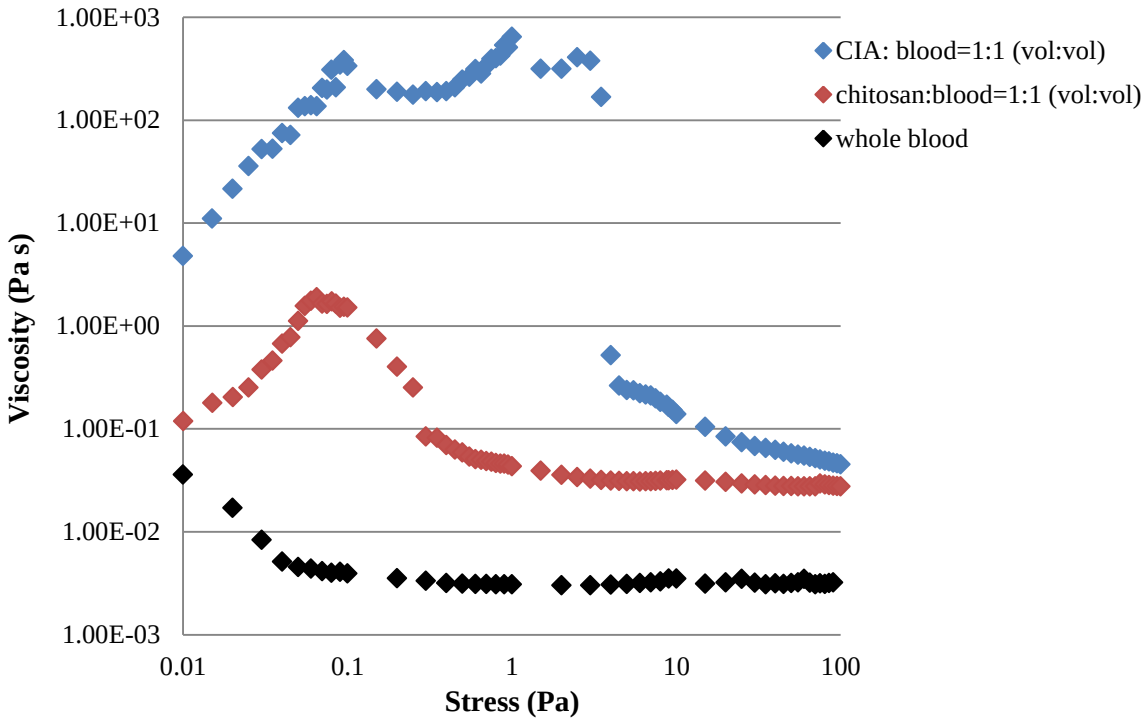

Figure 4-15 Steady-shear rheological data for the viscosity vs. shear stress. The CIA/blood mixture (blue symbol) shows a significantly higher viscosity relative to both the chitosan/blood mixture (red symbol) as well as a Na-citrated horse blood with no polymer solution (black symbol).

The viscosity of blood at 37 ˚C has been reported as 3 x 10^{-3} to 4 x 10^{-3} Pa s.[223] As seen in Figure 4-15, the blood itself has the apparent viscosity of around 3 x 10^{-3} Pa s that is consistent with the literature data. The CIA solution or chitosan solution showed anywhere from three to five order of magnitude increase in viscosity at low stresses. Unmodified chitosan/blood mixture has a low shear viscosity of around 1 Pa s, which is about 300 times that of blood alone. However, this high viscosity does not last with increasing applied stress, indicating that unmodified chitosan is not capable enough of inducing the stable blood gelation. It is notable that CIA/ blood mixture, on the other hand, exhibits a zero-shear plateau at low stresses, and then eventually shear thinning occurs once higher stresses (>2 Pa) have been obtained. This mixture has a low shear viscosity around 3000 Pa s, which is nearly a million-fold higher than that of blood, moreover, this high viscosity can be retained until the stress increases up to around 2 Pa. Under the stress above around 2 Pa, the viscosity of the mixture exhibited the steep drop. This figure indicates that the CIA derivative/blood mixture turns to an elastic gel with the applied stress and hardly flows at stress below 2 Pa. At stress above 2 Pa, the gel structure breaks. Similarly, other groups reported that their hydrophobically modified chitosan solution exhibited the comparable increase in the viscosity after mixing with blood and had a yield stress of 2 Pa.[97] The CIA solution of 2 % (w/v) has a dynamic viscosity of about 0.01 Pa s in the low shear regime, indicating that the sample is slightly viscous but far from being a gel (ex. dynamic viscosity of water at 37˚C ≈ 0.7x10^{-3} Pa s). This explains the gelation behavior seen in photographs in previous section (Figure 4-5), where the sample turned to be an elastic gel and does not flow down in the inverted tube.

4.3.5 Blood Coagulation Tests of Chitosan Derivative Film

The blood coagulation test was conducted by measuring the time of red blood cell sedimentation in the Na-citrated blood. A standardized method called erythrocyte sedimentation rate (ESR) has been widely used for one of the diagnosis of various diseases.[216] The ESR is a simple non-specific screening test that indirectly measures the presence of inflammation in the body. It reflects the tendency of red blood cells to settle more rapidly in the face of some disease states, usually because of increases in plasma fibrinogen, immunogloblins, and other acute-phase reaction proteins. Changes in red blood cell shape or numbers may also affect the ESR. When anti-coagulated whole blood is allowed to stand in a narrow vertical tube for a period of time, the red blood cells settle out from the plasma under the influence of gravity. The rate at which they settle is measured as the number of millimeters of clear plasma present at the top of the column after 1 hour (mm/hr). There are two main methods used to measure the ESR: the Westergren method and the Wintrobe method. The Westergren method is frequently used, which 2 mL of venous blood containing 0.5 mL of sodium citrate is drawn into a specific glass tube (2.5 x 300 mm) to the 200 mm mark. The tube is placed in a rack in a strictly vertical position for 1 hour at room temperature, at which time the distance from the lowest point of the surface meniscus to the upper limit of the red blood cell sediment is measured. The distance of fall of erythrocytes, expressed as millimeters in 1 hour, is the ESR. As described in Chapter 1, the mechanism of hemostatic action by chitosan has been known to occur outside of the coagulation pathways, either the extrinsic or intrinsic pathway. Also, the proposed rapid clot formation by iodoacetic acid is considered as a result of the covalent crosslinking formation

between the sulfhydryl compounds in the blood, that is, it similarly works outside of pathways without influencing the plasma coagulation factors. Therefore, any change in the blood sedimentation rate for the whole blood added the CIA film would be concluded that the film brings about the change in the red blood cell shape and resultant change in ESR.

In this study, conventional glass tubes (7.5 x 10 mm) were used to see whether the blood sedimentation is observed or not, by addition of fabricated chitosan and CIA derivative films into the tube with 1 mL of whole blood containing 3.8% of sodium citrate (coagulant ratio against blood is 1:9). The blood sedimentation time for various films, which the time when the supernatant and erythrocyte agglutination were separated as equal phases at 1:1, was measured.

In conclusion, the separation of the 3.8% Na-citrated blood into the supernatant and erythrocyte agglutination by adding the film was not observed for either the chitosan or the derivative during the entire measurements of up to 150 minutes. However, the incubated blood with the CIA film clearly showed the increased viscosity from round the film (Figure 4-16). After 10 minutes of incubation, the blood in the test tube upside down was almost gelled even though it was not stable. It is, however, noted that the blood with the derivative film again started flowing around after 1 hour and did not turn to be a perfect gel after 150 minutes-incubation although the film taken out from the test tube after the measurement had some blood clots on it. On the other hand, the control blood sample and the blood with the chitosan film did not show such increase in the viscosity over time, as shown in Figure 4-17, 4-18. These controls support the effect of the derivative film on formation of blood clots. Surprisingly, the films did not dissolve in the blood pool during the experiments. However, a

certain amount of shrinkage was observed for CIA film. This suggests that the obvious dissolution of the films could not be seen, however, it might gradually have dissolved from the surface and increased the sample viscosity.

The blood used in this study contained sodium citrate as the anti-coagulant agent, which can chelate calcium ions that are crucial for the coagulation cascade reaction. Therefore, the result indicates that the derivative film promoted the clot formation in the absence of enough calcium ions, suggesting a possibility that it works independently from the natural coagulation pathways. Chitosan generally activates platelets during hemostasis by the ionic affinity. At this point, the detailed mechanism how the derivative triggers and induces the clot formation is unclear. One possibility is the interaction with the blood cells, including red blood cells and platelet, chemically through the sulfide bonds.

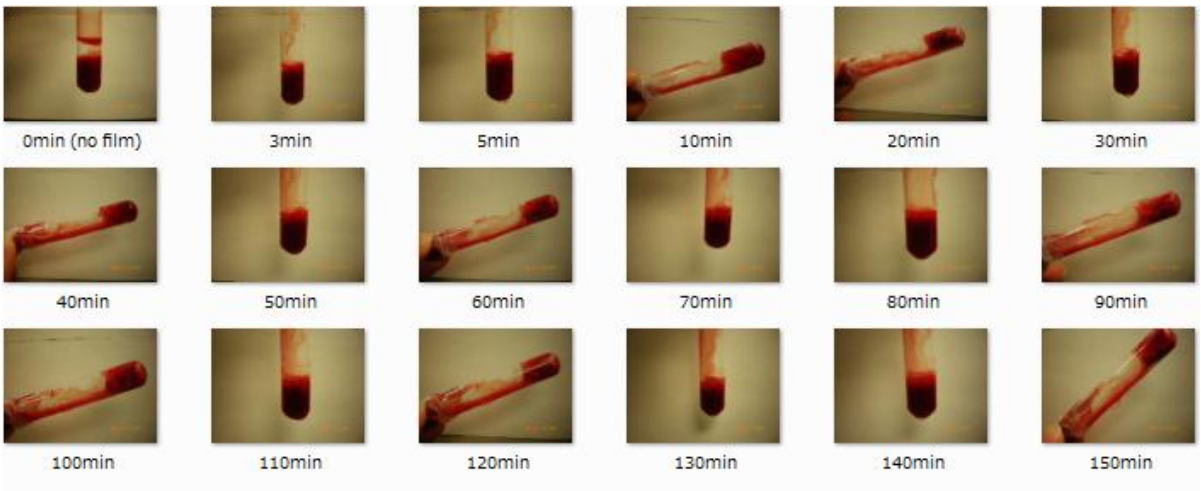

Figure 4-16 The Na-citrated bovine blood with the addition of the CIA film in a test tube (7.5 x 10 mm) incubated in a water bath at 37˚C for 150 min. The test tube was taken out from the bath and photographed periodically.

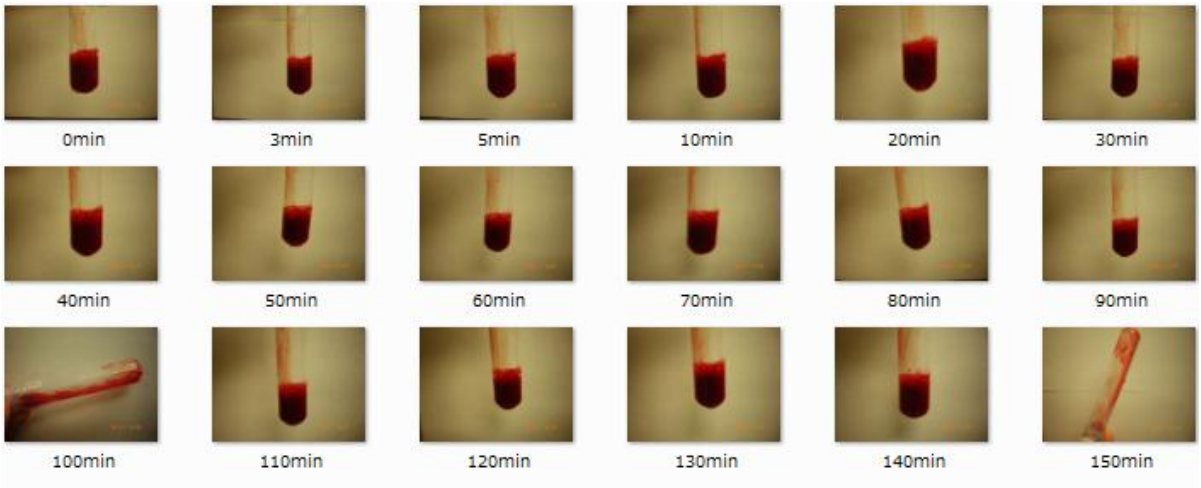

Figure 4-17 The Na-citrated bovine blood without any film in a test tube (7.5 x 10 mm) incubated in a water bath at 37˚C for 150 min.

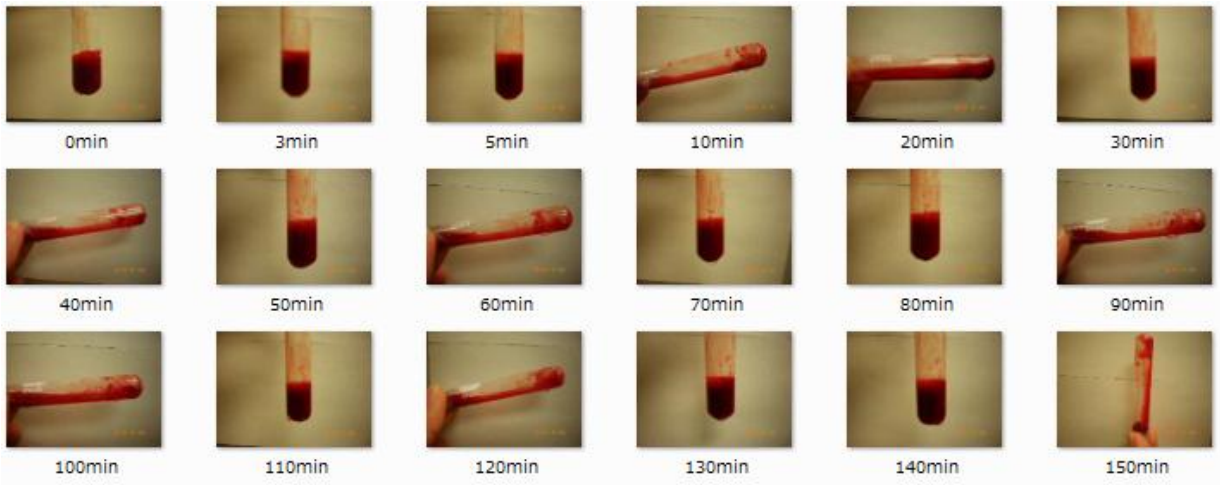

Figure 4-18 The Na-citrated bovine blood with the addition of the unmodified chitosan film in a test tube (7.5 x 10 mm) incubated in a water bath at 37˚C for 150 min.

Figures 4-19 and 4-20 show the CIA derivative film and the unmodified chitosan film respectively that were taken out from the blood pool after the incubation at 37˚C for 150 minutes. First, the CIA film shrunk and wrinkled up once it was put into the warmed blood

tube, on the other hand, the unmodified chitosan remained its original form even after the incubation. This result indicates that the crystallinity of the CIA became lower than the chitosan and the amorphous region was increased due to the introduction of the bulky iodoacetyl groups, resulting in the lower mechanical strength of the CIA film than that of unmodified chitosan film. In addition, a larger amount of blood clots were observed on the CIA film after 150 minutes.

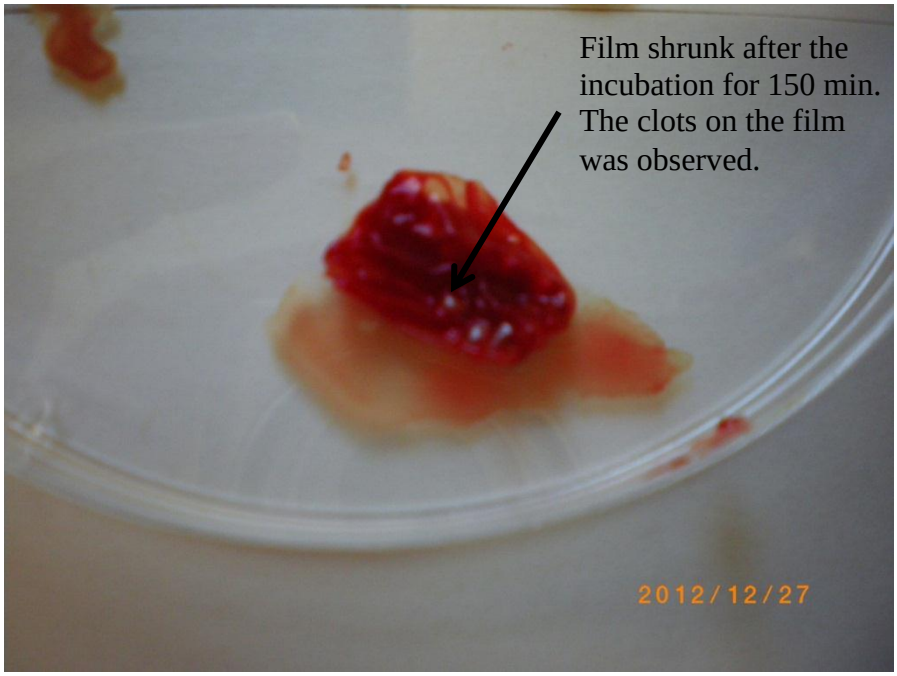

Figure 4-19 The photo of the CIA film taken out from the Na-citrated blood after 150 min of the incubation.

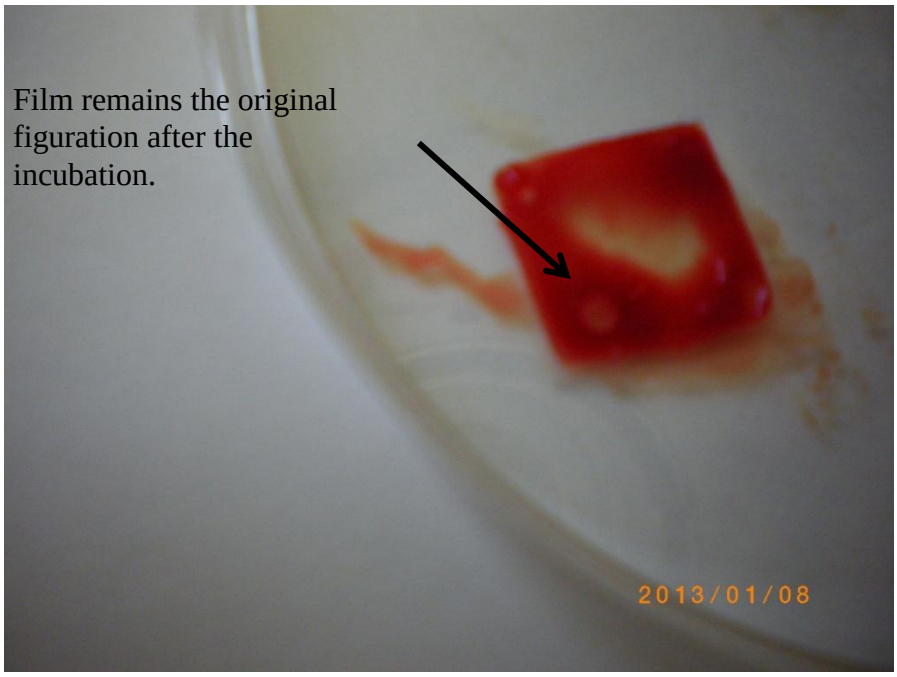

Figure 4-20 The photo of the chitosan film taken out from the Na-citrated blood after 150 min of the incubation.

4.4 Conclusion

The rheological studies are a key for this study. This chapter focused on the gelation behavior of the whole blood sample induced by the interaction with CIA derivative. The blood gelation could be optically observed. Dynamic oscillatory measurements and steady shear measurements revealed that the CIA derivative solution apparently gave rise to blood coagulation. The time for the blood to transform from a viscous liquid to an elastic gel highly depended on the polymer content in the total mixture. The study elucidated that there is a specific polymer content that induces the quickest blood coagulation. The ratio of CIA solution content against blood content was controlled, as a result, blood of three times as

many as the derivative solution could cause the quickest blood gelation. In this case, the blood turned to a gel right after the mixing with the derivative solution. The addition of larger volume of the derivative solution reduced the blood viscosity, on the other hand, the blood gelation proceeded slowly or it did not even happen. The blood clots which formed were later weakened after a few hours. The firm clot was formed after the mixing and it returned to liquid state (although red blood cells were partially aggregated) after several hours. Fibrinolysis is a process that prevents blood clots, which has two types: primary fibrinolysis (a normal body process) and secondary fibrinolysis (a breakdown of clots due to a medicine, a medical disorder, or some other cause). In fibrinolysis, a fibrin clot is broken down by the action of an enzyme, called as plasmin. Through a positive feedback mechanism, plasmin cleaves fibrin, generating soluble degradation products that are cleared by other proteases or by the kidney and liver. Initiation of fibrinolysis occurs through a number of orchestrated interactions between fibrin, plasminogen and its activator tPA which result in generation of plasmin. The CIA system works outside of the coagulation pathways, but the clot it forms, would eventually undergo the physiological fibrinolysis process, nevertheless, we can still expect its potential as a first-aid hemostatic system.

As revealed in Chapter 3, the reaction between iodoacetic acid and free sulfhydryl groups of L-cysteine preferably occurs at slightly basic condition. The solution pH of around 8 (at least above 5) is required to maximize this reaction. Thus, the pH environment of the reaction mixture is an important parameter. The pH value of CIA in 0.3 M AcOH is around pH 3 and the normal blood is regulated to stay within the narrow range of pH 7.35 to 7.45, making the mixture almost neutral.[224] In practice at the moment, the addition of chitosan

derivative solution reduces the blood pH outside of the normal value. This is a challenge for future studies. Presently, the chitosan derivative needs an acidic solvent to be dissolved. If a more water soluble derivative can be obtained, that would be a useful. As one of the potential solutions, it has been reported that chitin with around 50% of deacetylation is soluble in water.[225] This improved solubility of chitin with 50%DD would be attributed to the partial deacetylation which brought about the amorphousness of the polymer by the destruction of secondary structure and also the increase of the hydrophilic property on account of the increased number of amino groups.

The iodine content in the CIA would be another parameter that affects the interaction with the blood. We have prepared several CIA derivatives with different iodine contents, 4wt%~10wt%. If more iodine atoms are present, the greater opportunity there would be to react with cysteine in the blood proteins. However, the higher iodo substitution of amino groups of chitosan resulted in a lower solubility. Also, the cationic property of chitosan would be lost for the higher substitution. The positively charged chitosan in acidic condition has been considered to be involved in the blood coagulation by the ionic interaction between negatively charged red blood cell membrane.[81] Therefore, the iodo contents in the chitosan derivative might not be proportional to the induced blood coagulation. The relationship between iodine content in the derivative and the resultant blood coagulation has not been addressed in this research. Further studies are needed to clarify the best substitution ratio that causes the interaction with blood proteins to a maximum extent.

CHAPTER 5

5 Rheological Properties of Blood Plasma Protein

The previous chapter confirmed that the CIA derivative has the ability to induce blood clot formation, imitating the formation of the natural fibrin clots. Although the detail mechanism of the observed formation of blood gel is still uncertain, we strongly assume that the blood cells are chemically crosslinked in the network rather than being physically trapped in a polymer mesh through the sulfide bonds between sulfhydryl moiety and iodoacetic acid. In order to accelerate gel formation, there is a need to understand the gelling behavior and identify and induce crosslinking reactions to interact with as many blood proteins as possible. The objective of this chapter is to investigate the rheological properties of blood plasma proteins involved in the observed rapid transformation of a liquid blood into a gel.

5.1 Introduction

It is generally accepted that pronounced red blood cell (RBC) aggregation is a major factor contributing to an increase in whole blood viscosity at low shear. RBC aggregation affects blood viscosity most markedly in areas of low shear stress (< 4 dyn/cm^2 (or < 0.4 Pa)), which is prevalent at atherosclerosis (or thrombogenesis)-prone sites.[226] Increased RBC aggregation and the resulting elevated blood viscosity promote low-flow blood stream, i.e., a condition that favors thrombogenesis.[227] Regional low flow resulting from RBC aggregation can, therefore, set the stage for vascular thrombosis. Aggregation of RBCs is governed by opposing forces that dis-aggregate RBCs: the repulsive electrical force between negatively

charged cells and the shear force exerted by blood flow. On the other hand, the cohesive force induced by the presence of various plasma proteins promotes the formation of rouleaux structures and larger aggregates.[228,229] A rouleaux structure is described as stacks of RBCs which form because of the unique discoid shape of the cells. The flat surface of the discoid RBCs give them a large surface area to contact and stick to each other when the plasma protein concentration is high. The equilibrium between these forces determines the extent of RBC aggregation and thus a key element in hemorheology.[230] The rheological properties of the plasma proteins, fibrinogen, albumin, and globulins in RBC aggregation, however, are not clear. Chien et al.[231] shows the baseline values of these plasma proteins, which is shown in Table 5-1. The purpose of this chapter is to investigate the plasma factors which are involved in the blood coagulation.

Table 5-1 Baseline concentrations of plasma proteins in the various patient groups studied[231]

	n	Fibrinogen, mg/dL	Ig, g/dL	Albumin, g/dL
Patients receiving intravenous Ig	13	325.8 ± 26.5	3.5 ± 0.5	3.8 ± 0.1
Patients with ischemic heart disease	15	380.6 ± 31	2.7 ± 0.1	4.0 ± 0.1
Control subjects	4	268.9 ± 28.4*	2.7 ± 0.1	5.2 ± 0.1†

Values are means ± SE; n, no. of subjects. *Value smaller than in patients with ischemic heart disease ($P = 0.02$); †value greater than in patients with ischemic heart disease ($P = 0.001$) and in patients receiving intravenous Ig ($P < 0.001$).

Whatever the force that causes the adsorption of fibrinogen or other macromolecules to erythrocytes, it is relatively weak and can be overcome by the increased shear stress. At low shear rates, the large aggregates cause greater fluid immobilization, resulting in higher suspension viscosity, whereas high shear conditions cause the dispersion of aggregates, leading to reduced fluid immobilization and suspension viscosity. Thus, an increase in shear stress disperses the rouleaux, which are formed again when the shear stress is reduced. According to some previous viscometric data,[232,233] it appears that erythrocytes in normal blood are mono-dispersed at a shear rate of approximately 200 sec^{-1} or a shear stress of the order of 5 $dynes/cm^2$ (= 0.5 Pa). It is interesting that maximal deformation of erythrocytes can also occur at such shearing conditions.[231] Therefore, when the erythrocytes are completely dis-aggregated by high shear, they are also maximally deformed and further increases in shear rate above 200-300 sec^{-1} would not reduce blood viscosity, therefore the Newtonian regime can be seen over these high shear rates.

It is believed that fibrinogen, a 340-kDa fibrous hexamer, is the most potent aggregator of RBC in plasma. Some studies[234,235] have shown that immunoglobulin (Ig) induces RBC aggregation, whereas others have found no effect.[236] Some described enhancement of fibrinogen-induced RBC aggregation by albumin,[237,238] but one study showed inhibition.[239] Also, some reported that Ig-induced RBC aggregation has been inhibited by albumin,[237] but the other mentioned the enhancement by albumin.[240] Reinhart and Nagy[241] found that albumin increased the erythrocyte sedimentation rate when added to fibrinogen and Ig, but inhibited it when added to either alone. Lately, Ben-Ami et al.[242] revealed that high concentrations of both albumin and fibrinogen are susceptible to Ig-induced RBC aggregation (Figure 5-1).

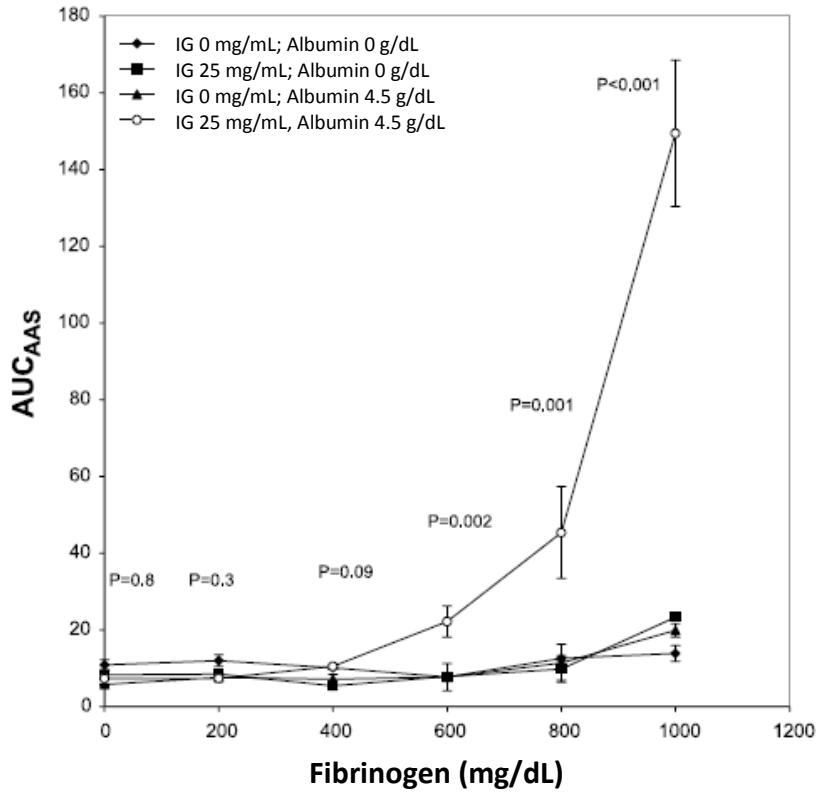

Figure 5-1 RBC aggregation (AUC_{AAS}) as a function of fibrinogen (Fib) concentration in four sets of suspensions with controlled concentrations of albumin (Alb) and immunoglobulin (Ig). Log AUC_{AAS} correlates with Fib concentration in a suspension containing Ig (25 mg/mL) and Alb (4.5 g/dL) but not in an Alb-free suspension. AUC_{AAS} is significantly greater at Fib concentrations above 400 mg/dL in a suspension containing Ig and Alb compared with the other three suspensions.[242]

Previously, Chien et al.[231] reported the shear-dependent interaction of plasma proteins with erythrocytes in blood rheology. They added the fibrinogen to suspensions of erythrocytes in serum as well as in Ringer solution. The addition of purified fibrinogen to erythrocytes suspended in serum or Ringer solution increases the blood viscosity with the shear dependence (Figure 5-2). The increase in the viscosity with increasing fibrinogen concentration in the serum was observed especially at low shear rates, but became saturated

at high fibrinogen concentrations (0.6 g/100mL). On the other hand, fibrinogen added to RBC suspensions in Ringer or Ringer-albumin solution (4g/100mL) exerted less effect than in serum suspensions. This difference in the hemorheological effects between fibrinogen added-RBC suspensions in serum and in Ringer (or Ringer-albumin) indicates that serum globulins possess a significant fibrinogen-like action, and the total serum globulins are approximately equivalent to the total fibrinogen present in their ability to interact with red cells. Therefore, the addition of further quantities of purified fibrinogen to serum suspensions causes no further increase in viscosity and does not markedly alter this fibrinogen equivalence of serum globulins, indicating that the hemorheological effects of fibrinogen and globulins are essentially additive.

As mentioned above, fibrinogen causes erythrocyte aggregation to form rouleaux. It has been shown that the RBC aggregate size varies with the fibrinogen concentration in a similar manner as the suspension viscosity does.[243] Fibrinogen has been found to be adsorbed onto the surface of the erythrocyte membrane. Because of the molecular length of fibrinogen (650-700 Å), it is possible that adsorption of the ends of the same fibrinogen molecule to two adjacent erythrocytes may bridge the negatively charged surfaces of the erythrocytes without significant electrical repulsion, resulting in the formation of rouleaux. The relative inability of albumin to bring erythrocytes together as rouleaux is probably because of its much shorter molecular distance of 150 Å that is not long enough to bring adjacent erythrocytes together and overcome the greater electrical repelling forces between them, indicating that albumin may actually exert a protective effect against erythrocyte aggregation.

Also, low shear viscometry shows time-dependent characteristics when fibrinogen is added. The larger plasma proteins (fibrinogen and globulins) can increase the shear dependence and time dependence of blood viscosity, whereas the smaller plasma protein (albumin) has little effect.

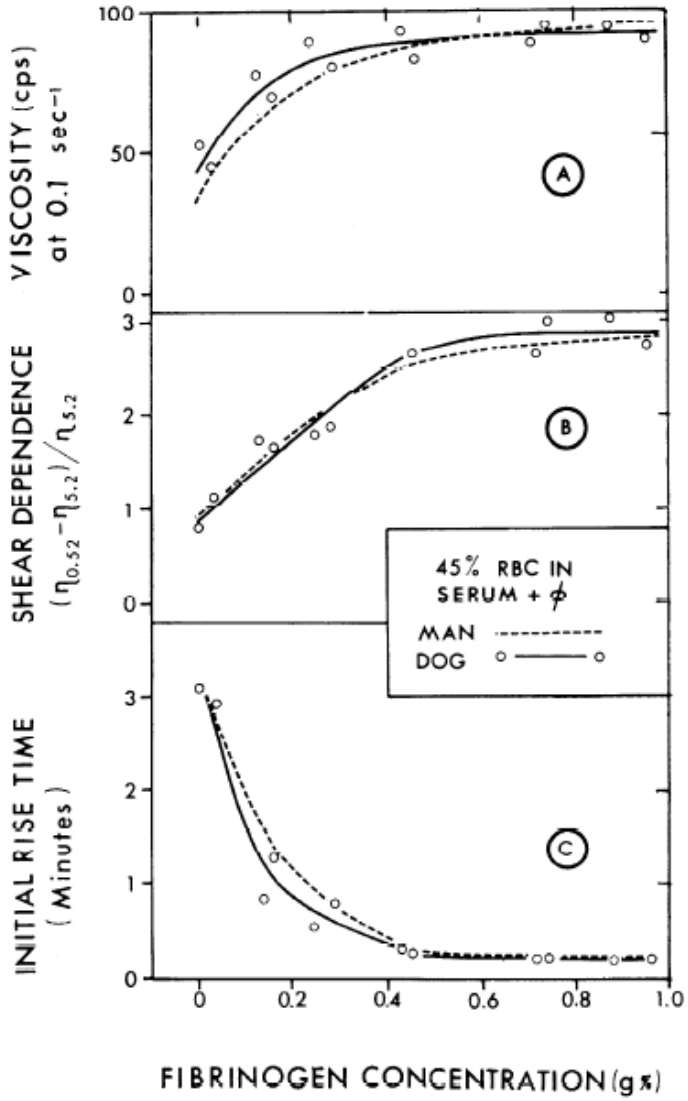

Figure 5-2 Relationships between viscosity at 0.1 sec^{-1} (A), shear dependence between 0.52 and 5.2 sec^{-1} (B), and initial rise time at 0.01 rpm (C), and fibrinogen concentration in suspensions of 45% canine erythrocytes in Ringer (solid lines), serum (broken lines), and Ringer-albumin, 4g/100 mL (dotted lines).[231]

5.2 Materials and Methods

5.2.1 Preparation of Chitosan Derivative Solutions

Chitosan and the prepared chitosan derivative solutions were prepared by following the method of Section 4.2.1.

5.2.2 Obtaining Centrifuged Blood

The blood plasma (containing the blood-clotting proteins) and the blood cells were separated by centrifugation. An amount of 2 mL Na-citrated whole bovine blood (anticoagulant ratio against whole blood is 1:9, 3.8% Na-citrate) was transferred into a test tube (10mm x 75 mm) and the test tube was sealed. This tube and an equally weighted test tube (filled with water) were put into 50 mL-centrifuge tubes and they were placed in pairs in IEC HN-SII Centrifuge (International Equipment Co., A Division of Damon, Needham Heights, MA) to balance the centrifuge. The centrifugation was run at 2000 ppm for 10 minutes. The separated blood cells were resuspended in an equal volume of PBS and then mixed with 2 wt% CIA/0.3M AcOH. Also, the blood plasma was mixed the same CIA solution.

5.2.3 Fibrin Formation by $CaCl_2$

Na-citrated bovine whole blood of 1.5mL was transferred into a test tube. Calcium chloride ($CaCl_2$) 0.025 M aqueous solution was prepared and 1.5 mL of this solution was

added into the blood test tube and mixed. The test tube was incubated in a water bath at 37˚C for 10 minutes. After the incubation, gel-like blood clot formation was observed. The clot was removed from the test tube with tweezers. The rest of the blood/$CaCl_2$ was stored at 5˚C until it was used for the rheological measurements.

5.2.4 Rheological Tests on Chitosan Derivative/Blood Mixture

The rheological tests were carried out by following the methods described in Section 4.2.4.

5.3 Results and Discussion

5.3.1 Gelation of Centrifuged Blood

The gelation experiments with the components of whole blood were also conducted. For this, the blood plasma (containing the blood-clotting proteins) and the blood cells were separated by centrifugation. First, 1 mL of 2 wt% CIA solution was mixed with 0.8 mL of blood plasma (without cells). Then, a time sweep test was carried out at oscillatory stress of 0.2 Pa, frequency of 0.1 Hz, and at 37˚C. The result is shown in Figure 5-3 along with the result of whole blood, under the same experimental condition. The sample with the blood plasma shows a weakly viscous response in the dynamic rheology. In this case, G" is slightly higher than G' over the frequency range. We cannot optically see the blood clot formed, either.

Next, the separated blood cells were re-suspended in an equal volume of PBS and then mixed with 2 wt% CIA solution. Figure 5-4 shows the result of the oscillatory time sweep tests for CIA derivative solution with separated blood cells resuspended in PBS. In contrast with the sample of separated blood plasma, this sample shows an elastic gel response over time under the same dynamic oscillatory stress. The result for the same derivative solution with blood plasma was also shown here as control. This confirmed that this blood coagulation induced by CIA derivative takes place only in the presence of blood cells and the blood cells are a key factor that facilitates blood clot formation, which is consistent with the previously reported result.[97] In this study, the induced blood gelation is explained as the sulfide bond formation between iodoacetic acid moiety of the derivative and sulfhydryl groups in blood proteins. Therefore, it is reasonable that the gelation occurs only when the blood cells that contain cysteine are present in the sample. Also, the blood plasma did not proceed with sufficient blood clot formation even though the coagulation factors exist in it, suggesting the aggregation of blood cells, including red blood cells and platelets, at the site of injury is necessary for the clot formation as mentioned in Chapter 1.

This sample shows a gel response as observed earlier with whole blood, however, the gel state was reached later than the sample of whole blood, as seen in Figure 5-5. The crossover of G' and G" was observed at around 50 minutes after the mixing, while the crossover occurs in approximately 15 minutes for the sample with whole blood (Table 5-2). Also, this is even relatively slower than that observed for unmodified chitosan/whole blood sample. Thus, the replacement of the plasma containing the blood coagulation factors with PBS retards the coagulation process. However, as seen in Table 5-2 the CIA derivative has

the greatest coagulating effect on whole blood. It is also notable that G' > G" was stably-maintained for the CIA/cells in PBS sample after their crossover, suggesting the fibrinolysis did not occur due to the replacement of the plasma with PBS, as shown in Figure 5-5.

Table 5-2 Gel time of the CIA (and unmodified chitosan)/Na-citrated blood systems at 37 ˚C; with separated blood plasma, with separated blood cells in PBS, and with whole blood

Sample	Time (min) at G"/G' = 2	Time (min) at G"/G' = 1	Time (min) at G"/G' = 1/2
CIA/blood cells in PBS	42.02	51.85	63.83
CIA/blood plasma	N/A	N/A	N/A
CIA/whole blood	8.30	15.01	26.30
Chitosan/whole blood	23.10	39.87	67.21

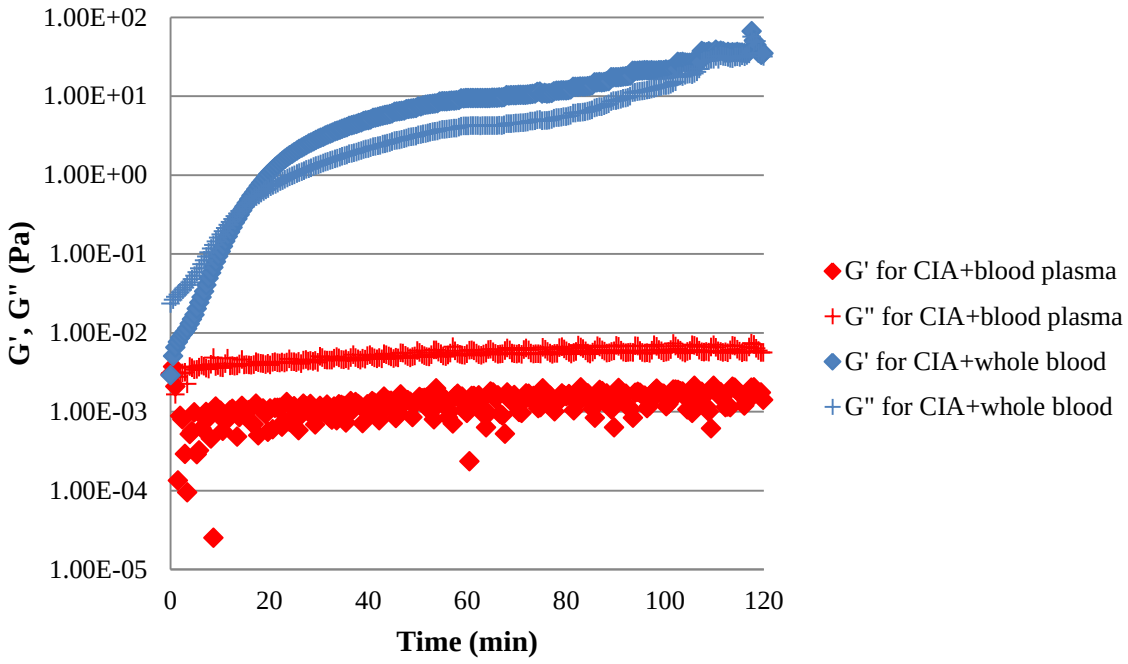

Figure 5-3 The dynamic rheological data for the elastic modulus (G') and the viscous modulus (G") versus time for the two samples. The CIA/blood plasma mixture (red symbols) shows the rheology of a liquid (G' < G") over entire measurement time whereas the CIA/Na-citrated whole blood mixture (blue symbols) responds like an elastic gel (G' > G").

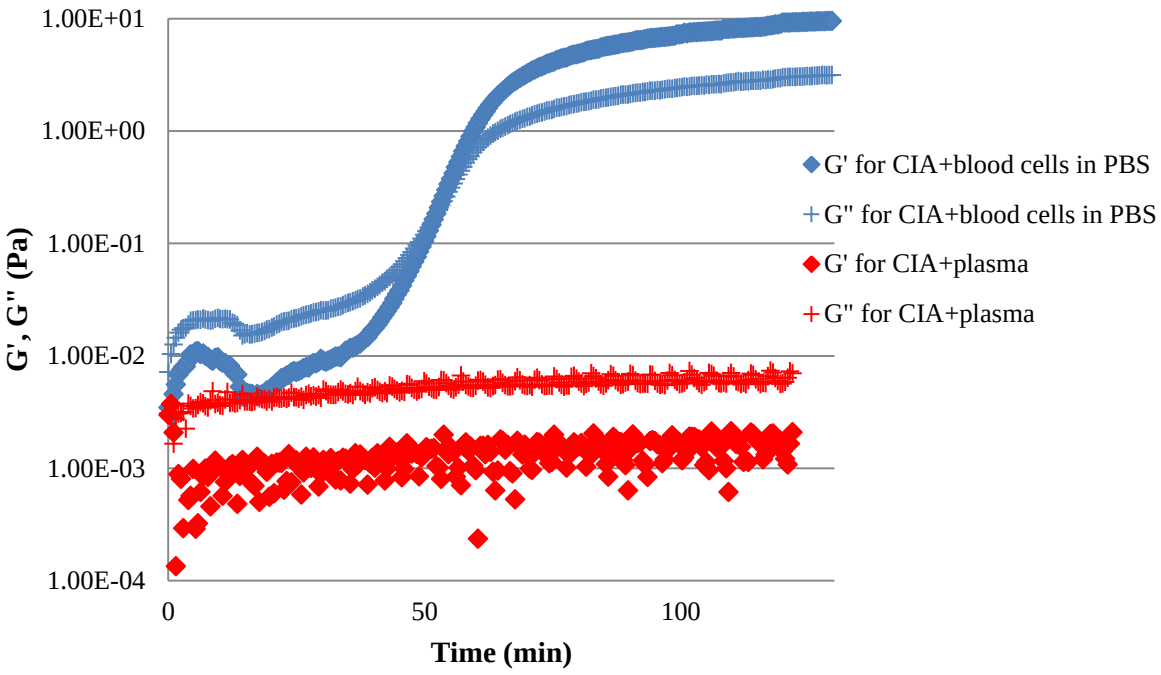

Figure 5-4 The dynamic rheological data for the elastic modulus (G') and the viscous modulus (G") versus time for the two samples. The CIA/blood cells resuspended in PBS mixture (blue symbols) shows the rheology of an elastic gel (G' > G") whereas the CIA/blood plasma mixture (red symbols) responds like a viscous solution over the measurement time.

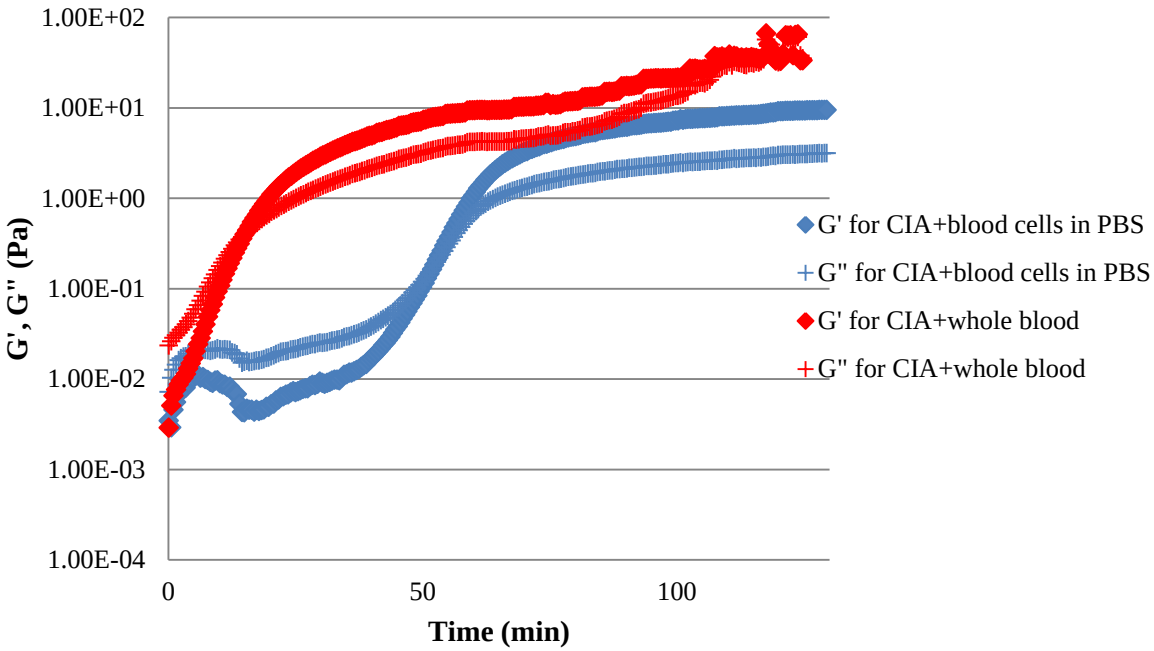

Figure 5-5 The dynamic rheological data for the elastic modulus (G') and the viscous modulus (G") versus time for the two samples; the CIA/blood cells resuspended in PBS mixture (blue symbols) and the CIA/Na-citrated whole blood mixture (red symbols).

The obtained results indicate a specific interaction happens between CIA and red blood cells. One aspect of the interaction of CIA with red blood cells is hemoglobin, which is the protein that makes up about 97% of the red blood cells in mammals,[244] and carries the important regulatory molecule nitric oxide bound to the globin protein thiol groups, releasing oxygen.[245] In addition, Glutathione (GSH, γ-L-glutamyl-L-cysteinyl-glycine), a tripeptide with a gamma peptide linkage between the amine group of cysteine and the carboxyl group of the glutamate side-chain, is widely distributed in biological samples as an important pathophysiological marker substance. Since thiol groups are reducing agents, GSH reduces

disulfide bonds formed within cytoplasmic proteins to cysteines by serving as an electron donor, while GSH itself is converted to its oxidized form glutathione disulfide (GSSG).

Some groups determined the amount of GSH in the blood.[246,247] Kosower et al.[247] reported on the oxidation of GSH into GSSG by two intracellular thiol-oxidising diazenes for the human red cell and rat red cell, in respect to the quantity of oxidant needed for GSH oxidation, to the fate of GSH, and to the reactivity of hemoglobin. They measured GSH and GSSG contents of human and rat red cells following treatment with excess diazene oxidants. In human red cells, the total GSH content of the cells is found as GSSG in the non-protein fraction of the lysate after complete GSH oxidation. In contrast, none or very little GSSG is found in rat blood cells after complete GSH oxidation, as summarized in Table 5-3. The –SH content of hemoglobin from human red cells treated with oxidants even in large excess shows almost no change from that found for hemoglobin of untreated red cells. The –SH content of hemoglobin from rat red cells diminishes significantly under similar conditions, as the data in Table 5-4.

Table 5-3 GSSG in red cells after oxidation of GSH[247]

Red cell suspensions were mixed with oxidants at 2˚C and kept for 10-15 min; cell suspensions then washed, cells resuspended in buffer and aliquots used for determination of GSH and of GSSG.

Cell origin	Oxidant	GSH, initial concentration (µmol/mL red cells)	Oxidant added/GSH (µmol/mL red cells)	GSH oxidized (%)	GSH recovered as GSSG (%)
Human	diamide	2.74	1.20	97	98
	diamide	2.45	2.05	100	95
	compound I	2.45	2.05	100	104
Rat	diamide	1.88	2.08	92	9
	diamide	2.10	2.38	100	6
	compound I	2.10	2.38	100	11
	compound I	2.28	2.20	98	14

* diamide: diazenedicarboxylic acid bis-*N'*-methylpiperazinide
compound I: diazenedicarboxylic acid bis-*N'*-ethylpiperazinide

Table 5-4 Hemoglobin –SH groups in oxidant-treated red cells[247]

Cell origin	Oxidant		Hemoglobin -SH (μmol/mL red cells)	Decrease in hemoglobin –SH (μmol/mL red cells)
	name	Amount (μmol/mL red cells)		
Human	none		30.5	
	diamide	5	30.5	0
	compound I	5	30.5	0
Human	none		29.25	
	diamide	4.8	29.0	0.25
	diamide	8.0	28.5	0.75
Rat	none		40.0	
	diamide	5	37.5	2.5
	diamide	6	35.0	5.0
Rat	none		39.5	
	diamide	5	36.5	3.0
	compound I	5	34.5	5.0
Rat	none		43.5	
	compound I	5	39.5	4.0

Red cell suspensions were mixed with solutions of the oxidants at 2 ˚C for 10-15 min; after washing, the cells were hemolysed and prepared for the determination of hemoglobin -SH groups. Note that for hemoglobin - SH, GSH thiol groups have been subtracted from the total thiol group determination. Hemoglobin - SH was measured as μmol/μmol hemoglobin. It was assumed that 5 μmol hemoglobin were present in each mL of red blood cells. Variation in the hemoglobin content of the red cells might account for a part of the small variation observed in those experiments to which no oxidant was added.

5.3.2 Gelation of Diluted Blood

We also conducted the gelation tests on the CIA solution with water-diluted blood to identify the factors which are involved in quick blood coagulation triggered by CIA derivative. In this test, the whole blood was diluted with deionized water or PBS by certain concentrations. The mixture of 1mL of 2 wt% CIA solution and 0.8 mL of whole blood was set as a standard. The amount of CIA solution was kept constant at 1 mL and certain amounts

of blood were replaced with deionized water (or PBS). The detail concentrations of the samples are summarized in Table 5-5.

Table 5-5 Summary of the concentration of the CIA/diluted horse blood mixture samples

Blood: H_2O (or PBS) (vol:vol)	1:0	1:2	1:3	1:4	1:3
Blood dilution ratio	1	1/3	1/4	1/5	1/4
Whole blood (mL)	0.8	0.266	0.200	0.160	0.200
Deionized water (mL)	0	0.532	0.600	0.640	0
PBS (pH 7.4, mL)	0	0	0	0	0.600
2 wt% CIA in 0.3M AcOH (mL)	1	1	1	1	1

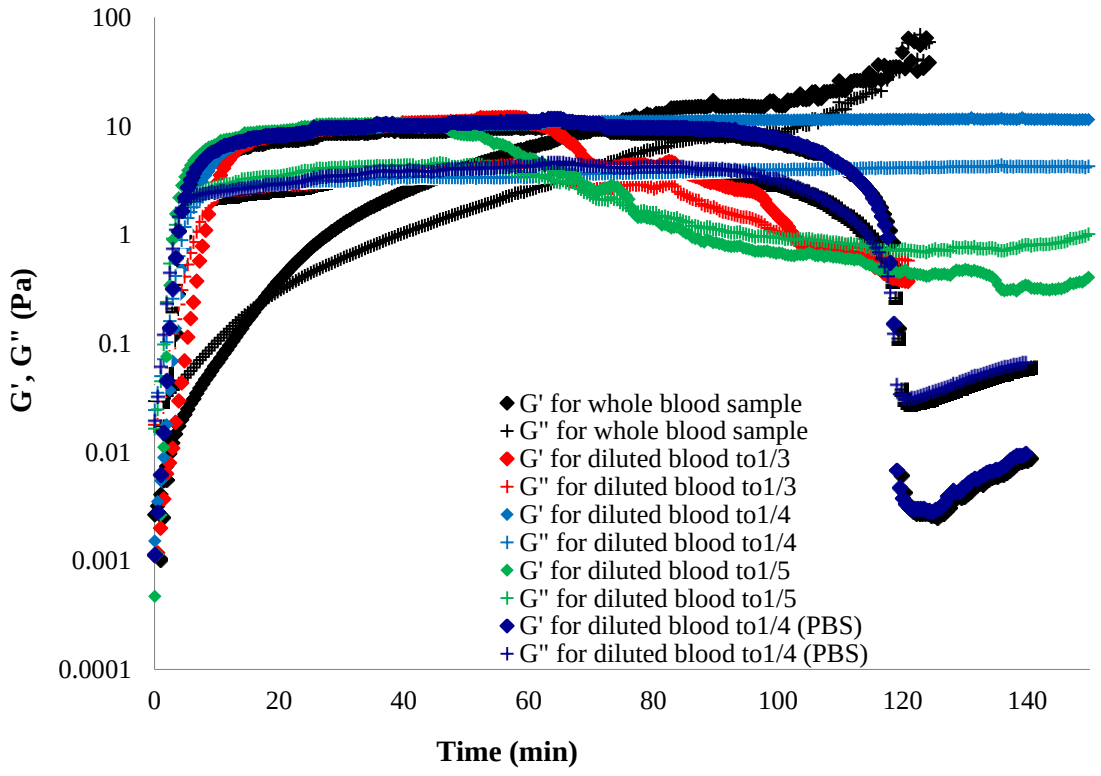

Figure 5-6 The changes in G' and G" over time for the CIA/horse whole blood mixture (black) and the deionized water (or PBS)-diluted horse whole blood mixtures with the different dilution ratio; diluted blood to 1/3 (red), diluted blood to 1/4 (light blue), diluted blood to 1/5 (green), and PBS-diluted blood to 1/4 (dark blue).

Figure 5-6 shows the changes in G’ and G” over time for CIA and diluted blood samples. The diluted blood samples show apparently different G’ and G” curves from those of the normal whole blood sample. It should be noted that the diluted samples exhibit the somewhat regular changes in both elastic and viscous moduli over time in proportion as the dilution ratio. As shown in Figure 5-7, the crossover point of G’ and G” tends to shift to shorter time with the increase in the dilution ratio, i.e., with the increase in water content in the mixture. This tells us that the diluted blood sample move to an elastic state from a viscous liquid in a much shorter time. However, the viscosity of the entire sample decreases due to the dilution of the blood and it cannot visibly be observed that the further rapid gelation occurs, than that for the normal whole blood sample. Furthermore, the red blood cells put in deionized water would bust due to the difference in osmotic pressure. Thus, the ionized water was replaced by the same amount of PBS and the same measurement was conducted for the diluted blood sample which the dilution ratio was 1/4. From Figure 5-7, the PBS diluted blood also exhibited a very rapid transition to an elastic gel state. Surprisingly then, the deionized water-diluted blood sample with the same dilution ratio, the sample diluted with PBS only shows a slightly shorter crossover time.

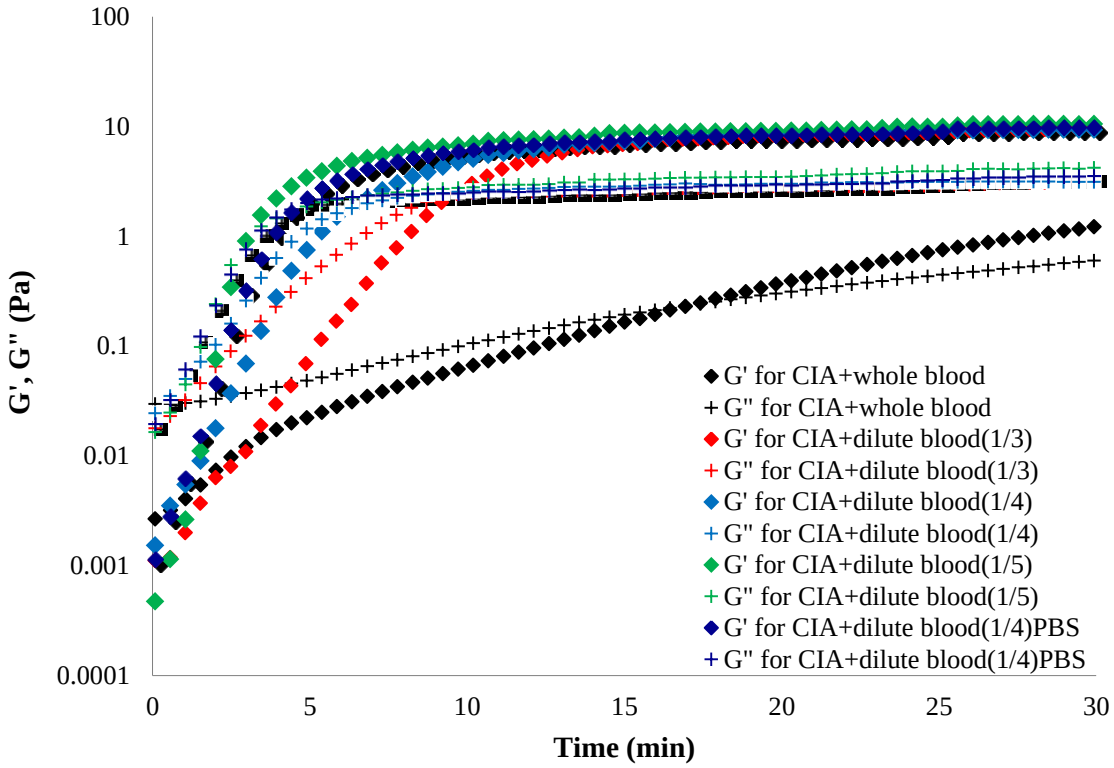

Figure 5-7 The expanded plot of Figure 5-6 in the region between 0min and 30 mins after mixing.

The loss tangent (tan δ) is plotted against time in Figure 5-8. Each curve starts to exhibit a different profile after 2 minutes, corresponding to an increase in the rate of the viscosity change. We can see the proportionally increased rate of crossover with the increase in dilution ratio. Comparing the diluted blood with the deionized water to the diluted blood with PBS, both with a dilution ratio of 1:4, the PBS-diluted blood mixture reaches the crossover point slightly faster.

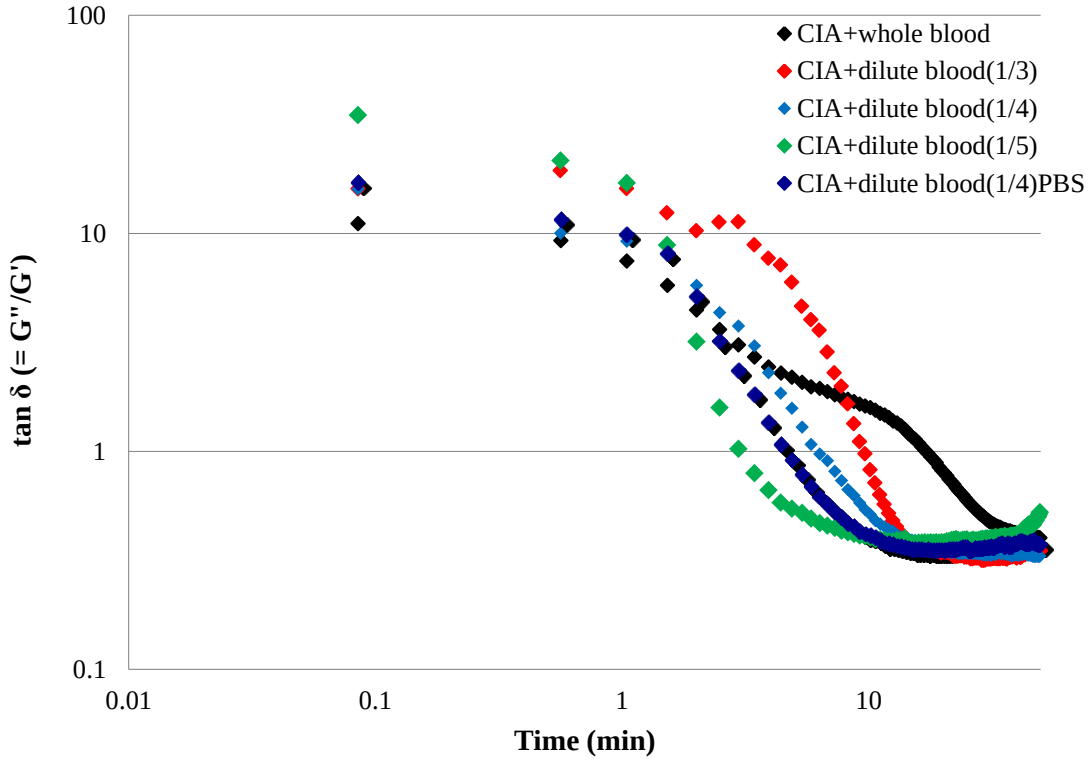

Figure 5-8 The plot of tan δ over time for the CIA/horse whole blood mixture (black) and those of the diluted horse whole blood mixtures by the dilution ratio of: 1/3 (red), 1/4 (light blue), 1/5 (green), and ¼ with PBS (dark blue).

5.3.3 Gelation Mechanism

In order to understand the influence of the natural fibrin crosslinking formation on the blood gelation induced by CIA derivative, the removal of fibrin from the blood was attempted. In the process of fibrin formation, calcium ions (Ca^{2+}) are involved with the activation steps of blood coagulation factors that finally lead to the crosslinked fibrin formation (Figure 1-1). This is why Na-citrate works as an anticoagulant, the citrate ion chelates calcium ions in the blood by chelating the calcium which disrupts the blood clotting

mechanism.Thus, adding calcium ions into the blood would cause the formation of fibrin. For this purpose, 0.025M $CaCl_2$ aq. was mixed with the same amount of the Na-citrated whole blood and maintained at 37˚C. After 10 minutes of incubation, the gel-like blood clot was formed in the blood/$CaCl_2$, as shown in Figure 5-9. The clot was removed from the blood and the rest of the blood containing $CaCl_2$ was mixed with 2% CIA/0.3M AcOH and the rheological tests were carried out.

Figure 5-9 Blood clot formed after mixing Na-citrated bovine whole blood with 0.025 M $CaCl_2$ solution.

After adding $CaCl_2$ solution, most of the coagulation factors should have been converted to their activated forms and caused the cascade reactions to form fibrin gelation. The clot in the photo indicates that this occurred.

Next, the rest of the blood containing $CaCl_2$ solution was mixed with the CIA derivative solution and the rheological test was run. Figure 5-10 shows the changes in G' and G" over time at a constant oscillatory stress (0.2 Pa), frequency (0.1Hz), and temperature (37˚C). The sample of CIA solution mixed with blood/$CaCl_2$ turned to a gel state after 40 minutes, while the sample of chitosan derivative solution mixed with the normal whole blood turned to a gel in around 10 minutes. This tells us that even though the fibrin has been removed, it is still able to form a clot. The amount of fibrin formed would be proportional to the amount of fibrinogen that existed in the blood (ref. Figure 1-1). Assuming all the fibrinogen (precursor of fibrin) was converted by the thrombin with addition of Ca^{2+} and was then removed, there was no fibrinogen available, for forming the fibrin clot. However, the blood cells have interacted with the CIA derivative solution. This result supports the previous result that re-suspended blood cells in PBS (where most of coagulation factors were removed) still exhibits gelation behavior with the derivative although it took 50 minutes for G' and G" to crossover. This clarifies that the observed blood gelation induced by CIA works by interacting with the blood cells, and not by the natural coagulation pathways.

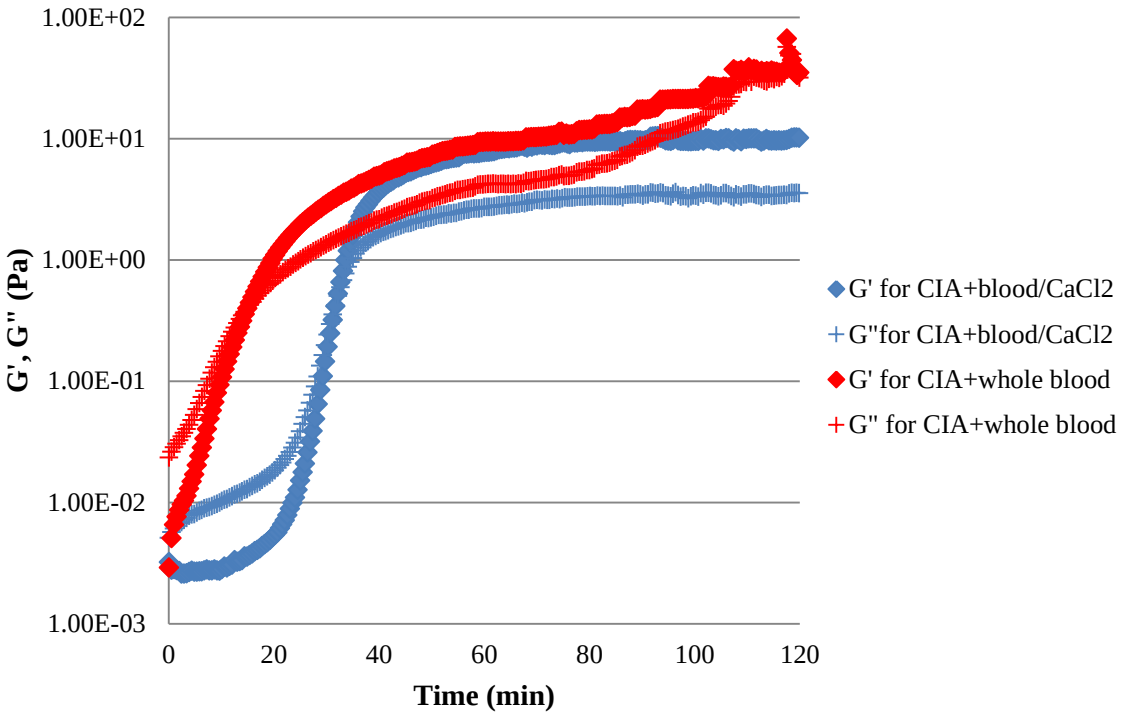

Figure 5-10 The dynamic oscillatory time sweep test for CIA solution mixed with the whole blood which fibrin was pre-removed by $CaCl_2$ addition (blue symbols) and for that mixed with the normal whole blood (red symbols).

5.4 Conclusion

The purpose of this chapter is to specify the factors that are involved in the enhanced clot formation of the whole blood by the interaction of CIA derivative and to determine the detail mechanism of the blood gelation. First of all, we assumed the sulfide covalent bonds formation between iodoacetic acid moiety of the derivative and cysteine residue in the blood could occur through the reaction discussed in Chapter 3. This study will be helpful to understand whether the crosslinking reaction with blood proteins is possible and maximizes blood clot formation.

First of all, we questioned what is crucial for the observed enhanced clot formation. It is known that a cascade of the activation of the blood coagulation factors in the blood plasma leads to the formation of the polymerized fibrin, followed by the aggregation of the blood cells on the fibrin mesh, thus forming a clot. In order to clarify which is more involved in the very rapid blood coagulation by the CIA system, whole blood was separated into the cells and the plasma and each was mixed with CIA solution, and the rheology was observed. The dynamic oscillatory measurements confirmed that the existence of the blood cells is necessary to complete the clot formation. In the case of only plasma mixed with CIA solution, we could not see any gelation. In addition, the separated blood cells were resuspended in PBS (eliminating most of the coagulation factors) and mixed with the derivative solution as well. This sample exhibited the gel behavior although it took a much longer time to reach the gel state, than the case for whole blood. These results indicate that the CIA system would not affect the reactions of the blood coagulation factors and works to enhance the coagulation rate independently of the natural coagulation cascade, supposedly through the interaction with the cysteine residue that are associated with the cells. Also, the CIA system works maximally in the presence of both the cells and plasma.

Next, some of whole blood was replaced with deionized water (or PBS) to investigate the limitation of the blood concentration required for the coagulation. The results obtained here were surprising. The more the whole blood was replaced with water, the quicker was the gelation time of the CIA/blood mixture. However, the lower concentration of blood, i.e., less amounts of blood cells and coagulation factors, would generally cause a

slower coagulation rate. The reason why this result was obtained is unclear and further studies are needed.

Finally, there is still a question on how the CIA derivative works to induce the rapid blood coagulation. In the coagulation pathways, the last step is to prepare the polymerized fibrin mesh that catches the platelets and the red blood cells in it and turns to being a clot. Therefore, removing fibrin out of the blood in advance of mixing with the chitosan derivative solution would help address the question. As a result, fibrin was artificially formed by addition of $CaCl_2$ and removed from the blood. The rest of the blood/$CaCl_2$ system could form a clot with addition of the CIA solution, suggesting that the CIA would work independently from the natural coagulation pathways, however, it cannot work in the absence of red blood cells.

In this study, the bovine serum albumin (BSA) aqueous solution of 4 wt% was mixed with CIA in order to verify that CIA reacts with cysteine (ref. Appendix B). The blood serum contains 4.4~5% albumin. However, we could not obtain reportable gelation behaviors from the mixture of CIA and the BSA solution. As described in Chapter 3, some groups previously found that iodoacetic acid reacted with only a portion or with none of the sulfhydryl groups of native proteins, on the other hand, the heat-denatured egg albumin was completely interacted with iodoacetic acid at pH 7.3 within 3 hours.[202] Another study found the value of cysteine (0.55%) in heat-denatured egg albumin which is available for the reaction with iodoacetate.[203] This would be a considerable reason why the native BSA solution did not show any gelation with iodoacetic acid. The denaturation of proteins involves the disruption and possible destruction of both the secondary and tertiary structures, while it is not strong

enough to break the peptide bonds thus the primary structure (sequence of amino acids) remains the same after a denaturation. Heat added to a protein disrupts hydrogen bonds and non-hydrophobic interactions. Therefore, the number of segments of amino acid sequence is increased, which leads to the increase in the amount of free cysteine (or other iodo-reacting amino acids) available for the reaction with iodoacetate. The relationship between the denatured protein and iodoacetic acid is an interesting subject to understand the mechanism of the observed blood gelation and to maximize the reaction between the sulfhydryl compounds in the blood and iodoacetic acid residue.

CHAPTER 6

6 Rheological Properties of Thiolated Chitosan

In previous chapters, it was discussed that thiolated polymers have been known to provide much higher adhesive properties than the existing mucoadhesive polymers. The enhancement of mucoadhesion can be explained by the formation of covalent disulfide bonds between the polymer and the mucus layer. These thiolated polymers, known as thiomers, interact with cysteine-rich subdomains of mucus glycoproteins via disulfide exchange reactions and/or simple oxidation process. Currently, various thiolated chitosan derivatives have been developed, such as chitosan-thioglycolic acid (chitosan-TGA) conjugates,[107,108,110,125] chitosan-cysteine conjugates,[124,126] and chitosan-4-thio-butyl-amidine (chitosan-TBA) conjugates[109] based on the immobilization of thiol bearing moieties on the polymeric backbone of chitosan. These thiolated chitosans have some useful features, including significantly improved mucoadhesive and enhanced permeation properties as well as *in situ* gelling property at physiological pH values, which give them promising applications.

The improved mucoadhesive properties of thiolated chitosans are explained by the formation of covalent bonds between thiol groups of the polymer and cysteine-rich subdomains of glycoproteins in the mucus layer. The cationic chitosan can also interact with anionic substructures of the mucus layer through the ionic interactions. In addition, thiolated chitosans provide another stronger interaction with them by forming disulfide bonds. Some groups confirmed the improve mucoadhesiveness by measuring *in vitro* adhesion time of

thiolated chitosan tablets on intestinal mucosa. For instance, chitosan-TGA conjugates show a 5~10-fold increase in mucoadhesion in comparison to unmodified chitosan,[107] also further improvement of mucoadhesive properties of chitosan-TBA was achieved.[109] This highly improved mucoadhesion of chitosan-TBA can be explained in that the chitosan-TBA conjugate provides additional ionic interactions between its cationic amidine moieties and anionic substructures within the mucus layer. In addition, the strong enhanced permeability of thiolated chitosans, chitosan-cysteine[124] and chitosan-TBA,[248] have been observed. Bernkop-Schnurch et al.[249] reported the permeation enhancing effect of the 0.5% (m/v) chitosan-TBA conjugate in combination with the permeation mediator glutathione (GSH), which contains 0.001% (m/v) rhodamine 123 as a model compound. The passive uptake of the rhodamine 123 into freshly excised small intestinal mucosa from guinea pigs, showed a 3-fold higher permeation, compared to unmodified chitosan.

Due to these enhanced properties, thiolated chitosans have been studied for biomedical applications, such as non-invasive matrices for controlled drug release and tissue engineering. The incorporation of cationic drugs in anionic mucoadhesive polymer matrices leads to a strong reduction in the mucoadhesive properties and would hinder drug release as a result of strong ionic interactions between the drug and the polymeric network. On the other hand, thiolated chitosans, as non-ionic polymers, seems to be a favorable tool for the oral administration of cationic hydrophilic macromolecules. The thiol groups introduced on the chitosan backbone enable thiolated chitosans not only to form disulfide bonds with mucus glycoproteins, but also to form inter- and intra-molecular disulfide bonds. This crosslinking of the polymeric structure results in high stability as drug carrier systems. Guggi et al.[133,250]

reported that chitosan-TBA conjugate matrix tablet loaded calcitonin (linear polypeptide hormone that acts to reduce blood calcium) demonstrated that oral administration of the chitosan-TBA tablet led to a significant reduction in the blood calcium level of rats for at least 12h. Thiolated chitosans seem to be useful not only as oral delivery systems but also for other non-invasive carriers of peptide drug administration, i.e., the nasal, vaginal, buccal and ocular mucosas are interesting targets. In order to improve the bioavailability of peptide or protein drugs administered via mucosal routes, the enhanced permeation property of thiolated chitosan is attractive for the delivery system. Kast et al.[251] designed a chitosan-TGA bioadhesive vaginal drug delivery system for clotrimazole. The adhesion on vaginal mucosal tissue was significantly improved with 26x greater adhesion time of chitosan-TGA on vaginal mucosa than unmodified chitosan.

Another interesting application of thiolated chitosans is their use in tissue engineering. The expanding field of tissue engineering applications has accelerated the need for materials which are tissue compatible, biodegradable and with mechanical properties similar to the target tissues. Biodegradable and biocompatible polymers have been attractive candidates for scaffolding materials because they eventually degrade as the new tissues are formed, without inflammatory reactions or toxic degradation. Recently, Kast et al.[252] demonstrated the biodegradability of thiolated chitosan, paving the way for its use as novel scaffold material. Further, studies in this direction were performed with L-929 mouse fibroblasts seeded onto chitosan-TGA sheets. The results of this study showed that thiolated chitosan can provide a porous scaffold structure guaranteeing cell anchorage, proliferation and tissue formation in three dimensions.

6.1 Introduction

An important feature of thiolated chitosans is the *in situ* gelling property. The crosslinking process of thiolated chitosan occurs due to the oxidation of thiol groups at the physiological pH values of 5-6.8, which results in the formation of inter- and intramolecular disulfide bonds. The *in situ* gelling behavior of thiolated chitosans has been characterized *in vitro* by rheological measurements.[109,110]

Bernkop-Schnurch et al.[109] characterized the *in situ* gelling behavior of chitosan-TBA conjugates with different ratios of immobilized TBA to chitosan (Figure 6-1). The rheological measurements showed that the sol-gel transition of the chitosan-TBA conjugate was completed at the physiological pH of 5.5 after 2 hours when highly crosslinked gels were formed along with a significant decrease in the thiol group content within the polymers, indicating the formation of disulfide bonds. Rheological investigation of thiolated chitosans, furthermore, demonstrated a clear correlation between the total amount of introduced thiol groups and the increase in elasticity of the formed gel. The more thiol groups that were immobilized on chitosan, a higher increase in elastic modulus in solutions of thiolated chitosan was observed.[109,110]

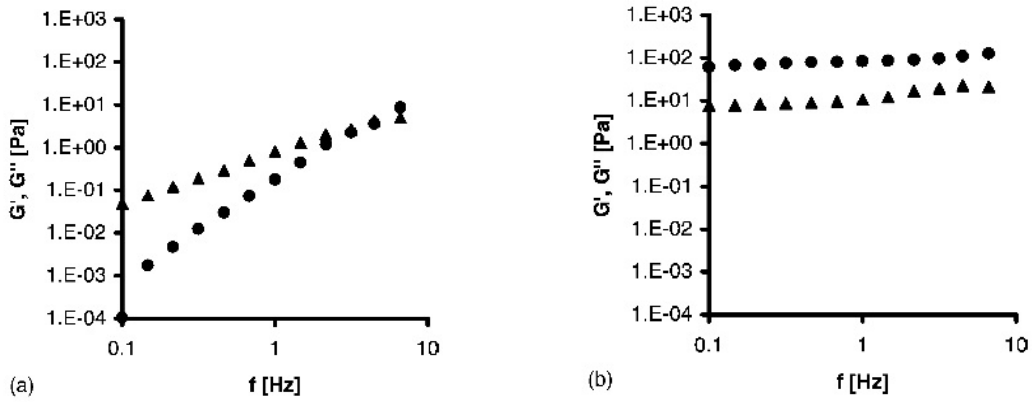

Figure 6-1 Effect of the oscillatory frequency on the storage modulus *G'* (●) and the loss modulus *G"* (▲) of a 1.5% (m/v) chitosan-TBA conjugate solution at the beginning of the observation period (a) and after 2h at pH 5.5 and 37°C (b).[109]

Thiolated chitosan derivatives, therefore, seem to be promising new excipients for liquid or semisolid formulations, which should stabilize themselves once applied on the site of drug delivery. One requirement for drug delivery systems is a prolonged residence time of the drug administered at the delivery site. A very promising strategy to achieve this is to increase the viscosity of a drug formulation based on *in situ* gel formation of a thiolated chitosan matrix. Moreover, the *in situ* crosslinking within the pH range of 5-6.8 would make it possible for thiolated chitosans to be applied on vaginal, nasal, and ocular mucosa. In addition, the *in situ* gelling properties of thiolated chitosans would provide a new type of tissue scaffold material.[252] When a liquid thiolated chitosan cell suspension is injected at the site of tissue damage, it rapidly becomes a gel as it is contacted by oxygen (disulfide formation by oxidation occurs).

6.2 Materials and Methods

6.2.1 Preparation of Chitosan-L-Cysteine Derivative

Chitosan of 1g (312 kDa, 96%DD) was dissolved in 1.0 wt % acetic acid of 100 mL to prepare chitosan/acetic acid solution of 1 % (w/v). The solution pH was raised to ~5 by 1N NaOH. L-cysteine (3 g, bioreagent ≥98%) was dissolved in 50 mL of deionized water, then, 1.48 g of 1-ethyl-3-(3-dimethylaminopropyl) carbodiimide hydrochloride (EDAC HCl, crystalline) (150 mM in final concentration) was added as a coupling agent to the L-cysteine solution and it was kept stirring for 20 minutes. The solution pH was set to 5 by 1N NaOH. The carboxyl groups of L-cysteine are activated by EDAC, the L-cysteine solution and the chitosan solution were mixed and incubated with continuous stirring for 6h at room temperature. After 6h, 1N NaOH was added gradually until a white precipitate was obtained. Then, the precipitate was filtered, washed by deionized water, and dried in the vacuum desiccator. The reaction scheme is shown in Figure 6-2. All chemicals were purchased from Sigma Aldrich.

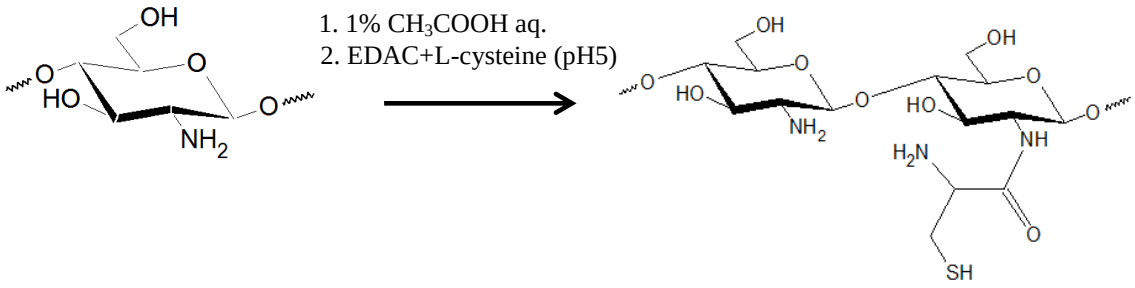

Figure 6-2 Synthetic scheme of chitosan-L-cysteine by a reaction coupled with 1-ethyl-3-(3-dimethylaminopropyl) carbodiimide hydrochloride (EDAC HCl).

6.2.2 Preparation of Chitosan Derivative Solutions

Chitosan and the chitosan derivative solutions were prepared by following the methods of Section 4.2.1.

6.2.3 FTIR Spectroscopy

The same equipment and the procedure described in Section 2.3.2 were used.

6.2.4 Rheological Tests on Chitosan Derivatives/Blood Mixture

The rheological tests were carried out by following the methods described in Section 4.2.4.

6.3 Results and Discussion

6.3.1 Characterization of Chitosan-L-Cysteine by FTIR

The structure of the prepared chitosan-L-cysteine conjugate was confirmed by FTIR. The IR spectra of the unmodified chitosan and chitosan-L-cysteine are shown in Figure 6-3 and 6-4, respectively. Comparing to the spectrum of the unmodified chitosan in Figure 6-3 (ref. Section 2.4.1), the derivative shows a single peak at 3363 cm^{-1} that is assigned for N-H stretching vibration. The peak at 2905 cm^{-1} is attributed to C-H stretching. The Amide I (C=O stretching) band appears at 1622 cm^{-1}. The strong band at 1582 cm^{-1} and 1486 cm^{-1} are attributed to N-H bending of a primary amine and a secondary amide, respectively. L-cysteine has a free amino group in its structure. Since the unmodified chitosan exhibited only

one N-H bending band, these two peaks that appeared in the derivative's spectrum, confirmed the modification of chitosan with L-cysteine. Moreover, the strong peak at 1408 cm^{-1} with a shoulder at 1382 $cm^{-1}$are assigned for CH_2 bend and the peaks at 1338 cm^{-1} and 1249 cm^{-1} indicate CH_3 bending and C-N stretch, respectively. In addition, the peaks at 1149 cm^{-1}, 1081 cm^{-1}, and 1036 cm^{-1} are attributed to asymmetric and symmetric C-O-C stretches and C-O stretch. Finally, the peak at 1193 cm^{-1} should be the C-S adsorption.

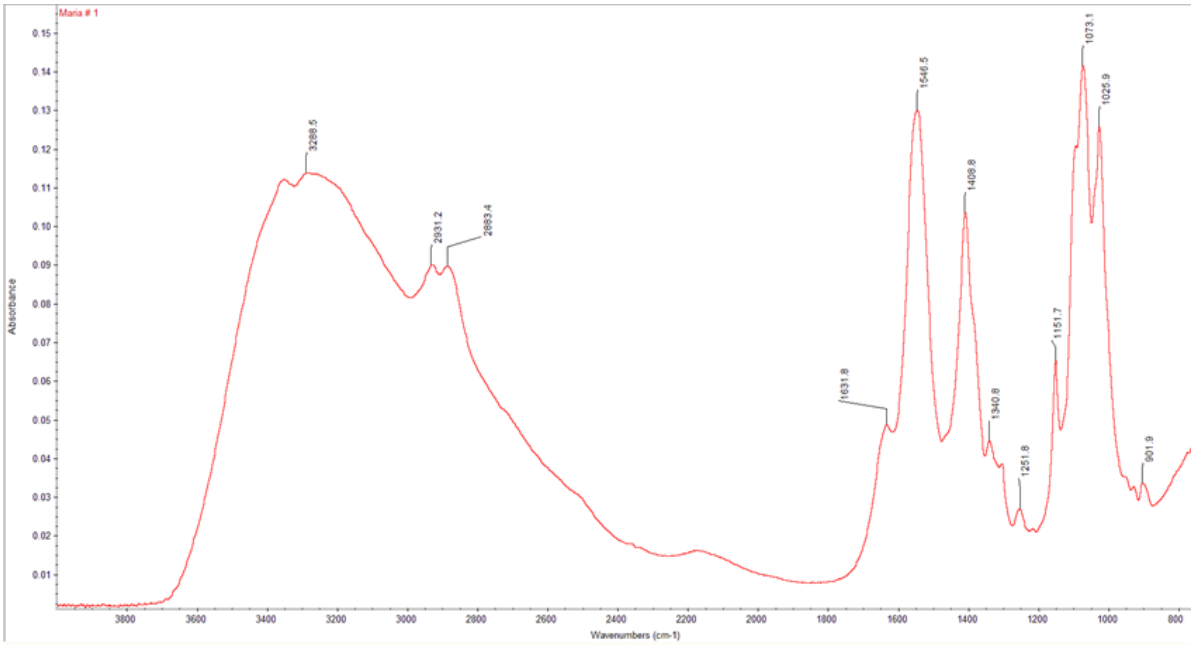

Figure 6-3 FTIR spectrum of the chitosan sample used in this study.

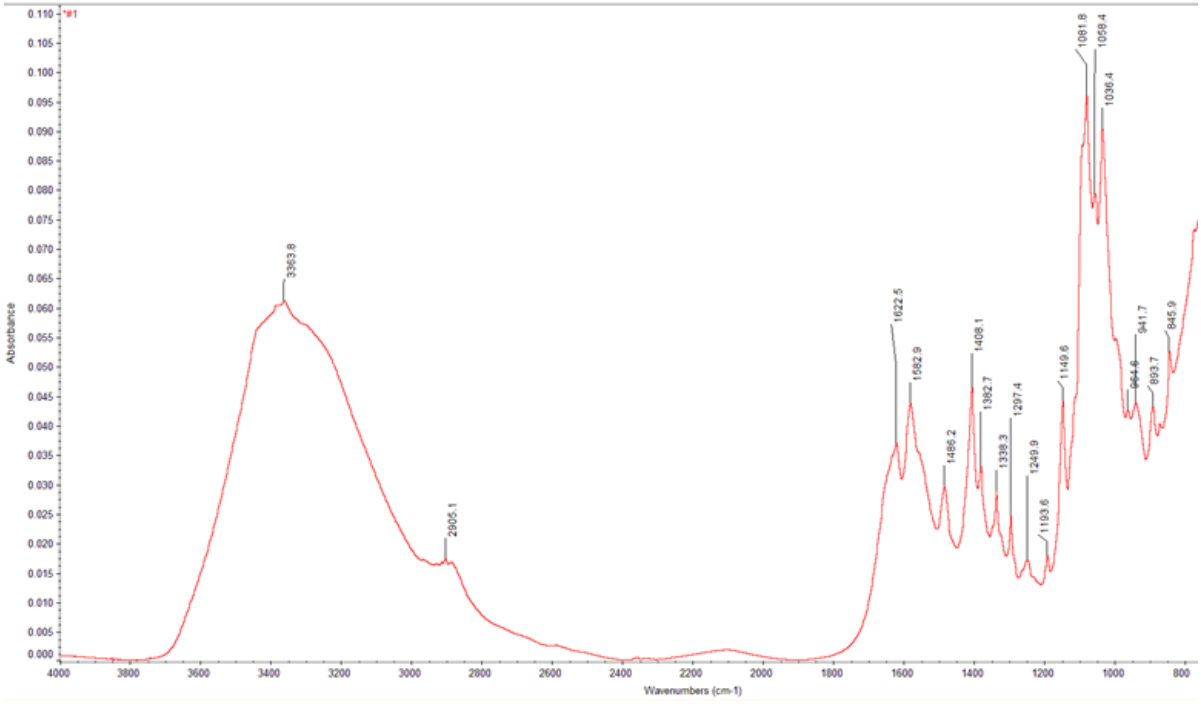

Figure 6-4 FTIR spectrum of the chitosan-L-cysteine sample used in this study.

6.3.2 Gelation of Chitosan-L-Cysteine Derivative and Blood

In this work, one of the thiolated chitosan derivatives, chitosan-L-cysteine conjugate, was prepared and its interaction with the whole blood under the same procedure done on the CIA derivative was investigated. As mentioned in Chapter 1, the thiolated polymers are able to form disulfide crosslinkings between cysteine-rich subdomains of mucus glycoproteins by an oxidation process between free thiol groups and/or thiol disulfide exchange reactions, providing the mucoadhesive properties. This could be another candidate that is capable of crosslinking covalently with cysteine residues in blood proteins. In order to check its effect

on the blood gelation and to compare the results with those of CIA, the rheological experiments were carried out on chitosan-L-cysteine derivative.

Following the previous procedure, the Na-citrated bovine whole blood of 0.8 mL was mixed with chitosan-L-cysteine/0.3M AcOH solution of 1 mL (0.02 g in 0.3M acetic acid aqueous solution) and the dynamic oscillatory tests were conducted under a constant stress (frequency sweep and time sweep). Figure 6-5 shows the result of the frequency sweep test, by changing the frequency from 0.01 Hz to 100 Hz under the constant oscillatory stress of 0.2 Pa and at 37˚C. The result indicates that the mixture exhibits a solution property at low frequencies and turned to an elastic gel with the increase in the frequency as well as seen in CIA/whole blood mixture. In addition, a time sweep test under a constant stress of 0.2 Pa and frequency of 0.1 Hz at 37 ˚C was conducted. The results are summarized in Figure 6-6 and Table 6-1. The changes in G' and G" over time explain the phase transition from a liquid into a gel and the clear crossover of G' and G" (G' > G") was observed after 35 minutes of mixing. Compared with the result of CIA under the exact same condition (red symbols in Figure 6-6), the time to reach the crossover point was approximately 2.5 times slower for chitosan-L-cysteine/blood mixture, however, the stable gel state was achieved after 40 minutes. Although it does not induce the rapid gelation as seen in CIA, these results indicate that chitosan-L-cysteine derivative has the ability to interact with the blood protein, specifically sulfhydryl compounds in the blood, giving a potential as a hemostatic agent. The synthesis of chitosan-L-cysteine followed the same procedure to prepare CIA. However, L-cysteine easily bonds with itself as the cystine dimer. Therefore, the substitution ratio of cysteine residue against amino groups of chitosan might not be high enough for inducing

blood gelation. The modification of the synthesis process would lead to an enhancement of its effect against the blood.

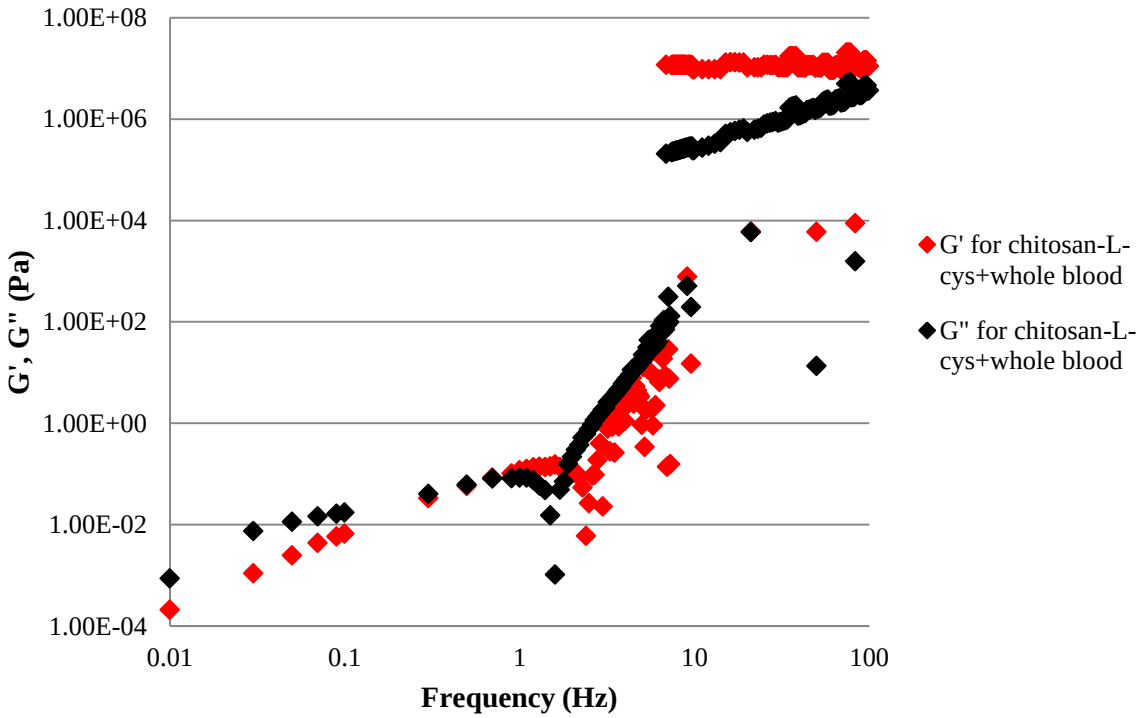

Figure 6-5 The elastic modulus (G') and the viscous modulus (G") versus frequency at 0.2 Pa, 37˚C for the chitosan-L-cysteine/Na-citrated bovine whole blood mixture sample.

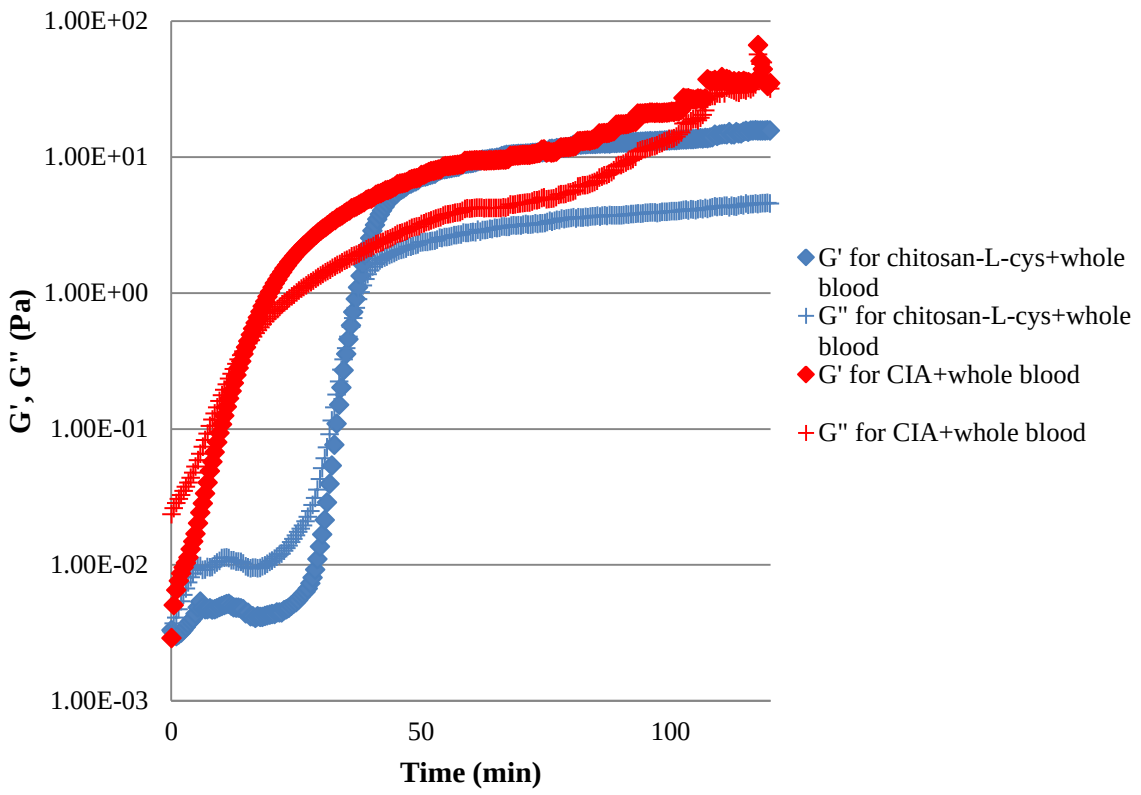

Figure 6-6 The elastic modulus (G') and the viscous modulus (G") versus time at 0.2 Pa, 0.1 Hz, 37˚C for the chitosan-L-cysteine/Na-citrated bovine blood mixture sample (blue symbols), the CIA/Na-citrated bovine blood mixture sample (red symbols).

Table 6-1 Gel time of the chitosan-L-cysteine/, CIA/, and unmodified chitosan/Na-citrated whole bovine blood systems at 37 ˚C

Sample	Time (min) at G"/G' = 2	Time (min) at G"/G' = 1	Time (min) at G"/G' = 1/2
CIA/whole blood	8.30	15.01	26.30
Chitosan-L-cysteine/whole blood	8.23	35.55	41.07
Chitosan/whole blood	23.10	39.87	67.21

Next, Figure 6-7 shows the change in complex viscosity (η*) over time for chitosan-L-cysteine/blood mixture and CIA/blood mixture. The steeper increase in the viscosity upon mixing was observed for the CIA/blood sample. On the other hand, it took 30 minutes for chitosan-L-cysteine/blood sample to increase its viscosity. Also, the viscosity value after 120 minutes was approximately three times higher for CIA derivative, compared with chitosan-L-cysteine derivative.

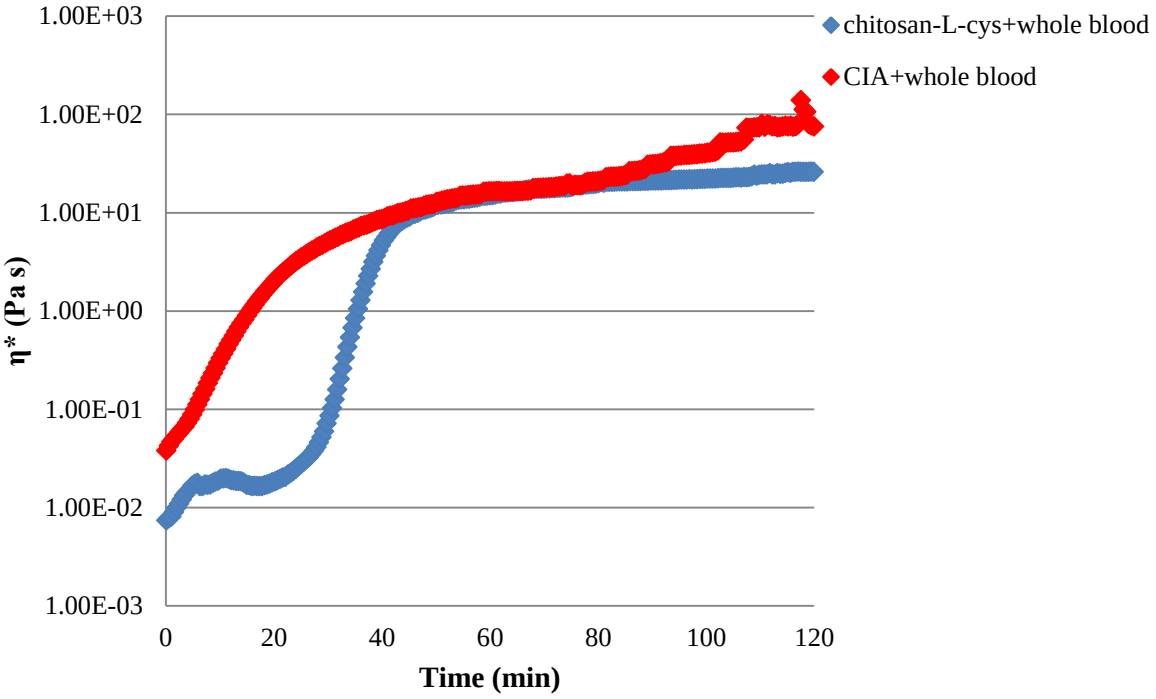

Figure 6-7 Complex dynamic viscosity versus time for chitosan-L-cysteine/Na-citrated whole blood mixture and CIA/Na-citrated whole blood mixture.

6.3.3 *In situ* Gelling of Chitosan-L-Cysteine Derivative

Next, *in situ* gelling of chitosan-L-cysteine conjugate was tested. As a thiolated polymer, chitosan-L-cysteine derivative was expected to undergo inter- and intramolecular interactions, followed by its own self-gelation. The result is shown in Figure 6-8. Chitosan-L-cysteine in 0.3M AcOH (2 wt%) was prepared and the solution pH was raised to 5-5.5 by 1N NaOH right before the rheological test was done. In contrast to the expectation, *in situ* gelation was not observed. The pKa value of free thiol groups is known to be ~8-9 and minimum value of 5 is needed to make them become thiolated anion form (SH^-). After stopping the measurement, white precipitations were found in the sample solution. The L-cysteine residues in the derivative apparently turned into the insoluble cystine dimer form and separated out of the solution.

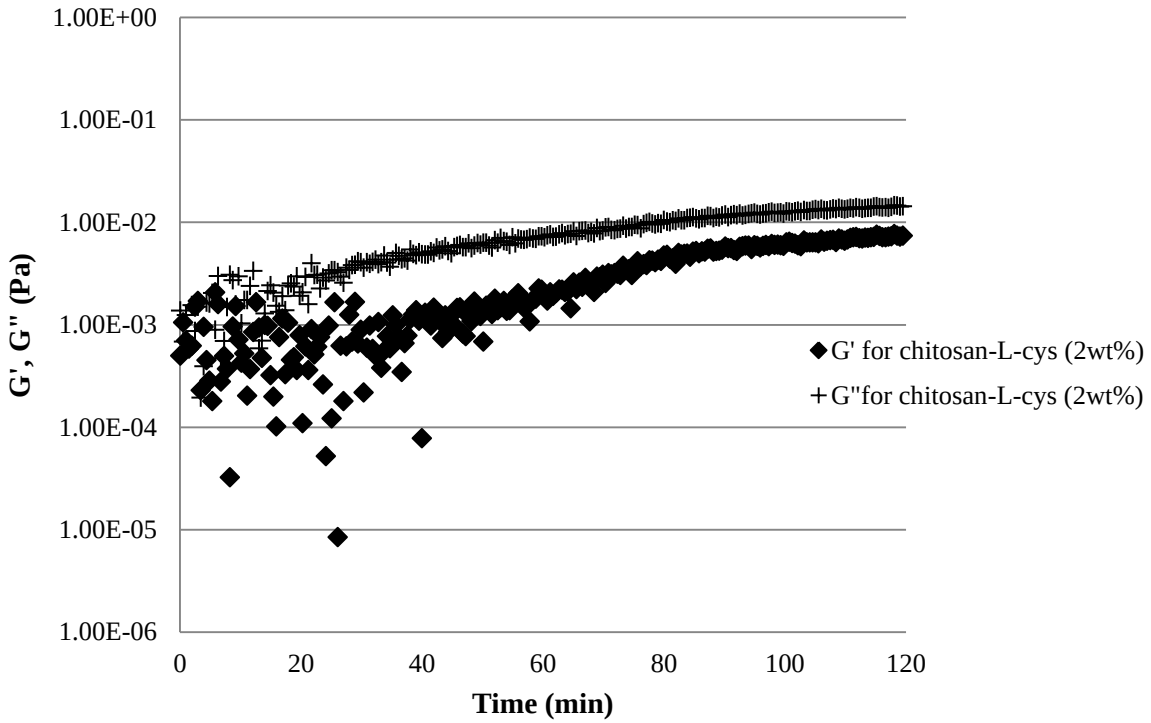

Figure 6-8 The dynamic rheological data for the elastic modulus (G') and the viscous modulus (G") versus time for the 2 wt% chitosan-L-cysteine/0.3M AcOH.

6.3.4 Rheology of CIA and Chitosan-L-Cysteine

Assuming the reaction occurs between iodoacetic acid and thiol groups, the CIA derivative and chitosan-L-cysteine derivative were studied in terms of their interaction with each other. The rheological measurement was carried out on the solution mixture of the two derivatives. As shown in Figure 6-9, the gelation behavior between these two derivatives was not observed in 0.3M acetic acid solution of pH ~3 during the entire measurement of 120 minutes.

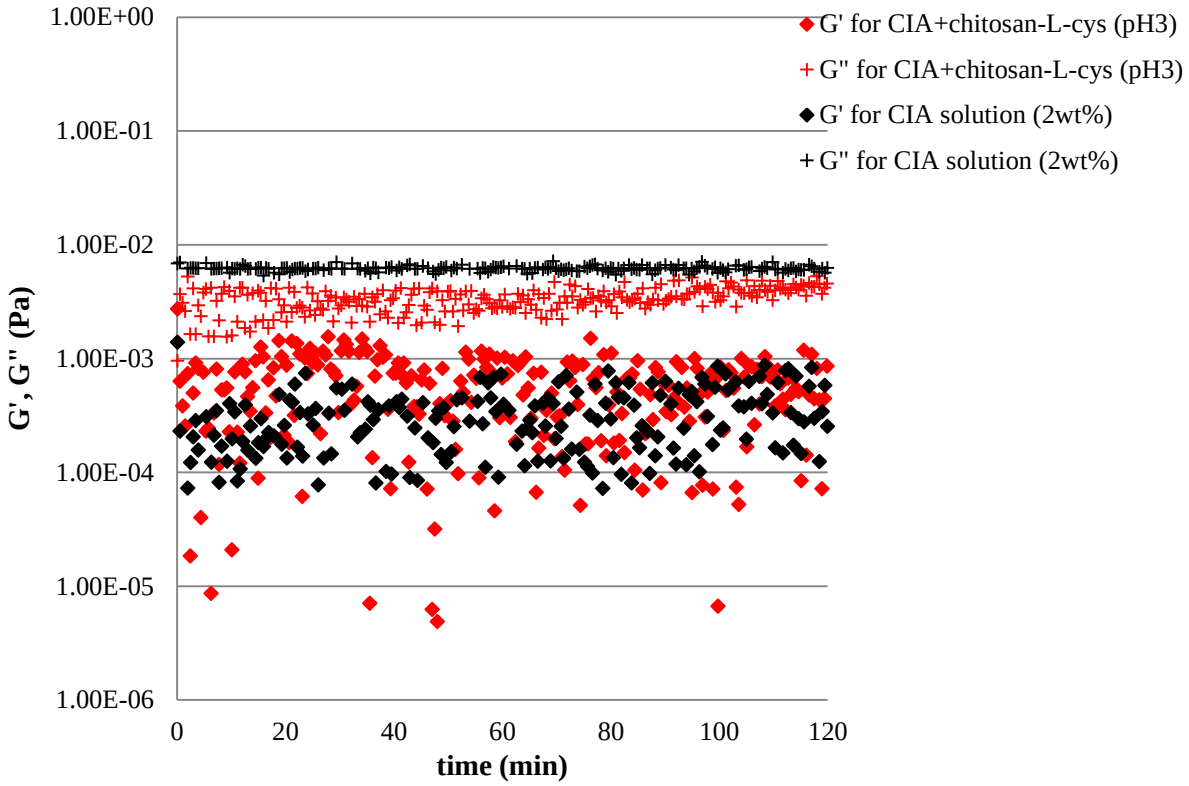

Figure 6-9 The dynamic rheological data for the elastic modulus (G') and the viscous modulus (G") versus time for the two samples. The CIA solution/chitosan-L-cysteine solution mixture (red symbols) shows the continuous liquid state (G' < G") and no changes in the viscosity over entire measurement time. The CIA solution itself (black symbols) remains the liquid state although the increase in the viscosity over time is seen.

Since the pH value seemed not to be sufficient to cause the reaction between them, the solution pH was raised to 5-5.5 by addition of 1N NaOH solution and the same measurement was repeated, as shown in Figure 6-10. As a result, the gelation behavior was not yet observed at this pH value, either. After the measurement was stopped, the white precipitates were found in the tested sample, which is the reason why the obtained data was erratic. This might be cystine dimers formed by the inter-molecular interaction of cysteine moieties. The result suggests that the inter-molecular interaction of chitosan-L-cysteine

would happen more easily than the reaction between iodoacetic acid and cysteine residues. Moreover, no changes in the viscosity were seen at the two different pH values, suggesting that a higher reactivity of both derivatives is required. As a possible improvement, the increase in the concentrations of sample solutions is worth trying. In addition, the amounts of both iodoacetic acid and L-cysteine residues introduced into chitosan were around 4~6 wt%, suggesting that the number of crosslinks formed between them is not enough to achieve sample-spread crosslinking system that holds its flow up. The higher degree of substitution of the derivative would be a solution about this. In this research, chitosan-L-cysteine was focused on, since the reaction between iodoacetic acid and cysteine is a key reaction over the entire study. Other thiolated chitosans, however, would be interesting candidates.

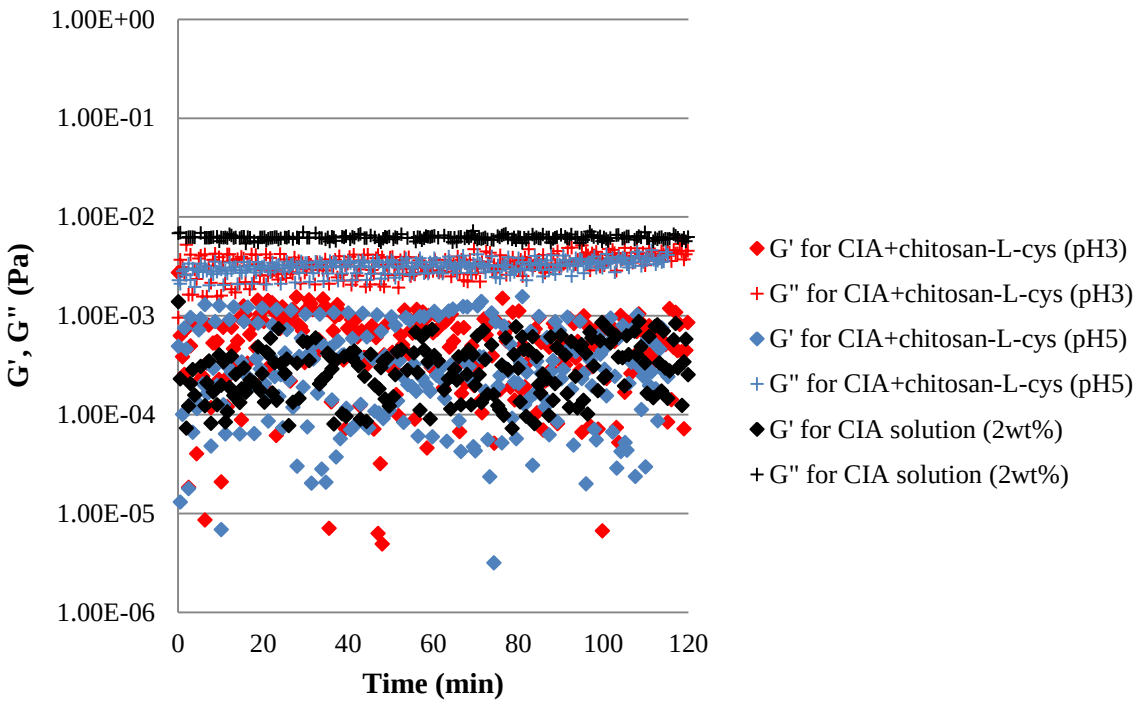

Figure 6-10 The dynamic rheological data for the elastic modulus (G') and the viscous modulus (G") versus time for the three samples. The CIA solution/chitosan-L-cysteine solution mixture at pH 3 (red symbols), CIA solution/chitosan-L-cysteine solution mixture at pH 5 (blue symbols), and CIA solution itself (black symbols).

6.4 Conclusion

In this chapter, the rheological properties of a thiolated chitosan have been tested. Thiolated chitosans bear free thiol groups on the backbone chain of chitosan. This gives them the possibility that they may be candidates that cause interaction with sulfhydryl compounds in the blood. In order to compare to CIA in terms of the induced rapid clots formation, chitosan-L-cysteine derivative was prepared and its rheological behavior with the blood was studied. The obtained results showed that chitosan-L-cysteine/whole blood mixture exhibited

a considerable increase in complex viscosity although it took 2.5 times longer to reach the gel state than the CIA/whole blood mixture. Nevertheless, there is a potential for chitosan-L-cysteine that a modification of the synthesis process to yield higher introduction of L-cysteine residue would develop a more effective system that interacts with blood proteins. The advantage of chitosan-L-cysteine is that it can interact not only with free thiol groups (-SH) by oxidation but also with disulfide groups (-S-S-) by disulfide exchange reaction, which enhances the points of interaction between the derivative and the proteins.

Rheological measurements were obtained on mixed CIA and chitosan-L-cysteine solutions. Theoretically, the iodoacetic acid moiety and thiol group of L-cysteine react with each other, forming hydrogen iodide (HI) as a side product. In conclusion, no gelation behavior occurred upon the mixing of two solutions at either pH 3 or pH 5. The self-gelation of chitosan-L-cysteine derivative was not observed as well. Bernkop-Schnurch et al.[109], however, reported the *in situ* gelling properties of chitosan-TBA, thus, there is a potential for a reaction between them. Hintzen et al.[253] investigated the effect of molar mass on *in situ* gelling properties of thiomers and concluded that low molar mass thiomers in a high concentration are most suitable for *in situ* gelling systems. The improved substitution ratio of L-cysteine moiety into chitosan might give a better result.

CHAPTER 7

7 Conclusions and Recommendations for Future Work

In Chapter 1 the concept of this study was discussed. Many current hemostatic wound dressings mainly attempt to absorb blowing blood and body fluids, but do not get actively involved with the physiological blood coagulation factors. A recent promising approach has adopted the self-assembly of a synthetic peptide into a nano-fibrous network, however, the synthetic peptides are expensive and difficult to synthesize. The objective of this study is to propose a novel hemostatic system based on chitosan that induces blood clot formation by simultaneous gelation of blood via the chemical crosslinking with sulfhydryl compounds in the blood. For this purpose, several chitosan derivatives were chosen as candidates for the new hemostat matrices, which are thiolated chitosans and chitosan-iodoacetamide (CIA). The iodoacetic acid is known as an irreversible inhibitor of all cysteine peptidases with the mechanism of inhibition occurring from alkylation of the catalytic cysteine residue. Based on this feature of iodoacetic acid, this study focused on forming strong chemical bonds between CIA and cysteine residues in the blood protein, trying to achieve the formation of three-dimensional crosslinked network that transforms a liquid blood into an elastic gel. A series of rheological measurements were conducted to understand the rheological behavior of the blood protein and the chitosan derivative hemostat and resultant induced blood coagulation mechanism.

In Chapter 2, several characterization tests were first carried out on the chitosan sample. ^{1}H NMR and FTIR, and conductometric titration demonstrated that the chitosan used

is highly deacetylated and the calculated degree of deacetylation was 96%. Also, the viscometry revealed that it has a molecular weight of 312,000 g/mol. Through the entire project the same chitosan sample was used. Next, the CIA conjugate was synthesized through the reaction of amino group of chitosan at C-2 position and carboxyl group of iodoacetic acid, as coupled by EDAC. This is a novel form of chitosan not previously reported. Also, some research groups have successfully reported the synthesis of chitosan-sulfhydryl conjugates, such as chitosan-TGA and chitosan-TBA. The same synthesis mechanism was applied to prepare CIA conjugate. ^{1}H-NMR and FTIR confirmed the introduction of iodoacetic acid moiety into the chitosan. In addition, elemental analysis clarified the amount of introduced iodoacetic acid moiety is in the range of 4 wt% to 10 wt%. According to the higher solubility in 0.3M aq. acetic acid and its better ability to induce rapid blood gelation, a CIA derivative with the degree of substitution of 4 wt% was used in this study. Further work would be helpful to investigate the relationship between the amount of introduced iodoacetic acid contents and the degree of the induced blood gelation. If assumed that considerable amounts of iodoacetic acid content are needed for the desired chemical crosslinking between the derivative and sulfhydryl compounds in the blood, a better synthesis procedure would be required to maximize the reaction between chitosan and iodoacetic acid and introduce as much iodoacetic acid contents as possible.

In Chapter 3, the proof of reactivity between iodoacetic acid and cysteine was presented since the reaction between them is crucial for this study in order to create sulfur crosslinks between the CIA derivative and sulfhydryl compounds existing in blood. Theoretically, cysteine bonds with iodoacetic acid, resulting in the side product HI. First, ^{1}H-

NMR was attempted on the mixed solution of L-cysteine and iodoacetic acid. As a result, the NMR result could not exactly confirm the reaction occurred since the two compounds bond to each other by forming sulfide bonds and the magnetic environment of existed protons does not change even after the reaction. ^{13}C NMR would be worth trying, it could give us additional useful information to prove the reaction. Consequently, mass spectrometry was attempted as well. The obtained result successfully demonstrated the presence of the reaction product in the mixed solution. As was expected, this reaction proceeded smoothly at alkaline condition (pH 8.5), associated with the formation of intermolecular disulfide bonds of L-cysteine and the resultant cystine dimers. What is more, the reactivity at physiological pH was tested in the same way and revealed that the reaction between iodoacetic acid and L-cysteine is still favorable at physiological conditions.

In Chapter 4, a series of dynamic oscillatory measurements and steady shear measurements were carried out to investigate the rheological behaviors of CIA/Na-citrated whole blood samples. As observed, the dynamic viscosity of the whole blood increased by addition of CIA derivative solution with several interesting findings. First, the gel point highly depended on the derivative content in the total mixture. Approximately three times the blood volume against the derivative solution volume was required for the most rapid blood gelation. At present, the formed clot returned to the liquid state after several hours, indicating the crosslinking is not very strong to support the sample-spanned gel network over hours. For the purpose of mixing with the blood, the derivative was dissolved in 0.3M AcOH. This acidic condition might be an inhibition for the reaction between iodoacetic acid residue and sulfhydryl residue to proceed. Finally, the substitution ratio of iodoacetic acid on chitosan

would be another parameter. In general, the higher introduction of iodoacetic acid content leads to an increase in the crosslinking points, resulting in the stronger interaction between the derivative and blood. On the other hand, it decreases the solubility and cationic feature of chitosan. Further studies are needed to clarify the best substitution ratio that will cause the interaction with blood proteins to be at a maximum extent.

In Chapter 5, the detail mechanism of how the CIA derivative works to induce the observed blood gelation, was studied. First of all, the necessary factors for the observed enhanced blood coagulation were clarified. The whole blood was separated into the cells and the plasma, then, they were mixed with CIA solution, respectively, and the rheological measurements were carried out. As a result, the presence of the blood cells is found necessary for clot formation. The plasma mixed with the derivative solution never reached the gel state. The separated cells which re-suspended in PBS could exhibit the gelation with the derivative solution as well, although the rate was much slower. This result indicates that the CIA derivative works independently of the natural coagulation pathways. Moreover, certain amounts of the whole blood were replaced with the deionized water then mixed with the derivative solution, and the same rheological measurements were done in order to investigate the need of the coagulation factors that exist in the plasma for the induced blood gelation. In contrast to the expectation, an increased gelation rate was observed for lower plasma concentration samples. The protein concentration of the samples were decreased with the addition of water, therefore, the gelation rate should be principally reduced by replacing blood with water. Also, the effect of water on the osmotic pressure of the blood cells needs to be considered. Furthermore, the need of fibrin for the complement of blood coagulation was

demonstrated. The blood from which fibrin was removed in advance, still demonstrated blood gelation, suggesting the interaction between the derivative and blood cells is important for this gelation.

In Chapter 6, chitosan-L-cysteine conjugate, a thiolated chitosan, was synthesized and its rheological properties were tested. First, we assumed that the induced blood coagulation observed for CIA derivative would be caused by the covalent crosslinking between the derivative and sulfhydryl groups in the blood. If this assumption is correct, chitosan-L-cysteine derivative also may interact with the blood via disulfide crosslinking formation with the sulfhydryl compounds in the blood. As a result of the rheological measurements, chitosan-L-cysteine also caused blood gelation. However, the detailed mechanism for the observed increased blood viscosity was still unclear. In order to clarify this, CIA and chitosan-L-cysteine were mixed and rheological measurements were carried out. In contrast to the expectation, two solutions mixture did not show any gelation behaviors. Some numbers of crosslinks must have been formed, but the formed crosslinking networks were not enough to span the volume of the liquid medium of the mixture since the substitution ratio of amino groups of chitosan with iodoacetic acid and/or L-cysteine was limited. In the same way, *in situ* gelation of chitosan-L-cysteine could not be observed. We still believe that the covalent crosslinking formation between the chitosan derivatives and the sulfhydryl compounds in the blood is possible, judging from the results of mass spectrometry in Chapter 3 and the rheological measurements on the derivative/whole blood mixtures in Chapter 4. Also, several groups reported on the gelling behaviors of thiolated chitosans. Further studies would be needed to confirm the gelling mechanism and expand the future applications.

However, very early work[202,203] indicates that many of the native protein sulfhydryl groups are inhibited, somehow, and are not reactive with iodoacetic acid. This is in contrast to the reactivity of sulfhydryl groups found in the reactive sites of many enzymes. Sulfhydryl compounds in denatured blood serum proteins, such as albumin, heat treated at 100˚C or with hydrogen bonding disruptors such as urea, have much greater reactivity against iodoacetic acid. This distinction between these groups needs further study.

In the future, further studies that elucidate a more accurate mechanism for the enhanced blood coagulation are necessary. As a next step, *in vivo* tests that allow us to test the hemostats with non-coagulated fresh blood would be highly recommended. Also, the model blood solutions, such as BSA solution and cysteine solution, are useful to further clarify the reaction between iodoacetic acid and the sulfhydryl compounds. In terms of this, the chemistry of the denatured proteins and iodoacetic acid should be studied.

In this study, several batches of the CIA derivative were obtained, however, one that has an ability to cause a strong and rapid blood gelation is still sought. The control of substitution ratio of iodoacetic acid moiety with the amino group at the C-2 position of chitosan would be an approach to synthesize a derivative with the desired properties. Moreover, the detailed study on the relationship between the amount of introduced iodoacetic acid moiety and blood gelation would be helpful. The prepared CIA is insoluble in water, this is why, 0.3M acetic acid was used to make its solution. In terms of higher reactivity of iodoacetic acid moiety at slightly alkaline condition and considering the biocompatibility of the hemostat system, a water-soluble chitosan derivative would be promising. Thiolated

chitosans have further hopeful properties that are worth studying, not only for wound healing but for mucoadhesiveness and enhanced permeability.

Other water soluble polymers could be candidates for this approach to hemostasis. For a first-aid wound dressing, any matrices that absorb quickly the running blood and body fluid is required at the same time as the positive enhancement of the clots formation. The remarkable feature of PVA is its high water absorption. The combination of PVA and iodoacetic acid would be a promising candidate for a great hemostatic wound dressing material. Additional mechanical and rheological experimentation on this is desired.

REFERENCES

1. Colman, R.W.; Hirsh, J.; Marder, V.J.; Salzman, E.W. Hemostasis and thrombosis: Basic principles and clinical practice, 3rd ed. Philadelphia: J.B. Lippincott Company 1993; 1–1632.

2. Forbes, C.D.; Courtney, J.M. Thrombosis and artificial surfaces. In: Bloom, A.L.; Thomas, D.P., editors. Haemostasis and thrombosis, 2nd ed. New York: Churchill Livingstone 1987; 902–921.

3. Champion, H.R.; Bellamy, R.F.; Roberts, C.P.; Leppaniemi, A. A profile of combat injury. *J. Trauma* **2003**, 54, S13–S19.

4. Stewart, R.M.; Myers, J.G.; Dent, D.L.; Ermis, P.; Gray, G.A.; Villarreal, R.; Blow, O.; Woods, B.; McFarland, M.; Garavaqlia, J.; Root, H.D.; Pruitt, B.A. Jr. Seven hundred fifty-three consecutive deaths in a level I trauma center: The argument for injury prevention. *J. Trauma* **2003**, 54, 66 –71.

5. Kauvar, D.S.; Lefering, R.; Wade, C.E. Impact of hemorrhage on trauma outcome; An overview of epidemiology, clinical presentations, and therapeutic considerations. *J. Trauma* **2006**, 60, S3–S11.

6. Acosta, J.A.; Yang, J.C.; Winchell, R.J. et al. Lethal injuries and time to death in a level I trauma center. *J. Am. Coll. Surg.* **1998**, 186, 528 –533.

7. Sauaia, A.; Moore, F.A.; Moore, E.E. et al. Epidemiology of trauma deaths: A reassessment. *J. Trauma* **1995**, 38, 185–193.

8. Stewart, R.M.; Myers, J.G.; Dent. D.L. et al. Seven hundred fifty-three consecutive deaths in a level I trauma center: the argument for injury prevention. *J. Trauma* **2003**, 54, 66 –70.

9. Hoyt, D.B.; Bulger, E.M.; Knudson, M.M. et al. Death in the operating room: an analysis of a multi-center experience. *J. Trauma* **1994**, 37, 426–432.

10. Heckbert, S.R.; Vedder, N.B.; Hoffman, W. et al. Outcome after hemorrhagic shock in trauma patients. *J. Trauma* **1998**, 45, 545–549.

11. Bellamy, R.F. Combat trauma overview. In: Zajtchuk, R.; Grande, C.M., editors. *Textbook of Military Medicine, Anesthesia and Perioperative Care of the Combat Casualty*. Falls Church, VA: Office of the Surgeon General, United States Army; 1995:1–42.

12. Bellamy, R.F. The causes of death in conventional land warfare: implications for combat casualty care research. *Mil. Med.* **1984**, 149, 229–230.

13. Harker, L.A.; Ratner, B.D.; Didisheim, P., editors. Cardiovascular biomaterials and biocompatibility. Published as a supplement to Cardiovascular Pathology 1993, 2 (3), 219 pp.

14. Bogdanov, V.Y.; Balasubramanian, V.; Hathcock, J.; Vele, O.; Lieb, M.; Nemerson, Y. Alternatively spliced human tissue factor: A circulating, soluble, thrombogenic protein. *Nat. Med.* **2003**, 9, 458–462.

15. Holcomb, J.B.; Pusateri, A.E.; Harris, R.A. et al. Effect of dry fibrin sealant dressings versus gauze packing on blood loss in grade V liver injuries in resuscitated swine. *J. Trauma* **1999**, 46, 49 –57.

16. Larson, M.J.; Bowersox, J.C.; Lim, R.C. Jr.; Hess, J.R. Efficacy of a fibrin hemostatic bandage in controlling hemorrhage from experimental arterial injuries. *Arch Surg.* **1995**, 130, 420–422.

17. Pusateri, A.E.; Modrow, H.E.; Harris, R.A.; Holcomb, J.B.; Hess, J.R.; Mosebar, R.H.; Reid, T.J.; Nelson, J.H.; Goodwin, C.W. Jr.; Fitzpatrick, G.M.; McManus, A.T.; Zolock, D.T.; Sondeen, J.L.; Cornum, R.L.; Martinez, R.S. Advanced hemostatic dressing development program: Animal model selection criteria and results of a study of nine hemostatic dressings in a model of severe large venous hemorrhage and hepatic injury in swine. *J. Trauma* **2003**, 55, 518 –526.

18. Sondeen, J.L.; Pusateri, A.E.; Coppes, V.G.; Gaddy, C.E.; Holcomb, J.B. Comparison of 10 different hemostatic dressings in an aortic injury. *J. Trauma* **2003**, 54, 280 –285.

19. Alam, H.B.; Burris, D.; DaCorta, J.A.; Rhee, P. Hemorrhage control in the battlefield: role of new hemostatic agents. *Mil Med.* **2005**, 170, 63–69.

20. Alam, H.B.; Uy, G.B.; Miller, D.; Koustova, E.; Hancock, T.; Inocencio, R.; Anderson, D.; Llorente, O.; Rhee, P. Comparative analysis of hemostatic agents in a swine model of lethal groin injury. *J. Trauma* **2003**, 54, 1077–1082.

21. King, D.R.; Cohn, S.M.; Proctor, K.G. Modified rapid deployment hemostat bandage terminates bleeding in coagulopathic patients with severe visceral injuries. *J. Trauma* **2004**, 57, 756 –759.

22. Blood Coagulation Materials (http://tollefsen.wustl.edu/coagulation/coagulation.html) provided from Tollefsen, D., MD, Ph.D. Lab: Washington University in St. Louis, School of Medicine, Division of Hematolkogy and Oncology. St. Lois, WA

23. Dee, K.C.; Puleo, D.A.; Bizios, R. An introduction to tissue-biomaterial interactions. New York: Wiley-Liss 2002, pp. 53-88.

24. Kheirabadi, B.J. Determination of Efficacy of New Hemostatic Dressings in a Model of Extremity Arterial Hemorrhage in Swine. *J. Trauma* **2009**, 67, 450-460.

25. McKee, P. A.; Mattock, P.; Hill, R.L. Subunit structure of human fibrinogen, soluble fibrin, and cross-linked insoluble fibrin. *Proceeding of the National Academy of Sciences* **1970**, 66 (3), 738-744.

26. Lorand, L. Factor XIII: structure, activation, and interactions with fibrinogen and fibrin. *Ann. N.Y. Acad. Sci.* **2001**, 936, 291–311.

27. Shen, L.; Lorand, L. Contribution of fibrin stabilization to clot strength. Supplementation of factor XIII-deficient plasma with the purified zymogen. *J. Clin. Invest.* **1983**, 71, 1336–1341.

28. Siebenlist, K.R.; Mosesson, M.W. Progressive cross-linking of fibrin gamma chains increases resistance to fibrinolysis. *J. Biol. Chem.* **1994**, 269, 28414–28419.

29. Medved, L.; Nieuwenhuizen, W. Molecular mechanisms of initiation of fibrinolysis by fibrin. *Thromb. Haemost.* **2003**, 89, 409–419.

30. Folk, J.E.; Finlayson, J.S. The ε-γ-(glutamyl)lysine crosslink and the catalytic role of transglutaminases. *Adv. Protein. Chem.* **1977**, 31, 130–133.

31. Zoucas, E.; Goransson, G.; Bengmark, S. Comparative evaluation of local hemostatic agents in experimental liver trauma. A study in the rat. *J. Surg. Res.* **1984**, 37, 145–147.

32. Silverstein, M.E.; Chvapil, M. Experimental and clinical experiences with collagen fleece as a hemostatic agent. *J. Trauma* **1981**, 21, 389–393.

33. Raccuia, J.S.; Simonian, G.; Dardik, J.; Hallac, D.; Salvatore, R.V.; Stahl, R.; Dardik, H. Comparative efficacy of topical hemostatic agents in a rat kidney model. *Am. J. Surg.* **1992**, 163, 235–239.

34. Reiss, R.F. Oz, M.C. Autologous fibrin glue: production and clinical use. *Transfus. Med. Rev*. **1996**, 10, 85-92.

35. Kram, H.B.; Reuben, B.I.; Fleming, A.W.; Shoemaker, W.C. Use of fibrin glue in hepatic trauma. *J. Trauma* **1988**, 28, 1195–1201.

36. Kram, H.B.; Shoemaker, W.C.; Hino, S.T.; Harley, D.P. Splenic salvage using biologic glue. *Arch. Surg.* **1984**, 119, 1309-1311.

37. Sierra, D.H. Fibrin sealant adhesive systems: A review of their chemistry material properties and clinical applications. *J. Biomater. Appl.* **1993**, 7, 309–350.

38. Spotniz, W.D.; Dalton, M.S.; Baker, J.W.; Nolan, S.P. Successful use of fibrin glue during two years of surgery at a University Medical Centre. *Am. Surg.* **1989**, 55, 166–168.

39. Matras, H. Fibrin seal: The state of the art. *J. Oral. Maxillofac. Surg.* **1985**, 43, 605–611.

40. Andreassen, T.T.; Jorgensen, P.H. Biomechanical properties and collagen formation in subcutaneously implanted cellulose sponges treated with fibrin sealant. *Eur. Surg. Res.* **1985**, 17, 264-268.

41. Schelling, G.; Block, T.; Gokel, M.; Blanke, E.; Hammer, C.; Brendel, W. Application of a fibrinogen-thrombin-collagen-based hemostyptic agent in experimental injuries of liver and spleen. *J. Trauma* **1988**, 28, 472-475.

42. Jacob, H.; Campbell, C.D.; Stemberger, A. et al. Combined application of heterologous collagen & fibrin sealant for liver injuries. *J. Surg. Res.* **1984**, 36, 571–577.

43. Scheele, J.; Gentsch, H.H.; Matterson, E. Splenic repair by fibrin tissue adhesive & collagen fleece. *Surgery* **1984**, 95, 6–10.

44. Krishnan, L.K.; Mohanty, M.; Umashankar, P.R.; Arthur Vijayan Lal, A. Comparative evaluation of absorbable hemostats: advantages of fibrin-based sheets. *Biomaterials* **2004**, 25, 5557-5563.

45. Noorjahan, S.E.; Sastry, T.P. Hydrogels based on physiologically clotted fibrin-gelation composites. *J. Polym. Sci., Part A: Polym. Chem.* **2004**, 42, 2241–2252.

46. Ravi Kumar, M.N.V. A review of chitin and chitosan applications. *React. Funct. Polym.* **2000**, 46, 1-27.

47. El-Kamel, A.; Sokar, M.; Naggar, V.; Al Gamal, S. Chitosan and sodium alginate based bioadhesive vaginal tablets. AAPS *PharmSci.* **2002**, 4, 224-230.

48. Kumar, G.; Smith, P. J.; Payne, G. F. Enzymatic grafting of a natural product onto chitosan to confer water solubility under basic conditions. *Biotechnol. Bioeng.* **1999**, 63, 154-165.

49. Chenite, A.; Chaput, C.; Wang, D.; Combes, C.; Buschmann, M.D.; Hoemann, C.D.; Leroux, J.C.; Atkinson, B.L.; Binette, F.; Selmani, A. Novel injectable neutral solutions of chitosan form biodegradable gels *in situ*. *Biomaterials* **2000**, 21, 2155-2161.

50. Kim, I.-Y.; Seo, S.-J.; Moon, H.-S.; Yoo, M.-K.; Park, I.-Y.; Kim, B.-C.; Cho, C.-S. Chitosan and its derivatives for tissue engineering applications. *Biotechnol. Adv.* **2008**, 26, 1-21.

51. Krajewska, B. Membrane-based processes performed with use of chitin/ chitosan materials. *Sep. Purif. Technol.* **2005**, 41, 305–312.

52. Okamoto, Y.; Shibazaki, K.; Minami, S.; Matsuhashi, A.; Tanioka, S.; Shigemasa, Y. Evaluation of chitin and chitosan on open wound healing in dogs. *J. Vet. Med. Sci.* **1995**, 57, 851–854.

53. Okamoto, Y.; Watanabe, M.; Miyatake, K.; Morimoto, M.; Shigemasa, Y.; Minami, S. Effects of chitin/chitosan and their oligomers/monomers on migrations of fibroblasts and vascular endothelium. *Biomaterials* **2002**, 23, 1975–1979.

54. Miyazaki, S.; Yamaguchi, H.; Yokouchi, C.; Takada, M.; Hou, W.M. Sustained release and intra gastric floating granules of indomethacin using chitosan in rabbits. *Chem. Pharm. Bull. (Tokyo)* **1988**, 36, 4033-4038.

55. Sawayanagi, Y.; Nambu, N.; Nagai, T. Use of chitosan for sustained-release preparations of water-soluble drugs. *Chem. Pharm. Bull. (Tokyo)* **1982**, 30, 4213-4215.

56. Miyazaki, T.; Komuro, T.; Yomota, C.; Okada, S. Use of chitosan as a pharmaceutical material: effectiveness as an additional additive of sodium alginate. *Eisei Shikenjo Hokoku* **1990**, 108, 95-97.

57. Macleod, G.S.; Collett, J.H.; Fell, J.T. The potential use of mixed films of pectin, chitosan and HPMC for bimodal drug release. *J. Controlled Release* **1999**, 58, 303-310.

58. Kristmundsdottir, T.; Ingvarsdottir, K.; Saemundsdottir, G. Chitosan matrix tablets: the influence of excipients on drug release. *Drug Dev. Ind. Pharm.* **1995**, 21, 1591-1598.

59. Bernkop-Schnurch, A.; Krajicek, M.E. Mucoadhesive polymers as platforms for peroral peptide delivery and absorption: synthesis and evaluation of different chitosan-EDTA conjugates. *J. Controlled Release* **1998**, 50, 215-223.

60. Bernkop-Schnurch, A.; Pasta, M. Intestinal peptide and protein delivery: Novel bioadhesive drug carrier matrix shielding from enzymatic attack. *J. Pharm. Sci.* **1998**, 87, 430-434.

61. Bernkop-Schnurch, A.; Scerbe-Saiko, A. Synthesis and *in vitro* evaluation of chitosan-EDTA-protease-inhibitor conjugates which might be useful in oral delivery of peptides and proteins. *Pharm. Res*. **1998**, 15, 263-269.

62. Bernkop-Schnurch, A.; Paikl, C.; Valenta, C. Novel bioadhesive chitosan-EDTA conjugate protects leucine enkephalin from degradation by aminopeptidase N. *Pharm. Res*. **1997**, 14, 917-922.

63. Bernkop-Schnurch, A.; Humenberger, C.; Valenta, C. Basic studies on bioadhesive delivery systems for peptide and protein drugs. *Int. J. Pharm*. **1998**, 165, 217-225.

64. Yuan, Z. Study on the synthesis and catalyst oxidation properties of chitosan bound nickel(II) complexes. *J. Agric. Food. Chem.* **2007**, 21, 22–24.

65. Errington, N.; Harding, S.E.; Varum, K.M.; Illum, L. Hydrodynamic characterisation of chitosans varying in degree of acetylation. *Int. J. Biol. Macromol*. **1993**, 15, 113-117.

66. Skaugrud, O. Chitosan - New biopolymer for cosmetics and drugs. *Drug Cosmetic Ind*. **1991**, 148, 24-29.

67. Duarte, M.L.; Ferreira, M.C.; Marvao, M.R.; Rocha, J. An optimised method to determine the degree of acetylation of chitin and chitosan by FTIR spectroscopy. *Int. J. Biol. Macromol.* **2002**, 31, 1-8.

68. Baxter, A.; Dillon, M.; Taylor, K.D.A.; Roberts, G.A.F. Improved method for IR determination of the degree of *N*-acetylation of chitosan. *J. Biol. Macromol.* **1992**, 14, 166-169.

69. Abdou, E.S.; Nagy, K.S.A.; Elsabee, M.Z. Extraction and characterization of chitin and chitosan from local sources. *Bioresour. Technol.* **2008**, 99, 1359–1367.

70. Zhang, Y.; Xue, C.; Xue, Y.; Gao, R.; Zhang, X. Determination of the degree of deacetylation of chitin and chitosan by X-ray powder diffraction. *Carbohydr. Res.* **2005**, 340, 1914–1917.

71. Aiba, S.-I. Determination of the degree of *N*-acetylation of chitosan by ultraviolet spectrophotometry and gel-permeation chromatography. *Int. J. Biol. Macromol.* **1986**, 8, 173-176.

72. Liu, D.; Wei, Y.; Yao, P.; Jiang, L. Determination of the degree of acetylation of chitosan by UV spectrophotometry using dual standards. *Carbohydr. Res.* **2006**, 341, 782–785.

73. Wu, T.; Zivanovic, S. Determination of the degree of acetylation (DA) of chitin and chitosan by an improved first derivative UV method. *Carbohydr. Polym.* **2008**, 73, 248–253.

74. Desbrie`res, J.; Martinez, C.; Rinaudo, M. Hydrophobic derivatives of chitosan: Characterization and rheological behaviour. *Int. J. Biol. Macromol.* **1996**, 19, 21–28.

75. Raymond, L.; Morin, F.G.; Marchessault, R.H. Degree of deacetylation of chitosan using conductometric titration and solid-state NMR. *Carbohydr. Res.* **1993**, 246, 331-336.

76. Cesteros, L.C.; Ramirez, C.A.; Pecina, A.; Katime, I. Poly (ethylene glycol-β-cyclodextrin) gels: Synthesis and properties. *J. Appl. Polym. Sci.* **2006**, 100, 1162–1166.

77. Jiang, X.; Chen, L.; Zhong, W. A new linear potentiometric titration method for the determination of deacetylation degree of chitosan. *Carbohydr. Polym.* **2003**, 54, 457–463.

78. Hayes, E.R.; Davies, O.H. In: Muzzarelli, R.A.A.; Pariser, E., editors. Proceeding of the first international conference on chitin/chitosan. Cambridge, MA: MIT Sea Gant Program, 1978. pp. 406-420.

79. Shive, M.S.; Brodbeck, W.G.; Colton, E.; Anderson, J.M. Shear stress and material surface effects on adherent human monocyte apoptosis. *J. Biomed. Mater. Res.* **2002**, 60, 148–158.

80. Singla, A.K.; Chawla, M. Chitosan: some pharmaceutical and biological aspects - an update. *J. Pharm. Pharmacol.* **2001**, 53, 1047–1067.

81. Whang, H.S.; Kirsch, W.; Zhu, H.; Yang, C.Z.; Hudson, S.M. Hemostatic agents derived from chitin and chitosan. *J. Macromol. Sci. Polym. Rev*. **2005**, C45, 309-323.

82. Rao, S.B.; Sharma, C.P. Use of chitosan as a biomaterial: Studies on its safety and hemostatic potential. *J. Biomed. Mater. Res.* **1997**, 34, 21-28.

83. Wang, H.-S.; Kirsch, W.; Zhu, Y.H.; Yang, C.Z.; Hudson, S.M. Hemostatic agents derived from chitin and chitosan. *Polym. Rev.* **2005**, 45, 309-323.

84. Granville-Chapman, J; Jacobs, N.; Midwinter, M.J. Pre-hospital haemostatic dressings: A systematic review. *Injury* **2011**, 42, 447-459.

85. Kozen, B.G.; Kircher, S.J.; Henao, J.; Godinez, F.S.; Johnson, A.S. An alternative hemostatic dressing: Comparison of CELOX, HemCon, and QuikClot. *Acad. Emerg. Med.* **2008**, 15, 74-81.

86. Granville-Chapman, J.; Jacob, N.; Midwinter, M.J. Pre-hospital haemostatic dressings: A systematic review. *Injury* **2011**, 42, 447-459.

87. King, K.; Neuffer, M.C.; McDivitt, J.; Rose, D.; Cloonan, C.C.; Vayer, J. Homeostatic dressings for the first responder: A review. *Mil. Med.* **2004**, 169, 716-720.

88. Coughlin, S.R. Protease-activated receptors in vascular biology. *Thromb. Haemost.* **2001**, 86, 298–307.

89. Hanson, S.R.; Harker, L.A.; Ratner, B.D.; Hoffmann, A.S. *In vivo* evaluation of artificial surfaces using a nonhuman primate model of arterial thrombosis. *J. Lab. Clin. Med.* **1980**, 95, 289-304.

90. Slack, S.M.; Cui, Y.; Turitto, V.T. The effects of flow on blood coagulation and thrombosis. *Thromb. Haemost.* **1993**, 70, 129–134.

91. Tsai, G.J.; Su, W.H. Antibacterial activity of shrimp chitosan against Escherichia coli. *J. Food Prot.* **1999**, 62, 239-243.

92. Valenta, C.; Christen, B.; Bernkop-Schnurch, A. Chitosan-EDTA conjugate: A novel polymer for topical used gels. *J. Pharm. Pharmacol*. **1998**, 50, 445-452.

93. Klollevold, P.R.; Lew, D.S.; Ellis, D.G.; Bertolami, C.N. Effect of chitosan on lingual hemostasis in rabbit. *J. Oral Maxillofac. Surg.* **1991**, 49, 858-863.

94. Klokkevold, P.R.; Subar, P.; Fukuyama, H.; Bertolami, C.N. Effect of chitosan on lingual hemostasis in rabbits with platelet dysfunction induced by epoprostenol. *J. Oral Maxillofac. Surg.* **1992**, 50, 41-45.

95. Klokkevold, P.R.; Fukuyama, H.; Sung, E.C.; Bertolami, C.N. The effect of chitosan (poly-*N*-Acetyl Glucosamine) on lingual hemostasis in heparinized rabbits. *J. Oral Maxillofac. Surg.* **1999**, 57, 49-52.

96. Okamoto, Y.; Yano, R.; Miyatake, K.; Tomohiro, I.; Shigemasa, Y.; Minami, S. Effect of chitin and chitosan on blood coagulation. *Carbohydr. Polym.* **2003**, 53, 337-342.

97. Dowling, M.B.; Kumar, R.; Keibler, M.A.; Hess, J.R.; Bochicchio, G.V.; Raghavan, S.R. A self-assembling hydrophobically modified chitosan capable of reversible hemostatic action. *Biomaterials* **2011**, 32, 3351-3357.

98. Kurita, K. Chitin and chitosan: functional biopolymers from marine crustaceans. *Mar. Biotechnol.* **2006**, 8, 203–226.

99. Peniche, C.; Monal, W.A.; Goycoolea, F.M. Chitin and chitosan: major sources, properties and applications. In: Belgacem, M.N.; Gandini, A., editors. Monomers, polymers and composites from renewable resources, 1st Ed. Amsterdam: Elsevier 2008, pp. 517–542.

100. Pillai, C.; Paul, W.; Sharma, C.P. Chitin and chitosan polymers: chemistry, solubility and fiber formation. *Progr. Polym. Sci.* **2009**, 34, 641–678.

101. Jayakumar, R.; New, N.; Tokura, S.; Tamura, H. Sulfated chitin and chitosan as novel biomaterials. *Int. J. Biol. Macromol.* **2007**, 40, 175–181.

102. Yalpani, M.; Hall, L.D. Some chemical and analytical aspects of polysaccharide modifications. III. Formation of branched-chain, soluble chitosan derivatives. *Macromolecules* **1984**, 17, 272-281.

103. Desbrires, J.; Martinez, C.; Rinaudo, M. Hydrophobic derivatives of chitosan: Characterization and rheological behaviour. *Int. J. Biol. Macromol.* **1996**, 19, 21-28.

104. Kheirabadi, B.S.; Acheson, E.M.; Deguzman, R.; Sondeen, J.L.; Ryan, K.L.; Delgado, A.; Dick, E.J. Jr.; Holcomb, J.B. Hemostatic efficacy of two advanced dressings in an aortic hemorrhage model in swine. *J. Trauma* **2005**, 59, 25-34.

105. Macosko, C.W. Rheology: Principles, measurements and applications, Part I Constitutive Relations. New York: Wiley/VCH Publishers; 1994, pp. 1-172.

106. Bernkop-Schnurch, A.; Schwarz, V.; Steininger, S. Polymers with thiol groups: A new generation of mucoadhesive polymers. *Pharm. Res.* **1999**, 16, 876-881.

107. Kast, C.E.; Bernkop-Schnurch, A. Thiolated polymers: Development and *in vitro* evaluation of chitosan-thioglycolic acid conjugates. *Biomaterials* **2001**, 22, 2345-2352.

108. Kast, C.E.; Frick, W.; Losert, U.; Bernkop-Schnurch, A. Chitosan-thioglycolic acid conjugate: A new scaffold material for tissue engineering. *Int. J. Pharm.* **2003**, 256, 183-189.

109. Bernkop-Schnurch, A.; Hornof, M.; Zoidl, T. Thiolated polymers-thiomers: Synthesis and *in vitro* evaluation of chitosan-2-iminothiolane conjugates. *Int. J. Pharm.* **2003**, 260, 229-237.

110. Hornof, M.; Kast, C.E.; Bernkop-Schnurch, A. *In vitro* evaluation of the viscoelastic behavior of chitosan-thioglycolic acid conjugates. *Eur. J. Pharm. Biopharm.* **2003**, 55, 185–190.

111. Bernkop-Schnurch, A. Thiomers: A new generation of mucoadhesive polymers. *Adv. Drug Delivery Rev.* **2005**, 57, 1569-1582.

112. Bernkop-Schnurch, A.; Kast, C.E.; Richter, M.F. Improvement in the mucoadhesive properties of alginate by the covalent attachment of cysteine. *J. Controlled Release* **2001**, 71, 277-285.

113. Snyder, G.H.; Reddy, M.K.; Cennerazzo, M.J.; Field, D. Use of local electrostatic environments of cysteines to enhance formation of a desired species in a reversible disulfide exchange reaction. *Biochem. Biophys. Acta.* **1983**, 749, 219-226.

114. Leitner, V.M.; Walker, G.F.; Bernkop-Schnurch, A. Thiolated polymers: Evidence for the formation of disulfide bonds with mucus glycoproteins. *Eur. J. Pharm. Biopharm.* **2003**, 56, 207-214.

115. Bernkop-Schnurch, A.; Schwarz, V.; Steininger, S. Polymers with thiol groups: A new generation of mucoadhesive polymers. *Pharm. Res.* **1999**, 16, 876–881.

116. Bernkop-Schnurch, A.; Steininger, S. Synthesis and characterisation of mucoadhesive thiolated polymers. *Int. J. Pharm.* **2000**, 194, 239–247.

117. Bernkop-Schnurch, A.; Clausen, A.E.; Hnatyszyn, M. Thiolated polymers, synthesis and *in vitro* evaluation of polymer-cysteamine conjugates. *Int. J. Pharm.* **2001**, 226, 185– 194.

118. Bernkop-Schnurch, A.; Leitner, V.; Moser, V. Synthesis and *in vitro* characterization of a poly(acrylic acid)-homocysteine conjugate. *Drug Dev. Ind. Pharm.* **2004**, 30, 1- 8.

119. Clausen, A.E.; Bernkop-Schnurch, A. Development and *in vitro* evaluation of a peptide drug delivery system based on thiolated polycarbophil. *Pharm. Ind.* **2001**, 63, 312– 317.

120. Kast, C.E.; Guggi, D.; Langoth, N.; Bernkop-Schnurch, A. Development and *in vivo* evaluation of an oral delivery system for low molecular weight heparin based on thiolated polycarbophil. *Pharm. Res.* **2003**, 20, 931– 936.

121. Leitner, V.; Guggi, D.; Bernkop-Schnurch, A. Thiomers in non-invasive peptide delivery: *in vitro* and *in vivo* characterisation of a polycarbophil–cysteine/ glutathione gel formulation for hGH. *J. Pharm. Sci.* **2004**, 93, 1682– 1691.

122. Sharma, R.; Ahuja, M. Thiolated pectin: Synthesis, characterization and evaluation as a mucoadhesive polymer. *Carbohydr. Polym.* **2011**, 85, 658–663.

123. Bernkop-Schnurch, A.; Kast, C.E.; Richter, M.F. Improvement in the mucoadhesive properties of alginate by the covalent attachment of cysteine. *J. Controlled Release* **2001**, 71, 277-285.

124. Bernkop-Schnurch, A.; Brandt, U.M.; Clausen, A.E. Synthesis and *in vitro* evaluation of chitosan-cysteine conjugates. *Sci. Pharm.* **1999**, 67, 196-208.

125. Bernkop-Schnurch, A.; Hopf, T.E. Synthesis and *in vitro* evaluation of chitosan-thioglycolic acid conjugates. *Sci. Pharm.* **2001**, 69, 109– 118.

126. Schmitz, T.; Hombach, J.; Bernkop-Schnurch, A. Chitosan-*N*-acetyl cysteine conjugates: *In vitro* evaluation of permeation enhancing and P-glycoprotein inhibiting properties. *Drug Deliv.* **2008**, 15, 245-252.

127. Kafedjiiski, K.; Krauland, A.H.; Hoffer, M.H.; Bernkop-Schnurch, A. Synthesis and *in vitro* evaluation of a novel thiolated chitosan. *Biomaterials* **2005**, 26, 819-826.

128. Kafedjiiski, K.; Foger, F.; Werle, M.; Bernkop-Schnurch, A. Synthesis and *in vitro* evaluation of a novel chitosan-glutathione conjugate. *Pharm. Res.* **2005**, 22, 1480-1488.

129. Millotti, G.; Samberger, C.; Frohlich, E.; Bernkop-Schnurch, A. Chitosan-graft-6-mercaptonicotinic acid: synthesis, characterization, and biocompatibility. *Biomacromolecules* **2009**, 10, 3023-3027.

130. Millotti, G.; Samberger, C.; Frohlich, E.; Sakloetsakun, D.; Bernkop-Schnurch, A. Chitosan-4-mercaptobenzoic acid: Synthesis and characterization of a novel thiolated chitosan. *J. Mater.Chem*. **2010**, 20, 2432-2440.

131. Sarti, F.; Bernkop-Schnurch, A. Chitosan and Thiolated chitosan, *Adv. Polym. Sci.* **2011**, 243, 93-110.

132. Marschütz, M.K.; Caliceti, P.; Bernkop-Schnürch, A. Design and *in vivo* evaluation of an oral delivery system for insulin. *Pharm. Res.* **2000**, 17, 1468–1474.

133. Guggi, D.; Krauland, A.H.; Bernkop-Schnürch, A. Systemic peptide delivery via the stomach: *in vivo* evaluation of an oral dosage form for salmon calcitonin. *J. Controlled Release* **2003**, 92,125–135.

134. Bernkop-Schnürch, A. Chitosan and its derivatives: Potential excipients for peroral peptide delivery systems. *Int. J. Pharm.* **2000**, 194, 1–13.

135. Guggi, D.; Kast, C.E.; Bernkop-Schnürch, A. *In vivo* evaluation of an oral salmon calcitonin-delivery system based on a thiolated chitosan carrier matrix. *Pharm. Res.* **2003**, 20, 1989–1994.

136. Hornof, M.D.; Weyenberg, W.; Ludwig, A.; Bernkop-Schnürch, A. A mucoadhesive ocular insert: Development and *in vivo* evaluation in humans. *J. Controlled Release* **2003**, 89, 419–428.

137. Triantaphyllopoulos, E.; Triantaphyllopoulos, D.C. Amino acid composition of human fibrinogen and anticoagulant derivatives. *Biochem. J.* **1967**, 105, 393-400.

138. Wilson, J.M.; Bayer, R.J.; Hupe, D. Structure-reactivity correlations for the thiol-disulfide interchange reaction. *J. Am. Chem. Soc.* **1977**, 99, 7922–7926.

139. Millotti, G.; Samberger, C.; Fröhlich, E.; Bernkop-Schnürch, A. Chitosan-graft-6-mercaptonicotinic acid: Synthesis, characterization, and biocompatibility. *Biomacromolecules* **2009**, 10, 3023–3027.

140. Shaltiel, S.; Soria, M. Dinitrophenylation and thiolysis in the reversible labeling of a cysteine residue associated with the nicotinamide adenine dinucleotide site of rabbit muscle glyceraldehyde-3-phosphate dehydrogenase. *Biochemistry* **1969**, 8, 4411–4415.

141. Pusateri, A.E.; Holcomb, J.B.; Kheirabadi, B.S.; Alam, H.B.; Wade, C.E.; Ryan, K.L. Making sense of the preclinical literature on advanced hemostatic products. *J. Trauma* **2006**, 60, 674-82.

142. Kheirabadi, B.S.; Scherer, M.R.; Estep, J.S.; Dubick, M.A.; Holcomb, J.B. Determination of efficacy of new hemostatic dressings in a model of extremity arterial hemorrhage in swine. *J. Trauma* **2009**, 67, 450-60.

143. Kheirabadi, B.S.; Acheson, E.M.; Deguzman, R.; Sondeen, J.L.; Ryan, K.L.; Delgado, A., et al. Hemostatic efficacy of two advanced dressings in an aortic hemorrhage model in swine. *J. Trauma* **2005**, 59, 25-34.

144. Ellis-Behnke, R.G.; Liang, Y.-X.; Tay, D.K.C.; Kau, P.W.F.; Schneider, G.E.; Zhang, S.; Wu, W.; So, K.F. Nano hemostat solution: immediate hemostasis at the nanoscale. *Nanomedicine* **2006**, 2, 207-15.

145. Ellis-Behnke, R.G.; Liang, Y.-X.; You, S.W.;Tay, D.K.C.; Zhang, S.; So, K.-F.; Schneider, G.E. Nano neuro knitting: peptide nanofiber scaffold for brain repair and axon regeneration with functional return of vision. *Proc. Natl. Acad. Sci. U S A* **2006**, 103, 5054-5459.

146. Richardson, S.C.; Kolbe, H.V.; Duncan, R. Potential of low molecular mass chitosan as a DNA delivery system: biocompatibility, body distribution and ability to complex and protect DNA. *Int. J. Pharm*. **1999**, 178, 231-243.

147. Tomihata, K.; Ikada, Y. *In vitro* and *in vivo* degradation of films of chitin and its deacetylated derivatives. *Biomaterials* **1997**, 18, 567-575.

148. Lahiji, A.; Sohrabi, A.; Hungerford, D.S.; Frondoza, C.G. Chitosan supports the expression of extracellular matrix proteins in human osteoblasts and chondrocytes. *J. Biomed. Mater. Res.* **2000**, 51, 586-595.

149. Muzzarelli, R.A.A.; Biagini, G.; Bellardini, M.; Simonelli, L.; Castaldini, C.; Fratto, G. Osteoconduction exerted by methylpyrrolidinone chitosan used in dental surgery. *Biomaterials* **1993**, 14, 39-43.

150. Onishi, H.; Machida, Y. Biodegradation and distribution of water-soluble chitosan in mice. *Biomaterials* **1999**, 20, 175-182.

151. Kato, Y.; Onishi, H.; Machida, Y. *N*-succinyl-chitosan as a drug carrier: water-insoluble and water-soluble conjugates. *Biomaterials* **2004**, 25, 907-915.

152. Brown, C.D.; Kreilgaard, L.; Nakakura, M.; Caram-Lelham, N.; Pettit, D.K.; Gombotz, W.R.; Hoffman, A.S. Release of PEGylated granulocyte-macrophage colony-stimulating factor from chitosan/ glycerol films. *J. Controlled Release* **2001**, 72, 35-46.

153. Cui, Y.L.; Qi, A.D.; Liu, W.G.; Wang, X.H.; Wang, H.; Ma, D.M.; Yao, K.D. Biomimetic surface modification of poly(L-lactic acid) with chitosan and its effects on articular chondrocytes *in vitro*. *Biomaterials* **2003**, 24, 3859-3868.

154. Wang, X.H.; Li, D.P.; Wang, W.J.; Feng, Q.L.; Cui, F.Z.; Xu, Y.X.; Song, X.H.; van der Werf, M. Crosslinked collagen/chitosan matrix for artificial livers. *Biomaterials* **2003**, 24, 3213-3220.

155. El-Mekawy, A.; Hudson, S.M.; El-Baz, A.; Hamza, H.; El-Halafawy, K. Preparation of chitosan films mixed with superabsorbent polymer and evaluation of its haemostatic and antibacterial activities. *J. Appl. Polym. Sci.* **2010**, 117, 3489-3496.

156. Yamane, S.; Iwasaki, N.; Majima, T.; Funakoshi, T.; Masuko, T.; Harada, K.; Minami, A.; Monde, K.; Nishimura, S. Feasibility of chitosan-based hyaluronic acid hybrid biomaterial for a novel scaffold in cartilage tissue engineering. *Biomaterials* **2005**, 26, 611-619.

157. Iwasaki, N.; Yamane, S. T.; Majima, T.; Kasahara, Y.; Minami, A.;Harada, K.; Nonaka, S.; Maekawa, N.; Tamura, H.; Tokura, S.;Shiono, M.; Monde, K.; Nishimura, S. Feasibility of polysaccharide hybrid materials for scaffolds in cartilage tissue engineering: Evaluation of chondrocyte adhesion to polyion complex fibers prepared from alginate and chitosan. *Biomacromolecules* **2004**, 5, 828-833.

158. Wei, Y.C.; Hudson, S.M.; Meyer, J.M.; Kaplan. D.L. The cross-linking of chitosan fibers with epichlorohydrin. *J. Polym. Sci. Polym. Chem. Ed.* **1992**, 30, 2187-2193.

159. Knaul, J.Z.; Hudson, S.M.; Creber, K. Cross-linking of chitosan fibers with dialdehydes: Proposal of a new reaction mechanism. *J. Polym. Sci., Part B: Polym. Phys.* **1999**, 37, 1079-1094.

160. Park, Y.J.; Lee, Y.M.; Park, S.N.; Sheen, S.Y.; Chung, C.P.; Lee, S.J. Platelet derived growth factor releasing chitosan sponge for periodontal bone regeneration. *Biomaterials* **2000**, 21, 153-159.

161. Ma, L.; Gao, C.; Mao, Z.; Zhou, J.; Shen, J.; Hu, X.; Han, C. Collagen/chitosan porous scaffolds with improved biostability for skin tissue engineering. *Biomaterials* **2003**, 24, 4833-4841.

162. Suh, J.-K Francis; Matthew, H.W. Application of chitosan-based polysaccharide biomaterials in cartilage tissue engineering: A review. *Biomaterials* **2000**, 21, 2589-2598.

163. Ishihara, M.; Obara, K.; Ishizuka, T.; Fujita, M.; Sato, M.; Masuoka, K.; Saito, Y.; Yura, H.; Matsui, T.; Hattori, H.; Kikuchi, M.; Kurita, A. Controlled release of fibroblast growth factors and heparin from photocrosslinked chitosan hydrogels and subsequent effect on *in vivo* vascularization. *J. Biomed. Mater. Res.* **2003**, 64A, 551-559.

164. Bernkop-Schnu¨rch, A.; Hornof, M.; Zoidl, T. Thiolated polymers—thiomers: Synthesis and *in vitro* evaluation of chitosan–2-iminothiolane conjugates. *Int. J. Pharm.* **2003**, 260, 229-237.

165. Biagini, G.; Pugnaloni, A.; Damadei, A.; Bertani, A.; Belligolli, A.; Bicchiega, V.; Muzzarelli, R. Morphological study of the capsular organization around tissue expanders coated with *N*-carboxybutyl chitosan. *Biomaterials* **1991**, 12, 287-291.

166. Suzuki, M.; Itoh, S.; Yamaguchi, I.; Takakuda, K.; Kobayashi, H.; Shinomiya, K.; Tanaka, J. Tendon chitosan tubes covalently coupled with synthesized laminin peptides facilitate nerve regeneration *in vivo*. *J. Neurosci. Res.* **2003**, 72, 646-659.

167. Nishioka, Y.; Kyotani, S.; Okamura, M.; Miyazaki, M.; Sakamoto,Y.; Morita, M.; Okazaki, K.; Ohnishi, S.; Yamamoto, Y.; Ito, K. A study of embolizing materials for chemo-embolization therapy of hepatocellular carcinoma: embolic effect of cisplatin albumin microspheres using chitin and chitosan in dogs, and changes of cisplatin content in blood and tissue. *Chem. Pharm. Bull. (Tokyo)* **1992**, 40, 267-268.

168. Aiedeh, K.; Gianasi, E.; Orienti, I.; Zecchi, V. Chitosan microcapsules as controlled release systems for insulin. *J. Microencapsulation* **1997**, 14, 567-576.

169. Huang, M.; Ma, Z.; Khor, E.; Lim, L.Y. Uptake of FITC-chitosan nanoparticles by A549 cells. *Pharm. Res.* **2002**, 19, 1488-1494.

170. Xu, Y.; Du, Y.; Huang, R.; Gao, L. Preparation and modification of *N*-(2-hydroxyl) propyl-3-trimethyl ammonium chitosan chloride nanoparticle as a protein carrier. *Biomaterials* **2003**, 24, 5015-5022.

171. Xu, Y.; Du, Y. Effect of molecular structure of chitosan on protein delivery properties of chitosan nanoparticles. *Int. J. Pharm.* **2003**, 250, 215-226.

172. Mitra, S.; Gaur, U.; Ghosh, P. C.; Maitra, A. N. Tumour targeted delivery of encapsulated dextran–doxorubicin conjugate using chitosan nanoparticles as carrier. *J. Controlled Release* **2001**, *74*, 317-323.

173. Rinaudo, M. Chitin and chitosan: Properties and applications. *Prog. Polym. Sci.* **2006**, 31, 603-632.

174. Sosa, M.A.; Fazely, F.; Koch, J.A.; Vercellotti, S.V.; Ruprecht, R.M. *N*-carboxymethylchitosan-N,O-sulfate as an anti-HIV-1 agent. *Biochem. Biophys. Res. Commun.* **1991**, 174, 489-496.

175. Muzzarelli, R.; Tarsi, R.; Filippini, O.; Giovanetti, E.; Biagini, G.; Varaldo, P.E. Antimicrobial properties of *N*-carboxybutyl chitosan. *Antimicrob. Agents Chemother.* **1990**, 34, 2019-2023.

176. Qin, C.; Du, Y.; Xiao, L.; Li, Z.; Gao, X. Enzymic preparation of water-soluble chitosan and their antitumor activity. *Int. J. Biol. Macromol.* **2002**, 31, 111-117.

177. Kato, Y.; Onishi, H.; Machida, Y. *N*-Succinyl-chitosan as a drug carrier: Water-insoluble and water-soluble conjugates. *Biomaterials* **2004**, 25, 907-915.

178. Vongchan, P.; Sajomsang, W.; Subyen, D.; Kongtawelert, P. Anticoagulant activity of a sulfated chitosan. *Carbohydr. Res.* **2002**, 337, 1239-1242.

179. Suzuki, M.; Itoh, S.; Yamaguchi, I.; Takakuda, K.; Kobayashi, H.; Shinomiya, K.; Tanaka, J. Tendon chitosan tubes covalently coupled with synthesized laminin peptides facilitate nerve regeneration *in vivo*. *J. Neurosci. Res.* **2003**, 72, 646-659.

180. Hudson S.M.; Jenkins, D.W. Chitin and chitosan. In: Mark, H.F., editor. EPST. vol. 1. 3rd ed. New York: Wiley; 2003. pp 569–580.

181. Roberts, G.A.F. Chitin chemistry. London: The MacMillan Press Ltd, 1992. 350 pp.

182. Morimoto, M.; Saimoto, H.; Shigemasa, Y. Control of functions of chitin and chitosan by chemical modifications. *Trends Glycosci. Glycotech*. **2002**, 14, 205–222.

183. Rinaudo, M.; Reguant, J. Polysaccharide derivatives. In: Frollini, E.; Leão, A.L.; Mattoso, L.H.C. editors. Natural polymers and agrofibers composites. São Carlos, Brésil: CIP-BRASIL, 2000. pp. 15-39.

184. Nishimura, K.; Nishimura, S.; Nishi, N.; Saiki, I.; Tokura, S.; Azuma, I. Immunological activity of chitin and its derivatives. *Vaccine* **1984**, 2, 93-99.

185. Schipper, N.G.; Olsson, S.; Hoogstraate, J.A.; deBoer, A.G.; Varum, K.M.; Artursson, P. Chitosan as absorption enhancers for poorly absorbable drug2: mechanism of absorption enhancement. *Pharm. Res.* **1997**, 14, 923-929.

186. Biagini, G.; Bertani, A.; Muzzarelli, R.; Damadei, A.; DiBenedetto, G.; Belligolli, A.; Riccotti, G.; Zucchini, C.; Rizzoli, C. Wound management with *N*-carboxybutyl chitosan. *Biomaterials* **1991**, 12, 281-286.

187. Chen, X.G.; Wang, Z.; Liu, W.S.; Park, H. J. The effect of carboxymethyl-chitosan on proloferation and collagen secretion of normal and keloid skin fibroblasts. *Biomaterials* **2002**, 23, 4609-4614.

188. Ueno, H.; Yamada, H.; Tanaka, I.; Kaba, N.; Matsuura, M.; Okumura, M.; Kadosawa, T.; Fujinaga, T. Accelerating effects of chitosan for healing at early phase of experimental open wound in dogs. *Biomaterials* **1999**, 20, 1407-1414.

189. Hirai, A.; Odani, H.; Nakajima, A. Determination of degree of deacetylation of chitosan by ^{1}H NMR spectroscopy. *Polym. Bull.* **1991**, 26, 87-94.

190. Knaul, J.Z.; Kasaai, M.R.; Bui, V.T.; Creber, K.A.M. Characterization of deacetylated chitosan and chitosan molecular weight review. *Can. J. Chemistry* **1998**, 76, 1699-1706.

191. Wang, W.; Bo, S.; Li, S.; Qin, W. Determination of the Mark-Houwink equation for chitosans with different degree of deacetylation. *Int. J. Biol. Macromol.* **1991**, 13, 281-285.

192. Domard, A.; Rinaudo, M. Preparation and characterization of fully deacetylated chitosan. *Int. J. Biol. Macromol.* **1983**, 5, 49-52.

193. Pavia, D.L.; Lampman, G.M.; Kriz, G.S. Introduction to spectroscopy: A guide for students of organic chemistry, 2nd ed. Fort Worth: Harcourt Brace College Publishers, 1996. 511 pp.

194. Gum Jr., J.R.; Hicks, J.W.; Toribara, N.W.; Rothe, E.-M.; Lagace, R.E.; Kim, Y.S. The human *MUC*2 intestinal mucin has cysteine-rich subdomains located both upstream and downstream of its central repetitive region. *J. Biol. Chem.* **1992**, 267, 21375–21383.

195. Bernkop-Schnu¨rch, A.; Schwarz, V.; Steininger, S. Polymers with thiol groups: A new generation of mucoadhesive polymers. *Pharm. Res.* **1999**, 16, 876–881.

196. Kast, C.E.; Bernkop-Schnu¨rch, A. Thiolated polymers: development and *in vitro* evaluation of chitosan–thioglycolic acid conjugates. *Biomaterials* **2001**, 22, 2345-2352.

197. Gurd, F.N. Carboxymethylation. *Methods Enzymol.* **1967**, 11, 532-541.

198. Cole, R.D.; Stein, W.H.; Moore, S. On the cysteine content of human hemoglobin. *J. Biol. Chem.* **1958**, 233, 1359-1363.

199. Dickens, F. Interaction of halogenacetates and SH compounds: The reaction of halogenacetic acids with glutathione and cysteine. The mechanism of iodoacetate poisoning of glyoxalase. *Biochem. J.* **1933**, 27, 1141-1151.

200. Smythe, C.V. The reaction of iodoacetate and of iodoacetamide with various sulfhydryl groups, with urease, and with yeast preparations. *J. Biol. Chem.* **1936**, 114, 601-612.

201. Rapkine, L. The effect of monoiodo-acetic acid on the sulph-hydrate groups of proteins. *Comptes Rendus des Seances de la Societe de Biologie et de ses Filiales* **1933**, 112, 1294-1296.

202. Mirsky, A.E.; Anson, M.L. Sulfhydryl and disulfide groups of proteins: I. Methods of estimation. *J. Gen. Physiol.* **1935**, 18, 307-323.

203. Rosner, L. The Reaction between iodoacetic acid and denatured egg albumin. *J. Biol. Chem.* **1940**, 132, 657-662.

204. Michaelis, L.; Schubert, M.P. The reaction of iodoacetic acid on mercaptans and amines. *J. Biol. Chem.* **1934**, 106, 331-341.

205. Greenstein, J.P. Sulfhydryl groups in proteins: I. Egg albumin in solutions of urea, guanidine, and their derivatives. *J. Biol. Chem.* **1938**, 125, 501-513.

206. Anson, M.L.; Mirsky, A.E. Protein coagulation and its reversal: Serum albumin. *J. Gen. Physiol*. **1931**, 14, 725-732.

207. Cuculo, J.A.; Aminuddin, N.; Frey, M.W. Solvent spun cellulose fibers. In: Salem, D. R., editor. Structure Formationin Polymeric Fibers. Munich: Hanser Publishers 2000; pp. 296–328.

208. Krajewska, B.; Zaborska, W.; Leszko, M. Inhibition of chitosan-immobilized urease by boric acid as determined by integration methods. *J. Mol. Catal. B: Enzym* **1997**, 3, 231-238.

209. Krajewska, B.; Leszko, M.; Zaborska, W. Urease immobilized on chitosan membrane: Preparation and properties. *J. Chem. Technol. Biotechnol.* **1990**, 48, 337-350.

210. Muzzarelli, R.A.A. Immobilization of enzymes on chitin and chitosan. *Enzyme Microb. Technol.* **1980**, 2, 177-184.

211. Cestari, A.R.; Airoldi, C. Diamine immobilization on silica gel through the sol−gel process and increase in the organic chain by using glutaraldehyde followed by ethylenediamine. *Langmuir* **1997**, 13, 2681-2686.

212. Ishii, H.; Minegishi, M.; Lavitpichayawong, B.; Mitani, T. Synthesis of chitosan-amino acid conjugates and their use in heavy metal uptake. *Int. J. Biol. Macromol.* **1995**, 17, 21-23.

213. Hsien, T.-Y.; Rorrer, G.L. Effects of acylation and crosslinking on the material properties and cadmium ion adsorption capacity of porous chitosan beads. *Sep. Sci. Technol.* **1995**, 30, 2455-2475.

214. Knaul, J.Z.; Hudson, S.M.; Creber, K.A.M. Cross-linking of chitosan fibers with dialdehydes: Proposal of a new reaction mechanism. *J. Polym. Sci., Part B: Polym. Phys.* **1999**, 37, 1079–1094.

215. Winter, H.; Chambon, F. Analysis of linear viscoelasticity of a crosslinking polymer at the gel point. *J. Rheol.* **1986**, 30, 367-382.

216. Sengupta, S.; Lohse, C.M.; Cheville, J.C.; Leibovich, B.C.; Thompson, R.H.; Webstar, W.S.; Frank, I; Zincke, H.; Blute, M.L.; Kwon, E.D. The preoperative erythrocyte sedimentation rate is an independent prognostic factor in renal cell carcinoma. *Cancer* **2006**, 106, 304-312.

217. Klossner R.R.; Queen, H.A.; Coughlin, A.J.; Krause, W.E. Correlation of chitosan's rheological properties and its ability to electrospin. *Biomacromolecules* **2008**, 9, 2947–2953.

218. Wang W.; Xu, D. Viscosity and flow properties of concentrated solutions of chitosan with different degrees of deacetylation. *Int. J. Biol. Macromol.* **1994**, 16, 149–152.

219. Desbrieres, J. Viscosity of semiflexible chitosan solutions: Influence of concentration, temperature, and role of intermolecular interactions. *Biomacromolecules* **2002**, 3, 342–349.

220. Mucha, M. Rheological characteristics of semi-dilute chitosan solutions. *Macromol. Chem. Phys.* **1997**, 198, 471–484.

221. Park, J.B.; Lakes, R.S. Biomaterials: An Introduction, 2 nd ed. New York: Plenum Press 1992.

222. Dobrynin, A.V.; Colby, R.H.; Rubinstein, M. Scaling theory of polyelectrolyte solutions. *Macromolecules* **1995**, 28, 1859–1871.

223. Glenn Elert. Viscosity. The Physics Hypertextbook-Viscosity (http://physics.info/viscosity/). Physics.info. Retrieved 2010-09-14.

224. Waugh, A.; Grant, A. In: Ross and Wilson: Anatomy and Physiology in Health and Illness (10th ed.). Philadelphia: Churchill Livingstone Elsevier. 2007. pp. 22.

225. Sannan, T.; Kurita, K.; Iwakura, Y. Studies of Chitin, 2: Effect of deacetylation on solubility. *Makromol. Chem.* **1976**, 177, 3589-3600.

226. Malek, A.M.; Alper, S.L.; Izumo, S. Hemodynamic shear stress and its role in atherosclerosis. *JAMA.* **1999**, 282, 2035-2042.

227. Karino, T.; Goldsmith, H.L. Role of blood cell-wall interactions in thrombogenesis and atherogenesis: a microrheological study. *Biorheology* **1984**, 21, 587–601.

228. Nash, G.B.; Wenby, R.; Sowemimo-Coker, S.O.; Meiselman, H.J. Influence of cellular properties on red cell aggregation. *Clin. Hemorheol.* **1987**, 7, 93–108.

229. Shalak, R.; Zarda, P.; Jan, K.M.; Chien, S. Mechanism of rouleaux formation. *Biophys. J.* **1981**, 35, 771–781.

230. Chien, S. Rheology in the microcirculation in normal and low flow states. *Adv. Shock. Res.* **1982**, 8, 71–80.

231. Chien, S.; Usami, S.; Dellenback, R.J.; Gregersen, M.I. Shear-dependent interaction of plasma proteins with erythrocytes in blood rheology. *Am. J. Physiol.* **1970**, 219, 143-153.

232. Cerny, L.C.; Cook, F.B.; Walker, C.C. Rheology of blood. *Am. J. Physiol.* **1962**, 202, 1188-1194.

233. Cokelet, G.R.; Merrill, E.W.; Gilliland, E.R.; Shin, H. The rheology of human blood-measurement near and at zero shear rate. *Trans. Soc. Rheol.* **1963**, 7, 303-317.

234. Fusman. R.; Zeltser, D.; Rotstein, R.; Chapman, J.; Avitzour, D.; Shapira, I.; Eldor, A.; Elkayam, O.; Caspi, D.; Arber, N.; Berliner, S. INFLAMET: an image analyzer to display erythrocyte adhesiveness/aggregation. *Eur. J. Intern. Med.* **2000**, 11, 271–276.

235. Yamamoto, M. Effects of fibrinogen, globulin, albumin and hematocrit on the kinetics of erythrocyte aggregation in man. *Angiology* **1986**, 37, 663–671.

236. Madl, C.; Koppensteiner, R.; Wendelin, B.; Lenz, K.; Kramer, L.; Grimm, G.; Kranz, A.; Schneeweiss, B.; Ehringer, H. Effect of immunoglobulin administration on blood rheology in patients with septic shock. *Circ. Shock* **1993**, 40, 264–267.

237. Maeda, N.; Shiga, T. Opposite effect of albumin on the erythrocyte aggregation induced by immunoglobulin G and fibrinogen. *Biochim. Biophys. Acta*. **1986**, 85, 127–135.

238. Rampling, M.W.; Martin, G. Albumin and rouleaux formation. *Clin. Hemorheol.* **1992**, 12, 761–765.

239. Lacombe, C.; Bucherer, C.; Ladjouzi, J.; Lelievre, J.C. Competitive role between fibrinogen and albumin on thixotropy of red cell suspensions. *Biorheology* **1988**, 25, 349–354.

240. Weng, X.; Roederer, G.O.; Beaulieu, R.; Cloutier, G. Contribution of acute-phase proteins and cardiovascular risk factors to erythrocyte aggregation in normolipidemic and hyperlipidemic individuals. *Thromb. Haemost.* **1998**, 80, 903–908.

241. Reinhart, W.H.; Nagy, C. Albumin affects erythrocyte aggregation and sedimentation. *Eur. J. Clin. Invest.* **1995**, 25, 523–528.

242. Ben-Ami, R.; Barshtein, G.; Mardi, T.; Deutch, V.; Elkayam, O.; Yedgar, S.; Berliner, S. A synergistic effect of albumin and fibrinogen on immunoglobulin-induced red blood cell aggregation. *Am. J. Physiol. Heart. Circ. Physiol.* **2003**, 285, H2663–H2669.

243. Chien, S.; Usami, S.; Dellenback, R.J.; Gregersen, M.I.; Nanninga, L.B.; Guest, M.M. Blood viscosity: influence of erythrocyte aggregation. *Science* **1967**, 157, 829-831.

244. Weed, R.I.; Reed, C.F.; Berg, B. Is hemoglobin an essential structural component of human erythrocyte membranes? *J. Clin. Invest.* **1963**, 42, 581–588.

245. Connie, C.W.; Hsia, M.D. Respiratory function of hemoglobin. *N. Engl. J. Med.* **1998**, 338, 239-248.

246. Fukunaga, K.; Nakazono, N.; Yoshida, M. Determination of reduced-form glutathione and total glutathione in blood and plasma by high performance liquid chromatography with on-column fluorescence derivatization. *Chromatographia* **1998**, 48, 690-694.

247. Kosower, N.S.; Kosower, E.M.; Koppel, R.L. Sensitivity of hemoglobin thiol groups within red blood cells of rat during oxidation of glutathione. *Eur. J. Biochem.* **1977**, 77, 529-534.

248. Bernkop-Schnurch, A.; Guggi, D.; Pinter, Y. Thiolated chitosans: development and *in vitro* evaluation of a mucoadhesive, permeation enhancing oral drug delivery system. *J. Controlled Release* **2004**, 94, 177-186.

249. Bernkop-Schnürch,A.; Guggi, D.; Pinter, Y. Thiolated chitosans: development and *in vivo* evaluation of a mucoadhesive permeation enhancing oral drug delivery system. *J. Controlled Release* **2004**, 94,177–186.

250. Roldo, M.; Hornof, M.; Caliceti, P.; Bernkop-Schnurch, A. Mucoadhesive thiolated chitosans as platforms for oral controlled drug delivery: Synthesis and *in vitro* evaluation. *Eur. J. Pharm. Biopharm.* **2004**, 67, 116-121.

251. Kast, C., Valenta, C., Leopold, M. Bernkop-Schnurch, A. Design and *in vitro* evaluation of a novel bioadhesive vaginal drug delivery system for clotrimazole. *J. Controlled Release* **2002**, 81, 347-364.

252. Kast, C.E.; Frick, W.; Losert, U.; Bernskop-Schnurch, A. Chitosan thioglycolic acid conjugate: a new scaffold material for tissue engineering. *Int. J. Pharm.* **2003**, 256, 183–189.

253. Hintzen, F.; Laffleur, F.; Sarti, f.; Shahnaz, G.; Bernkop-Schnurch, A. Thiomers: influence of molar mass on *in situ* gelling properties. *Int. J. Pharm.* **2012**, 436, 120-126.

APPENDICES

Appendix A Poly(vinyl alcohol) (PVA)-Iodoacetyl Ester

A hydrogel matrix, which is a three-dimensional structure, is generally made up of hydrophilic polymers, such as poly(vinyl alcohol)(PVA), poly(vinyl pyrrolidone), poly(acrylic acid), etc. and holds significant amount of water in its porous structure. PVA is one of the most widely studied hydrophilic polymers that is soluble in water where the optimum conditions for dissolutions are primary governed by the degree of hydrolysis, molecular weight, particle size distribution, and crystallinity. PVA hydrogel is preferable due to its greater biocompatibility, as well as industrial adaptability for large scale manufacture and environmental friendly disposal. On the other hand, it has low mechanical strength and thermal stability. In order to improve its properties and increase the potential use of PVA, chemical modifications have been performed by various methods. Esterification of PVA by reaction with various acid chlorides or acid anhydrides to develop functional materials is one route. As a potential hemostatic wound dressing material, its hydrophilicity is useful to absorb the running blood. Moreover, iodoacetic acid has been successfully demonstrated to interact with sulfhydryl compounds. For this purpose, PVA-iodoacetyl ester derivative was prepared via esterification of PVA with iodoacetic acid and its potential to cause enhanced blood clots formation was preliminarily studied. In contrast to chitosan derivatives that have ionic interactions with the negatively charged blood cells, this derivative would be a good candidate to evaluate the covalent interaction of iodoacetic acid residue with the blood serum proteins and blood cells, eliminating the ionic interaction.

A-1 Esterification of PVA with Iodoacetic acid

PVA 2g (45.5 mmol repeat units, Aldrich 87~89% hydrated, MW=124000-186000) was dissolved in 100 mL deionized water, heated to 80˚C, to make a 2 wt% PVA aqueous solution. Iodoacetic acid 1.7g (9.12 mmol, ≥ 99.0% Sigma-Aldrich) was dissolved in 40 mL of 7N HCl. The iodoacetic acid solution was added dropwise into PVA solution over 20 minutes. The reaction was conducted for 12h at 80˚C. After 8h, the reacted solution was slowly poured into methanol. The obtained white precipitate was filtered, washed repeatedly by methanol, and dried under free from moisture at room temperature.

A-2 Characterization by FTIR

Figure A-1 and A-2 show the FTIR spectra of modified PVA and the prepared PVA-iodoacetyl ester, respectively. In Figure A-1, a very strong and broad O-H stretch vibration appears at 3360 cm^{-1}. The peaks between 2930 cm^{-1} and 2850 cm^{-1} are typical C-H stretching vibrations. The sharp peak at 1732 cm^{-1} appears, which is due to C=O stretch of an ester group of unhydrolyzed polyvinyl acetate repeat unit. The PVA used in this experiment has the degree of hydrolysis of 85-87%. Also, the peak at 1427 cm^{-1} is attributed to C-OH stretching vibration. In Figure A-2 of the derivative spectrum, the strong broad peak of OH group still appeared at 3340 cm^{-1}. Also, C-H stretching vibration bands were observed at 2946 cm^{-1} and 2839 cm^{-1}. The peaks at 1251 cm^{-1} and 1092 cm^{-1} are assigned for C-O-C stretch of the vinyl acetate units and C-O stretch of the vinyl units, respectively. On the other hand, the sharp peak of C=O stretch of vinyl acetate at 1732 cm^{-1} disappeared, while a new

peak appeared at 1652 cm^{-1}, which is due to C=O stretch of the introduced ester groups via the reaction with iodoacetic acid. The iodo group shifts the C=O peak to this lower value. The weak peak of C-OH stretching appeared at 1418 cm^{-1}, indicating some OH groups of the vinyl units were used for the reaction.

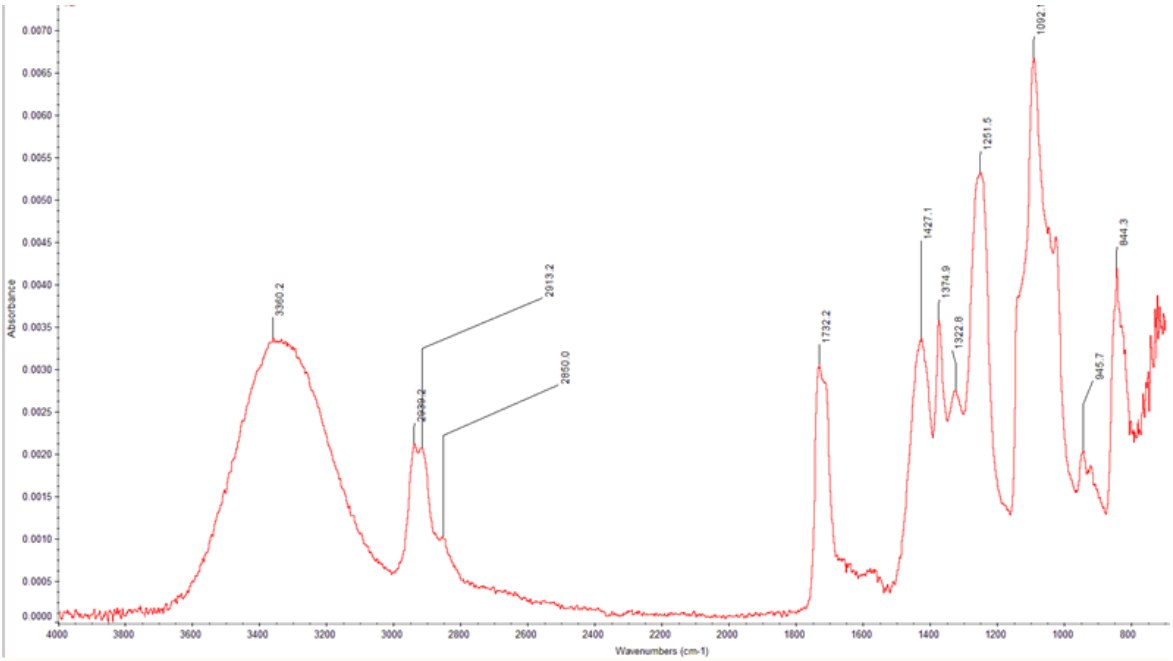

Figure A-1 FTIR spectrum of PVA sample used.

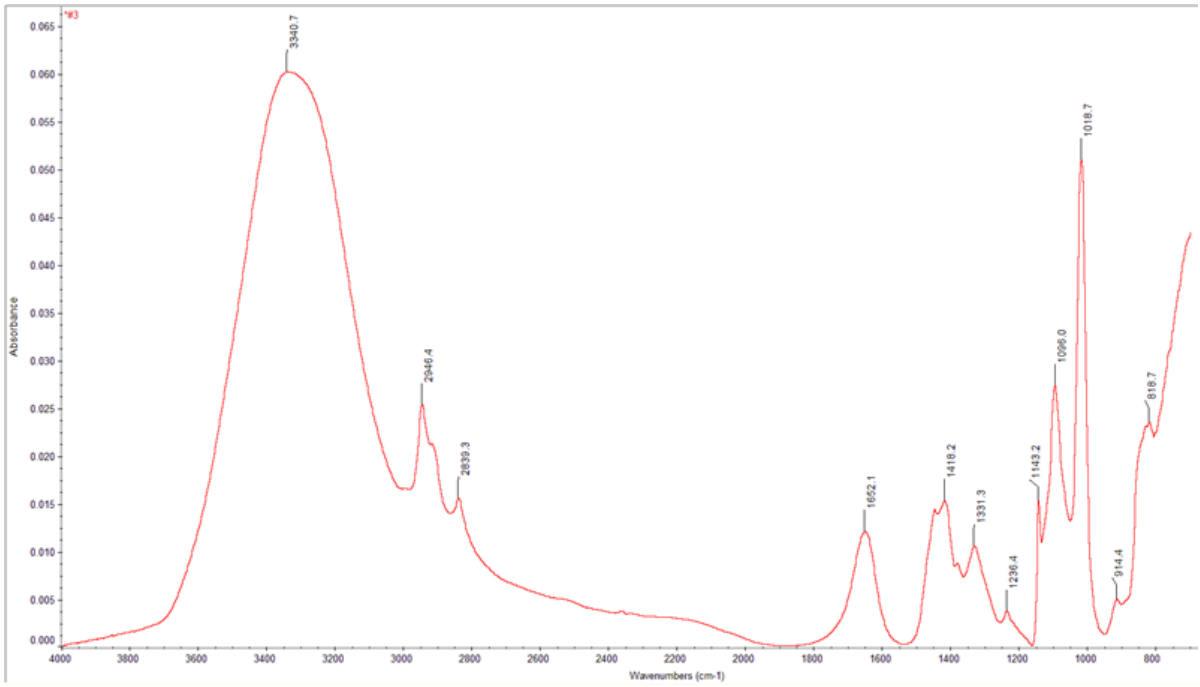

Figure A-2 FTIR spectrum of prepared PVA-iodoacetyl ester sample.

Appendix B Reactivity between CIA and BSA

This study demonstrated that the CIA is capable of inducing the rapid clot formation of whole blood. The mechanism of the observed rapid clot formation is assumed to result from the interaction between CIA and blood serum protein, especially at cysteine residue site. For the purpose of confirming this, albumin, which is contained in the blood serum at a rate of 4.4~5%, was tested on its reaction with CIA. The native albumin, nevertheless, has been reported to exhibit the less reactivity for iodoacetamide and iodoacetate.[201,202] On the other hand, these studies stated that it took only three hours to complete the reaction between denatured albumin and iodo-compounds. Moreover, the denatured albumin contains 0.55% of free cysteine that is available for the reaction. This finding indicates that the denatured albumin is worth trying as a model blood to demonstrate the interaction between CIA and cysteine (or other sulfhydryl compounds) in the blood through sulfide bonds formation.

B-1.1 Preparation of Denatured Albumin

Bovine serum albumin (BSA, ≥98% Sigma-Aldrich) was dissolved in 0.05 N HCl to prepare a 5 wt% solution. Then, this solution was added into 10 times volume of acetone containing 0.2 wt% of 5N HCl under stirring. The white precipitate was washed by acetone.

B-1.2 Preparation of CIAsolution and Denatured BSA solution

2 wt% of CIA/0.3M AcOH (0.5mL) was mixed with 4wt% BSA aq. (1mL). The solution pH was then raised to ~7 by 1N NaOH. This mixture was incubated in 37˚C water

bath for 3 hours. In the same manner, 2 wt% of chitosan/0.3M AcOH mixed with 4 wt% BSA aq. and 2 wt% of CIA/0.3M AcOH itself without the BSA aq. were prepared and incubated as controls.

B-2 Reaction between CIA and Denatured BSA

In order to study the reactivity of the denatured BSA toward the CIA, both solutions were mixed and reacted for 3 hours at pH~7, 37˚C. Figure B-1 shows pictures of the reaction mixture at each point. The mixture was totally miscible before the pH was raised (the solution originally showed the pH value of 5.5), on the other hand, a white precipitate started appearing right after 1N NaOH was added to the mixture until the pH reached 7. After the incubation for 3 hours, the precipitate was separated from the solution. Two controls, unmodified chitosan solution mixed with the BSA solution and CIA solution only, also formed gel-like precipitates after raising their pH values. However, the obtained precipitates were more like wet and clear gels and different from that obtained from the CIA/BSA mixture, as showed in Figure B-2. Also, the precipitate from CIA/BSA could not be dissolved in 0.3M AcOH any longer, suggesting this would be a reaction product between the CIA and the denatured BSA. These results indicate that CIA is capable of reacting with the denatured BSA, possibly through iodoacetic acid residue and sulfhydryl compounds in BSA.

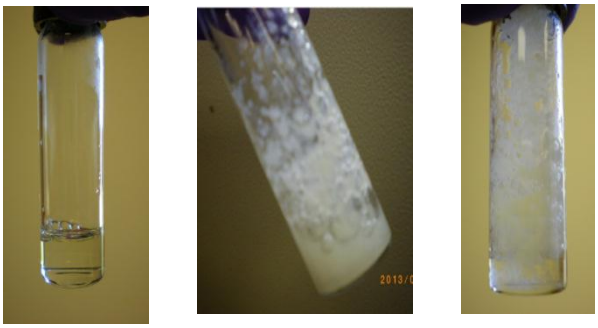

Figure B-1 Photographs of 2 wt% CIA/0.3M AcOH (0.5 mL) mixed with 4 wt% denatured BSA aq. (1 mL); before pH was raised (left), right after pH was raised to 7 (middle), and after incubated for 3h at 37˚C (right).

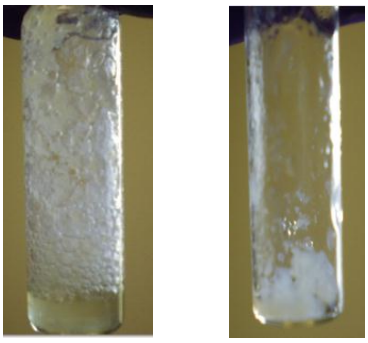

Figure B-2 Photographs of 2 wt% Chitosan/0.3M AcOH (0.5 mL) mixed with 4 wt% denatured BSA aq. (1 mL) (left), 2wt% CIA/0.3M AcOH (0.5 mL) (right) after incubation for 3h at 37˚C.

The reactivity of CIA and the denatured BSA was furthermore, studied by a colorimetric analysis. As described earlier, iodoacetic acid residue is supposed to get involved in the reaction against the sulfhydryl groups releasing HI, thus, the presence of the reaction might be confirmed by using a soluble starch solution. In fact, the clear CIA/AcOH with a starch solution turned to exhibit a blue color when H_2O_2 (an oxidant) was added. This is considered that iodide ions in CIA derivative were oxidized and formed free iodine

molecule, which slides into amylose coil and give the characteristic color. This blue color of the CIA solution disappeared by adding the BSA aq. solution. On the other hand, the CIA/BSA mixture after 3 hour-reaction did not exhibit the blue color with starch and H_2O_2 although the solution showed slightly yellow color (Figure B-3). This is different from what was expected that the mixture solution would turn to the blue color again due to the presence of reaction product, HI.

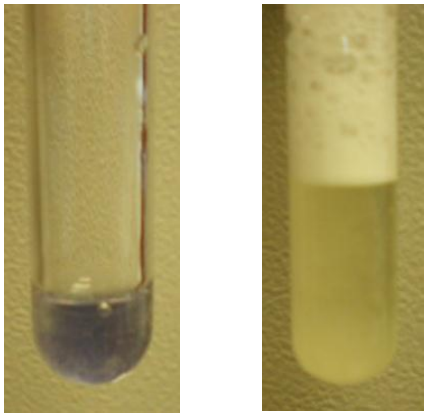

Figure B-3 Photographs of 2 wt% CIA/0.3M AcOH (0.3 mL) mixed with starch aq. and H_2O_2 (0.2 mL) (left), 2 wt% CIA/0.3M AcOH (0.1 mL)/4 wt% denatured BSA aq. (0.275 mL) after incubation for 3 h at 37˚C, then, starch aq. and H_2O_2 (~0.8 mL) was added (right).

The depth of the blue of starch-iodine complex is a function of the starch (or iodine) concentration. Specifically, I_2 reacts with I^- to yield a soluble triiodide ion, I_3^-. This triiodide ion is embedded inside of the starch chain, forming a non-covalent starch-triiodide complex, which gives a blue-black color. That is, only iodine element in the presence of iodide ion

gives the characteristic color. Neither iodine element alone nor iodide ions alone gives the color. Since HI is supposed to be oxidized to I_2 by added H_2O_2, the sample solution seems to lack the iodide ions. Thus, the yellow color indicates that iodide ions in the CIA would perfectly have reacted with the sulfhydryl compounds in the denatured BSA and no iodide ions were remained in the CIA units. Another experiment was carried out to demonstrate this. In this experiment, 2 wt% CIA/AcOH solution was mixed with soluble starch aq. solution and H_2O_2, exhibiting the blue color. Next, 4 wt% BSA aq. solution was gradually added into the CIA solution. It caused the proportional disappearance of the color to the amount of added BSA solution (Figure B-4). With the increase in the BSA content, the iodoacetic acid residue in CIA was more likely to react with the sulfhydryl group in BSA, resulting in the less iodide ions remained in the solution and the disappearance of the blue color. This concludes that the CIA solution, that was reacted with BSA for 3 hours, did not give the blue color since the iodoacetic acid residues totally reacted with BSA and there were no iodide ions available to form I_3^-, consequently, I_3^--starch complex.

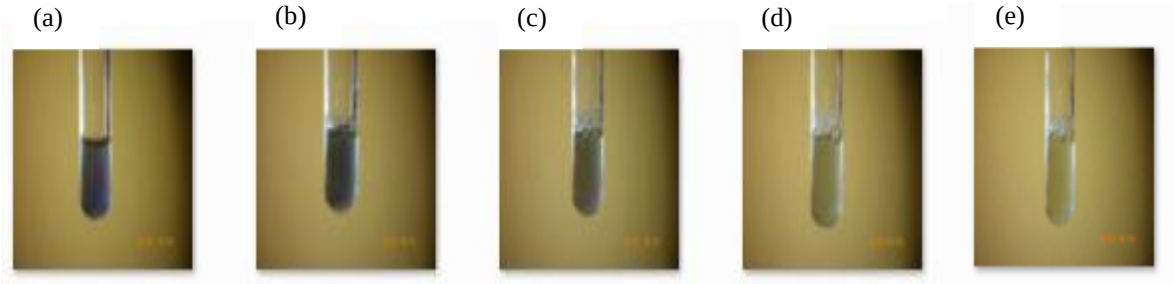

Figure B-4 Photographs of 2 wt% CIA/0.3M AcOH (0.3 mL)/ 4 wt% denatured BSA aq. mixed with starch aq. and H_2O_2 (0.2 mL); (a) 0 mL BSA, (b) 0.1 mL BSA, (c) 0.2 mL BSA, (d) 0.3 mL BSA, (e) 0.4 mL BSA.